Design and application of emulsion-based delivery systems as carriers of antimicrobials or bioactive compounds into complex food matrices

Anna Molet Rodríguez

http://hdl.handle.net/10803/675083

Universitat de Lleida

Design and application of emulsion-based delivery systems as carriers of antimicrobials or bioactive compounds into complex food matrices
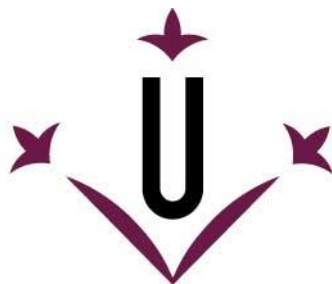
Anna Molet Rodríguez

Memòria presentada per optar al grau de Doctor per la Universitat de Lleida
Programa de Doctorat en Ciència i Tecnologia Agrària i Alimentària

Director/a
Olga Martín Belloso
Laura Salvia Trujillo

Tutor/a
Olga Martín Belloso

2022

Acknowledgements-Agradecimientos-Agraïments

En aquest moment, a punt de finalitzar la meva tesi doctoral i tancar aquesta etapa de la meva vida, miro enrere, respiro i satisfeta prenc consciència del camí recorregut. Un camí molt intens i amb grans reptes, però ple d'aprenentatge tant en l'àmbit professional com en el personal. Per sort, he caminat sempre acompanyada de la meva gent i de les persones que han compartit el mateix recorregut que jo. A tots i cadascun d'ells els hi agraeixo els moments compartits i l'ajuda que m'han brindat en tot moment.

En primer lloc, voldria agrair a les meves directores de tesi, la Dra. Olga Martín Belloso i la Dra. Laura Salvia Trujillo per recolzar-me en els moments importants i haver-me guiat durant tots aquests anys. Acabo aquesta etapa amb uns aprenentatges que valoro molt i que estic segura que em seran molt útils pel futur. Olga, gracias por darme la oportunidad de realizar la tesis doctoral y formar parte del grupo de Nuevas Tecnologías. También por compartir tus conocimientos, así como haberme ayudado a desarrollar un pensamiento crítico y a estructurar mis ideas. Laura, moltes gràcies per compartir amb mi la teva passió per la ciència i tots els teus coneixements. M'he sentit molt recolzada, he gaudit i he après moltíssim al teu costat.

Voldria agrair, també, a totes les persones que formen o han format part del grup i que en algun moment o altre hem coincidit, passat una bona estona o m'han ofert la seva ajuda. En especial a la Magda, la Gemma Charles i el Manel. També a les persones amb qui he compartit el meu dia a dia, els predocs i els que han passat pel departament en algun moment o altre, en especial a l'Ana Turmo, l'Ana Álvarez, la Gloria, la Winnie, l'Heloísa, el Gustavo, la Raquel i la Tere. I com no, a les meves nenetes "sin espuma", Ari, Clara, Júlia, María i Sara, per aquest "bon rollo" i alegria que despreneu. Heu sigut un pilar imprescindible per a mi durant aquesta etapa. M'enduc cinc amigues per a tota la vida.

I would also like to thank Prof. Alan Mackie for giving me the opportunity to join his group at the University of Leeds during my internship and for his confidence and support. I am also deeply thankful to Dr. Amelia Torcello Gómez and Neil Rigby for their help and advice. During my time in Leeds, I met incredible people, especially Alberto, Andrea, Emma, Vicente and Suvro, who welcome me with much kindness and made the experience unforgettable.

Gràcies a l'espai de ioga per tots els divendres de parar, respirar i recarregar piles.

A vosaltres, la Colla de Guapos i Guapes, els que sempre hi sou i sempre hi sereu. Gràcies pels moments de desconnexió, sempre plens de rialles i aventures. I per molts més!

A les Floretes, Lourdes i Tere, quina sort tinc que els nostres camins s'hagin creuat. Gràcies per l'afecte i suport que em doneu sempre.

A la meva família, els de Barcelona i els de Bellpuig. A la família del Xavier pel seu suport i amor incondicionals. A l'Helena pel disseny de la portada de la tesi, ets una artista!

A tu Xavier, perquè compartir la vida amb tu és un regal. Moltes gràcies per fer-ho tot tan fàcil sempre, per donar-me tanta pau, pel teu suport, per ser incondicional, per regalar-me tants moments, tant aprenentatge i per veure'm amb els millors ulls de món.

I finalment als meus pares, l'Ana María i el Toni, pels valors que m'heu donat, de compromís, il·lusió, perseverança i implicació, els quals m'han ajudat a convertir-me en la persona que sóc i aconseguir les fites que em proposo. A la meva germana, la Daniel·la, que em guia, m'aconsella i m'aixeca quan és necessari. I el més important, gràcies per fer-me costat sempre i pel vostre amor infinit.

A l'Ana María, el Toni, la Daniel·la i el Xavier,
per caminar sempre al meu costat

RESUM

Les emulsions s'han descrit com a prometedors sistemes de protecció i alliberament de compostos actius en productes alimentaris. Tanmateix, es disposa de poca informació sobre l'impacte que poden tenir la composició i les característiques de les matrius alimentàries sobre l'estabilitat col·loidal i la funcionalitat de les emulsions en condicions d'emmagatzematge i digestió gastrointestinal. Per tant, l'objectiu d'aquesta tesi doctoral va ser estudiar el comportament de diferents sistemes d'alliberament basats en emulsions (emulsions i nanoemulsions oli-aigua o emulsions dobles aigua-oli-aigua) portadors d'antimicrobians (olis essencials, OE) o compostos bioactius (β-carotè o clorofilina) un cop incorporats a productes alimentaris aquosos (begudes a base de suc de poma, productes làctics o productes a base de civada), que diferien en composició i característiques de la matriu. Amb aquesta finalitat, es van formar emulsions portadores de compostos actius estabilitzades amb Tween 80 i es van incorporar a productes alimentaris aquosos. Posteriorment, es van emmagatzemar a temperatura ambient amb un cultiu d'*Escherichia coli (E.coli)* o es van sotmetre a digestió gastrointestinal simulada.

L'estabilitat col·loidal de les emulsions i nanoemulsions un cop incorporades als productes alimentaris estudiats, així com durant el seu posterior emmagatzematge o digestió gastrointestinal no sols es va mantenir sinó que en alguns casos, fins i tot va millorar. Durant l'emmagatzematge, les nanoemulsions portadores d'OE van ser més estables en una beguda a base de suc de poma que en aigua. Les emulsions portadores de β-carotè van mantenir la seva estabilitat col·loidal un cop incorporades a productes làctics o productes a base de civada, així com durant la posterior digestió gastrointestinal. La funcionalitat de les emulsions i nanoemulsions va dependre de la composició i les característiques de la matriu de l'aliment en el qual es van incorporar. L'eficàcia de les nanoemulsions portadores d'OE contra *E.coli* es va veure compromesa en una beguda a base de suc de poma. El buidatge gàstric de l'emulsió portadora de β-carotè va ser més ràpid quan aquesta es va digerir juntament amb llet sencera que amb una matriu més viscosa a base de civada. La incorporació de l'emulsió portadora de β-carotè a productes alimentaris que contenien glòbuls de greix va incrementar-ne la lipòlisi. A més, la incorporació d'emulsions a productes làctics o a base de civada va ajudar a millorar la retenció de β-carotè durant la digestió gastrointestinal, però en va comprometre la bioaccessibilitat.

Pel que fa a les emulsions dobles portadores de clorofilina amb fase lipídica gelificada, la seva formació i estabilitat col·loidal durant la digestió gastrointestinal van dependre principalment de la composició de la fase lipídica. La barreja de triglicèrids de cadena mitja (TCM) amb estearat de

gliceril (EG) a una concentració del 5%, va ser eficaç en la formació d'emulsions dobles que van ser estables en condicions gastrointestinals. En canvi, l'ús de triglicèrids de cadena llarga, com l'oli de palma hidrogenat (OPH), va conduir a la separació de fases. El grau de lipòlisi durant la digestió gastrointestinal d'emulsions dobles portadores de clorofilina amb fase lipídica gelificada, va ser determinat per la composició de la fase lipídica en lloc del seu estat físic, cosa que podria atribuir-se a la fusió de la fase lipídica en condicions gastrointestinals. Fins i tot, quan es van incorporar a la llet sencera, l'estabilitat col·loidal i el grau de lipòlisi de les emulsions dobles portadores de clorofilina van dependre de la composició de la fase lipídica. De fet, l'estabilitat col·loidal i el grau de lipòlisi no es van alterar quan l'emulsió doble (TCM-EG) es va digerir juntament amb llet sencera, mentre que la incorporació de l'emulsió doble amb OPH a la llet sencera, va resultar en un augment de l'estabilitat col·loidal i de la lipòlisi. Per una altra banda, la bioaccessibilitat de la clorofilina en les emulsions dobles amb fase lipídica gelificada abans i després de ser incorporades a la llet sencera, va estar relacionada amb el grau de lipòlisi.

Els resultats obtinguts en aquesta tesi doctoral, proporcionen nous coneixements sobre el comportament de diferents sistemes d'alliberament basats en emulsions una vegada incorporats a productes alimentaris aquosos, així com durant el seu posterior emmagatzematge o digestió gastrointestinal. Aquesta informació podria ser molt útil en el futur per desenvolupar emulsions amb propietats fisicoquímiques específiques depenent de les característiques de la matriu alimentària d'interès i de la funcionalitat desitjada.

RESUMEN

Las emulsiones se han descrito como prometedores sistemas de protección y liberación de compuestos activos en productos alimentarios. Sin embargo, se desconoce el impacto que pueden tener la composición y las características de la matriz alimentaria en la estabilidad coloidal y la funcionalidad de las emulsiones en condiciones de almacenamiento y digestión gastrointestinal. Por lo tanto, el objetivo de esta tesis doctoral fue estudiar el comportamiento de sistemas de liberación basados en emulsiones (emulsiones y nanoemulsiones aceite-agua o emulsiones dobles agua-aceite-agua) para la incorporación de antimicrobianos (aceites esenciales, AE) o compuestos bioactivos (β-caroteno o clorofilina) a alimentos acuosos (bebidas a base de jugo de manzana, productos lácteos y productos a base de avena), que difirieron en composición y características de la matriz alimentaria. Para ello, sistemas de liberación basados en emulsiones estabilizados con Tween 80 y portadores de compuestos activos se incorporaron a alimentos acuosos y, posteriormente, se almacenaron a temperatura ambiente con un cultivo de *Escherichia coli (E.coli)* o se sometieron a digestión gastrointestinal simulada.

La estabilidad coloidal de las emulsiones y las nanoemulsiones se mantuvo e incluso mejoró, una vez incorporadas a los alimentos estudiados, así como también durante su posterior almacenamiento y digestión gastrointestinal. Durante condiciones de almacenamiento, las nanoemulsiones portadoras de AE mostraron una mayor estabilidad coloidal en una bebida a base de jugo de manzana que en agua. Las emulsiones portadoras de β-caroteno mantuvieron su estabilidad coloidal una vez incorporadas a productos lácteos o a base de avena, así como durante su posterior digestión gastrointestinal. La funcionalidad de las emulsiones y nanoemulsiones dependió de la composición y las características de la matriz alimentaria en la que se incorporaron. La eficacia de las nanoemulsiones portadoras de AE contra *E.coli* se vio comprometida en una bebida a base de jugo de manzana. El vaciado gástrico de la emulsión portadora de β-caroteno fue más rápido cuando esta fue digerida con leche entera que con una matriz más viscosa que consistía en productos a base de avena. La incorporación de la emulsión portadora de β-caroteno a alimentos que contenían glóbulos de grasa resultó en una mayor lipólisis. Además, la incorporación de emulsiones a productos lácteos o a base de avena ayudó a mejorar la retención de β-caroteno durante la digestión gastrointestinal, pero comprometió su bioaccesibilidad.

Respecto a las emulsiones dobles portadoras de clorofilina con fase lipídica gelificada, su exitosa formación y posterior estabilidad coloidal durante la digestión gastrointestinal dependieron principalmente de la composición de la fase lipídica. La mezcla de triglicéridos de cadena media

(TCM) con estearato de glicerilo (EG) a una concentración del 5%, fue eficaz en la formación de emulsiones dobles, que además fueron estables en condiciones gastrointestinales. En cambio, el uso de triglicéridos de cadena larga, como el aceite de palma hidrogenado (APH), condujo a la separación de fases. Durante la digestión gastrointestinal, el grado de lipólisis de las emulsiones dobles portadoras de clorofilina con fase lipídica gelificada, fue determinado por la composición de la fase lipídica en lugar de su estado físico, probablemente debido a la fusión de la fase lipídica en condiciones gastrointestinales. Incluso cuando se incorporaron a la leche entera, su estabilidad coloidal y lipólisis dependieron de la composición de la fase lipídica. De hecho, la estabilidad coloidal y el grado de lipólisis no variaron cuando la emulsión doble (TCM-EG) se digirió juntamente con leche entera, mientras que la incorporación de la emulsión doble con APH a la leche entera, resultó en una mayor estabilidad coloidal y grado de lipólisis. Por otro lado, la bioaccesibilidad de la clorofilina en las emulsiones dobles con fase lipídica gelificada antes y después de ser incorporadas a la leche entera, estuvo relacionada con el grado de lipólisis.

Los resultados obtenidos en esta tesis doctoral, proporcionan nuevos conocimientos sobre el comportamiento de distintos sistemas de liberación basados en emulsiones una vez incorporados a productos alimentarios acuosos comunes, así como durante su posterior almacenamiento o digestión gastrointestinal simulada. Esta información podría ser muy útil en el futuro para el desarrollo de emulsiones con propiedades fisicoquímicas específicas dependiendo de las características de la matriz alimentaria de interés y de la funcionalidad deseada.

ABSTRACT

Emulsions are promising systems for the protection and delivery of active compounds into food products. However, little is known about the effect of food matrix composition and characteristics on emulsion-based delivery systems colloidal stability and functionality during storage and gastrointestinal (GI) conditions. Therefore, this doctoral thesis aimed to study the behaviour of emulsion-based delivery systems (oil-in-water (O/W) emulsions and nanoemulsions or $W_1/O/W_2$ emulsions) carrying antimicrobials (essential oils, EOs) or bioactive compounds (β-carotene or chlorophyllin, CHL) into water-based food products (apple juice-based beverage, dairy products or oatmeal-based products), differing in food matrix composition and characteristics. For this, Tween 80-stabilized emulsion-based delivery systems carrying active compounds were incorporated into water-based food products and subsequently stored at room temperature with an *Escherichia coli (E.coli)* culture or subjected to simulated GI digestion.

The colloidal stability of O/W emulsions and nanoemulsions was maintained and, even enhanced, once incorporated into water-based food products and during their subsequent storage or GI digestion conditions. EOs-O/W nanoemulsions showed higher colloidal stability into an apple juice-based beverage than in water during storage. In the case of the β-carotene-loaded O/W emulsions into dairy and oatmeal-based products, their colloidal stability was maintained before and during GI conditions. The functionality of O/W emulsions and nanoemulsions depended on the composition and matrix characteristics of the food in which were incorporated. EOs-O/W nanoemulsions killing efficacy against *E.coli* was compromised once incorporated into apple juice-based beverage. The gastric emptying rate of β-carotene-loaded O/W emulsion was faster when co-digested with whole milk than with a more viscous matrix consisting of oatmeal-based products. The incorporation of the β-carotene-loaded O/W emulsion in food products containing fat globules resulted in faster and higher lipolysis compared to water. Besides this, the incorporation of β-carotene-loaded O/W emulsions into dairy or oatmeal-based products helped in enhancing the bioactive compound retention during GI conditions, yet they compromised its bioaccessibility.

Regarding the CHL-loaded $W_1/O/W_2$ emulsions with gelled lipid phase, their successful formation and subsequent colloidal stability during GI digestion mainly depended on the lipid phase composition. Blends of medium-chain triglyceride (MCT) oil with glyceryl stearate (GS) at a concentration of 5% were efficient in forming $W_1/O/W_2$ emulsions, which were stable upon GI conditions. Instead, using hydrogenated palm oil (HPO) as a lipid phase led to phase separation. The lipolysis extent during simulated GI digestion of CHL-loaded $W_1/O/W_2$ emulsions with gelled lipid

phase was determined by the lipid phase composition rather than the physical state, which might be attributed to the melting of the lipid phase at GI conditions. Even when incorporated into whole milk, the colloidal stability and lipolysis extent of CHL-loaded $W_1/O/W_2$ emulsions was still dependent on the lipid phase composition. Indeed, the colloidal stability and lipolysis extent were not altered when the $W_1/O/W_2$ emulsion (MCT-GS) was co-ingested with whole milk, whereas the incorporation of the $W_1/O/W_2$ emulsion with HPO into whole milk resulted in enhanced colloidal stability and lipolysis extent. The CHL bioaccessibility of $W_1/O/W_2$ emulsions with gelled lipid phase before and after incorporated into whole milk was linked with the lipolysis extent.

The results obtained in this doctoral thesis provide novel insights on the behaviour of different emulsion-based delivery systems once incorporated into common water-based food products, as well as, during their subsequent storage or GI digestion. This information could be very useful in the future for the development of emulsions with specific physicochemical properties depending on the characteristics of the food matrix of interest and its desired functionality.

TABLE OF CONTENTS

INTRODUCTION

1 Introduction

In the last decades, consumers' awareness of the relationship between foods and well-being has evolved into a growing claim for healthier and safer foods. Thus, foods are no more intended only to satisfy hunger and to provide the necessary nutrients, yet also contribute to higher functionality. On the one hand, the interest in food products with enhanced health benefits is growing among consumers. On the other hand, there is an ongoing demand for safer food products with longer shelf life, yet rejecting highly processed foods and the presence of synthetic ingredients. In this way, the incorporation of active compounds into foods is being regarded as an interesting approach to develop food products with added functional benefits (Burt, 2004; Gleeson, Ryan, & Brayden, 2016; Granato et al., 2020; Gunathilake, Rupasinghe, & Pitts, 2013). Fruits, vegetables, legumes, nuts, herbs and spices, among others, are rich sources of macro-, and micro-nutrients, as well as active compounds that exhibit a wide range of biological activities (Pan, Lai, Dushenkov, & Ho, 2009; Sell, 2010). However, many active compounds present low water-solubility, poor chemical stability, high flavour, and/or low absorption through biological membranes, making their incorporation into food products a challenge as their functional properties can be diminished (Boon, McClements, Weiss, & Decker, 2010; Ferruzzi & Schwartz, 2005; Sell, 2010). In this regard, there is a growing interest among the scientific community regarding the design of delivery systems of active compounds into food products (Salvia-Trujillo, Artiga-Artigas, Molet-Rodríguez, Turmo-Ibarz, & Martín-Belloso, 2018). A wide variety of food-grade emulsion-based structures have been described as delivery systems of active compounds (Mao & Miao, 2015). In general, emulsion consists of two immiscible liquids (usually oil and water), with one liquid being dispersed as spherical droplets in the other liquid, which acts as a continuous phase (McClements, 2015). They can be classified according to the spatial organization of the lipid (oil) and aqueous (water) phases. A system that consists of oil droplets dispersed in an aqueous continuous phase is called an oil-in-water (O/W) emulsion, whereas a system that consists of water droplets dispersed in a lipid phase is called a water-in-oil (W/O) emulsion. In this context, O/W and W/O emulsions can carry lipophilic and hydrophilic active compounds, respectively. When their droplet size is below 100 nm, they are defined as O/W and W/O nanoemulsions. In addition, depending on the state of the lipid core, whether it is a liquid oil or solid fat, nanoemulsions or solid lipid nanoparticles can be formed, respectively. It is also possible to prepare double emulsions, being oil-in-water-in-oil ($O_1/W/O_2$) or water-in-oil-in-water ($W_1/O/W_2$) emulsions that are able to carry both hydrophilic and lipophilic active compounds (Muschiolik & Dickinson, 2017). Nevertheless, the incorporation of emulsion-based delivery systems into food products remains limited due to the lack of scientific evidence about whether they preserve or not

their physicochemical properties and colloidal stability as well as active compound functionality once incorporated into food matrices. Food matrix composition and characteristics may allow them to interact with the oil/water interface compromising the colloidal stability of the emulsion-based delivery systems and consequently the functionality of the encapsulated compound (Aguilera, 2019).

Thus, this section aims to discuss the benefits and limitations of food-grade emulsions as delivery systems of active compounds into food matrices. We provide an overview of the recent developments concerning the formation, physicochemical properties, colloidal stability and functionality of emulsion-based delivery systems carrying active compounds. In addition, the composition and characteristics of the selected water-based food matrices and their possible interactions with emulsion-based delivery systems are presented.

2 Active compounds

Active compounds from natural origin have been widely used as a source of medication since ancient times. Nowadays, there is strong scientific evidence of the wide range of biological activity of these natural compounds. On the one hand, antimicrobial compounds have been regarded as an alternative natural decontamination strategy to chemical preservatives against food-borne microorganisms (Burt, 2004). On the other hand, bioactive compounds have been observed to be involved in physiological processes, as well as to exhibit antioxidant and anti-inflammatory activities, thus reducing the risk of certain diseases (Estruch et al., 2013; Zulueta, Esteve, Frasquet, & Frígola, 2007). Despite the potential benefits of antimicrobial and bioactive compounds, they need a prior emulsification step in order to be incorporated into food products (Donsì, Annunziata, Sessa, & Ferrari, 2011; Mao & Miao, 2015; Qian, Decker, Xiao, & McClements, 2012). Table 1 shows a list of active compounds with interest for being incorporated into foods using emulsion-based delivery systems.

Table 1. Active compounds with interest for the development of foods with added functional benefits through their encapsulation into emulsion-based delivery systems.

Type	Source	Chemical	Name	Polarity	Functionality	Limitations	Reference
Antimicrobial	Fruit peels, plants and herbs	Essential oils	Thyme, oregano, sage, lemongrass, mandarin, cinnamon, rosemary, marjoram, clove	Lipophilic	Flavourings and food preservation	Low solubility Strong flavour and volatility	(Burt, 2004)
Bioactive compounds	Fish oil, krill oil, flax-seed and walnut oil	Fatty acids	Omega-3 Fatty acids (eicosapentaenoic acid and docosahexaenoic acid)	Lipophilic	Cardiovascular disease, inflammatory disease, brain function and mental health	Susceptibility to degradation Low chemical stability Off-flavours	(Ruxton, Reed, Simpson, & Millington, 2004)
	Milk, rice, eggs, salmon skin	Bioactive peptide and protein	Val-Tyr-Pro, lactoglobulin and lactoferrin	Hydrophilic	Blood pressure lowering effect, cholesterol-lowering effect, anti-inflammatory activity, anticancer effect and Immunomodulatory activity	Low solubility Low chemical stability Loss of bioactivity Bitter taste	(Cicero, Fogacci, & Colletti, 2017)
	Plants, whole grains, fish	Micronutrients	Vitamins (A, D and folic acid) and minerals (zinc, magnesium)	Lipophilic and hydrophilic	Co-enzymes for metabolic processes, antioxidants to remove reactive oxygen species and modulation of gene transcription	Low solubility (lipophilic) Susceptibility to degradation Low bioavailability	(Gleeson et al., 2016)
	Plant, fruits and vegetables	Phytochemicals	Chlorophylls, carotenoids, flavonoids and betalains	Lipophilic and hydrophilic	Colourings, antioxidant activity, anti-inflammatory and anti-hyperlipidemic activity	Low solubility (lipophilic) Susceptibility to degradation Low bioavailability	(Miller, Owens, & Rørslett, 2011)

2.1   Antimicrobials

Antimicrobials are substances that exhibit outstanding efficacy against spoilage microorganisms in food. Organic acids are added frequently to foods as preservatives since pH has a great impact on the survival and growth of spoilage microorganisms (Raybaudi-Massilia, Mosqueda-Melgar, Soliva-Fortuny, & Martín-Belloso, 2009). Nevertheless, consumers are currently demanding safe foods without the addition of chemically synthesized preservatives. Therefore, the application of natural antimicrobials to assure the safety of food is a promising alternative. Essential oils (EOs) are natural lipophilic antimicrobial compounds obtained from the distillation of aromatic herbs, plants and fruit peels (Tu, Thanh, Une, Ukeda, & Sawamura, 2002). EOs also present a strong antioxidant activity, thus being good candidates to enhance the antioxidant properties of foods (Adorjan & Buchbauer, 2010; Olszowy & Dawidowicz, 2016). However, their incorporation in water-based food matrices is a challenge due to their hydrophobicity and extreme volatility (Burt, 2004). In addition, although a number of EO components, including carvacrol, carvone, cinnamaldehyde, citral, p-cymene, eugenol, limonene, menthol and thymol have been recognized as safe (GRAS) by the European Commission for use as flavourings in foods, their use as preservatives is often limited due to their strong flavour and possible toxicity at the high concentrations needed for it to be an efficient food preservative (Dima & Dima, 2015; Espina, García-Gonzalo, & Pagán, 2014).

2.2   Bioactive compounds

Bioactive compounds are food-derived substances with biological activity, thus capable of modulating metabolic processes, which results in a maintenance of the normal physiological function in the human body (Das, Bhaumik, Raychaudhuri, & Chakraborty, 2012). Bioactive compounds can be classified depending on their chemical nature as omega 3 (ω-3) fatty acids, bioactive peptide and protein prebiotics, micronutrients and phytochemical plant pigments (Gleeson et al., 2016). Besides the biological activity, phytochemical plant pigments have an attractive colour, which makes them useful to obtain visually appealing food products (Costell, Tárrega, & Bayarri, 2010; Miller et al., 2011). They can be divided into four major categories: chlorophylls, carotenoids, flavonoids and betalains. Chlorophyll is the most abundant family of phytochemicals in nature and is responsible for the colour of all green plants (Miller et al., 2011). Chlorophyll and its various derivates have demonstrated significant biological activities *in vitro* and *in vivo* consistent with the prevention of certain chronic diseases (Ferruzzi & Blakeslee, 2007). Nevertheless, they present different chemical structures, from lipophilic (natural chlorophylls) to highly hydrophilic (commercial sodium copper chlorophyllin) and so, variable sensitivities to pH (Hayes & Ferruzzi, 2020). In this regard, the

biological activity of chlorophylls and their derivates depends on their stability throughout the gastrointestinal (GI) tract and route of absorption in the small intestine. Carotenoids are long-chain lipophilic natural molecules responsible for the yellow, orange, and red colours in various fruits and vegetables. They have been classified in xanthophylls (lutein and zeaxanthin), containing oxygen as a functional group and carotenes (α-carotene, β-carotene and lycopene), which contain only a hydrocarbon chain without any functional group (Saini, Nile, & Park, 2015). The consumption of a diet rich in carotenoids is well-known to have a positive impact on human health as they have been associated with biological functions, such as provitamin A activity, antioxidant capacity and enhancement of the immune system (Maiani et al., 2009). Nevertheless, the bioaccessibility of lipophilic carotenes from foods is usually fairly low (Boon et al., 2010). In this regard, studies have shown that the absorption of ingested dietary carotenoids may be greatly improved when they are consumed in the presence of lipids (Maiani et al., 2009). Flavonoids are a class of plant secondary metabolites widely found in fruits and vegetables (Ignat, Volf, & Popa, 2011). They present a polyphenolic hydrophilic structure, which gives them antioxidative, anti-inflammatory, anti-mutagenic and anti-carcinogenic properties and the capacity to modulate key cellular enzyme functions (Panche, Diwan, & Chandra, 2016). Among them, anthocyanins are the main responsible for the blue, purple, red and orange colouration in flowers and fruits (Miller et al., 2011). Nevertheless, they can adopt multiple different structures in solution depending on the pH of the solvent, which can compromise their health-related properties. Betalains are also hydrophilic molecules with proven antioxidant activity, but sensitive to high temperature, pH, light and oxygen (Cai, Sun, & Corke, 2003; Herbach, Stintzing, & Carle, 2006).

3 Emulsion-based delivery systems

There has been a marked increase in the number of publications focusing on the development of food-grade emulsion-based delivery systems carrying active compounds. The selection of the emulsion-based delivery system type and formulation based on the polarity (lipophilic or hydrophilic) of active compounds, food product composition and matrix characteristics and the desired functional performance is of crucial importance. Particularly, to incorporate active compounds into water-based food products, O/W emulsions, O/W nanoemulsions and $W_1/O/W_2$ emulsions have a special interest, as they have a structure consisting of oil droplets dispersed in a continuous aqueous phase (Fig. 1).
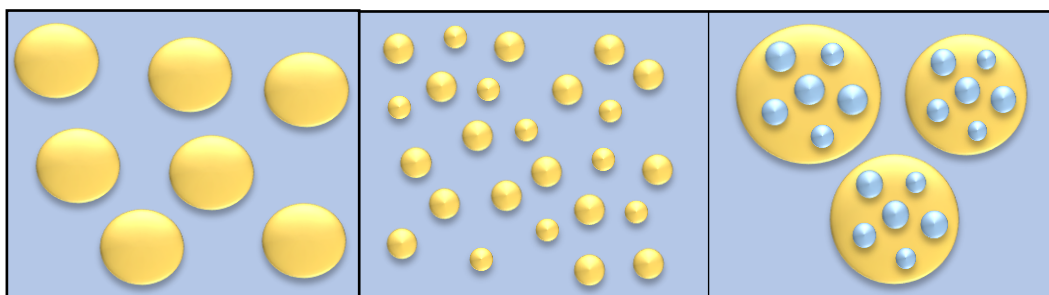
Figure 1. Oil-in-water (O/W) emulsions (left panel), O/W nanoemulsions (middle panel) and water-in-oil-in-water (W_1/O/W_2) emulsions (right panel) as delivery systems of active compounds.

3.1 Oil-in-water (O/W) emulsions and nanoemulsions

O/W emulsions and nanoemulsions both consist of lipid droplets dispersed into a continuous aqueous phase. The lipid droplet size is the main difference between O/W emulsions (0.1-10 μm) and O/W nanoemulsions (<100 nm), which confers them with variable physicochemical properties and functional performance (McClements & Li, 2010). Due to their reduced oil droplet size, O/W nanoemulsions barely scatter the light, having a higher optical clarity than O/W emulsions, which strongly scatter the light (McClements, 2002; Salvia-Trujillo, Rojas-Graü, Soliva-Fortuny, & Martín-Belloso, 2013c). In addition, O/W nanoemulsions have higher stability to particle aggregation and gravitational separation than O/W emulsions, thus remaining with the initial characteristics during longer periods (Mason, Wilking, Meleson, Chang, & Graves, 2006). O/W nanoemulsions have a larger oil/water interfacial area than O/W emulsions, thus favouring: (*i*) the interaction of antimicrobials with biological membranes, such as the bacterial cell membrane (Donsì et al., 2011; Salvia-Trujillo, Rojas-Graü, Soliva-Fortuny, & Martín-Belloso, 2014) and (*ii*) the contact between the oil droplets and the digestive enzymes, so that facilitating the lipid digestibility. This has been related to an enhanced lipophilic bioactive compound bioaccessibility (Rao & McClements, 2011; Salvia-Trujillo, Qian, Martín-Belloso, & McClements, 2013a).

3.1.1 *Formation*

High-speed homogenizers such as Ultraturrax are sufficient for the formation of large oil droplets with diameters > 100 nm, as is the case of O/W emulsions. O/W nanoemulsion formation requires the subsequent breakdown of larger oil droplets into smaller ones (oil droplet diameter < 100 nm), which can be achieved by the use of high energy or low energy methods (Acosta, 2009; Tadros, Izquierdo, Esquena, & Solans, 2004). However, high energy methods are generally more extended as they have shown to reduce the oil droplet size more effectively in a wide range of formulations and

are regarded as easier methods to scale up at the industrial level (Salvia-Trujillo, Soliva-Fortuny, Rojas-Grau, McClements, & Martin-Belloso, 2017). All these devices work on the general principle of high-shear produced by cavitation, collision and turbulence, which causes the breakdown of the oil droplets and their uniform dispersion in a continuous aqueous phase. On the one hand, ultrasounds have been reported to produce O/W nanoemulsions with average oil droplet sizes smaller than 100 nm (Kentish et al., 2008; Salvia-Trujillo, Rojas-Graü, Soliva-Fortuny, & Martín-Belloso, 2013d). The main factors affecting the fabrication of O/W nanoemulsions by sonication are the output frequency, amplitude and treatment time, which determines the intensity of the cavitation phenomena and therefore oil droplet disruption (Abbas, Hayat, Karangwa, Bashari, & Zhang, 2013; Salvia-Trujillo et al., 2013d). On the other hand, high-pressure homogenizers, such as valve-homogenizers or microfluidizers, are widely used to produce O/W nanoemulsions. In general, the higher the homogenization pressure and the number of cycles, the smaller the oil droplet size. Several authors have reported the formation of O/W nanoemulsions with droplet sizes smaller than 50 nm using high-pressure homogenizers (Qian & McClements, 2011; Salvia-Trujillo et al., 2013c).

Besides the fabrication method and processing parameters, the droplet size of O/W emulsions and nanoemulsions highly depends on the lipid phase physicochemical characteristics (Qian & McClements, 2011). Different kinds of oils and fats can be used for their formulation, whether from different origins (vegetal or animal) or variable molecular composition (fatty acids chain length or unsaturation degree). Vegetable and essential oils are mainly composed of unsaturated fatty acids, but they differ in the fatty acid chain length of triglycerides (Gao et al., 2017). Vegetable oils are mostly composed of long-chain fatty acids ($\geq C_{12}$) and medium-chain fatty acids (C_8-C_{10}) while essential oils mainly contain short-chain fatty acids (C_4-C_6). Animal fat has a high content of short- and medium-chain fatty acids mainly saturated (Lubary, Hofland, & ter Horst, 2011). These differences in the chain length and unsaturation degree of triglycerides between oils and fats confers them with varying physicochemical characteristics such as viscosity and water solubility that ultimately may alter O/W emulsion and nanoemulsion droplet size. It has been observed that long-chain triglycerides (LCT) oils, such as many vegetable oils, render O/W nanoemulsions with oil droplets larger than those with medium-chain (MCT) and short-chain triglycerides (SCT) (Komaiko & McClements, 2015; Ostertag, Weiss, & McClements, 2012; Salvia-Trujillo, Qian, Martín-Belloso, McClements, 2013b). It is well-known that LCT oils present high viscosity, thus reducing their droplet size during emulsification by high energy methods is less efficient than for oils with lower viscosity, as is the case of MCT or SCT (Qian & McClements, 2011; Walker, Gumus, Decker, & McClements, 2017; Wooster, Golding, & Sanguansri, 2008). For instance, Qian & McClements (2011) showed that O/W emulsions formulated

with corn oil, which have a viscosity of 30 mPa·s, presented oil droplet sizes of 125 nm, while increasing the percentage of octadecane in the lipid phase lead to O/W nanoemulsions with smaller oil droplet sizes (90 nm) due to a viscosity reduction (< 9 mPa·s). Moreover, it has also been observed that the higher the water solubility of oil, the smaller the produced oil droplets, which has been attributed to a reduction of the interfacial tension at the oil/water interface (Ziani, Fang, & Julian, 2012). In fact, Salvia-Trujillo, Rojas-Graü, Soliva-Fortuny, & Martín-Belloso (2015) have formed O/W nanoemulsions with droplet sizes ranging from 13.16 ± 0.92 to 86.49 ± 4.31 nm, when using different essential oils (lemongrass, clove, tea tree, thyme, geranium, marjoram, palmarosa, rosewood, sage and mint), which are well-known to present different water solubilities due to variations in their chemical composition (Espina et al., 2011).

3.1.2 *Stabilization*

O/W emulsions and nanoemulsions are both thermodynamically unstable, so they will tend to break down over time. It is normally caused by some physicochemical mechanisms, such as creaming, sedimentation, Ostwald ripening and flocculation which normally ends with coalescence (McClements, 2015) (Fig. 2).
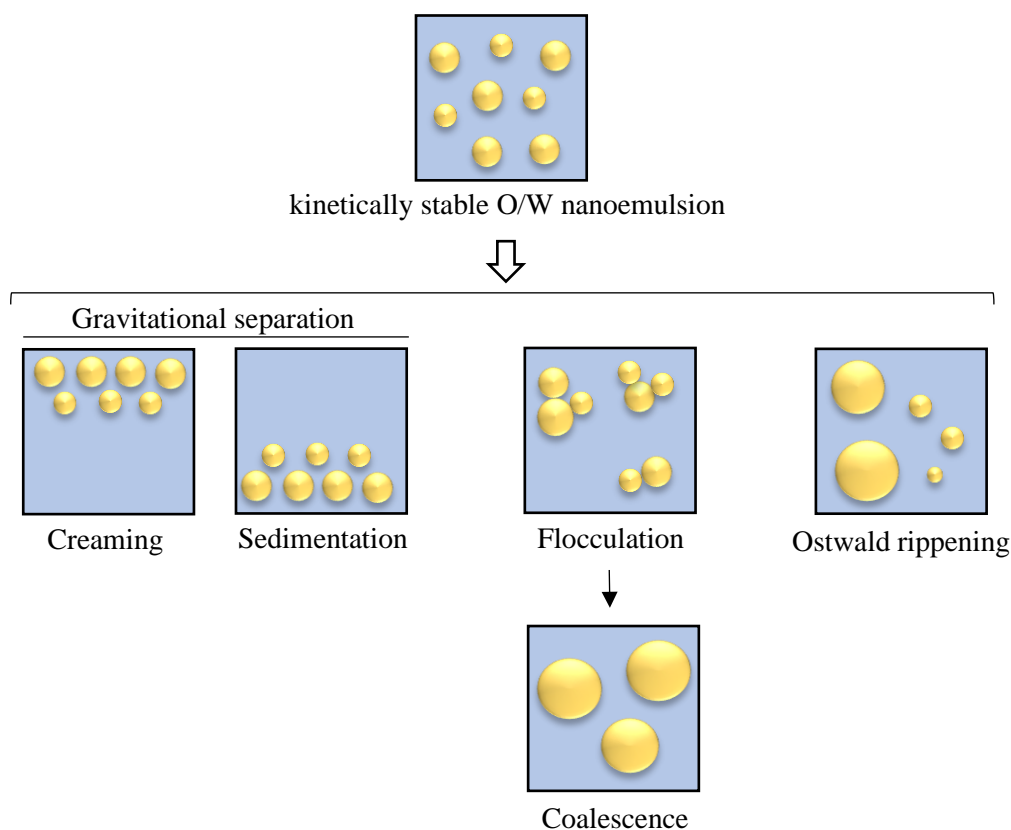
Figure 2. Instability mechanisms in O/W nanoemulsions.

Creaming and sedimentation are gravitational separations caused by density differences between the oil and the water phases. As a result, oil droplets migrate to the top (creaming) or the bottom (sedimentation), yet the latter is less likely to occur in O/W emulsions and nanoemulsions. By contrast, flocculation refers to the formation of oil droplet aggregates. Moreover, flocculation may lead to coalescence, the process by which oil droplets merge, resulting in a larger droplet. Finally, Ostwald ripening consists of the growth of large droplets, *via* the diffusion of lipid molecules through the water until they deposit into larger oil droplets. Therefore, one of the most important challenges to be faced for the formulation of O/W emulsions and nanoemulsions is to guarantee their kinetical stability, which is achieved by the proper selection of the emulsifier and lipid phase components. O/W emulsions and nanoemulsions stabilization require the presence of hydrophobic emulsifiers, which have the ability to adsorb and remain at the oil/water interface, thus forming a stable layer surrounding the oil droplet surface and preventing the breakdown of the O/W emulsion and nanoemulsion structure once it is formed. Table 2 presents the emulsifiers that are suitable for the formation and stabilization of food-grade O/W emulsion and nanoemulsion, which maximum permitted doses in food are regulated by current legislation (EU 1333/2008) (Kralova & Sjöblom, 2009; Molet-Rodríguez, Salvia-Trujillo, & Martín-Belloso, 2018).

Small-molecule surfactants are amphiphilic molecules, meaning that they present a hydrophilic head with a high affinity for water and a lipophilic tail that has a strong affinity for oil. The capacity of small-molecule surfactant to form O/W emulsions and nanoemulsions mainly depends on its hydrophilic-lipophilic balance (HLB), defined as the ratio of hydrophilic and lipophilic groups in the molecule (Kralova & Sjöblom, 2009). HLB numbers >10 refer to surfactants that have a high affinity for water (hydrophilic) and numbers <10 for the ones that have a strong affinity for oil (lipophilic). In this context, O/W emulsions and nanoemulsions can be prepared using surfactants with a high HLB (8-16) such as polyoxyethylene sorbitan esters of monoglycerides (Tweens), sucrose esters, sodium dodecyl sulphate (SDS) and lecithin. Apart from that, the head group of surfactant molecules might be either uncharged (non-ionic) or charged (ionic or zwitterionic) (Table 2). According to Tadros (2013), the most effective small-molecule surfactant to form O/W emulsions and nanoemulsions are those non-ionic (*e.g.,* Tweens and sucrose esters), since repulsion between the head groups is smaller than in those charged surfactant (*e.g.,* SDS and lecithin) and low concentrations are sufficient for oil droplet emulsification. For instance, Chang & McClements (2016) have obtained stable orange oil nanoemulsions using only 0.5% of Tween 80, which polyoxyethylene chains strongly adsorbed at the oil/water interface contributing to enhancing the stability *via* steric repulsions. Although the absorption of charged surfactants into the oil droplets surface is less easy

than that of non-ionic ones, they are also considered a good option for the production of O/W emulsions and nanoemulsions. On the one hand, ionic surfactants, such as SDS, have been observed to form negatively charged oil droplets of around ~300 nm that are stable against creaming (Mun, Decker, & McClements, 2005). On the other hand, lecithin (zwitterionic), which consists of a mixture of phospholipids whose polar head groups contain ionizable phosphate and nitrogen moieties, has been reported to form oil droplets surrounded by a viscoelastic oil/water interface able to resist deformation and protect O/W emulsions and nanoemulsions against destabilization phenomena such as coalescence or flocculation (Artiga-Artigas, Lanjari-Pérez, & Martín-Belloso, 2018c).

Table 2. Emulsifiers with potential interest for the formation and stabilization of food-grade O/W emulsion and nanoemulsion.

Type	Emulsifier	Charge	HLB	Droplet size (nm)	Reference
Small-molecule surfactant	Tweens	Non-ionic	10-16	7–127	(Jo & Kwon, 2014; Salvia-Trujillo et al., 2013c; Teo et al., 2016)
	Sucrose esters	Non-ionic	1-16	<150	(McClements, Decker, & Choi, 2014)
	Lecithin	Zwitterionic	12	>250	(Gasa-Falcon, Odriozola-Serrano, Oms-Oliu, & Martín-Belloso, 2019; Ma et al., 2018)
	SDS	Ionic	40	~300	(Mun et al., 2005)
Protein	Whey protein isolate			70–369	(Cornacchia & Roos, 2011; Jo & Kwon, 2014; Teo et al., 2016)
	Lactoferrin	Ionic	-	70–300	(Teo et al., 2016; Tokle & McClements, 2011)
	Sodium caseinate			93–335	(Cornacchia & Roos, 2011; Jo & Kwon, 2014; Kanafusa, Chu, & Nakajima, 2007)
Polysaccharide	Gum Arabic	Ionic		384–1000	(Klein, Aserin, Svitov, & Garti, 2010; Ozturk, Argin, Ozilgen, & McClements, 2015)
	Octenyl succinic anhydride starch		-	142–157	(Liang, Shoemaker, Yang, Zhong, & Huang, 2013)
	Pectin and alginate			350–850	(Artiga-Artigas, Guerra-Rosas, Morales-Castro, Salvia-Trujillo, & Martín-Belloso, 2018a)

Hydrophilic-lipophilic balance (HLB); polyoxyethylene sorbitan esters of monoglycerides (Tweens); sodium dodecyl sulphate (SDS)
Adapted from Molet-Rodríguez et al. (2018)

Protein from natural origin and certain types of polysaccharides have also shown interfacial properties, thus being able to act as natural emulsifiers. Protein especially from milk and eggs can adsorb at the oil/water interface, protecting O/W emulsions and nanoemulsions from the destabilization phenomena (Kanafusa et al., 2007). Nevertheless, protein-stabilized O/W emulsions and nanoemulsions typically exhibit higher oil droplets sizes compared to those stabilized by a small-molecule surfactant, since their large molecular size occupies a space at the oil/water interface that contributes to the final oil droplet size (Jo & Kwon, 2014). In addition, they tend to adsorb less effectively at the oil/water interface in comparison with small-molecule surfactants, so higher amounts of protein need to be used for emulsion stabilization (Gomes, Costa, & Cunha, 2018). Recently, Raikos, Duthie, & Ranawana (2017) observed gravitational separation in sodium caseinate-stabilized nanoemulsions, mainly caused by a lack of surfactant concentration, whereas Tween 80-stabilized nanoemulsions were stable at the same concentration. Nevertheless, these authors have shown that when the concentration of protein is enough to cover all the surface area, these emulsions are highly stable. This can be attributed to the high electrostatic repulsions between oil droplets due to the charged protein adsorbed at the oil/water interface. Moreover, protein can exhibit denaturation during adsorption, thus strengthening intramolecular interactions, which results in higher emulsion stability *via* steric repulsion (Cornacchia & Roos, 2011). Nevertheless, changes in the pH result in changes in the ionization degree of the functional groups of protein and the electrical charge of droplets, which may compromise O/W emulsion and nanoemulsion colloidal stability (Teo et al., 2016).

Finally, polysaccharides including gum arabic (GA), octenyl succinic anhydride starch, pectin and alginate have also been shown to effectively contribute to the stabilization of oil droplets (Liang et al., 2013; Sweedman, Tizzotti, Schäfer, & Gilbert, 2013; Xiang et al., 2015). In general, they do not present a strong interfacial activity, yet the surface activity of these hydrocolloids is mainly determined by (*i*) the non-polar character of chemical groups attached to the hydrophilic polysaccharide backbone (*e.g.,* starch) or (*ii*) the presence of protein moieties in their molecular structure (*e.g.,* gums, pectin and alginate) (Dickinson, 2009). In fact, GA has been reported to adsorb at the oil/water interface forming a thick layer surrounding the oil droplets and conferring great steric stability (up to 3 weeks) to flocculation and coalescence (Raikos et al., 2017). Moreover, Artiga-Artigas et al. (2018a) obtained submicron essential oil nanoemulsions with pectin concentrations above 1% (w/w) in the absence of other emulsifiers. Besides their activity as emulsifiers, they may provide a significant increase of the aqueous phase viscosity, minimizing oil droplets movement and thus providing additional colloidal stability to the O/W emulsion and nanoemulsion (Dickinson, 2009).

The origin (vegetal or animal) and molecular composition (fatty acids chain length or unsaturation) of the oils or fats used as lipid phase of O/W emulsion and nanoemulsion and consequently its physicochemical properties (density and water solubility) may also affect their physicochemical characteristics (see section 3.1.1), yet also their colloidal stability. Density differences between the lipid and the aqueous phases have a direct impact on O/W emulsion and nanoemulsion stability. When the density difference between the aqueous phase and the lipid phase is high, O/W emulsion and nanoemulsions tend to separate into a system that consists of a layer of oil (lower density) on top of a layer of water (higher density) (McClements, 2015). For instance, Meroni & Raikos (2017) have reported higher O/W nanoemulsion stability using corn oil, which has a density (0.9188 g/cm^3) closer to the aqueous phase density (~0.998 g/cm^3), than using orange oil (0.8423 g/cm^3) (Meroni & Raikos, 2017). Besides this, some lipids, such as EOs, present a relatively high-water solubility due to the presence of monoterpenes in their composition (Rao & McClements, 2012). These oils are highly prone to suffer Ostwald ripening, which leads to the diffusion of lipid material from small droplets into larger ones and consequently droplet size increases (Liang et al., 2012; Zhang, Zhang, Zhang, Decker, & McClements, 2015).

3.2 Water-in-oil-in-water (W$_1$/O/W$_2$) emulsions

W$_1$/O/W$_2$ emulsions consist of a water-in-oil (W$_1$/O) emulsion dispersed in an outer aqueous phase (Muschiolik & Dickinson, 2017). The use of W$_1$/O/W$_2$ emulsions presents important advantages over O/W emulsions and nanoemulsions due to their compartmentalized internal structure (Lamba, Sathish, & Sabikhi, 2015). On the one hand, they allow the encapsulation of both hydrophilic active ingredients in the inner water (W$_1$) droplets and lipophilic active compounds in the lipid core (Artiga-Artigas, Molet-Rodríguez, Salvia-Trujillo, & Martín-Belloso, 2018b). On the other hand, they can protect and release in a controlled manner the encapsulated compounds during GI digestion (Frank et al., 2012). As a consequence of their compartmentalized structure with water droplets inside the oil droplets, W$_1$/O/W$_2$ emulsions have been proposed to fabricate low-fat foods (Giroux et al., 2013). Nevertheless, the formation and stabilization of such emulsion-based delivery systems remain a challenge.

3.2.1 Formation

The formation of W$_1$/O/W$_2$ emulsions is generally achieved with a two-step emulsification procedure in which a W$_1$/O emulsion is first formed and subsequently dispersed in a continuous aqueous phase (Muschiolik & Dickinson, 2017). High shear rate devices including high-speed homogenizers, ultrasonicator, valve-homogenizer and microfluidizer, can be used for the W$_1$/O emulsion formation,

yet rendering to W_1 droplets with comparable sizes, ranging between 0.2 to 38.06 μm (Artiga-Artigas et al., 2018b). In a second emulsification step, the W_1/O emulsion is used as the dispersed phase that will be further dispersed in an outer aqueous phase to form the final $W_1/O/W_2$ emulsion. In general, devices used for preparing the primary W_1/O emulsion can be used in the second step, but under more moderate dispersing conditions so as to try to avoid over-processing, and consequently, destabilization of the previously formed W_1/O emulsion (Ghasemi, Darjani, Mazloomi, & Mozaffari, 2020; Jafari, Assadpoor, He, & Bhandari, 2008; Muschiolik & Dickinson, 2017). Ultrasonicator, valve-homogenizer and microfluidizer are generally more efficient at disrupting droplets than high-speed homogenizers in which the energy provided is generally dissipated (Choi, Choi, Lee, & Jo, 2020). Nevertheless, the smaller the W_1/O droplets, the more W_1 droplets get in contact with the interface, causing their coalescence (Schuch, Deiters, Henne, Köhler, & Schuchmann, 2013). For that reason, gentle high-speed homogenizers are often used for the dispersion of W_1/O into the outer aqueous phase, rendering to W_1/O droplet sizes typically between 5 and 50 µm and long-term stability (Artiga-Artigas et al., 2018b; Carrillo-Navas et al., 2012; Sapei, Naqvi, & Rousseau, 2012; Schuch et al., 2013).

3.2.2 Stabilization

Multiple instability mechanisms can occur during $W_1/O/W_2$ emulsion formation and storage (Fig. 3). Coalescence of the lipid droplets and/or inner water droplets, and the coalescence of the inner water droplets with the outer water phase, leads to water migration between both water phases (Dickinson, 2011). Also, inner water droplets may shrink or swell as a result of the water transfer between the inner and the outer aqueous phases (Yan & Pal, 2001). In this sense, it is recommended to balance the concentration of salt in both aqueous phases, since an excess or lack of salt in one of them may cause water migration, and ultimately the breakdown of $W_1/O/W_2$ emulsions structure (Artiga-Artigas et al., 2018b). In principle, in order to stabilize a $W_1/O/W_2$ emulsion, a lipophilic emulsifier is used for the stabilization of the inner water/oil interface. Polyglycerol polyricinoleate (PGPR) has been demonstrated to be highly effective as a W_1/O stabilizer, due to its ability to form small W_1 droplets, and because it forms a physical barrier around them preventing their coalescence (Artiga-Artigas et al., 2018b; Lamba et al., 2015).
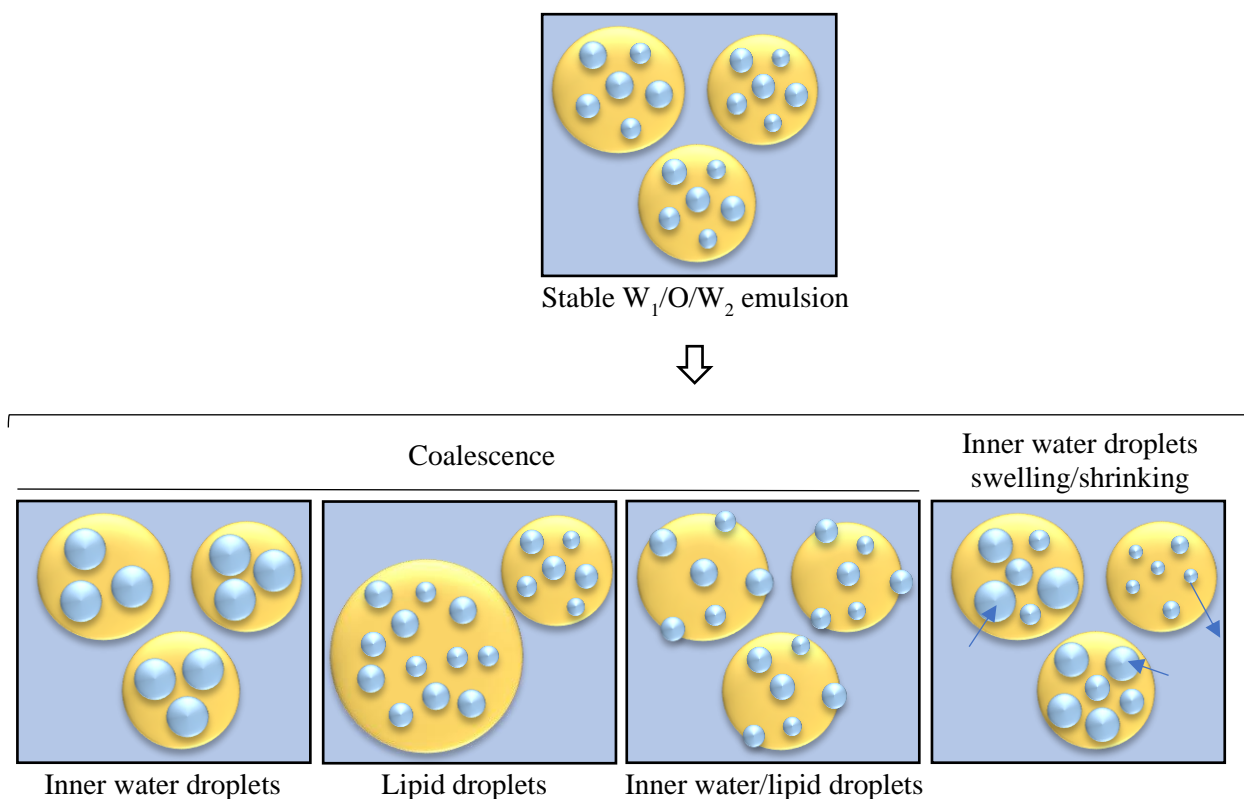
Figure 3. Instability mechanisms in $W_1/O/W_2$ emulsions.

To stabilize the second interface, it is necessary to use a hydrophilic emulsifier. In this case, it has been reported that small-molecule surfactant and protein can be effective stabilizers of the secondary oil/water interface (Lamba et al., 2015). Nevertheless, in $W_1/O/W_2$ emulsions, the lipid phase is filled with nanometric inner water droplets, implying that the size of the lipid droplets is typically larger than 1 μm, which in turn renders highly unstable emulsions (Mason et al., 2006). Therefore, strategies for improving the colloidal stability of $W_1/O/W_2$ emulsions are needed, which require modifying the properties of both the lipid and aqueous phases. On the one hand, the addition of biopolymers in the outer aqueous phase to increase its viscosity, can reduce the oil droplet mobility and subsequently the colloidal stability of $W_1/O/W_2$ emulsions may be enhanced (Carrillo-Navas et al., 2012; Teixé-Roig, Oms-Oliu, Velderrain-Rodríguez, Odriozola-Serrano, & Martín-Belloso, 2018). On the other hand, formulating solid, semi-solid or gelled lipid phases by using solid crystalline oils or fats, such as those containing high percentages of saturated triglycerides, has been proposed as a strategy to minimize the diffusion rates between the two aqueous phases. The most significant research studies that contributed to describing the colloidal stability of $W_1/O/W_2$ emulsions formulated with solid oils or fats as lipid phases are summarized in Table 3.

Table 3. Overview of studies that investigate the effect of solid, semi-solid or gelled lipid phases on the $W_1/O/W_2$ emulsions colloidal stability.

Inner aqueous phase	Lipid phase	Lipophilic Emulsifier	Outer aqueous phase	Colloidal stability	Reference
20% (w/w) sucrose	Soybean oil or hydrogenated soybean oil fat	5% (w/w) PGPR	10% (w/w) WPI, 1% v/v saponin, and 20% (w/w) sucrose	At 25°C, $W_1/O/W_2$ emulsion formulated with hydrogenated soybean oil fat (solid lipid phase) showed lower water migration under applied osmotic gradients compared to soybean oil (liquid lipid phase) At >60 °C, W_1/O droplets in the hydrogenated soybean oil fat-emulsions swelled due to fat melting	(Liu et al., 2020)
KCl 0.1 M, 0.02% (w/w) NaN$_3$	Soft palm mid fraction or high oleic sunflower oil	5% (w/w) PGPR	KCl 0.1 M, 0.02% (w/w) NaN$_3$, 1.25% (w/w) sodium caseinate, and 0.3% (w/w) xanthan gum	$W_1/O/W_2$ emulsion formulated with soft palm (solid lipid phase) showed lower water migration than with high oleic sunflower oil (liquid lipid phase) W_1/O globule size of $W_1/O/W_2$ emulsion formulated with soft palm remained stable under applied osmotic gradients	(Nelis et al., 2019)
Phosphate buffer (0.001 M, pH 6.8), NaCl 0.1 M, 0.2% (w/v) Vitamin B$_{12}$ and 0.02% (w/v) NaN$_3$	Butter oil	8% (w/w) PGPR	skim milk or NaCN dispersion (0.5%; pH 6.8; containing NaCl 0.1 M) preheated	$W_1/O/W_2$ emulsion formulated with butter oil (solid lipid phase) were very effective in preventing vitamin B$_{12}$ release during *in vitro* gastric digestion	(Giroux et al., 2013)
800 mM tetramethylammonium chloride, 1.25% (w/v) sodium caseinate and phosphate buffer 0.1M	Soft palm mid fraction or high oleic sunflower oil	2.5% (w/w) PGPR	0.2% (w/w) xanthan gum and 1.4% (w/w) Tween 80	$W_1/O/W_2$ emulsion formulated with soft palm mid fraction (solid lipid phase) presented lower water migration than with high oleic sunflower oil (liquid lipid phase)	(Vermeir et al., 2016)
5.84 g/L aqueous solution of NaCl and 0.03 g/100 mL riboflavin	Chia oil, sunflower oil, olive oil or rendered pork backfat	6% (w/w) PGPR	5.84 g/L NaCl and 0.5 g/100 mL sodium caseinate	$W_1/O/W_2$ emulsion with rendered pork backfat (solid lipid phase) stored at room temperature had encapsulated riboflavin more efficiently than using chia oil, sunflower oil, olive oil (liquid lipid phase)	(Bou, Cofrades, & Jiménez-Colmenero, 2014)

Polyglycerol polyricinoleate (PGPR); whey protein isolate (WPI)

Table 3. Overview of studies that investigate the effect of solid, semi-solid or gelled lipid phases on the $W_1/O/W_2$ emulsions colloidal stability *(Continuation)*.

Inner aqueous phase	Lipid phase	Lipophilic Emulsifier	Outer aqueous phase	Colloidal stability	Reference
$MgCl_2,6H_2O$ 0.1 M	Cocoa butter/miglyol oil, anhydrous milkfat, olein or stearin	2 or 5% (w/w) PGPR	3.1% Sodium caseinate, lactose 0.3 M, 0.08% NaN_3 and 0.5% xanthan	For $W_1/O/W_2$ emulsions formulated with cocoa butter/miglyol oil, the rate of magnesium release was gradually lowered by increasing the percentage of fat crystals, whereas with milk fat fractions, the rate of magnesium release was independent of the percentage of fat crystals	(Herzi & Essafi, 2018)
0.1 M NaCl aqueous solution	Pure olive oil or mixed with Verols (V10 or V50)	3 or 6% (w/w) PGPR	NaCl 0.1 M, 0.5% (w/v) sodium caseinate and 0.02% (w/w) NaN_3	Creaming of $W_1/O/W_2$ emulsions decreased with the addition of Verols to the lipid phase. V10 plus 3 or 6% PGPR formed crystalline $W_1/O/W_2$ emulsions with presence of lyotropic mesophases, which yielded W/O Pickering stabilization effects, whereas V50 produced essentially glassy matrices, thus impeding Pickering effects	(Fernández-Martín, Freire, Bou, Cofrades, & Jiménez-Colmenero, 2017)
1.6% (w/w) KCl and 0.01% (w/w) NaN_3	Mixture of 1.25% saturated monoglyceride and 2.5% tripalmitin	1% (w/w) PGPR	1% sodium caseinate, 0.01% NaN_3 and 4–16% glucose or 1–5% NaCl	$W_1/O/W_2$ emulsions formulated with a mixture of 1.25% saturated monoglyceride and 2.5% tripalmitin (solid lipid phase) did not present water migration even when subjected to osmotic pressure gradients	(Frasch-Melnik, Spyropoulos, & Norton, 2010)
0.3 g of Hydroxysafflor yellow A and Hydroxypropyl methylcellulose (150 mg, 15 mg, and 0 mg)	Caprylic/capric triglyceride and glyceryl monostearate	Labrafil M 1944 CS	1% (v/v) Tween 80	At 4 and 30 °C, $W_1/O/W_2$ emulsions formulated with caprylic/capric triglyceride and glyceryl monostearate (solid lipid phase) were relatively stable during 10 days, yet W_1/O droplet size increased at 60 °C	(Zhao et al., 2018)

Polyglycerol polyricinoleate (PGPR)

Gelation or solidification of the lipid phase, by using solid oils or fats, can help in reducing the molecular water exchange between the two aqueous phases of $W_1/O/W_2$ emulsions. For instance, Liu et al. (2020) found that the W_1/O droplets in soybean oil (liquid) $W_1/O/W_2$ emulsions swelled/shrank when the external sucrose concentration was below/above the internal concentration, whereas there was no change in the size of $W_1/O/W_2$ emulsions formulated with hydrogenated soybean oil, which is solid at room temperature. Nevertheless, two other main factors might be determining the effectiveness of gelling or solidifying the lipid phase in $W_1/O/W_2$ emulsions, being the distribution of oil or fat crystals within the lipid phase and their melting point. It has been stated that oil or fat crystals in W_1/O emulsions can locate in the bulk lipid phase forming a continuous fat network or in the water/oil interface forming a crystalline shell around droplets, as shown in Fig. 4, with the latter being more effective in stabilizing the W_1/O emulsion (Ghosh & Rousseau, 2011). Namely, research conducted by Herzi & Essafi (2018) evidenced that the retention of the inner water phase in $W_1/O/W_2$ emulsions formulated with mixtures of cocoa butter (located at the bulk lipid phase) and miglyol oil increased with the percentage of fat crystals, whereas for $W_1/O/W_2$ emulsions with milk fat fractions (located at the water/oil interface), the rate of magnesium release was independent of the percentage of fat crystals. Therefore, the surface-active properties of the oil or fat crystals determine their location in the lipid phase, and consequently their ability to avoid inner water migration.
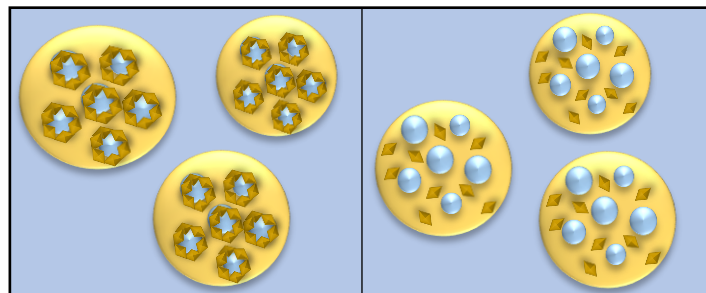
Figure 4. $W_1/O/W_2$ emulsions with solid lipid phase. Lipid crystals in W_1/O emulsions located at the oil/water interface forming a crystalline shell around droplets (left panel) or in the bulk lipid phase forming a continuous fat network (right panel).

Apart from that, W_1/O droplets in the $W_1/O/W_2$ emulsions formulated with gelled lipid phase can swell/shrank appreciably when the temperature is raised, which is indicative of water exchange between the aqueous phases (Liu et al., 2020; Zhao et al., 2018). This phenomenon can be attributed to the melting of the oil or fat crystals in the lipid phase,

which would behave as a liquid lipid phase, thereby reducing $W_1/O/W_2$ emulsion stability. The use of crystallization agents (oleogelators) can also allow the conversion of liquid oils into fat-like lipids, which could be an alternative to saturated fats or oils. For instance, mono-glycerides are amphiphilic molecules that are located at the oil/water interface forming a crystal shell (Abreu-Martins, Artiga-Artigas, Hilsdorf Piccoli, Martín-Belloso, & Salvia-Trujillo, 2020). In this sense, Fernández-Martín et al. (2017) have demonstrated the ability of $W_1/O/W_2$ emulsions with solid lipid phase based on olive oil and a mixture of mono- and diglycerides, to reduce creaming of the W_1/O globules. In addition, Zhao et al. (2018) have reported the formation of stable $W_1/O/W_2$ emulsions with a solid lipid phase consisting of MCT oil mixed with glyceryl stearate (GS). Nevertheless, in the latter study, authors have also used a gelling hydrophilic surfactant, which, as mentioned earlier, can diminish the water migration in $W_1/O/W_2$ emulsions. Thus, there is a need for information regarding the use of monoglycerides to crystalize liquid oils and their potential use to stabilize $W_1/O/W_2$ emulsions, in absence of gelling hydrophilic surfactant.

4 Emulsion-based delivery systems functionality

4.1 Antimicrobial activity

The antimicrobial activity of EOs relies on their lipophilic nature, which allows them to partition in the lipids of the microbial cell membrane and mitochondria, altering their structure and making them more permeable (Lambert, Skandamis, Coote, & Nychas, 2001; Oussalah, Phane, & Lacroix, 2006). As a consequence, the leakage of the cellular content occurs, causing the viability loss of microbial cells (Helander et al., 1998). Encapsulation of EOs into O/W nanoemulsions has been extensively reported to enhance their antimicrobial activity against food-borne microorganisms (Donsì, & Ferrari, 2016). Although the exact mechanisms of action of EO-O/W nanoemulsions are still unclear, different theories regarding the way in which they promote the interaction between EOs and the cell membranes of microorganisms have been proposed (Donsì, & Ferrari, 2016). Firstly, due to their small oil droplets and large surface-area, O/W nanoemulsions favour the contact between the EO and the bacterial cell membrane as well as oil droplets are effectively transported through the porin protein of the outer membrane of the bacteria, enabling the delivery of EOs. In this context, Salvia-Trujillo et al., (2014) have observed that an LEO-O/W emulsion reduced the *E. coli* population up to 5.85 log-units after 30 min of contact time, whereas the O/W nanoemulsion achieved 7.07 log-

reductions. Secondly, the fusion of the emulsified oil droplets with the phospholipid bilayer of the cell membrane likely promotes the release of the EOs at the desired sites. Lastly, EOs partition between the oil droplets and the aqueous phase prolongs their antimicrobial activity. Apart from that, the bacterial killing performance of EOs-O/W nanoemulsions has been reported to be dependent on the chemical composition of each EO, being aldehyde compounds (*e.g.,* cinnamaldehyde, citral, citronellal) and phenolic compounds (*e.g.,* carvacrol, eugenol, and thymol) the ones with higher antimicrobial activity due to their strong interactions with the lipids of the cell membrane (Salvia-Trujillo et al., 2015). It is also known that the membrane permeability and cellular absorption depend on the surfactant used in the formulation of O/W nanoemulsions since the charge of the oil droplets is known to influence its electrostatic interaction with the microbial cell wall (Donsì, Annunziata, Vincensi, & Ferrari, 2012). Moreover, gram-negative and gram-positive bacteria have been shown to present different resistance against EOs-O/W nanoemulsions, due to differences in the cell wall composition and thickness (Guerra-Rosas, Morales-Castro, Cubero-Márquez, Salvia-Trujillo, & Martín-Belloso, 2017).

O/W nanoemulsions enable disperse the EOs in aqueous phases at a higher concentration than their water solubility, thus being good candidates to enhance the antimicrobial activity of EOs into water-based food products. So far, only a limited number of studies has addressed the application of EOs-O/W nanoemulsions in fruit juices (Donsì & Ferrari, 2016). These studies have shown a significant extension of fruit juice's shelf life by the antimicrobial action of EOs-O/W nanoemulsions. For instance, Ghosh, Mukherjee, & Chandrasekaran (2014) have observed that eugenol-O/W nanoemulsions exhibited better preservation of orange juice against *Staphylococcus aureus* spoilage than the same concentration of sodium benzoate, a synthetic preservative extensively used in the food industry. Nevertheless, other authors have observed that the antimicrobial activity of EOs-O/W nanoemulsions has a certain dependence on the juice matrix and microorganism species (Donsì & Ferrari, 2016; Jo et al., 2015). In general, these studies evidence the potential advantages of using EOs-O/W nanoemulsions as preservatives in fruit juice, but further studies regarding their effectivity against other microorganisms and in other fruit juices would be needed in order to fully understand their bacterial killing mechanism in complex food matrices.

4.2   Lipid digestibility and bioactive compound bioaccessibility

Emulsion-based delivery systems need to be specifically designed to control the lipid digestion and active compound release and absorption within the GI tract (Li, Kim, Park, & McClements, 2012). In this regard, *in vitro* digestion models have been used for decades to simulate *in vivo* digestion by mimicking the physiological conditions of the upper GI tract, being the oral, gastric and small intestinal phases (Bohn et al., 2018; Li et al., 2012). In general, static models takes into account the presence of digestive enzymes and their concentrations, pH, digestion time, and salt concentrations, among other factors (Brodkorb et al., 2019; Minekus et al., 2014). Figure 5 shows a representation of the human gastrointestinal tract and the *in vitro* conditions in oral, gastric and small intestinal phases.

Oral
pH: 5-7
Time: 5-120 s
Salts, mucins, α-amylase
High shear

Gastric
pH: 1-3
Time: 30 min-4 h
Salts, pepsin, gastric lipase
Low shear

Small intestine
pH: 6-7.5
Time: 1-2 h
Salts, bile, pancreatin
Moderate shear
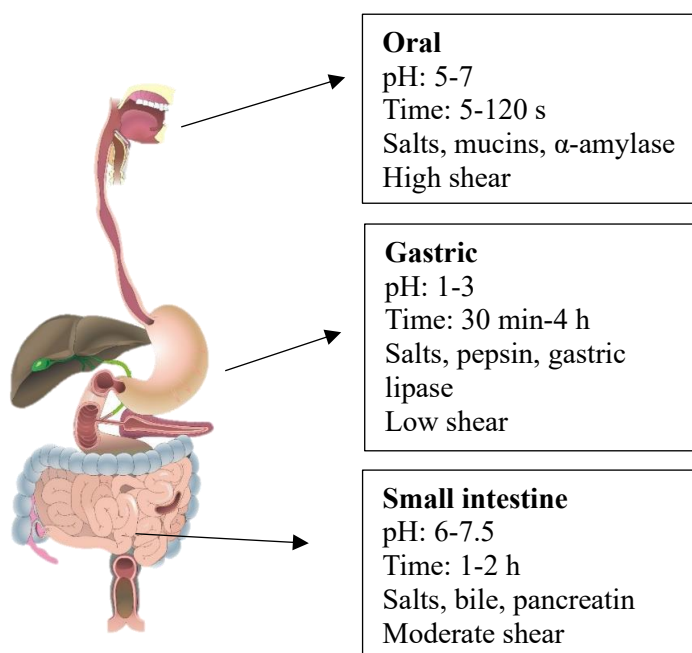
Figure 5. Schematic representation of the human digestive apparatus and *in vitro* gastrointestinal conditions along oral, gastric and small intestinal phases. The image is taken from the database of the Spanish Ministry of Education (http://recursostic.educacion.es/bancoimagenes/web/).

Emulsions may undergo physical alteration when they are subjected to an *in vitro* GI digestion process, since pH, ionic strength and temperature conditions may compromise their colloidal stability and consequently, lipid digestibility (Frank et al., 2012). The *in vitro* digestion process starts with the oral phase, where starch hydrolysis takes place by the action of α-amylase. In addition, salivary salts are secreted, which alters the ionic strength of the medium and can compromise the colloidal stability of emulsions. In the gastric phase, the emulsion is gradually mixed, acidified and digested with gastric fluids, acids, salts and enzymes. The colloidal stability of the lipid droplets within the gastric phase depended strongly on emulsifier type, *e.g.*, the lipid droplets stabilized by sodium caseinate and sucrose palmitate were highly susceptible to aggregation, whereas those stabilized by Tween 20 and lecithin were relatively stable (Gasa-Falcon et al., 2019). Proteolysis and partial lipolysis (~ 25%) are performed in the gastric phase by the action of pepsin and gastric lipase, respectively. In the small intestine, lipolysis is performed by the action of pancreatic lipase present in the intestinal fluids.

It has been found that the characteristics of the emulsion-based delivery system, such as the droplet size, lipid type and state as well as surfactant type, may influence the lipid digestibility rate and end-point. Firstly, smaller droplets have been reported to be digested faster and to a higher extent than bigger ones (Salvia-Trujillo et al., 2013a). This is due to the increased oil surface area available for enzymatic digestion. Secondly, the chain length of the lipid triglyceride may influence the rate of the *in vitro* lipid digestibility on the small intestine (Salvia-Trujillo et al., 2013b). For instance, SCT and MCT have been observed to be digested faster and to a higher extent in comparison with LCT. This has been attributed to the ability of SCT and MCT to migrate to the aqueous phase, whereas LCT would remain at the oil/water interface, hindering the action of lipase (Ahmed, Li, McClements, & Xiao, 2012; Li, Hu & McClements, 2011). Thirdly, pancreatin has stereospecificity for positions 1 and 3 of the triglycerides, thus the lipid digestion might depend on the glyceride chain organization within the triglyceride (Karupaiah & Sundram, 2007). Lastly, it has also been suggested that solid lipids could retard the initiation of lipolysis (Abreu-Martins et al., 2020). As the lipolysis takes place, free fatty acids and monoglycerides are generated and accumulated at the oil surface. Bile salts are responsible for removing these digestion products from the oil surface and solubilizing them in mixed micelles, thus facilitating the complete lipid digestion and bioactive compound absorption (Malaki Nik, Wright, & Corredig, 2011; Maldonado-Valderrama,

Wilde, Macierzanka, & Mackie, 2011). In this sense, it has been observed that LCT can better accommodate lipophilic compounds than MCT, due to their higher non-polar structure, enhancing their bioaccessibility.

Despite the utility of *in vitro* static models for understanding trends, they can not assess some of the important dynamic processes occurring during GI digestion. These processes are namely the gradual addition of acid, enzymes and gastric fluids, as well as continuous gastric emptying (Egger et al., 2017). In this sense, a recently developed semi-dynamic *in vitro* model has been reported in order to understand the behaviour of several food structures within the GI tract (Mulet-Cabero et al., 2020a). Mulet-Cabero et al. (2020b) reported that the emptying rate of the emulsions from the stomach could be affected by several parameters, such as droplet size, viscosity and colloidal stability. Nevertheless, there is limited information on the behaviour of emulsions when co-digested with food products using either the static or the semi-dynamic *in vitro* digestion models.

5 Complex food matrix composition and physicochemical properties

The incorporation of emulsion-based delivery systems carrying active compounds into complex food products represents a challenge, since it may compromise the emulsion physicochemical properties, colloidal stability and functionality. Foods are generally composed of protein, fats and carbohydrates, which can interact with lipid droplets compromising their physicochemical characteristics, colloidal stability and functionality. Nevertheless, foods are more than just the sum of macromolecular components, they form part of a complex structure, known as the food matrix, which physicochemical properties depend on macromolecular properties (composition and organization), but also matrix characteristics (physical state and pH). For that reason, understanding the emulsion-based delivery systems behaviour when incorporated into different food matrices containing protein, fat and carbohydrates is of relevance. Thus, in this doctoral thesis, the selected food products were clear fruit juices from concentrate, dairy products and oatmeal-based products. The food matrix composition and its physicochemical properties were summarized below in order to understand their possible implications on the colloidal stability and functionality of emulsion-based delivery systems.

5.1 Clear fruit juice-based beverage

Clear fruit juices from concentrate are of great importance within the food industry as they are non-alcoholic beverages able to fulfil several consumer needs because of their clear appearance, freshness, tastiness and easy storage and distribution. Their production process consists of clarification, concentration and reconstitution of the fresh juice. Clarified (clear) juices are obtained by technological processing (*i.e.,* ultrafiltration) of pressurized and pasteurized fruit juices, which results in a water solution of soluble solids (sugars, organic acids, salts, free amino acids, water-soluble vitamins, pigments, etc.) with particle sizes under 0.001 µm. Then, a clear-concentrated juice is obtained through the extraction of water from the clear juice, which leads to an increase of the percentage of soluble solids above 50 ᵒBrix. Finally, the clear-concentrated fruit juice is reconstituted with water to meet the minimum soluble solids concentration laid down in the regulation for clear fruit juices from concentrate (CODEX STAN 247-2005 and RD 781/2013). Thus, the final fruit juice is mostly composed of water and simple carbohydrates such as fructose, glucose and sucrose, which are found dissolved in water. In addition, in a lesser concentration, it can also contain active compounds and minerals, which impairs it with biological, physical and chemical properties. Firstly, active compounds, such as vitamins and polyphenols are well-known to have antioxidant properties (Maragò et al., 2015; Suárez-Jacobo et al., 2011). Secondly, polyphenols have also been reported to present surface-active properties (Di Mattia, Sacchetti, & Pittia, 2011). Lastly, the presence of minerals, which are cations ionized in water, might change the ionic strength of aqueous solutions (Teo et al., 2016).

5.2 Dairy products

5.2.1 Milk

Milk is an important element of the human diet as a natural source of bioactive peptides and fat-soluble vitamins, which are considered beneficial for human health (Nagpal et al., 2011). Its composition varies depending on mammalian species, genetic variations, age, lactation stage, diet, habitat, climate and storage conditions (Park, Juárez, Ramos, & Haenlein, 2007; Pereira, 2014). The most commonly consumed milk is bovine milk, which on average contains 87% water, 4-5% lactose, 3-4% fat, 3% of protein and 0.9% minerals and vitamins. The predominant carbohydrate in milk is lactose, which is a disaccharide comprised of glucose and galactose, and oligosaccharides are also present

in minor percentages. Milk fat is mostly composed of triacylglycerols (98%) and the remainder diacylglycerols, phospholipids, sterols (Nagpal et al., 2011). Triacylglycerols have a complex composition, which mostly contains long-chain fatty acids, yet it also contains a significant proportion (37%) of medium- and short-chain fatty acids (Park et al., 2007). Over 70% of the fatty acids in milk are saturated and a very small amount is unsaturated fatty acids (*e.g.*, $C_{18:1}$). The protein in milk is classified into two main groups, whey protein and caseins, which have been reported to have surface-active properties due to their amphiphilic structure (Dickinson, 2001; Luo et al., 2014). Nevertheless, they present differences in their molecular structure and pH-solubility characteristics. On the one hand, there are four different casein protein (αs1-, αs2-, β- and κ-casein), which have predominantly flexible structures and are insoluble near their isoelectric point, around pH 4.5-4.8 (Francis, Glover, Yu, Povey, & Holmes, 2019). They assemble as colloidal particles having a diameter of ~50-500 nm, called casein micelles, which are responsible for the turbid appearance of milk. Their structure is still a subject of discussion, but it is generally accepted that the micelle structure contains colloidal calcium phosphate and that κ-casein is responsible for the micelle stability against aggregation (Fox & Brodkorb, 2008). Briefly, at milk pH, the C-terminal chain of κ-casein acts as a steric barrier and/or the negative surface potential cause electrostatic repulsion. On the other hand, whey protein is a complex mixture of globular protein molecules comprising β-lactoglobulin, α-lactalbumin, bovine serum albumin, and immunoglobulins that are relatively soluble near their isoelectric point (pH 5.2) (Vasbinder, Alting, & De Kruif, 2003). In addition, they are rich in sulfur-containing amino acids that, within the protein complex structure, can be either forming disulfide bonds (-S-S-) or free sulfhydryl groups (-SH), but hidden inside their native form. Upon temperature increase (> 70 °C), whey protein denature, expose the free -SH residue, which can result in auto-aggregation or interaction with other milk protein molecules such as κ-casein, through sulphydryl–disulphide bonds (Law & Leaver, 2000; Vasbinder et al., 2003). Milk also contains a variety of organic and inorganic minerals, such as chlorides, phosphates, citrates, and bicarbonates of sodium, potassium, chloride, and magnesium that may be present as free ions or forming complexes (Haug, Høstmark, & Harstad, 2007). In particular, many of the multivalent minerals are incorporated within the casein micelles, avoiding electrostatic interactions and consequently, droplet flocculation.

The microstructure of milk naturally exhibits an O/W emulsion that consists of native fat globules of 3-5 µm homogeneously dispersed in an aqueous phase with numerous constituents, including protein, sugars, vitamins and minerals (Luo et al., 2014). Commercial milk is conventionally heat-treated and homogenized to improve consumer acceptance, ensure microbial stability and shelf life. This process results in size reduction of their native fat globules from 3-5 µm to below 1 µm (Sharma & Dalgleish, 1993). The fat globule interface is covered predominantly by surface-active protein adsorbed from the aqueous phase, that is, casein and whey protein isolate, and phospholipids and various other types of polar lipid and glycoprotein are also present in lower amounts, for example, diacylglycerols, monoacylglycerols, and free fatty acids (Fig. 6).
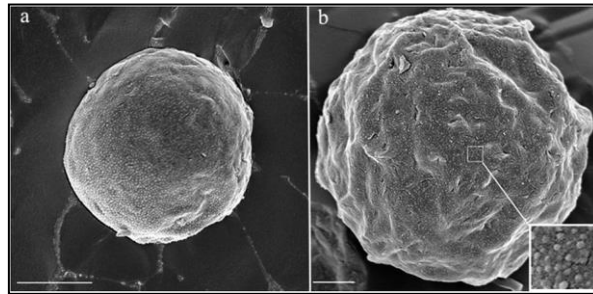
Figure 6. Cryo-SEM image of native milk fat globules (a) native fat globules (diameter 4.5 µm), Scale bar: 2 µm; (b) native fat globules (diameter 6.5 µm) with boxed area magnified by 10-fold, Scale bar: 1 µm. The image is taken from Luo et al. (2014).

5.2.2 Yogurt

Milk is used as raw material to obtain a wide variety of common dairy food products, including ice cream, cheese, butter and yogurt. In the process of yogurt production, milk lactose is fermented into lactic acid by the action of *Lactobacillus* and *Streptococcus* bacteria. It preserves the microstructure of milk in which the fat globules are dispersed in an aqueous phase. Nevertheless, yogurt presents a semi-solid aqueous phase due to the fermentation process (Fig. 7). The lactic acid production makes the milk more acidic (pH 4.6), which leads to casein aggregation (Hassan, Frank, Farmer, Schmidt, & Shalabi, 1995). In addition, yogurt production also causes the thermal denaturation of globular whey protein and subsequently their interaction with κ-caseins. Therefore, both the casein aggregates and denatured whey protein-casein complexes form a three-dimensional network responsible for the yogurt semi-solid texture.
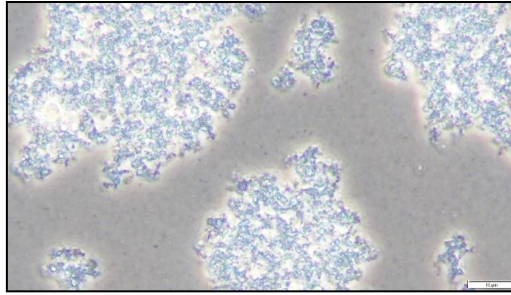
Figure 7. Phase contrast microscopic image of the three-dimensional network of protein in yogurt matrix. Scale bar: 10 μm. Adapted from chapter II of this doctoral thesis.

5.3   Oatmeal-based products

Oat *(Avena sativa L.)* consumption has been associated with the reduction of postprandial glycaemia and plasma lipoprotein-cholesterol, having a positive effect in reducing the incidence of cardiovascular diseases and diabetes (Daou & Zhang, 2012; Thongoun et al., 2013). Their health-enhancing properties have been attributed to their structure rich in starch and β-glucan (Wang & Ellis, 2014). Oat grain structure consists of three tissues (bran, endosperm and germ), where the nutrients are distributed (Grundy, Fardet, Tosh, Rich, & Wilde, 2018) (Fig. 8).
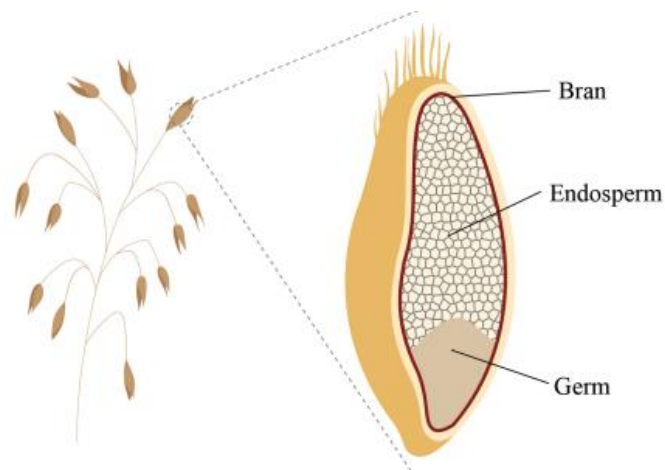
Figure 8. Structure of oat grain.

The chemical composition of oat grain is characterized by the high content of polysaccharides (66–76%), including starch and dietary fibre, and in minor proportion simple sugars. Starch is located in the endosperm, organized in concentric alternating semi-crystalline and amorphous layers in granules of various sizes. It is formed by two water-insoluble homoglucans, amylose (~ 25%) and amylopectin (~ 75%) linked via

intermolecular bonds, being the latter the responsible for the granular semicrystalline structure of starch (Schirmer, Höchstötter, Jekle, Arendt, & Becker, 2013). Starch is the only complex carbohydrate in whole grains that can be digested due to the presence of α-amylase in the human digestive system (Yu, Tao, & Gilbert, 2018). The rate of starch hydrolysis has been reported to modulate postprandial glycaemia (Holm, Lundquist, Bjorck, Eliasson, & Asp, 1988). Some factors can influence the rate and extent of starch digestibility. Firstly, the enzymatic attack by α-amylase is facilitated for smaller starch granules, since their specific surface-area is larger (Qi & Tester, 2016). Secondly, starch gelatinization and loss of crystallinity make the starch granule more susceptible to enzymatic attack (Holm et al., 1988). The extent of the gelatinization process of starch has been reported to depend on the size of the granule and the rate of amylose/amylopectin (Regina et al., 2012). This latter can be explained by the ability of amylose to form complexes with lipids and protein present in the endosperm, which may influence swelling by increasing the hydrophobicity (Chung, Liu, & Hoover, 2009). Lastly, the presence of dietary fibre may reduce starch digestibility by limiting water availability as a consequence of their hydration which, in turn, restricts starch gelatinization (Regand, Chowdhury, Tosh, Wolever, & Wood, 2011). Dietary fibre is a primary constituent of the cell walls and can be subdivided into water-soluble and water-insoluble. Water-soluble fibre is composed of polysaccharides, such as β-glucan (Knudsen, 2014; Roye et al., 2020). They are able to absorb water and form highly viscous solutions, which has been reported to delay nutrient gastric emptying from the stomach to the duodenum and consequently their absorption by the small intestine (Mackie, Rafiee, Malcolm, Salt, & van Aken, 2013). As a consequence, viscous water-soluble fibre may help in lowering serum cholesterol, postprandial blood glucose, and insulin levels. Water-insoluble fibre contains lignin, which is a lipophilic phenolic polymer that may be covalently linked to polysaccharides in the bran, making it very rigid and difficult to degrade by the microorganisms in the large intestine (Manthey, Hareland, & Huseby, 1999).

Protein is distributed over the whole grain with a concentration of approximately 15 to 20% (Mäkinen, Sozer, Ercili-Cura, & Poutanen, 2016). In particular, protein in the endosperm forms a dense network entrapping starch granules and therefore acting as a physical barrier to starch digestion by reducing contact between α-amylase and starch (Autio & Salmenkallio-Marttila, 2001; Rahimi et al., 2020).

Oats contain comparatively high amounts of lipid compared with other cereal species, with values between 5.6 and 8.8% (Rahimi et al., 2020). Unsaturated triglycerides with a fatty acid composition rich in linoleic, oleic and in minor proportion saturated palmitic acids are the predominant lipid class in oats (Brindzová et al., 2008).

6   Concluding remarks

In the last decades, the key variables concerning the formulation and stabilization of emulsion-based delivery systems for the delivery of active compounds (*i.e.,* EO antimicrobials and bioactive compounds) with functional properties into food products have been studied in detail. The functionality of EOs and bioactive compounds can be modulated by controlling the factors affecting the physicochemical properties, colloidal stability and functionality of emulsion-based delivery systems. In addition, it is of vital importance to choose the most suitable formulation taking into account the active compound and desired functionality of the final food product. However, there is still scarce scientific evidence about the behaviour of emulsion-based delivery systems in terms of physicochemical properties, colloidal stability and functionality once incorporated into food matrices and their subsequent behaviour during food storage and *in vitro* gastrointestinal digestion. Therefore, further investigations regarding the functionality of emulsion-based delivery systems with active compounds once incorporated into foods need to be carried out in order to provide a more comprehensive understanding of their real benefits.

7   References

Abbas, S., Hayat, K., Karangwa, E., Bashari, M., & Zhang, X. (2013). An Overview of Ultrasound-Assisted Food-Grade Nanoemulsions. *Food Engineering Reviews*, *5*(3), 139–157.

Abreu-Martins, H., Artiga-Artigas, M., Hilsdorf Piccoli, R., Martín-Belloso, O., & Salvia-Trujillo, L. (2020). The lipid type affects the in vitro digestibility and β-carotene bioaccessibility of liquid or solid lipid nanoparticles. *Food Chemistry*, *311*, 126024.

Acosta, E. (2009). Bioavailability of nanoparticles in nutrient and nutraceutical delivery. *Current Opinion in Colloid and Interface Science*, *14*(1), 3–15.

Adorjan, B., & Buchbauer, G. (2010). Biological properties of essential oils: An updated review. *Flavour and Fragrance Journal*, *25*(6), 407–426.

Aguilera, J. M. (2019). The food matrix: implications in processing, nutrition and health. *Critical Reviews in Food Science and Nutrition*, *59*(22), 3612–3629.

Ahmed, K., Li, Y., McClements, D. J., & Xiao, H. (2012). Nanoemulsion- and emulsion-based delivery systems for curcumin: Encapsulation and release properties. *Food Chemistry*, *132*(2), 799–807.

Artiga-Artigas, M., Guerra-Rosas, M. I. I., Morales-Castro, J., Salvia-Trujillo, L., & Martín-Belloso, O. (2018a). Influence of essential oils and pectin on nanoemulsion formulation: A ternary phase experimental approach. *Food Hydrocolloids*, *81*, 209–219.

Artiga-Artigas, M., Molet-Rodríguez, A., Salvia-Trujillo, L., & Martín-Belloso, O. (2018b). Formation of Double (W1/O/W2) Emulsions as Carriers of Hydrophilic and Lipophilic Active Compounds. *Food and Bioprocess Technology*, *12,* 422–435.

Artiga-Artigas, M., Lanjari-Pérez, Y., & Martín-Belloso, O. (2018c). Curcumin-loaded nanoemulsions stability as affected by the nature and concentration of surfactant. *Food Chemistry*, *266*, 466–474.

Autio, K., & Salmenkallio-Marttila, M. (2001). Light Microscopic Investigations of Cereal Grains, Doughs and Breads. *LWT - Food Science and Technology*, *34*(1), 18–22.

Bohn, T., Carriere, F., Day, L., Deglaire, A., Egger, L., Freitas, D., … Dupont, D. (2018). Correlation between in vitro and in vivo data on food digestion. What can we predict with static in vitro digestion models. *Critical Reviews in Food Science and Nutrition*, *58*(13), 2239–2261.

Boon, C. S., McClements, D. J., Weiss, J., & Decker, E. A. (2010). Factors influencing the chemical stability of carotenoids in foods. *Critical Reviews in Food Science and Nutrition*, *50*(6), 515–532.

Bou, R., Cofrades, S., & Jiménez-Colmenero, F. (2014). Physicochemical properties and riboflavin encapsulation in double emulsions with different lipid sources. *LWT - Food Science and Technology*, *59*(2P1), 621–628.

Brindzová, L., Čertík, M., Rapta, P., Zalibera, M., Mikulajová, A., & Takácsová, M. (2008). Antioxidant activity, β-glucan and lipid contents of oat varieties. *Czech Journal of Food Sciences, 26*(3), 163–173.

Brodkorb, A., Egger, L., Alminger, M., Alvito, P., Assunção, R., Ballance, S., … Recio, I. (2019). INFOGEST static in vitro simulation of gastrointestinal food digestion. *Nature Protocols*, *14*(4), 991–1014.

Burt, S. (2004). Essential oils: their antibacterial properties and potential applications in foods—a review. *International Journal of Food Microbiology*, *94*(3), 223–253.

Cai, Y., Sun, M., & Corke, H. (2003). Antioxidant activity of betalains from plants of the Amaranthaceae. *Journal of Agricultural and Food Chemistry*, *51*(8), 2288–2294.

Carrillo-Navas, H., Cruz-Olivares, J., Varela-Guerrero, V., Alamilla-Beltrán, L., Vernon-Carter, E. J., & Pérez-Alonso, C. (2012). Rheological properties of a double emulsion nutraceutical system incorporating chia essential oil and ascorbic acid stabilized by carbohydrate polymer-protein blends. *Carbohydrate Polymers*, *87*(2), 1231–1235.

Chang, Y., & McClements, D. J. (2016). Influence of emulsifier type on the in vitro digestion of fish oil-in-water emulsions in the presence of an anionic marine polysaccharide (fucoidan): Caseinate, whey protein, lecithin, or Tween 80. *Food Hydrocolloids*, *61*, 92–101.

Choi, M. J., Choi, D., Lee, J., & Jo, Y. J. (2020). Encapsulation of a bioactive peptide in a formulation of W1/O/W2-type double emulsions: Formation and stability. *Food Structure*, *25*, 100145.

Chung, H. J., Liu, Q., & Hoover, R. (2009). Impact of annealing and heat-moisture treatment on rapidly digestible, slowly digestible and resistant starch levels in native and gelatinized corn, pea and lentil starches. *Carbohydrate Polymers*, *75*(3), 436–447.

Cicero, A. F. G., Fogacci, F., & Colletti, A. (2017). Potential role of bioactive peptides in prevention and treatment of chronic diseases: a narrative review. *British Journal of Pharmacology*, *174*(11), 1378–1394.

Cornacchia, L., & Roos, Y. H. (2011). Stability of β-carotene in protein-stabilized oil-in-water delivery systems. *Journal of Agricultural and Food Chemistry*, *59*(13), 7013–7020.

Costell, E., Tárrega, A., & Bayarri, S. (2010). Food acceptance: The role of consumer perception and attitudes. *Chemosensory Perception*, *3*(1), 42–50.

Das, L., Bhaumik, E., Raychaudhuri, U., & Chakraborty, R. (2012). Role of nutraceuticals in human health. *Journal of Food Science and Technology*, *49*(2), 173–183.

Daou, C., & Zhang, H. (2012). Oat Beta-Glucan: Its Role in Health Promotion and Prevention of Diseases. *Comprehensive Reviews in Food Science and Food Safety, 11*(4), 355–365.

Di Mattia, C. D., Sacchetti, G., & Pittia, P. (2011). Interfacial Behavior and Antioxidant Efficiency of Olive Phenolic Compounds in O/W Olive oil Emulsions as Affected by Surface Active Agent Type. *Food Biophysics*, *6*(2), 295–302.

Dickinson, E. (2011). Double Emulsions Stabilized by Food Biopolymers. *Food Biophysics*, *6*(1), 1–11.

Dickinson, E. (2001). Milk protein adsorbed layers and the relationship to emulsion stability and rheology. *Studies in Surface Science and Catalysis*, *132*, 973–978.

Dickinson, E. (2009). Hydrocolloids as emulsifiers and emulsion stabilizers. *Food Hydrocolloids*, *23*(6), 1473–1482.

Dima, C., & Dima, S. (2015). Essential oils in foods: Extraction, stabilization, and toxicity. *Current Opinion in Food Science*, *5*, 29–35.

Donsì, F., Annunziata, M., Sessa, M., & Ferrari, G. (2011). Nanoencapsulation of essential oils to enhance their antimicrobial activity in foods. *LWT - Food Science and Technology*, *44*(9), 1908–1914.

Donsì, F., Annunziata, M., Vincensi, M., & Ferrari, G. (2012). Design of nanoemulsion-based delivery systems of natural antimicrobials: Effect of the emulsifier. *Journal of Biotechnology*, *159*(4), 342–350.

Donsì, F., & Ferrari, G. (2016). Essential oil nanoemulsions as antimicrobial agents in food. *Journal of Biotechnology*, *233*, 106–120.

Egger, L., Schlegel, P., Baumann, C., Stoffers, H., Guggisberg, D., Brügger, C., … Portmann, R. (2017). Physiological comparability of the harmonized INFOGEST in vitro digestion method to in vivo pig digestion. *Food Research International*, *102*, 567–574.

Espina, L., García-Gonzalo, D., & Pagán, R. (2014). Impact of essential oils on the taste acceptance of tomato juice, vegetable soup, or poultry burgers. *Journal of Food Science*, *79*(8), 1575–1583.

Espina, L., Somolinos, M., Lorán, S., Conchello, P., García, D., & Pagán, R. (2011). Chemical composition of commercial citrus fruit essential oils and evaluation of their antimicrobial activity acting alone or in combined processes. *Food Control*, *22*(6), 896–902.

Estruch, R., Ros, E., Salas-Salvadó, J., Covas, M.-I., Corella, D., Arós, F., … Martínez-González, M. A. (2013). Primary Prevention of Cardiovascular Disease with a Mediterranean Diet. *New England Journal of Medicine*, *368*(14), 1279–1290.

Fernández-Martín, F., Freire, M., Bou, R., Cofrades, S., & Jiménez-Colmenero, F. (2017). Olive oil based edible W/O/W emulsions stability as affected by addition of some acylglycerides. *Journal of Food Engineering*, *196*, 18–26.

Ferruzzi, M. G., & Blakeslee, J. (2007). Digestion, absorption, and cancer preventative activity of dietary chlorophyll derivatives. *Nutrition Research*, *27*(1), 1–12.

Ferruzzi, M. G., & Schwartz, S. J. (2005). Thermal degradation of commercial grade sodium copper chlorophyllin. *Journal of Agricultural and Food Chemistry*, *53*(18), 7098–7102.

Fox, P. F., & Brodkorb, A. (2008). The casein micelle: Historical aspects, current concepts and significance. *International Dairy Journal*, *18*(7), 677–684.

Francis, M. J., Glover, Z. J., Yu, Q., Povey, M. J., & Holmes, M. J. (2019). Acoustic characterisation of pH dependant reversible micellar casein aggregation. *Colloids and Surfaces A: Physicochemical and Engineering Aspects*, *568*, 259–265.

Frank, K., Walz, E., Gräf, V., Greiner, R., Köhler, K., & Schuchmann, H. P. (2012). Stability of Anthocyanin-Rich W/O/W-Emulsions Designed for Intestinal Release in Gastrointestinal Environment. *Journal of Food Science*, *77*(12), N50-7.

Frasch-Melnik, S., Spyropoulos, F., & Norton, I. T. (2010). *W1/O/W2 double emulsions stabilised by fat crystals – Formulation , stability and salt release*. *350*(1), 178–185.

Gao, B., Luo, Y., Lu, W., Liu, J., Zhang, Y., & Yu, L. (2017). Triacylglycerol compositions of sunflower, corn and soybean oils examined with supercritical CO2 ultra-performance convergence chromatography combined with quadrupole time-of-flight mass spectrometry. *Food Chemistry*, *218*, 569–574.

Gasa-Falcon, A., Odriozola-Serrano, I., Oms-Oliu, G., & Martín-Belloso, O. (2019). Impact of emulsifier nature and concentration on the stability of β-carotene enriched nanoemulsions during: In vitro digestion. *Food and Function*, *10*(2), 713–722.

Ghasemi, H., Darjani, S., Mazloomi, H., & Mozaffari, S. (2020). Preparation of stable multiple emulsions using food-grade emulsifiers: evaluating the effects of emulsifier concentration, W/O phase ratio, and emulsification process. *SN Applied Sciences*, *2*(12), 1–9.

Ghosh, S., & Rousseau, D. (2011). Fat crystals and water-in-oil emulsion stability. *Current Opinion in Colloid and Interface Science*, *16*(5), 421–431.

Ghosh, V., Mukherjee, A., & Chandrasekaran, N. (2014). Eugenol-loaded antimicrobial nanoemulsion preserves fruit juice against, microbial spoilage. *Colloids and Surfaces B: Biointerfaces*, *114*, 392–397.

Giroux, H. J., Constantineau, S., Fustier, P., Champagne, C. P., St-Gelais, D., Lacroix, M., & Britten, M. (2013). Cheese fortification using water-in-oil-in-water double emulsions as carrier for water soluble nutrients. *International Dairy Journal*, *29*(2), 107–114.

Gleeson, J. P., Ryan, S. M., & Brayden, D. J. (2016). Oral delivery strategies for nutraceuticals: Delivery vehicles and absorption enhancers. *Trends in Food Science and Technology*, *53*, 90–101.

Gomes, A., Costa, A. L. R., & Cunha, R. L. (2018). Impact of oil type and WPI/Tween 80 ratio at the oil-water interface: Adsorption, interfacial rheology and emulsion features. *Colloids and Surfaces B: Biointerfaces*, *164*, 272–280.

Granato, D., Barba, F. J., Bursać Kovačević, D., Lorenzo, J. M., Cruz, A. G., & Putnik, P. (2020). Functional Foods: Product Development, Technological Trends, Efficacy Testing, and Safety. *Annual Review of Food Science and Technology*, *11*, 93–118.

Grundy, M. M. L., Fardet, A., Tosh, S. M., Rich, G. T., & Wilde, P. J. (2018). Processing of oat: The impact on oat's cholesterol lowering effect. *Food and Function, 9*(3), 1328–1343.

Guerra-Rosas, M. I., Morales-Castro, J., Cubero-Márquez, M. A., Salvia-Trujillo, L., & Martín-Belloso, O. (2017). Antimicrobial activity of nanoemulsions containing essential oils and high methoxyl pectin during long-term storage. *Food Control*, *77*, 131–138.

Gunathilake, K. D. P. P., Rupasinghe, H. P. V., & Pitts, N. L. (2013). Formulation and characterization of a bioactive-enriched fruit beverage designed for cardio-protection. *Food Research International*, *52*(2), 535–541.

Hassan, A. N., Frank, J. F., Farmer, M. A., Schmidt, K. A., & Shalabi, S. I. (1995). Formation of Yogurt Microstructure and Three-Dimensional Visualization as Determined by Confocal Scanning Laser Microscopy. *Journal of Dairy Science*, *78*(12), 2629–2636.

Haug, A., Høstmark, A. T., & Harstad, O. M. (2007). Bovine milk in human nutrition - A review. *Lipids in Health and Disease*, *6*(25), 1–16.

Hayes, M., & Ferruzzi, M. G. (2020). Update on the bioavailability and chemopreventative mechanisms of dietary chlorophyll derivatives. *Nutrition Research*, *81*, 19–37.

Helander, I. M., Alakomi, H. L., Latva-Kala, K., Mattila-Sandholm, T., Pol, I., Smid, E. J., … Von Wright, A. (1998). Characterization of the Action of Selected Essential Oil Components on Gram-Negative Bacteria. *Journal of Agricultural and Food Chemistry*, *46*(9), 3590–3595.

Herbach, K. M., Stintzing, F. C., & Carle, R. (2006). Betalain stability and degradation - Structural and chromatic aspects. *Journal of Food Science*, *71*(4), 41–50.

Herzi, S., & Essafi, W. (2018). Different magnesium release profiles from W/O/W emulsions based on crystallized oils. *Journal of Colloid and Interface Science*, *509*, 178–188.

Holm, J., Lundquist, I., Bjorck, I., Eliasson, A. C., & Asp, N. G. (1988). Degree of starch gelatinization, digestion rate of starch in vitro, and metabolic response in rats. *American Journal of Clinical Nutrition, 47*(6), 1010–1016.

Ignat, I., Volf, I., & Popa, V. I. (2011). A critical review of methods for characterisation of polyphenolic compounds in fruits and vegetables. *Food Chemistry*, *126*(4), 1821–1835.

Jafari, S. M., Assadpoor, E., He, Y., & Bhandari, B. (2008). Re-coalescence of emulsion droplets during high-energy emulsification. *Food Hydrocolloids*, *22*(7), 1191–1202.

Jo, Y. J., Chun, J. Y., Kwon, Y. J., Min, S. G., Hong, G. P., & Choi, M. J. (2015). Physical and antimicrobial properties of trans-cinnamaldehyde nanoemulsions in water melon juice. *LWT - Food Science and Technology*, *60*(1), 444–451.

Jo, Y. J., & Kwon, Y. J. (2014). Characterization of β-carotene nanoemulsions prepared by microfluidization technique. *Food Science and Biotechnology*, *23*(1), 107–113.

Kanafusa, S., Chu, B. S., & Nakajima, M. (2007). Factors affecting droplet size of sodium caseinate-stabilized O/W emulsions containing β-carotene. *European Journal of Lipid Science and Technology*, *109*(10), 1038–1041.

Karupaiah, T., & Sundram, K. (2007). Effects of stereospecific positioning of fatty acids in triacylglycerol structures in native and randomized fats: A review of their nutritional implications. *Nutrition and Metabolism*, *4*(16), 1–17.

Kentish, S., Wooster, T. J., Ashokkumar, M., Balachandran, S., Mawson, R., & Simons, L. (2008). The use of ultrasonics for nanoemulsion preparation. *Innovative Food Science and Emerging Technologies*, *9*(2), 170–175.

Klein, M., Aserin, A., Svitov, I., & Garti, N. (2010). Enhanced stabilization of cloudy emulsions with gum Arabic and whey protein isolate. *Colloids and Surfaces B: Biointerfaces*, *77*(1), 75–81.

Knudsen, K. E. B. (2014). Fiber and nonstarch polysaccharide content and variation in common crops used in broiler diets. *Poultry Science*, *93*(9), 2380–2393.

Komaiko, J., & McClements, D. J. (2015). Low-energy formation of edible nanoemulsions by spontaneous emulsification: Factors influencing particle size. *Journal of Food Engineering*, *146*, 122–128.

Kralova, I., & Sjöblom, J. (2009). Surfactants used in food industry: A review. *Journal of Dispersion Science and Technology*, *30*(9), 1363–1383.

Lamba, H., Sathish, K., & Sabikhi, L. (2015). Double Emulsions: Emerging Delivery System for Plant Bioactives. *Food and Bioprocess Technology*, *8*(4), 709–728.

Lambert, R. J. W., Skandamis, P. N., Coote, P. J., & Nychas, G. J. E. (2001). A study of the minimum inhibitory concentration and mode of action of oregano essential oil, thymol and carvacrol. *Journal of Applied Microbiology*, *91*(3), 453–462.

Law, A. J. R., & Leaver, J. (2000). Effect of pH on the thermal denaturation of whey proteins in milk. *Journal of Agricultural and Food Chemistry*, *48*(3), 672–679.

Li, Y., Hu, M., & McClements, D. J. (2011). Factors affecting lipase digestibility of emulsified lipids using an in vitro digestion model: Proposal for a standardised pH-stat method. *Food Chemistry*, *126*(2), 498–505.

Li, Y., Kim, J., Park, Y., & McClements, D. J. (2012). Modulation of lipid digestibility using structured emulsion-based delivery systems: Comparison of in vivo and in vitro measurements. *Food and Function*, *3*(5), 528–536.

Liang, R., Shoemaker, C. F., Yang, X., Zhong, F., & Huang, Q. (2013). Stability and bioaccessibility of β-carotene in nanoemulsions stabilized by modified starches. *Journal of Agricultural and Food Chemistry*, *61*(6), 1249–1257.

Liang, R., Xu, S., Shoemaker, C. F., Li, Y., Zhong, F., & Huang, Q. (2012). Physical and antimicrobial properties of peppermint oil nanoemulsions. *Journal of Agricultural and Food Chemistry*, *60*(30), 7548–7555.

Liu, J., Kharat, M., Tan, Y., Zhou, H., Muriel Mundo, J. L., & McClements, D. J. (2020). Impact of fat crystallization on the resistance of W/O/W emulsions to osmotic stress: Potential for temperature-triggered release. *Food Research International*, *134*, 109273.

Lubary, M., Hofland, G. W., & ter Horst, J. H. (2011). The potential of milk fat for the synthesis of valuable derivatives. *European Food Research and Technology*, *232*(1), 1–8.

Luo, J., Wang, Z. W., Wang, F., Zhang, H., Lu, J., Guo, H. Y., & Ren, F. Z. (2014). Cryo-SEM images of native milk fat globule indicate small casein micelles are constituents of the membrane. *RSC Advances*, *4*(90), 48963–48966.

Ma, P., Zeng, Q., Tai, K., He, X., Yao, Y., Hong, X., & Yuan, F. (2018). Development of stable curcumin nanoemulsions: effects of emulsifier type and surfactant-to-oil ratios. *Journal of Food Science and Technology*, *55*(9), 3485–3497.

Mackie, A. R., Rafiee, H., Malcolm, P., Salt, L., & van Aken, G. (2013). Specific food structures supress appetite through reduced gastric emptying rate. *American Journal of Physiology - Gastrointestinal and Liver Physiology*, *304*(11), 1038–1043.

Maiani, G., Castón, M. J. P., Catasta, G., Toti, E., Cambrodón, I. G., Bysted, A., … Schlemmer, U. (2009). Carotenoids: Actual knowledge on food sources, intakes, stability and bioavailability and their protective role in humans. *Molecular Nutrition and Food Research*, *53*(S2), 194–218.

Mäkinen, O. E., Sozer, N., Ercili-Cura, D., & Poutanen, K. (2016). Protein From Oat: Structure, Processes, Functionality, and Nutrition. In S. R. Nadathur, J. P. D. Wanasundara, & L. Scanlin (1st ed.), *Sustainable Protein Sources* (pp.105–119). Academic Press.

Malaki Nik, A., Wright, A. J., & Corredig, M. (2011). Micellization of beta-carotene from soy-protein stabilized oil-in-water emulsions under in vitro conditions of lipolysis. *JAOCS, Journal of the American Oil Chemists' Society*, *88*(9), 1397–1407.

Maldonado-Valderrama, J., Wilde, P., Macierzanka, A., & Mackie, A. (2011). The role of bile salts in digestion. *Advances in Colloid and Interface Science*, *165*(1), 36–46.

Manthey, F. A., Hareland, G. A., & Huseby, D. J. (1999). Soluble and insoluble dietary fiber content and composition in oat. *Cereal Chemistry, 76*(3), 417–420.

Mao, L., & Miao, S. (2015). Structuring Food Emulsions to Improve Nutrient Delivery During Digestion. *Food Engineering Reviews*, *7*(4), 439–451.

Maragò, E., Iacopini, P., Camangi, F., Scattino, C., Ranieri, A., Stefani, A., & Sebastiani, L. (2015). Phenolic profile and antioxidant activity in apple juice and pomace: Effects of different storage conditions. *Fruits*, *70*(4), 213–223.

Mason, T. G., Wilking, J. N., Meleson, K., Chang, C. B., & Graves, S. M. (2006). Nanoemulsions: formation, structure, and physical properties. *Journal of Physics: Condensed Matter*, *18*(41), R635–R666.

McClements, D. J. (2002). Colloidal basis of emulsion color. *Current Opinion in Colloid and Interface Science*, *7*(5–6), 451–455.

McClements, D. J. (2015). *Food Emulsions: Principles, Practices, and Techniques* (3rd ed.). CRC Press, Taylor & Francis Group.

McClements, D. J., Decker, E. A., & Choi, S. J. (2014). Impact of environmental stresses on orange oil-in-water emulsions stabilized by sucrose monopalmitate and lysolecithin. *Journal of Agricultural and Food Chemistry*, *62*(14), 3257-3261.

McClements, D. J., Li, Y. (2010). Structured emulsion-based delivery systems: Controlling the digestion and release of lipophilic food components. *Advances in Colloid and Interface Science*, *159*(2), 213-228.

Meroni, E., & Raikos, V. (2017). Physicochemical stability, antioxidant properties and bioaccessibility of β-carotene in orange oil-in- water beverage emulsions: influence of carrier oil types. *Food & Function*, *9*(1), 320-330.

Miller, R., Owens, S. J., & Rørslett, B. (2011). Plants and colour: Flowers and pollination. *Optics and Laser Technology*, *43*(2), 282–294.

Minekus, M., Alminger, M., Alvito, P., Ballance, S., Bohn, T., Bourlieu, C., … Brodkorb, A. (2014). A standardised static in vitro digestion method suitable for food-an international consensus. *Food and Function*, *5*(6), 1113–1124.

Molet-Rodríguez, A., Salvia-Trujillo, L., & Martín-Belloso, O. (2018). Beverage Emulsions: Key Aspects of Their Formulation and Physicochemical Stability. *Beverages*, *4*(3), 70.

Mulet-Cabero, A. I., Egger, L., Portmann, R., Ménard, O., Marze, S., Minekus, M., … Mackie, A. (2020a). A standardised semi-dynamic: in vitro digestion method suitable for food-an international consensus. *Food and Function*, *11*(2), 1702–1720.

Mulet-Cabero, A. I., Torcello-Gómez, A., Saha, S., Mackie, A. R., Wilde, P. J., & Brodkorb, A. (2020b). Impact of caseins and whey proteins ratio and lipid content on in vitro digestion and ex vivo absorption. *Food Chemistry*, *319*, 126514.

Mun, S., Decker, E. A., & McClements, D. J. (2005). Influence of droplet characteristics on the formation of oil-in-water emulsions stabilized by surfactant-chitosan layers. *Langmuir*, *21*(14), 6228–6234.

Muschiolik, G., & Dickinson, E. (2017). Double Emulsions Relevant to Food Systems: Preparation, Stability, and Applications. *Comprehensive Reviews in Food Science and Food Safety*, *16*(3), 532–555.

Nagpal, R., Behare, P., Rana, R., Kumar, A., Kumar, M., Arora, S., … Yadav, H. (2011). Bioactive peptides derived from milk proteins and their health beneficial potentials: an update. *Food Funct.*, *2*(1), 18–27.

Nelis, V., Declerck, A., Vermeir, L., Balcaen, M., Dewettinck, K., & Van der Meeren, P. (2019). Fat crystals: A tool to inhibit molecular transport in W/O/W double emulsions. *Magnetic Resonance in Chemistry*, *57*(9), 707–718.

Olszowy, M., & Dawidowicz, A. L. (2016). Essential oils as antioxidants : their evaluation by DPPH , ABTS , FRAP , CUPRAC , and b -carotene bleaching methods. *Monatshefte Für Chemie - Chemical Monthly*, *147*(12), 2083–2091.

Ostertag, F., Weiss, J., & McClements, D. J. (2012). Low-energy formation of edible nanoemulsions: Factors influencing droplet size produced by emulsion phase inversion. *Journal of Colloid and Interface Science*, *388*(1), 95–102.

Oussalah, M., Phane, S., & Lacroix, M. (2006). Mechanism of Action of Spanish Oregano, Chinese Cinnamon, and Savory Essential Oils against Cell Membranes and Walls of Escherichia coli O157:H7 and Listeria monocytogenes. *Journal of Food Protection*, *69*(5), 1046–1055.

Ozturk, B., Argin, S., Ozilgen, M., & McClements, D. J. (2015). Formation and stabilization of nanoemulsion-based vitamin E delivery systems using natural biopolymers: Whey protein isolate and gum arabic. *Food Chemistry*, *188*, 256–263.

Pan, M. H., Lai, C. S., Dushenkov, S., & Ho, C. T. (2009). Modulation of inflammatory genes by natural dietary bioactive compounds. *Journal of Agricultural and Food Chemistry*, *57*(11), 4467–4477.

Panche, A. N., Diwan, A. D., & Chandra, S. R. (2016). Flavonoids: An overview. *Journal of Nutritional Science*, *5*(47), 1-15.

Park, Y. W., Juárez, M., Ramos, M., & Haenlein, G. F. W. (2007). Physico-chemical characteristics of goat and sheep milk. *Small Ruminant Research*, *68*(1–2), 88–113.

Pereira, P. C. (2014). Milk nutritional composition and its role in human health. *Nutrition*, *30*(6), 619–627.

Qi, X., & Tester, R. F. (2016). Effect of native starch granule size on susceptibility to amylase hydrolysis. *Starch/Staerke, 68*(9–10), 807–810.

Qian, C., Decker, E. A., Xiao, H., & McClements, D. J. (2012). Inhibition of β-carotene degradation in oil-in-water nanoemulsions: Influence of oil-soluble and water-soluble antioxidants. *Food Chemistry*, *135*(3), 1036–1043.

Qian, C., & McClements, D. J. (2011). Formation of nanoemulsions stabilized by model food-grade emulsifiers using high-pressure homogenization: Factors affecting particle size. *Food Hydrocolloids*, *25*(5), 1000–1008.

Rahimi, A., Naserian, A. A., Valizadeh, R., Tahmasebi, A. M., Dehghani, H., Sung, K. I., & Nejad, J. G. (2020). Effect of different corn processing methods on starch gelatinization, granule structure alternation, rumen kinetic dynamics and starch digestion. *Animal Feed Science and Technology*, *268*, 114572.

Raikos, V., Duthie, G., & Ranawana, V. (2017). Comparing the efficiency of different food-grade emulsifiers to form and stabilise orange oil-in-water beverage emulsions: influence of emulsifier concentration and storage time. *International Journal of Food Science and Technology*, *52*(2), 348-358.

Rao, J., & McClements, D. J. (2011). Formation of flavor oil microemulsions, nanoemulsions and emulsions: Influence of composition and preparation method. *Journal of Agricultural and Food Chemistry*, *59*(9), 5026–5035.

Rao, J., & McClements, D. J. (2012). Impact of lemon oil composition on formation and stability of model food and beverage emulsions. *Food Chemistry*, *134*, 749-757.

Raybaudi-Massilia, R. M., Mosqueda-Melgar, J., Soliva-Fortuny, R., & Martín-Belloso, O. (2009). Control of pathogenic and spoilage microorganisms in fresh-cut fruits and fruit juices by traditional and alternative natural antimicrobials. *Comprehensive Reviews in Food Science and Food Safety*, *8*(3), 157–180.

Regand, A., Chowdhury, Z., Tosh, S. M., Wolever, T. M. S., & Wood, P. (2011). The molecular weight, solubility and viscosity of oat beta-glucan affect human glycemic response by modifying starch digestibility. *Food Chemistry, 129*(2), 297–304.

Regina, A., Blazek, J., Gilbert, E., Flanagan, B. M., Gidley, M. J., Cavanagh, C., … Morell, M. K. (2012). Differential effects of genetically distinct mechanisms of elevating amylose on barley starch characteristics. *Carbohydrate Polymers*, *89*(3), 979–991.

Roye, C., Bulckaen, K., De Bondt, Y., Liberloo, I., Van De Walle, D., Dewettinck, K., & Courtin, C. M. (2020). Side-by-side comparison of composition and structural properties of wheat, rye, oat, and maize bran and their impact on in vitro fermentability. *Cereal Chemistry*, *97*(1), 20–33.

Ruxton, C. H. S., Reed, S. C., Simpson, M. J. A., & Millington, K. J. (2004). The health benefits of omega-3 polyunsaturated fatty acids: A review of the evidence. *Journal of Human Nutrition and Dietetics*, *17*(5), 449–459.

Saini, R. K., Nile, S. H., & Park, S. W. (2015). Carotenoids from fruits and vegetables: Chemistry, analysis, occurrence, bioavailability and biological activities. *Food Research International*, *76*, 735–750.

Salvia-Trujillo, L., Artiga-Artigas, M., Molet-Rodríguez, A., Turmo-Ibarz, A., & Martín-Belloso, O. (2018). Emulsion-Based Nanostructures for the Delivery of Active Ingredients in Foods. *Frontiers in Sustainable Food Systems*, *2*(79).

Salvia-trujillo, L., Qian, C., Martín-belloso, O., & McClements, D. J. (2013a). Influence of particle size on lipid digestion and β-carotene bioaccessibility in emulsions and nanoemulsions. *Food Chemistry*, *141*(2), 1472–1480.

Salvia-Trujillo, L., Qian, C., Martín-Belloso, O., & McClements, D. J. (2013b). Modulating β-carotene bioaccessibility by controlling oil composition and concentration in edible nanoemulsions. *Food Chemistry*, *139*(1–4), 878–884.

Salvia-trujillo, L., Rojas-graü, M. A., Soliva-fortuny, R., & Martín-belloso, O. (2015). Physicochemical characterization and antimicrobial activity of food- grade emulsions and nanoemulsions incorporating essential oils. *Food Hydrocolloids*, *43*, 547–556.

Salvia-Trujillo, L., Rojas-Graü, M. A., Soliva-Fortuny, R., & Martín-Belloso, O. (2013c). Effect of processing parameters on physicochemical characteristics of microfluidized lemongrass essential oil-alginate nanoemulsions. *Food Hydrocolloids*, *30*(1), 401–407.

Salvia-Trujillo, L., Rojas-Graü, M. A., Soliva-Fortuny, R., & Martín-Belloso, O. (2013d). Physicochemical characterization of lemongrass essential oil-alginate anoemulsions: effect of ultrasound processing parameters. *Food and Bioprocess Technology*, *6*(9), 2439–2446.

Salvia-Trujillo, L., Rojas-Graü, M. A., Soliva-Fortuny, R., & Martín-Belloso, O. (2014). Impact of microfluidization or ultrasound processing on the antimicrobial activity against Escherichia coli of lemongrass oil-loaded nanoemulsions. *Food Control*, *37*(1), 292–297.

Salvia-Trujillo, L., Soliva-Fortuny, R., Rojas-Graü, M. A., McClements, D. J., Martín-Belloso, O. (2017). *Edible Nanoemulsions as Carriers of Active Ingredients: A Review*. *8*, 439–466.

Sapei, L., Naqvi, M. A., & Rousseau, D. (2012). Stability and release properties of double emulsions for food applications. *Food Hydrocolloids*, *27*(2), 316–323.

Schirmer, M., Höchstötter, A., Jekle, M., Arendt, E., & Becker, T. (2013). Physicochemical and morphological characterization of different starches with variable amylose/amylopectin ratio. *Food Hydrocolloids*, *32*(1), 52–63.

Schuch, A., Deiters, P., Henne, J., Köhler, K., & Schuchmann, H. P. (2013). Production of W/O/W (water-in-oil-in-water) multiple emulsions: Droplet breakup and release of water. *Journal of Colloid and Interface Science*, *402*, 157–164.

Sell, C. (2010). Chemistry of Essential Oils. In K. H. Can Baser, & G. Buchbauer (2nd ed.), *Handbook of Essential oils. Science, Technology and Applications (pp. 165-194)*. CRC Press, Taylor & Francis.

Sharma, S. K., & Dalgleish, D. G. (1993). Interactions between Milk Serum Proteins and Synthetic Fat Globule Membrane during Heating of Homogenized Whole Milk. *Journal of Agricultural and Food Chemistry*, *41*(9), 1407–1412.

Suárez-Jacobo, Á., Rüfer, C. E., Gervilla, R., Guamis, B., Roig-Sagués, A. X., & Saldo, J. (2011). Influence of ultra-high pressure homogenisation on antioxidant capacity, polyphenol and vitamin content of clear apple juice. *Food Chemistry*, *127*(2), 447–454.

Sweedman, M. C., Tizzotti, M. J., Schäfer, C., & Gilbert, R. G. (2013). Structure and physicochemical properties of octenyl succinic anhydride modified starches: A review. *Carbohydrate Polymers*, *92*(1), 905–920.

Tadros, T. F. (2013). Emulsion Formation, Stability, and Rheology. In T. F. Tadros (1st ed.), *Emulsion Formation and Stability* (pp. 1-75). Wiley-VCH.

Tadros, T., Izquierdo, P., Esquena, J., & Solans, C. (2004). Formation and stability of nano-emulsions. *Advances in Colloid and Interface Science*, *108–109*, 303–318.

Teixé-Roig, J., Oms-Oliu, G., Velderrain-Rodríguez, G. R., Odriozola-Serrano, I., & Martín-Belloso, O. (2018). The Effect of Sodium Carboxymethylcellulose on the Stability and Bioaccessibility of Anthocyanin Water-in-Oil-in-Water Emulsions. *Food and Bioprocess Technology*, *11*, 2229–2241.

Teo, A., Goh, K. K. T., Wen, J., Oey, I., Ko, S., Kwak, H. S., & Lee, S. J. (2016). Physicochemical properties of whey protein, lactoferrin and Tween 20 stabilised nanoemulsions: Effect of temperature, pH and salt. *Food Chemistry, 197* (A), 297-306.

Thongoun, P., Pavadhgul, P., Bumrungpert, A., Satitvipawee, P., Harjani, Y., & Kurilich, A. (2013). Effect of oat consumption on lipid profiles in hypercholesterolemic adults. *Journal of the Medical Association of Thailand*, *96* (5), 25–32.

Tokle, T., & McClements, D. J. (2011). Physicochemical properties of lactoferrin stabilized oil-in-water emulsions: Effects of pH, salt and heating. *Food Hydrocolloids*, *25*(5), 976–982.

Tu, N. T. M., Thanh, L. X., Une, A., Ukeda, H., & Sawamura, M. (2002). Volatile constituents of Vietnamese pummelo, orange, tangerine and lime peel oils. *Flavour and Fragrance Journal*, *17*(3), 169–174.

Vasbinder, A. J., Alting, A. C., & De Kruif, K. G. (2003). Quantification of heat-induced casein-whey protein interactions in milk and its relation to gelation kinetics. *Colloids and Surfaces B: Biointerfaces*, *31*(1–4), 115–123.

Vermeir, L., Sabatino, P., Balcaen, M., Declerck, A., Dewettinck, K., Martins, J. C., … Van der Meeren, P. (2016). Effect of molecular exchange on water droplet size analysis as determined by diffusion NMR: The W/O/W double emulsion case. *Journal of Colloid and Interface Science*, *475*, 57-65.

Walker, R. M., Gumus, C. E., Decker, E. A., & McClements, D. J. (2017). Improvements in the formation and stability of fish oil-in-water nanoemulsions using carrier oils: MCT, thyme oil, & lemon oil. *Journal of Food Engineering*, *211*, 60–68.

Wang, Q., & Ellis, P. R. (2014). Oat β-glucan: Physico-chemical characteristics in relation to its blood-glucose and cholesterol-lowering properties. *British Journal of Nutrition, 112*(S2), 4–13.

Wooster, T. J., Golding, M., & Sanguansri, P. (2008). Impact of oil type on nanoemulsion formation and ostwald ripening stability. *Langmuir*, *24*(22), 12758–12765.

Xiang, S., Yao, X., Zhang, W., Zhang, K., Fang, Y., Nishinari, K., … Jiang, F. (2015). Gum Arabic-stabilized conjugated linoleic acid emulsions: Emulsion properties in relation to interfacial adsorption behaviors. *Food Hydrocolloids*, *48*, 110–116.

Yan, J., & Pal, R. (2001). Osmotic swelling behavior of globules of W/O/W emulsion liquid membranes. *Journal of Membrane Science*, *190*(1), 79–91.

Yu, W., Tao, K., & Gilbert, R. G. (2018). Improved methodology for analyzing relations between starch digestion kinetics and molecular structure. *Food Chemistry*, *264*, 284–292.

Zhang, R., Zhang, Z., Zhang, H., Decker, E. A., & McClements, D. J. (2015). Influence of lipid type on gastrointestinal fate of oil-in-water emulsions: In vitro digestion study. *Food Research International*, *75*, 71–78.

Zhao, B., Gu, S., Du, Y., Shen, M., Liu, X., & Shen, Y. (2018). Solid lipid nanoparticles as carriers for oral delivery of hydroxysafflor yellow A. *International Journal of Pharmaceutics*, *535*(1–2), 164–171.

Ziani, K., Fang, Y., & Julian, D. (2012). Fabrication and stability of colloidal delivery systems for flavor oils : Effect of composition and storage conditions. *FRIN*, *46*(1), 209–216.

Zulueta, A., Esteve, M. J., Frasquet, I., & Frígola, A. (2007). Vitamin C, vitamin A, phenolic compounds and total antioxidant capacity of new fruit juice and skim milk mixture beverages marketed in Spain. *Food Chemistry*, *103*(4), 1365–1374.

HYPOTHESIS AND OBJECTIVES

Based on the available literature, as it was introduced in the previous section, the incorporation of active compounds, such as natural antimicrobials and bioactive compounds, into food products has been proposed as a strategy to develop new food products with improved shelf-life and health benefits. Nevertheless, natural antimicrobials, such as essential oils, have strong flavour and volatility, as well as, some bioactive compounds like β-carotene and chlorophyllin are susceptible to degradation and/or have specific solubilities. In this regard, emulsions are effective systems to encapsulate, protect and deliver active compounds that are not easily incorporated into food products. The proper selection of the emulsifier and lipid phase components in the formulation of emulsions is of crucial importance to obtain systems that maintain their colloidal stability during storage and/or gastrointestinal conditions. In addition, emulsions need to be specifically designed to have the desired functionality, for instance, favouring the interaction of antimicrobials with bacterial cell membranes and/or controlling the lipid digestion and bioactive compound release, as well as, their absorption in the small intestine.

Nevertheless, there is a need for a better understanding of the behaviour of emulsions-based delivery systems carrying active compounds, in terms of colloidal stability and functionality, once incorporated into food products. In particular, the present doctoral thesis intends to focus on water-based food products differing in food matrix composition and characteristics: *(i)* apple juice-based beverages, composed of simple carbohydrates, being mainly fructose and sucrose, *(ii)* dairy products (*i.e.,* milk or yogurt) that contain fat, protein and simple carbohydrates, such as lactose, and *(iii)* oatmeal, which contains fat, protein and starch and fibre as complex carbohydrates. Thus, emulsions that have an aqueous continuous phase, being O/W emulsions, O/W nanoemulsions and $W_1/O/W_2$ emulsions, were the selected delivery systems. To elucidate the real benefits of bioactive compounds incorporated into water-based food products through the use of emulsions, not only the colloidal stability of emulsions once incorporated into water-based food matrices should be studied, but also their behaviour during *in vitro* gastrointestinal digestion conditions, in terms of emptying rate and lipid digestibility, as well as, bioactive compound bioaccessibility.

The main objective of this doctoral thesis was to study the physicochemical properties, colloidal stability and functionality of emulsion-based delivery systems, carrying active compounds once incorporated into water-based food products and during storage and *in vitro* gastrointestinal digestion conditions. To achieve this goal, the following specific objectives were proposed:

1. To study the colloidal stability and functionality (*i.e.,* antioxidant and antimicrobial activity) of O/W nanoemulsions carrying essential oils into apple juice-based beverage.

2. To elucidate the influence of dairy products with different food macromolecular composition and matrix characteristics on the colloidal stability and functionality of β-carotene-loaded O/W emulsions once co-digested together.

3. To understand the behaviour of β-carotene-loaded O/W emulsions into complex meals consisting of whole milk and oatmeal before and during *in vitro* gastrointestinal conditions.

4. To study the effect of the lipid phase composition and state on the formulation of chlorophyllin-loaded $W_1/O/W_2$ emulsions with gelled lipid and assess their behaviour during *in vitro* gastrointestinal digestion.

5. To evaluate the colloidal stability and functionality of $W_1/O/W_2$ emulsions with gelled lipid phase incorporated into whole milk before and during *in vitro* gastrointestinal digestion.

MATERIAL AND METHODS

The experimental design to fulfil the research objectives is depicted in Figures 1 and 2. It was divided into two sections depending on the emulsion-based delivery system used, O/W emulsions and O/W nanoemulsions or $W_1/O/W_2$ emulsions. The material and methodology used for emulsion-based delivery systems formation and incorporation into food products as well as characterization are described in detail below.
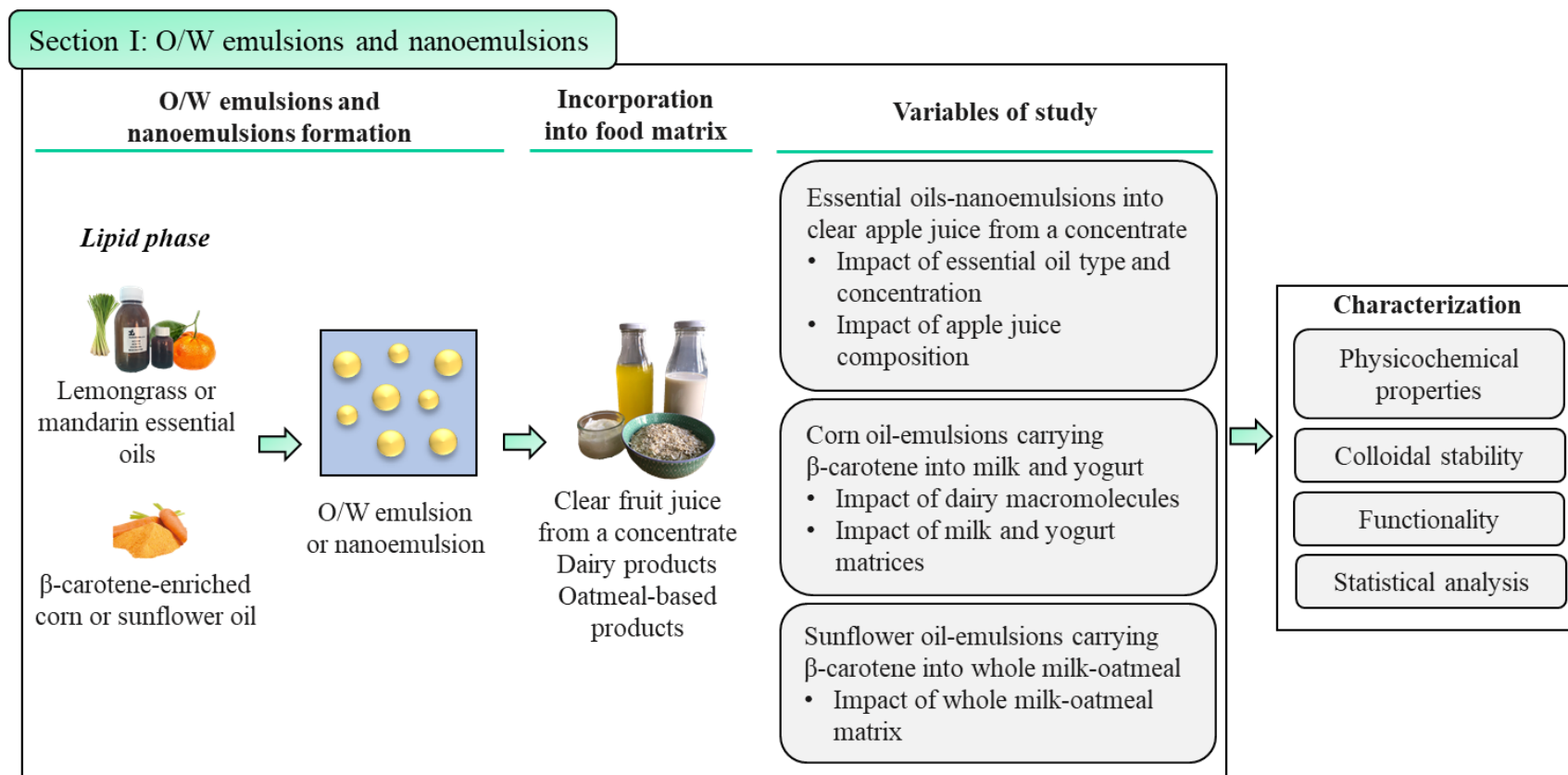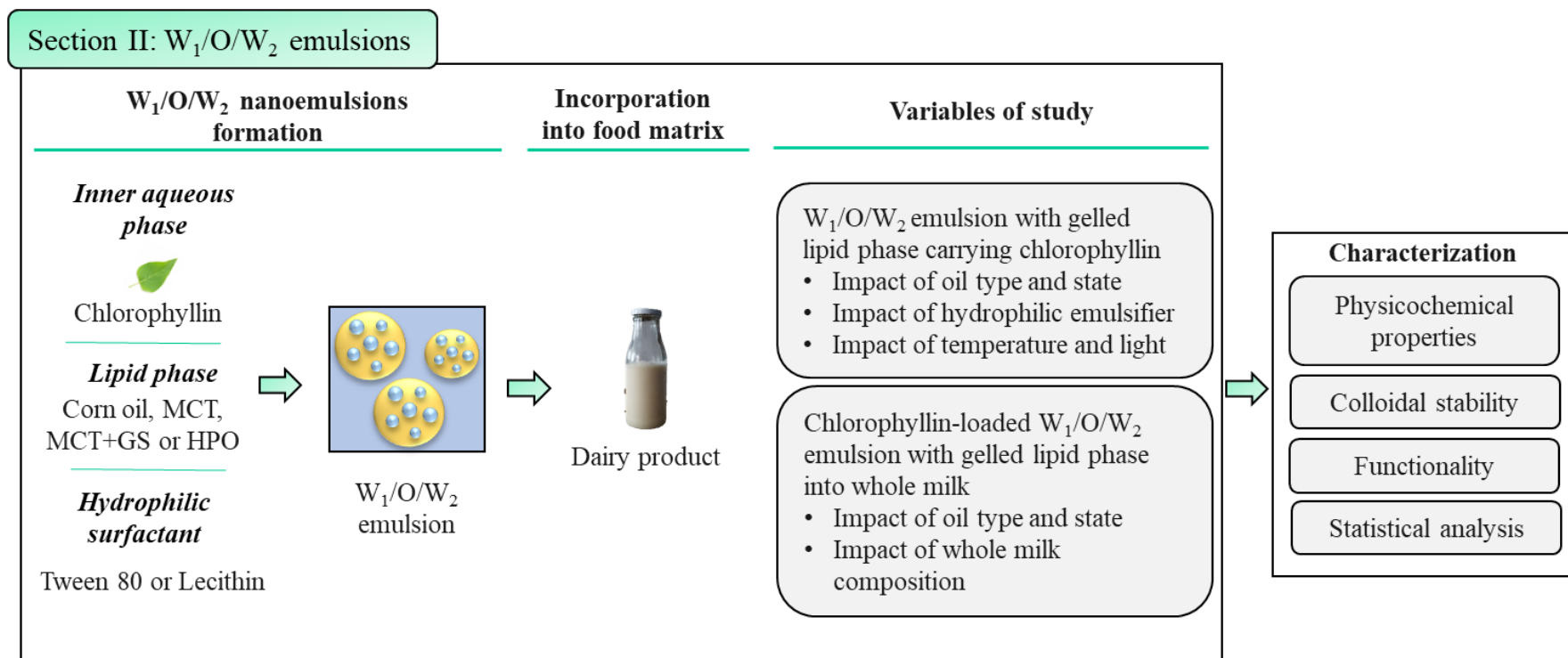

Figure 1. Project description to fulfil the proposed objectives of section I.

Figure 2. Project description to fulfil the proposed objectives of section II.

SECTION I: O/W emulsions and nanoemulsions

1 Formation of O/W emulsions and nanoemulsions carrying antimicrobials or bioactive compounds

A coarse oil-in-water (O/W) emulsion was firstly prepared by pre-homogenizing the lipid phase (*i.e.,* EOs: essential oils, CO: corn oil or sunflower oil) with the aqueous phase containing 2 or 10% w/w of polyoxyethylene sorbitan monooleate (Tween 80), using a laboratory T25 digital Ultra-Turrax mixer (IKA, Staufen, Germany). In those O/W emulsions carrying β-carotene, the lipid phase consisted of an oil carrier enriched with 0.1% (w/w) of β-carotene by sonication (5 min) and mild heating (< 50 ºC for 10 min) until complete dissolution. Then, in chapter I, O/W nanoemulsions were formed by ultrasounds (UP400S, Hielscher Ultrasound Technology, Teltow, Germany). Submicron O/W emulsions were formed by passing the coarse O/W emulsions through a microfluidizer (chapter II) (M110P, Microfluidics, Massachusetts, USA) or two-chamber Jet Homogenizer (chapter III) developed in the School of Food Science and Nutrition (University of Leeds, Leeds, UK).

2 Incorporation of O/W emulsions or nanoemulsions carrying antimicrobials or bioactive compounds into food products

2.1 Essential oil-O/W nanoemulsions into apple juice-based beverage

Three different formulations with increasing levels of complexity, being water, an apple juice model and an apple juice-based beverage were used as a continuous aqueous phase of the lemongrass or mandarin essential oil-O/W nanoemulsions. The soluble solids content and pH of both the apple juice model and the apple juice-based beverage were 9.5 °Brix and 3.7, respectively. The formulation of the apple juice model consisted of a mixture of D-fructose (9.5% w/w) and DL-malic acid (0.3% w/w) in order to adjust the concentration of soluble solids and the pH. To obtain the apple juice-based beverage with the same soluble solids as the apple juice model, the concentrated commercial clear apple juice was diluted. Sodium alginate (1% w/w) was added to all the continuous phases as emulsion stabilizer.

2.2 O/W emulsion carrying β-carotene into dairy macromolecule or products

Individual aqueous solutions of sodium caseinate (SC) 2.3% (w/w), whey protein isolate (WPI) 0.5% (w/w) and lactose 4.7% (w/w), as the main macromolecules present in the studied dairy products, were prepared by its dissolution in milli-Q water at the same concentration than found in commercial milk, and subsequent mixing for 4 h at 750 rpm and 25°C to allow its complete hydration. Then, 80% w/w of each solution was mixed with the O/W emulsion (20% w/w) to obtain the dairy macromolecule solutions fortified with the O/W emulsion (O/W-dairy macromolecule solutions). Additionally, the O/W emulsion (20% w/w) was diluted and mixed with milli-Q water (80% w/w) to reach the same concentration as in the other formulations.

A skimmed milk model solution consisting of a mixture of the main macromolecules present in the studied dairy products was prepared by dissolving SC (2.3% w/w), WPI (0.5% w/w) and lactose (4.7% w/w) in milli-Q water and mixing during 4 h at 750 rpm and 25 °C. Later, 80% w/w of this solution was mixed with the O/W emulsion (20% w/w) to obtain the fortified skimmed milk model, referred to as the O/W-skimmed milk model. In addition, 20% (w/w) of milli-Q water was added to the skimmed milk model (80% w/w) (750 rpm, 5 min), as a control.

Commercial bovine whole milk, skimmed milk, whole yogurt and skimmed yogurt (80% w/w) were mixed with the O/W emulsion (20% w/w) for 5 min at 750 (milk) and 1500 rpm (yogurt), to obtain the fortified dairy products, referred as O/W-whole milk, O/W-skimmed milk, O/W-whole yogurt and O/W-skimmed yogurt. Whole milk, skimmed milk, whole yogurt and skimmed yogurt (80% w/w) mixed with (20% w/w) milli-Q water (750 or 1500 rpm, 5 min) were used as dairy products control.

2.3 O/W emulsion carrying β-carotene into whole milk and/or oatmeal

First, two preliminary blends were prepared by mixing (750 rpm; 5 min) the O/W emulsion (20% w/w) with 80% w/w of milli-Q water (O/W emulsion:water) or whole milk (O/W emulsion:whole milk). Then, 87% (w/w) of the O/W emulsion:water or O/W emulsion:whole milk was diluted in milli-Q water (13% w/w) and subsequently, mixed and boiled (750 rpm; 5 min). These two systems are referred to as the O/W emulsion and O/W-whole milk. In addition, oat flakes were added to the O/W emulsion:water or O/W

emulsion:whole milk to a final ratio of 13/87 and, oatmeals were prepared by boiling and mixing at 750 rpm for 5 min. These two systems are referred to as the O/W-oatmeal and O/W-whole milk-oatmeal.

SECTION II: $W_1/O/W_2$ emulsions

3   Formation of $W_1/O/W_2$ emulsions carrying chlorophyllin

$W_1/O/W_2$ emulsions were prepared according to a two-step emulsification method previously reported by Artiga-Artigas, Molet-Rodríguez, Salvia-Trujillo, & Martín-Belloso (2018) with some modifications, consisting of the formation of the W_1/O emulsion followed by its dispersion in an outer aqueous phase.

Liquid phase W_1/O emulsion with pure medium-chain triglyceride (MCT) oil or CO and gelled lipid W_1/O emulsions with lipid phases consisting of (*i*) a blend of MCT or CO with 1 or 5% (w/w) of glyceryl stearate (GS) or (*ii*) pure hydrogenated palm oil (HPO) were formulated. GS and HPO were firstly melted by increasing the temperature to 50 and 60 °C, respectively. The development of a gelled lipid phase with GS involved its aggregation through self-assembly and/or crystallization. Specifically, the lipid phase containing GS was formulated with 1 or 5% (w/w) of GS and the rest MCT or CO by mixing for 5 min using a magnetic stirrer working at 450 rpm and 50 ºC. Then, each lipid phase (94% w/w) was mixed with 6% (w/w) of polyglycerol polyricinoleate (PGPR) at 450 rpm and 50 °C for 5 min. Afterwards, W_1/O emulsions were formed by mixing each lipid phase:PGPR mixture (70% w/w) with an aqueous phase (30% w/w) consisting of 112.5 or 7500 ppm chlorophyllin, coppered trisodium salt (CHL), 0.05 M NaCl and 2% (w/w) sodium alginate by using a laboratory T25 digital Ultra-Turrax mixer, working at 11000 rpm for 5 min. The temperature during the first emulsification step was kept at 50-60 °C in order to maintain the lipid phases containing GS and HPO in liquid state. In chapter IV, the physicochemical properties of W_1/O emulsions were analyzed. In this case, after W_1/O emulsions formation, two aliquots were taken and their temperature was reduced down to 4 °C for 2 h in order to allow lipid gelation. Subsequently, droplet size, viscosity and microscopic analysis were done. Otherwise, W_1/O emulsions were maintained at 50-60 ºC, for the following formation of the $W_1/O/W_2$ emulsions.

The second step was the dispersion of the previously prepared W_1/O emulsions in the outer aqueous phase using a laboratory T25 digital Ultra-Turrax mixer working at 4000 rpm for 2-3 min. From each W_1/O emulsion, two different $W_1/O/W_2$ emulsions were formed. On the one hand, the W_1/O emulsion (20% w/w) was dispersed in an outer aqueous phase (80% w/w) containing NaCl 0.05 M, sodium alginate (2% w/w) and Tween 80 (2.5% w/w). On the other hand, a percentage of 2% (w/w) of lecithin was previously mixed with the W_1/O emulsion (18% w/w) using a magnetic stirrer at 750 rpm for 5 min followed by its dispersion in an outer aqueous phase (80% w/w) containing NaCl 0.05 M and sodium alginate (2% w/w). Once the $W_1/O/W_2$ emulsions were formed, their temperature was reduced down to 4 °C for 2 h in order to allow lipid gelation in those $W_1/O/W_2$ emulsions with gelled lipid phase.

4 Incorporation of $W_1/O/W_2$ emulsions carrying chlorophyllin into whole milk

From the previously prepared $W_1/O/W_2$ emulsions (30.4% w/w), the ones formulated with pure MCT, a blend of MCT and GS (5% w/w) or pure HPO were incorporated into whole milk (69.6% w/w) and subsequently mixed at 900 rpm for 5 min, referred in the manuscript as $W_1/O/W_2$ emulsions in whole milk. In addition, $W_1/O/W_2$ emulsions (30.4% w/w) were also diluted in milli-Q water (69.6% w/w) and mixed at 450 rpm for 5 min, to reach the same final concentration as when incorporated in whole milk. They are referred to as $W_1/O/W_2$ emulsions in the manuscript.

Characterization of emulsion-based delivery systems before and after incorporation into food products

5 Physicochemical properties

5.1 Droplet size and size distribution

Droplet size and size distribution of the studied formulations were measured using dynamic light scattering (DLS) or static light scattering (SLS) techniques depending on the range of droplet sizes. DLS and SLS are suitable for droplets in the nano-range and micrometres, respectively.

5.1.1 Dynamic light scattering

Oil droplet size and size distribution were measured by DLS with a Zetasizer NanoZS laser diffractometer (Malvern Instruments Ltd., Worcestershire, U.K.) working at 633 nm, 25 ºC and equipped with a backscatter detector (173°). DLS measures the Brownian motion of nanosized droplets and relates this movement to an equivalent hydrodynamic diameter (Brar & Verma, 2011). Before measurements, each formulation was diluted in milli-Q water using a dilution ratio of 1:9 sample-to-solvent. The oil droplet size (nm) was characterized by distribution curves in intensity (%) and average droplet size. The oil absorbance at 633 nm and the oil refractive index were determined with a spectrophotometer and a refractometer, respectively.

5.1.2 Static light scattering

Using SLS (Mastersizer 2000, Malvern Instruments Ltd, Worcestershire, UK), each formulation was dispersed in distilled water at 2200 rpm and the measured average droplet size was reported as surface-weighted average ($D_{[3;2]}$) or volume-weighted average ($D_{[4;3]}$) and size distribution as volume (%).

5.2 ζ -potential

The ζ-potential of the oil droplets was measured by phase analysis light scattering (PALS) with a Zetasizer NanoZS laser diffractometer. Samples were diluted in milli-Q water with a dilution factor of 1:9 aliquot-to-solvent and placed in a capillary cell to assess the electrophoretic mobility of the particles. The ζ-potential was expressed in millivolts (mV).

5.3 Viscosity

Viscosity measurements (mPa·s) were performed by using a vibro-viscometer (SV-10 vibro-viscometer, A&D Company, Tokyo, Japan) vibrating at 30 Hz, with constant amplitude (0.4 mm) and working at 25 ºC. Aliquots of 10 mL of each sample were used for determinations.

5.4 Microstructure

5.4.1 Phase contrast optical microscopy

Phase contrast microscopy images of the studied formulations were taken with an optical microscope (BX41, Olympus, Göttingen, Germany) using a 100x oil immersion objective lens and equipped with UIS2 optical system. Images of some formulations were taken using fluorescence with the same optical microscope and a 40x objective lens. A stock solution of a fluorescent agent named Fluorescein 5-isothiocyanate (Fit C) was used to stain protein. The formulations were dyed in green using the stock solution of FitC (1 mg/mL of dimethyl sulfoxide). All images were processed using the instrument software (Olympus cellSense, Barcelona, Spain).

5.4.2 Confocal laser scanning microscopy (CLSM)

A stock solution of Nile Red (1 mg/mL in dimethyl sulfoxide) was used to stain the lipid, Fast Green (1 mg/mL in milli-Q water) was used to stain the protein and Methyl Blue (1 mg/mL in milli-Q water) was used to stain the β-glucan. The studied formulations were dyed with the stock solutions of Nile red and Fast Green or Methyl blue and excited at wavelengths of 488, 633 and 665 nm, respectively. The emission filters were set at 555–620 nm for Nile Red, 660–710 nm for Fast Green and 550-700 nm for Methyl Blue. A Zeiss LSM 880 inverted confocal microscope (Carl Zeiss MicroImaging GmbH, Jena, Germany) with an oil immersion 63× lens and the pinhole diameter maintained at 1 Airy Unit to filter out the majority of the scattered light was used to capture the confocal images. All images were processed using the instrument software Zen.

6 Colloidal stability

The colloidal stability of the studied formulations during storage or GI digestion was analyzed in terms of oil droplet size variations by DLS or SLS technique with a Zetasizer NanoZS laser diffractometer or a Mastersizer 2000 (sections 5.1 and 5.2) and backscattering (ΔBS) variations by multiple light scattering (MLS) technique, using a Turbiscan ™Classic MA 2000 (Formulation, Toulouse, France). It consists of a detection head composed of a pulsed near-infrared light source (λ_{air} = 850 nm) and two synchronous detectors. The transmission detector receives the light which goes through the sample (180° from the incident beam), while the BS detector receives the light scattered by the

sample at 45° from the incident beam. Samples are placed in cylindered glass cells and the detection head scans their entire length, acquiring transmission and BS data every 40 μm. Transmission is used to analyze clear or turbid dispersions and BS is used to analyze opaque dispersions, as is the case of the formulations used in this doctoral thesis. Thus, each formulation was placed in a cylindered glass cell and the BS data was acquired after formation and during storage time.

Each BS profile obtained can be split into three zones corresponding to the bottom (on the left), the intermediate part (in the middle) and the top of the cylindered glass cell (on the right). Emulsion destabilization mechanisms can be easily identified as ΔBS in the different parts of the BS profile. Variations in particle size (flocculation or coalescence) is shown as displacement of the horizontal lines from the intermediate part of the BS profile. Whereas, gravitational separation can show up peaks either on the left (sedimentation) or on the right (creaming) parts. Both sedimentation and creaming can cause clarification of the emulsions. Data analysis of the BS values is represented as ΔBS, which refers to the BS of each storage day relative to the initial storage day.

The stability of some formulations determined by the ΔBS was also evaluated under common food storage and gastrointestinal conditions, being different temperatures (4, 25 and 35 °C) and visible light (λ = 350–700 nm).

7 Functionality

7.1 Antioxidant activity

The antioxidant activity of EOs-nanoemulsions with water, an apple juice model or an apple juice-based beverage as a continuous phase was determined by the ferric reducing antioxidant power (FRAP) assay, which measures the ability to reduce ferric ion (Fe^{3+}) to ferrous ion (Fe^{2+}). The FRAP procedure was conducted according to the method described by Benzie & Strain (1996) with minor modifications. The FRAP reagent was freshly prepared from 300 mM acetate buffer (pH 3), 10 mM 2,4,6- tripyridyl-s-triazine (TPTZ) made up in a 40 mM HCl and 20 mM $FeCl_3$ solution. All three solutions were mixed in a 10:1:1 (w/w/w) ratio. Once the working solution was prepared, 150 μL of the sample or Trolox standard was mixed with 2.85 mL of the working solution. The absorption of the reaction mixture was measured at 630 nm after 30 min of incubation at 25 ºC using a Shimadzu (UV–2401PC, Japan) spectrophotometer. The antioxidant capacity was

calculated from a linear calibration curve and expressed as μg equivalents of Trolox ($FeSO_4 \cdot 7H_2O$) per mL of sample.

7.2 Antimicrobial activity against inoculated *Escherichia coli*

The antimicrobial activity of EOs-O/W nanoemulsions with water, an apple juice model or an apple juice-based beverage as a continuous phase was assessed by evaluating the inactivation of inoculated *Escherichia coli* (*E.coli*) during 28 days of storage. The method used was a modification of that previously described by Ferreira et al. (2010). *E. coli* 1.107 (Laboratoire de Repression des Fraudes, Montpellier, France) was cultured in tryptone soy broth (Bioakar Diagnostic; Beauvais, France) and incubated at 37 ºC with continuous agitation at 120 rpm for 11 h to obtain cells in stationary growth phase. The final concentration reached in the culture was 108 –109 colony-forming units/mL. A 0.5 mL-aliquot of overnight bacterial culture was mixed with 0.5 mL of lemongrass or mandarin essential oils-O/W nanoemulsions and 4.5 mL of the aqueous solution. To determine the inactivation of *E. coli* populations, a 100 mL-aliquot of the bacterial suspensions was taken immediately after 30 min and 1, 3, 6, 9, 13, 21 and 28 days of contact time to be serially diluted and spread on McConkey agar (Biokar Diagnostics, Beauvais, France) plates. A control was performed with the same method, replacing the EOs with CO. Additionally, milli-Q water was used as a blank. Colony counts were determined after incubation of agar plates at 37 ºC for 24 h.

7.3 Lipid digestibility

In chapters II and V, the study of lipid digestibility was conducted according to the INFOGEST international consensus (Minekus et al., 2014). In chapter III, oral and intestinal phases were performed following the INFOGEST static protocol (Brodkorb et al., 2019), while a semi-dynamic *in vitro* model recently described by Mulet-Cabero, et al. (2020) was used to mimic the gastric digestion.

7.3.1 *Stock solutions of simulated digestive fluids*

In general, the electrolyte stock solutions of digestion fluids (x1.25 concentrated) were prepared according to Brodkorb et al. (2019) and stored at −20 °C. Electrolyte simulated salivary fluid (eSSF: KCl, KH_2PO_4, $NaHCO_3$, $MgCl_2(H_2O)_6$, $(NH_4)_2CO_3$, HCl), adjusted to pH 7, electrolyte simulated gastric fluid (eSGF: KCl, KH_2PO_4, NaCl, $MgCl_2(H_2O)_6$,

$(NH_4)_2CO_3$), adjusted to pH 3 (static digestion) and pH 7 (semi-dynamic digestion) and electrolyte simulated intestinal fluid (eSIF: KCl, KH_2PO_4, NaCl, $MgCl_2(H_2O)_6$), adjusted to pH 7. The eSGF and eSIF solutions consisted of the mixture of electrolytes proposed by Brodkorb et al. (2019), but replacing the $NaHCO_3$ for NaCl, when an open vessel was used.

7.3.2 Oral phase

In the reaction vessel, which was a v-form vessel (Yorlab, UK) with a thermostat jacket (37°C), 30 g of the studied formulation were mixed with the oral mixture solution consisting of eSSF, $CaCl_2(H_2O)_2$ (0.3 M) and milli-Q water to a final ratio of 1:1 with the dry weight of food. Thus, the volume of oral mixture solution added varied slightly between formulations, ranging from 1.04 to 6.57 mL. In addition, α-amylase (150 U/mL oral mixture solution) was added to the gastric mixture solution for the formulations containing starch. Then, the pH of the mixture was adjusted to 7 and incubated at 37 ºC for 2 min with continuous agitation at 150 rpm using an overhead stirrer (Hei-TORQUE Value 100, Heidolph, Germany) with a 3D printed stirrer paddle.

7.3.3 Gastric phase

For the static method, the gastric mixture solution was prepared by dissolving pepsin (8.8 mg pepsin/ mL) in eSGF, followed by the addition of $CaCl_2(H_2O)_2$ 0.3 M, HCl 1 M and milli-Q water. The gastric digestion was performed by mixing each formulation with the gastric mixture to a final ratio of 1:1. It was incubated under dark conditions for 2 h at 37 °C and continuous agitation using an orbital shaker working at 100 rpm. After the gastric phase, three aliquots, referred to as gastric chyme aliquots, were collected for microscopic, droplet size and ζ-potential analysis and the rest was used for the subsequent intestinal digestion.

For the semi-dynamic method, a gastric mixture solution was prepared to have a final ratio of 1:1 with the oral bolus. The gastric mixture solution consisted of SGF (eSGF, $CaCl_2(H_2O)_2$ (0.3 M) and milli-Q water), HCl (1 M) and pepsin solution. The pH of the oral bolus was decreased to simulate the fasted state in the stomach by adding 10% of the SGF solution and HCl until reaching pH 2. During the gastric digestion, three solutions were added: (1) the remaining 90% of SGF solution at pH 7, (2) pepsin solution (4000

U/mL of gastric mixture solution) and (3) HCl (1 M). The volume of acid needed to decrease the pH of the tested formulations to 2 was determined previously, following the pH test protocol described in Mulet-Cabero et al. (2020a). A dosing device (800 Dosino, Metrohm, Switzerland) with an automatic titrator (902 Titrando, Metrohm, Switzerland) was used to deliver both the gastric mixture solution and HCl. The enzyme solution was delivered by a syringe pump (Legato, Kd Scientific, USA). The rate at which these solutions were delivered was dependent on the total gastric digestion time of each formulation. The gastric content was mixed at 10 rpm (using the same overhead stirrer as in the oral phase) and 37°C during the total gastric phase time determined for each sample.

7.3.4 *Gastric emptying*

The simulation of the gastric emptying (GE) was determined considering the composition of each formulation and calculating their caloric content (kcal/g of meal) based on the standard Atwater factors (1 g of lipid yields 9 kcal, 1 g of protein yields 4 kcal and 1 g of carbohydrates yields 4 kcal). The emptying rate used was constant and based on the caloric content of the studied meals and scaled-down from 2 kcal/min/mL of the realistic meal that would be digested *in vivo*, being 180 mL for the O/W emulsion and O/W-whole milk and 207 mL for the O/W-oatmeal and O/W-whole milk-oatmeal. Thus, the volume and time of each GE point differed between formulations. GE was simulated by taking five aliquots, referred to as GE1-5 in the text, corresponding to the portion of each formulation that would be delivered into the duodenum. Aliquots were taken from the bottom of the vessel using a 10 mL pipette tip, the aperture of which had a 2 mm diameter because it approximates the upper limit of particle size that has been seen to pass through the pyloric opening into the duodenum (Thomas, 2006). To inhibit pepsin activity, NaOH (2 M) was added to each GE sample to increase the pH above 7. Aliquots of GEs were collected for immediate analysis of particle size and particle size distribution (GE1 and GE5) as well as confocal microscopy (GE1, GE3 and GE5) and the rest was snap-frozen in liquid nitrogen and stored at -80 °C for subsequent *in vitro* small intestinal digestion.

7.3.5 *Intestinal phase*

Using the method proposed by Minekus et al. (2014) to simulate the small intestinal phase, a 30 mL-aliquot of the gastric chyme, that is the food from the gastric phase, was placed in a water bath at 37 °C. Subsequently, 3.5 mL of bile salts (54 mg/mL) diluted in

a phosphate buffer (0.005 M, pH 7) and 1.5 mL of intestinal salts (10 mM of $CaCl_2$ and 160 mM of NaCl) were also added, and the pH was adjusted to 7. Then, 2.5 mL of pancreatin solution (215 mg/mL) diluted in phosphate buffer was added to initiate the lipid hydrolysis.

Using the method proposed by Brodkorb et al. (2019), the intestinal mixture was prepared using 42.5 % (v/v) of eSIF, 0.2 % (v/v) of $CaCl_2(H_2O)_2$ (0.3 M) and 19.8 % (v/v) of milli-Q water and was added to each GE sample followed by an adjustment of pH to 7. Afterwards, 12.5 % (v/v) of bile bovine solution (20 mM intestinal mixture) and 25 % (v/v) of pancreatin solution (200 U of trypsin/mL intestinal mixture) were also added.

In both cases, the lipolysis reaction was monitored for 120 min with a titration unit (pH-stat, Metrohm USA Inc., Riverview, FL, USA). To compensate for the free fatty acids (FFAs) that were released during the lipid digestion, the pH was constantly maintained at 7.0 by adding dropwise a NaOH solution (0.25 M). The percentage of FFA release was calculated according to equation (1):

$$Free\ fatty\ acid\ release\ (\%) = \frac{V_{NaOH} \times C_{NaOH} \times M_{oil}}{2 \times m_{lipid}} \times 100 \tag{1}$$

where V_{NaOH} is NaOH volume (mL) used to compensate the FFAs released during the digestion, C_{NaOH} is NaOH molarity (0.25 M), M_{lipid} is lipid molecular weight, m_{lipid} is the total lipid weight in the sample placed in the titration unit.

Since the interest was in the lipid instead of protein, after the small intestinal digestion the digest was transferred into glass tubes and heat-shocked at 80 °C for 3 min in order to stop the lipolysis reaction and placed in an iced-water bath afterwards.

7.4   β-carotene retention after gastrointestinal digestion

The capacity of the studied formulations to retain β-carotene after being subjected to the prior described *in vitro* GI digestion was determined by the method reported by Liu, Wang, McClements, & Zou (2018) with minor modifications. A 1 mL-aliquot of the initial O/W emulsion or each GE digest was mixed with 1 mL of ethanol and 1.5 mL of hexane, vortexed for 10 s and centrifuged at 9000 rpm for 10 min at 4 °C (Universal 320R, Andreas Hettich GmbH & Co. KG, Tuttlingen, Germany). The hexane fraction was

analyzed spectrophotometrically (CECIL CE 2021; Cecil Instruments Ltd, Cambridge, UK) at 450 nm. The concentration of β-carotene extracted from the initial O/W emulsion or each GE digest was determined from a calibration curve of absorbance versus β-carotene concentration in hexane.

The β-carotene retention was then calculated using equation (2):

$$\beta - carotene\ retention\ (\%) = \frac{C_{digest}}{C_{initial}} \times 100 \tag{2}$$

where C_{digest} and $C_{initial}$ are the β-carotene concentration in each GE digest and in the initial O/W emulsion, respectively.

The total β-carotene retention of the formulations was calculated as the sum of the β-carotene retention in each of their individual GE samples after *in vitro* small intestinal digestion.

7.5   Bioactive compounds bioaccessibility
7.5.1   *β-carotene bioaccessibility*

The β-carotene bioaccessibility is defined as the fraction of β-carotene that can be incorporated into the mixed micelles and thus becomes available for absorption in the body. The β-carotene bioaccessibility of the formulations after being subjected to the prior described *in vitro* gastrointestinal digestion procedure was evaluated. The digest was centrifuged (AVANTI J-25, Beckman Instruments Inc., Fullerton, CA, USA) at 4000 rpm for 40 min at a temperature of 8 °C. The supernatant, being the aqueous fraction containing the mixed micelles, was collected and considered as the micellar fraction in which the β-carotene is solubilized. The β-carotene quantification was conducted following the method reported by Liu, Wang, McClements, & Zou (2018), where 0.5 mL of the initial or micellar fraction were mixed with 2 mL of ethanol and 3 mL of hexane and vortexed for 10 s at 1800 rpm. Afterwards, the upper hexane phase containing the β-carotene was analyzed spectrophotometrically with a V-670 spectrophotometer (Jasco, Tokyo, Japan) at 450 nm. The concentration of β-carotene extracted from the initial or micellar fractions was determined from a calibration curve of absorbance versus β-carotene concentration in hexane.

The β-carotene bioaccessibility was then calculated using the following equation (3):

$$\beta - carotene\ bioaccessibility\ (\%) = \frac{C_{micellar}}{C_{initial}} \times 100 \tag{3}$$

where $C_{micelle}$ is the β-carotene concentration of the micelle fraction and $C_{initial}$ is the initial β-carotene concentration of the initial formulations.

7.5.2   *Chlorophyllin bioaccessibility*

The CHL bioaccessibility of the $W_1/O/W_2$ emulsions and $W_1/O/W_2$ emulsion in whole milk after being subjected to the prior described *in vitro* GI digestion procedure was evaluated. The digest was centrifuged (AVANTI J-25, Beckman Instruments Inc., Fullerton, CA, USA) at 4000 rpm for 40 min at a temperature of 8 °C. The supernatant, being the aqueous fraction was collected and was considered to be the fraction in which CHL was solubilized. CHL quantification was conducted by a method in which a 0.5 mL-aliquot of the supernatant was mixed with 3 mL of Milli-Q water and 2 mL of hexane and vortexed for 10 s at 1800 rpm. The lower fraction containing the CHL was collected and filtered with a nonsterile nylon syringe filter, pore: 0.45 μm, ø13 mm (Branchia, Labbox labware, Barcelona, Spain) in order to remove the larger particles than 0.45 μm that cannot be absorbed by epithelium cells. Afterwards, the absorbance of the CHL in the filtrate was measured with a V-670 spectrophotometer (Jasco, Tokyo, Japan) at 405 nm. The concentration of CHL extracted from the digest was determined from a calibration curve of absorbance versus CHL concentration in Milli-Q water. The CHL bioaccessibility was then calculated using equation (4):

$$Chlorophyllin\ bioaccessibility\ (\%) = \frac{C_{digest}}{C_{theorethic}} \times 100 \tag{4}$$

where $C_{digesta}$ and $C_{theoretic}$ are the concentration measured in the aqueous fraction of the centrifuged digest and the CHL concentration used in the formulation of $W_1/O/W_2$ emulsions, respectively.

7.6 Encapsulation Efficiency of chlorophyllin in $W_1/O/W_2$ emulsions

The percentage of CHL entrapped in the inner aqueous phase of $W_1/O/W_2$ emulsions over 12 days of refrigerated storage (4 °C) was determined according to the methods described by Aditya et al. (2015) and Teixé-Roig, Oms-Oliu, Velderrain-Rodríguez, Odriozola-Serrano, & Martín-Belloso (2018) with minor modifications. Briefly, 10 mL of the $W_1/O/W_2$ emulsion was placed in a Falcon™ tube and centrifuged (AVANTI J-25, Beckman Instruments Inc., Fullerton, CA, USA) at 4500 rpm for 10 min at 4 °C. The outer aqueous phase at the bottom of the Falcon tube (which contained the unentrapped CHL) was collected using a syringe and centrifuged at 7500 rpm for 15 min at 4 °C, prior dilution at 1:4 with methanol. The process was repeated twice in order to extract all the unentrapped CHL. The methanol fraction containing the CHL was analyzed spectrophotometrically (V-670 spectrophotometer, Jasco, Tokyo, Japan) at 405 nm. Encapsulation efficiency (EE) was calculated using the following equation (5):

$$EE(\%) = \frac{N_{W1} - N_{W2}}{N_{W1}} \times 100 \tag{5}$$

where N_{W2} is the amount of CHL in the methanol phase and N_{W1} is the amount of CHL initially added to the inner aqueous phase.

8 Statistical analysis

All experiments were assayed in duplicate and data was expressed as the mean with standard deviation. An analysis of variance was carried out and the Student's t or Tukey HSD tests were run to determine significant differences at a 5% significance level (p < 0.05) with statistical software JMP Pro 14 (SAS Institute Inc.).

9 References

Aditya, N. P., Aditya, S., Yang, H., Kim, H. W., Park, S. O., & Ko, S. (2015). Co-delivery of hydrophobic curcumin and hydrophilic catechin by a water-in-oil-in-water double emulsion. *Food Chemistry*, *173*, 7-13.

Artiga-Artigas, M., Molet-Rodríguez, A., Salvia-Trujillo, L., & Martín-Belloso, O. (2018). Formation of Double (W1/O/W2) Emulsions as Carriers of Hydrophilic and Lipophilic Active Compounds. *Food and Bioprocess Technology*, *12,* 422–435.

Benzie, I.F.. & Strain, J. (1996). The Ferric Reducing Ability of Plasma (FRAP) as a Measure of "Antioxidant Power": The FRAP Assay. *Analytical Biochemistry*, *239*(1), 70–76.

Brar, S. K., & Verma, M. (2011). Measurement of nanoparticles by light-scattering techniques. *TrAC - Trends in Analytical Chemistry*, *30*(1), 4.

Brodkorb, A., Egger, L., Alminger, M., Alvito, P., Assunção, R., Ballance, S., … Recio, I. (2019). INFOGEST static in vitro simulation of gastrointestinal food digestion. *Nature Protocols*, *14*(4), 991–1014.

Ferreira, J. P., Alves, D., Neves, O., Silva, J., Gibbs, P. A., & Teixeira, P. C. (2010). Effects of the components of two antimicrobial emulsions on food-borne pathogens. *Food Control*, *21*(3), 227–230.

Liu, W., Wang, J., McClements, D. J., & Zou, L. (2018). Encapsulation of β-carotene-loaded oil droplets in caseinate/alginate microparticles: Enhancement of carotenoid stability and bioaccessibility. *Journal of Functional Foods*, *40*, 527–535.

Minekus, M., Alminger, M., Alvito, P., Ballance, S., Bohn, T., Bourlieu, C., … Brodkorb, A. (2014). A standardised static in vitro digestion method suitable for food-an international consensus. *Food and Function*, *5*(6), 1113–1124.

Mulet-Cabero, A. I., Egger, L., Portmann, R., Ménard, O., Marze, S., Minekus, M., … Mackie, A. (2020). A standardised semi-dynamic: in vitro digestion method suitable for food-an international consensus. *Food and Function*, *11*(2), 1702–1720.

Teixé-Roig, J., Oms-Oliu, G., Velderrain-Rodríguez, G. R., Odriozola-Serrano, I., & Martín-Belloso, O. (2018). The Effect of Sodium Carboxymethylcellulose on the Stability and Bioaccessibility of Anthocyanin Water-in-Oil-in-Water Emulsions. *Food and Bioprocess Technology*, 11, 2229–2241.

Thomas, A. (2006). Gut motility, sphincters and reflex control. *Anaesthesia and Intensive Care Medicine*, *7*(2), 57–58.

PUBLICATIONS

Section I

Chapter I

Incorporation of antimicrobial nanoemulsions into complex foods: A case study in an apple juice-based beverage

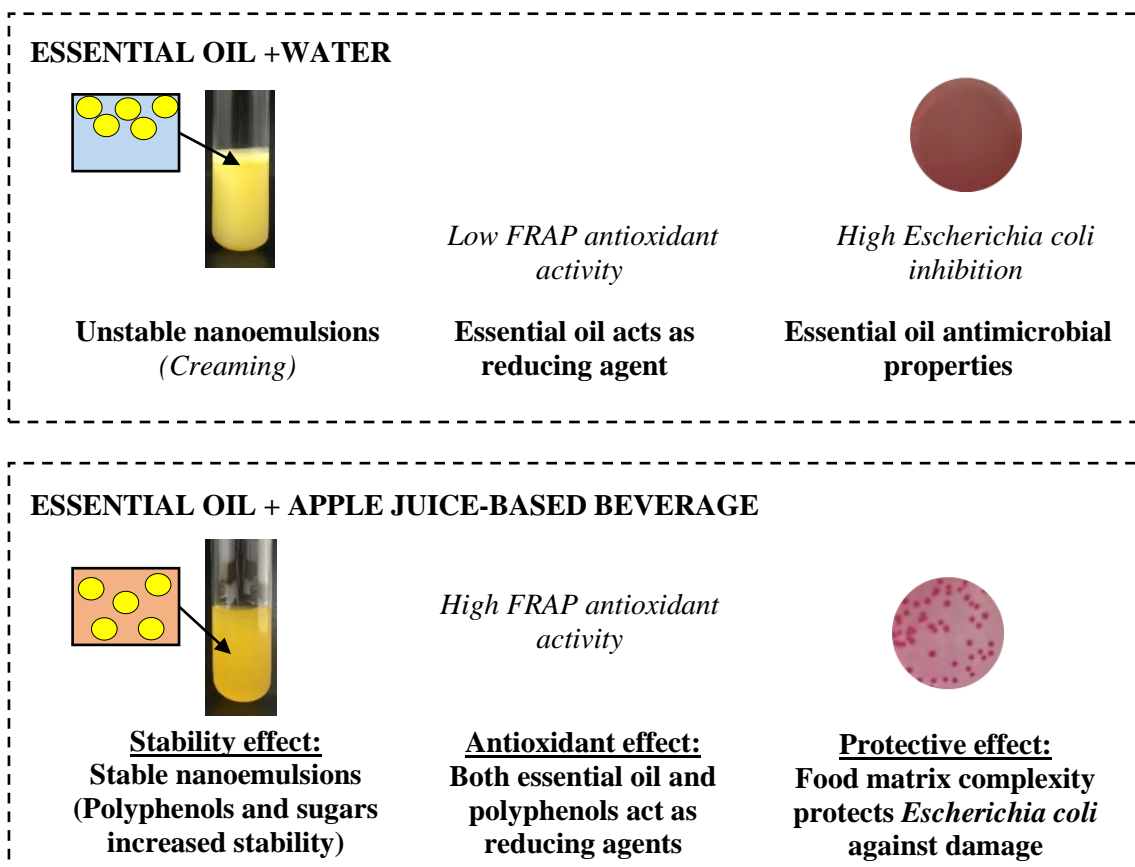Anna Molet-Rodríguez, Ana Turmo-Ibarz, Laura Salvia-Trujillo, Olga Martín-Belloso*

Abstract

Despite the proven antioxidant and antimicrobial efficiency of nanoemulsions as carriers of essential oils, there is scarce research on their behaviour once incorporated into complex food matrices. In the current work, lemongrass or mandarin essential oil (LEO or MEO) nanoemulsions were formulated using three different continuous phases (water, an apple juice model and an apple juice-based beverage). Droplet size, ζ-potential, colloidal stability as well as the antioxidant and antimicrobial activity were studied. The increase in the complexity of the continuous phase promoted the formation of nanoemulsions with smaller sizes. Consequently, creaming phenomena was prevented in complex systems. Moreover, nanoemulsions formulated using the apple juice-based beverage presented a high antioxidant activity, with values of up to 400 mg Eq. Trolox/mL, probably due to the presence of polyphenols. Nevertheless, nanoemulsions presented slower and lower inactivation kinetics at increasing complexity of the continuous phase, which may be related to the ability of sugars to protect cell damage. This work evidenced that antimicrobial nanoemulsions within complex food matrices lead to higher colloidal stability and antioxidant activity, but lower bactericidal activity than nanoemulsions alone. Hence, it provides valuable information for the design of complex foods with nanoemulsions as delivery systems of functional ingredients.

Graphical abstract

ESSENTIAL OIL +WATER

Low FRAP antioxidant activity

High Escherichia coli inhibition

Unstable nanoemulsions
(Creaming)

Essential oil acts as reducing agent

Essential oil antimicrobial properties

ESSENTIAL OIL + APPLE JUICE-BASED BEVERAGE

High FRAP antioxidant activity

Stability effect:
Stable nanoemulsions (Polyphenols and sugars increased stability)

Antioxidant effect:
Both essential oil and polyphenols act as reducing agents

Protective effect:
Food matrix complexity protects *Escherichia coli* against damage

Keywords

Nanoemulsions; essential oils; colloidal stability; antimicrobial activity; apple juice

Highlights

- The droplet size of nanoemulsions was reduced using an apple juice-based beverage.

- Apple juice-based beverage improved the creaming stability of nanoemulsions.

- Antioxidant activity was higher in the apple juice beverage than nanoemulsions.

- Lemongrass and mandarin essential oil nanoemulsions inactivated *Escherichia coli*.

- Nanoemulsions in a complex beverage have lower antimicrobial activity than in water.

1 Introduction

Essential oils (EOs) are natural hydrophobic substances obtained from the distillation of aromatic herbs, plants and fruit peels. They possess antimicrobial properties, thus being regarded as an alternative natural decontamination strategy to chemical preservatives against foodborne microorganisms (Hammer, Carson, & Riley, 1999). The principal components in EOs, which have been associated with their antimicrobial potential, are terpenoids and phenolic compounds (Burt, 2004; Pejin, Vujisic, Sabovljevic, Tesevic, & Vajs, 2011). Their hydrophobic nature allows them to interact with the bacterial cell membrane, altering its structure and making it more permeable (Lambert, Skandamis, Coote, & Nychas, 2001; Oussalah, Phane, & Lacroix, 2006). As a consequence, the leakage of the cellular content occurs, causing the viability loss of microbial cells (Helander et al., 1998). EOs also have been reported to present a strong antioxidant activity, thus being good candidates to enhance the antioxidant properties of foods (Adorjan & Buchbauer, 2010; Nikolić et al., 2013). However, their incorporation in aqueous food systems is a challenge due to their hydrophobicity, strong flavour and extreme volatility (Sell, 2010; Donsì & Ferrari, 2016; Sánchez-González, Vargas, González-Martínez, Chiralt, & Cháfer, 2011). In this regard, the encapsulation of EOs in oil-in-water nanoemulsions arises as an attempt to improve the stability and the delivery of antimicrobials to water-based food systems (Donsì, Annunziata, Sessa, & Ferrari, 2011; Jo et al., 2015). Due to their small droplet size (≤ 200 nm), nanoemulsions present several advantages over emulsions with larger droplet size. First, they are kinetically stable, thus remaining with the initial characteristics during long periods. Second, they scatter the light very weakly being almost transparent, which makes them suitable for being added into clear drinks and beverages. And third, nanoemulsions have a larger interfacial area than conventional emulsions and have been shown to interact with biological membranes to a higher extent. Thereby, in the last decade, nanoemulsions as delivery systems for EOs have been used as antimicrobial agents against foodborne microorganisms, such as *Escherichia coli (E.coli),* being one of the most pathogenic and resistant (Donsì et al., 2011; Salvia-trujillo, Rojas-Graü, Soliva-Fortuny, & Martín-Belloso, 2015). Despite the proven efficiency of EO-nanoemulsions as antimicrobial agents, there is scarce insight on their behaviour and antimicrobial activity once incorporated in food matrices. Plant-based foods such as fruit juices contain sugars (*e.g.,* fructose, glucose and sucrose) in the bulk continuous phase. In this regard, there is

evidence that EOs may weaken antimicrobial activities in fruit juices in comparison to water due to a possible protective effect of sugars in the bulk continuous phase (Friedman, Henika, & Mandrell, 2002; Guerra-Rosas, Morales-Castro, Ochoa-Martínez, Salvia-Trujillo, & Martín-Belloso, 2016). Moreover, sugars are also capable of modifying nanoemulsions oil/water interface composition by increasing the adsorbed surfactant (Ikeda, Miyanoshita, & Gohtani, 2013), which may result in an enhancement of their colloidal stability during storage.

The purpose of the present work was to address the potential of incorporating antimicrobial nanoemulsions into plant-based food matrices. In particular, the objective of this study was to determine the impact of the continuous phase composition being water, apple juice model (*i.e.,* fructose) and apple juice-based beverage on the stability and functionality of oil-in-water nanoemulsions containing EOs during 28 days of storage. In this study, creaming stability of the nanoemulsions was monitored by multiple light scattering (Turbiscan). Moreover, to evaluate their antioxidant activities, ferric reducing antioxidant power (FRAP) assay was used. In addition, *in vitro* antimicrobial activity against *E.coli* was assessed. The EOs used were lemongrass essential oil (LEO) (0.1 and 1% (w/w)) and mandarin essential oil (MEO) (1 and 2% (w/w)). Corn oil (CO) (0.1, 1 and 2% (w/w)) was used as a control.

2 Material and methods

2.1 Materials

LEO *(Cymbopogon citratus)* from Essential aroms[®] (Dietetica Intersa, Lleida, Spain), MEO (*Citrus reticulata L.)* kindly donated by Indulleida S.A. (Lleida, Spain) and CO (Koipesol Asua, Deoleo, Spain) were used as a lipid phase. Polyoxyethylene sorbitan monooleate (Tween 80) (Lab Scharlab, Barcelona, Spain) was used as non-ionic surfactant. Sodium alginate (MANUCOL[®]DH) was purchased from FMC Biopolymer Ltd. (Scotland, UK). D-Fructose obtained from Fisher Scientific (Thermo Fisher Scientific, GmbH, Karlsruhe, Germany) and DL-malic acid (99% purity) from Acros Organics (Thermo Fisher Scientific, GmbH, Karlsruhe, Germany) were utilized to formulate the apple juice model solution. A concentrated commercial clarified apple juice was kindly donated by Indulleida S.A. (Lleida, Spain).

Ultrapure Milli-Q water obtained from a Millipore filtration system (Merck, Darmstadt, Germany) was used for the preparation of all samples and solutions.

2.2 Formulation of the apple juice model and apple juice-based beverage.

Three different formulations with increasing levels of complexity, being water, an apple juice model and an apple juice-based beverage were used as a continuous phase of the emulsions and nanoemulsions, which composition is detailed in Table 1. Apple juice was chosen as emulsion destabilization can be easily observed due to its optical clarity. Soluble solids content and pH of both the apple juice model and the apple juice-based beverage were 9.5 ºBrix and 3.7, respectively. The formulation of the apple juice model consisted of a mixture of D-fructose (9.5% w/w) and DL-malic acid (0.3% w/w) in order to adjust the concentration of soluble solids and the pH. To obtain the apple juice-based beverage with the same soluble solids as the apple juice model, the concentrated commercial clarified apple juice was diluted. Sodium alginate (1% w/w) was added to all the continuous phases as emulsion stabilizer.

Table 1. Composition of the three continuous phases.

Continuous phase	Milli-Q water (% w/w)	Surfactant (Tween 80) (% w/w)	Thickening agent (Sodium alginate) (% w/w)	Sugar (D-Fructose) (% w/w)	Acid (DL-malic) (% w/w)	Concentrated clarified apple Juice (70ºBrix) (% w/w)
Water	97	2	1	-	-	-
Apple juice model	87.2	2	1	9.5	0.3	-
Apple juice-based beverage	83.4	2	1	-	-	13.6

2.3 Emulsion and nanoemulsion formation

The concentrations of each EO were set based on the reported minimum inhibitory concentration against *E. coli* (Hammer et al., 1999) to see if there is a reduction of the EO-nanoemulsions antimicrobial activity after being in contact with apple juice components. Thus, the lipid phase of the nanoemulsions consisted of 0.1 or 1% (w/w) for LEO and 1 or 2% (w/w) for MEO. Additionally, CO (0.1, 1 or 2% w/w) emulsion was

used as a control lipid phase. The formation of emulsions and nanoemulsions was carried out by mixing the lipid phase and Tween 80 (2% w/w) with water, the apple juice model solution or the apple juice-based beverage, respectively. Firstly, a coarse emulsion was made by blending the mixture with a laboratory T25 digital Ultra-Turrax mixer (IKA, Staufen, Germany) working at 13400 rpm for 2 min. Afterwards, the coarse emulsion was treated by ultrasonication (UP400S, Hielscher Ultrasound Technology, Teltow, Germany) for droplet size reduction. The ultrasound equipment had nominal power of 400 W and a frequency of 24 kHz equipped with a 22 mm sonotrode and was set at an amplitude of 30 μm. The coarse emulsion was pumped into a stainless steel ultrasonic flow cell with a peristaltic pump (model Selecta- PR 2003) set at 100 mL/min giving a residence time of 16.5 s. The ultrasonic flow cell was equipped with a stainless steel double layer with flowing cold water to avoid excessive heating of emulsions. The coarse emulsion was recirculated through the ultrasonic flow cell until it reached a total treatment time of 180s.

2.4 Physicochemical characterization

2.4.1 *Droplet size*

Oil droplet size was measured by dynamic light scattering (DLS) with a Zetasizer NanoZS laser diffractometer (Malvern Instruments Ltd., Worcestershire, U.K.) working at 633 nm, 25 ºC and equipped with a backscatter detector (173º). The average droplet diameter (nm) in intensity (%) was used to characterize the emulsions and nanoemulsions. Prior to measurements, samples were diluted in Milli-Q water using a dilution ratio of 1:9 sample-to-solvent. Refractive indexes of LEO, MEO and CO measured with a refractometer (ABBE-2WAJ, optic ivymen system®, Comecta SA, Barcelona, Spain) were 1.484, 1.475 and 1.473, respectively; and their absorbance was measured with a spectrophotometer (Jasco V-670, Tokyo, Japan) at 633 nm were 0.024, 0.004 and 0.010, respectively.

2.4.2 *ζ-potential*

The ζ -potential (mV) of the oil droplets was measured by phase analysis light scattering (PALS) with a Zetasizer NanoZS laser diffractometer (Malvern Instruments Ltd., Worcestershire, UK). Samples were diluted in Milli-Q water with a dilution factor of 1:9 sample-to-solvent and placed in a capillary cell to assess the electrophoretic mobility of the particles.

2.4.3 Continuous phase viscosity

Viscosity measurements (mPa·s) of the different continuous phases were performed by using a vibro-viscometer (SV-10, A&D Company, Tokyo, Japan) vibrating at 30 Hz, with constant amplitude (0.4 mm) and working at 25 °C. Aliquots of 10 mL of each sample were used for determinations.

2.4.4 Creaming stability

Creaming stability of emulsions and nanoemulsions was monitored by a Turbiscan ™Classic MA 2000 (Formulaction, Toulouse, France) during 28 days of storage at room temperature. The creaming phenomenon registered by the Turbiscan is shown as up peaks on the right part (< 50 mm) of the backscattering (BS) plot.

2.5 Antioxidant activity

The antioxidant activity of EO-nanoemulsions was determined by the ferric reducing antioxidant power (FRAP) assay, which measures the ability to reduce ferric ion (Fe^{3+}) to ferrous ion (Fe^{2+}). The FRAP procedure was conducted according to the method described by Benzie & Strain (1996) with minor modifications. The FRAP reagent was freshly prepared from 300 mmol/L acetate buffer (pH 3), 10 mmol/L 2,4,6- tripyridyl-s-triazine (TPTZ) made up in a 40 mmol/L HCl and 20 mmol/L $FeCl_3$ solution. All three solutions were mixed together in a 10:1:1 (w/w/w) ratio. Once the working solution was prepared, 150 µL of sample or Trolox standard was mixed with 2.85 mL of the working solution. The absorption of the reaction mixture was measured at 630 nm after 30 min of incubation at 25 ºC using a Shimadzu (UV-2401PC, Japan) spectrophotometer. The antioxidant capacity was calculated from a linear calibration curve and expressed as µg equivalents of Trolox ($FeSO_4·7H_2O$) per mL of sample.

2.6 Antimicrobial activity against inoculated *Escherichia coli*

Numerous studies have demonstrated the ability of *E. coli* to survive in acidic conditions, such as in fruit juices (Conner & Kotrola, 1995; Mazzotta, 2001). Moreover, it is one of the most pathogenic and resistant foodborne microorganisms. For that reason, the antimicrobial activity of emulsions and nanoemulsions with an apple juice-based beverage as continuous phase was assessed by evaluating the inactivation of inoculated

E.coli during 28 days of storage. The method used was a modification of that previously described by Ferreira et al. (2010). *E. coli* 1.107 (Laboratoire de Répression des Fraudes, Montpellier, France) was cultured in tryptone soy broth (Bioakar Diagnostic; Beauvais, France) and incubated at 37 ºC with continuous agitation at 120 rpm for 11 h to obtain cells in stationary growth phase. The final concentration reached in the culture was 10^8-10^9 colony-forming units/mL. A 0.5 mL-aliquot of overnight bacterial culture was mixed with 0.5 mL of nanoemulsions encapsulating LEO or MEO and 4.5 mL of aqueous solution. To determine the inactivation of *E. coli* populations, a 100 mL-aliquot of the bacterial suspensions was taken immediately after 30 min and 1, 3, 6, 9, 13, 21 and 28 days of contact time to be serially diluted and spread on McConkey agar (Biokar Diagnostics, Beauvais, France) plates. A control was performed with the same method, replacing the EOs by CO. Additionally, milli-Q water was used as a blank. Colony counts were determined after incubation of agar plates at 37 ºC for 24 h.

2.7   Statistical analysis

All experiments were assayed in duplicate and data was expressed as the mean with standard deviation. An analysis of variance was carried out and the Student's t test was run to determine significant differences at a 5% significance level ($p < 0.05$) with statistical software JMP Pro 14 (SAS Institute Inc.).

3 Results and discussion

3.1 Physicochemical characterization

3.1.1 *Initial droplet size and emulsion stability*

3.1.1.1 Initial droplet size

CO emulsions presented average droplet sizes above 400 nm, which were higher than those obtained for the nanoemulsions formulated with EOs (< 260 nm) (Fig. 1). The efficiency of droplet disruption within a high-pressure homogenizer usually increases as the viscosity of the disperse phase decreases (Walker, Gumus, Decker, & McClements, 2017). In general, long-chain triglycerides such as those of CO has high viscosity values, thus reducing their droplet size by high energy emulsification methods is less efficient than using oils with lower viscosity such as EOs (Qian & McClements, 2011). Moreover, it is well-known that smaller droplets are produced when the polarity of the oil phase used is high, which reduces the interfacial tension at the oil/water interface (Salvia-trujillo et al.,2015; Ziani, Fang, & McClements, 2012). Specifically, LEO stem from the *Poaceae* family and their major constituents (neral and geranial) are aldehydes, which are polar by nature (Viuda-Martos et al., 2010). Instead, MEO, which belongs to the *Rutaceae* family, is mainly constituted by cyclic hydrocarbons, which are non-polar (Espina et al., 2011; Raut & Karuppayil, 2014). Consequently, it would be expected LEO to be able to form smaller droplets than MEO.

In general, it was observed that the smallest oil droplets were obtained when the highest oil concentrations were used, regardless of the oil type (Fig. 1). In fact, decreasing the CO concentration from 1% to 0.1% (w/w) resulted in a significant increase in droplet size from 473.81 ± 129.50 to 829.81 ± 58.66 nm. Similarly, there was an appreciable increase in the average droplet size of LEO or MEO nanoemulsions when decreasing the lipid concentration in the formulation, which might be attributed to the high surfactant concentration used. When the surfactant concentration is higher than the oil concentration, there might be an excess of non-adsorbed Tween 80 molecules in the bulk aqueous phase, which in turn may promote the formation of surfactant micelles. These non-adsorbed surfactant micelles may lead to an increase in attraction forces between the droplets due to depletion flocculation that ultimately causes droplet coalescence and consequently a droplet size increase after emulsification (Jafari, He, & Bhandari, 2007; Teo et al., 2016).
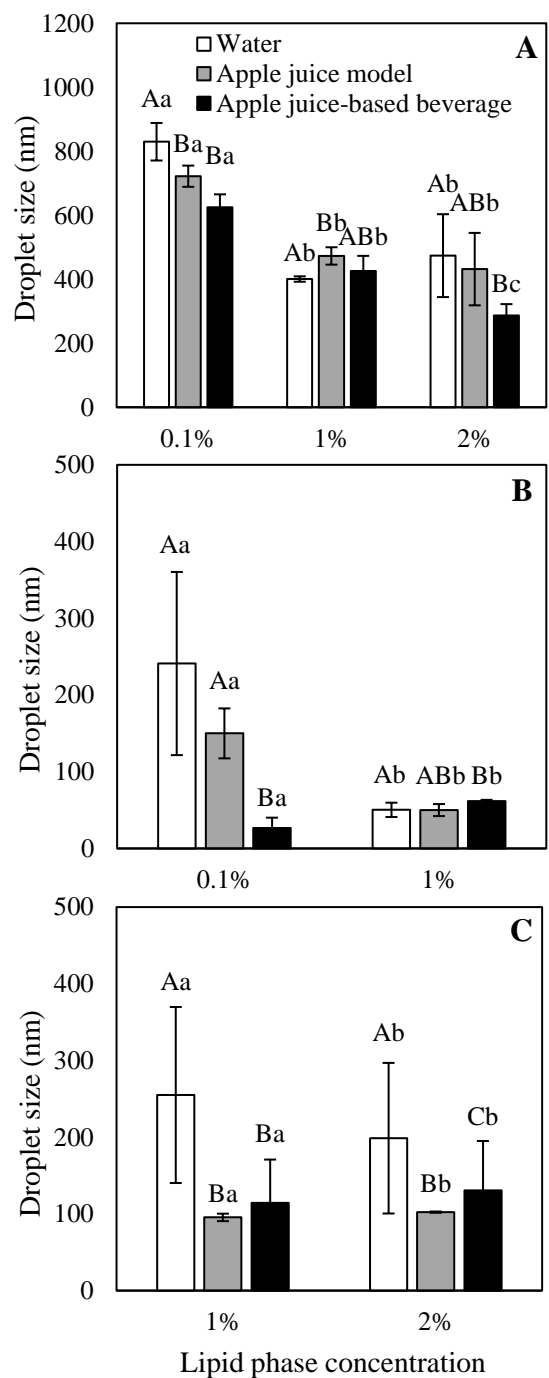
Figure 1. Average droplet size (nm) of emulsions and nanoemulsions formulated with corn oil (CO) (A), lemongrass essential oil (LEO) (B) or mandarin essential oil (MEO) (C) at different concentrations. The aqueous phase consisted of water (white bars), apple juice model (gray bars) or apple juice-based beverage (black bars). Different capital letters mean significant differences ($p < 0.05$) on the droplet size of each concentration, whereas different lowercase letters mean significant differences ($p < 0.05$) on the droplet size of each continuous phase. Mean ± SD, n=2.

Irrespective of the oil used in the system, a droplet size decrease was observed when the continuous phase contained sugars (*i.e.,* apple juice model and apple juice-based beverage) (Fig.1). For instance, the average droplet size of the nanoemulsions containing 0.1% (w/w) of CO and formulated with water was 829.81 ± 58.66 nm, while the apple juice model or the apple juice-based beverage led to smaller sizes, with values of 722.11 ± 33.12 and 625.40 ± 40.04 nm, respectively. Increasing the continuous phase viscosity has been reported to cause a decrease in the droplet size of nanoemulsions, due to an increased shear stress in high energy homogenizers (Qian & McClements, 2011). Accordingly, it was observed that the apple juice-based beverage had higher viscosity values than water and apple juice model continuous phases, being 56.87 ± 1.96, 22.10 ± 0.62 and 28.01 ± 1.14 mPa·s, respectively. Moreover, other authors have attributed the formation of smaller droplets in the presence of sugar to the modification of the surfactant affinity to the oil/water interface (Urakami, Ukada, Amano, & Ohtani, 2005). It was hypothesized that a single molecule of sugar in the continuous phase might bind with water molecules contributing to a higher surfactant hydrophobicity, thereby facilitating the deposition of Tween 80 at the interface of the oil droplets. Moreover, the presence of other surface-active molecular species such as phenolic compounds could contribute in explaining the smaller droplet size observed since they might adsorb to the oil-water interface and contribute in the overall droplet size reduction during emulsification (Di Mattia, Sacchetti, & Pittia, 2011).

3.1.1.2 Emulsion and nanoemulsion stability

Emulsions and nanoemulsions containing CO and MEO experienced a BS increase at the top part of the tube after 9 days of storage, which indicates droplet creaming (Fig. 2A and C). This effect can be attributed to the ability of the alginate molecules to promote droplet flocculation in emulsions through a bridging or depletion mechanism. Bridging flocculation occurs when a biopolymer simultaneously binds to the surfaces of two or more droplets. In contrast, depletion flocculation occurs due to the presence of sufficiently high levels of non-adsorbed biopolymer molecules in the aqueous phase surrounding the droplets (Dickinson, 2003). Consequently, the effective size of the droplets might increase and promote the upward movement of flocs due to their lower density compared to the surrounding liquid. It should be noted that any flocs present in an emulsion that are held together by osmotic attraction are usually dissociated when the

sample is diluted for droplet size measurements (Klang & Valenta, 2011), explaining that the mean droplet size did not change over 28 days of storage (Fig. 3). This phenomenon occurs because dilution causes the biopolymer concentration to fall below the critical amount required to induce bridging or depletion flocculation.
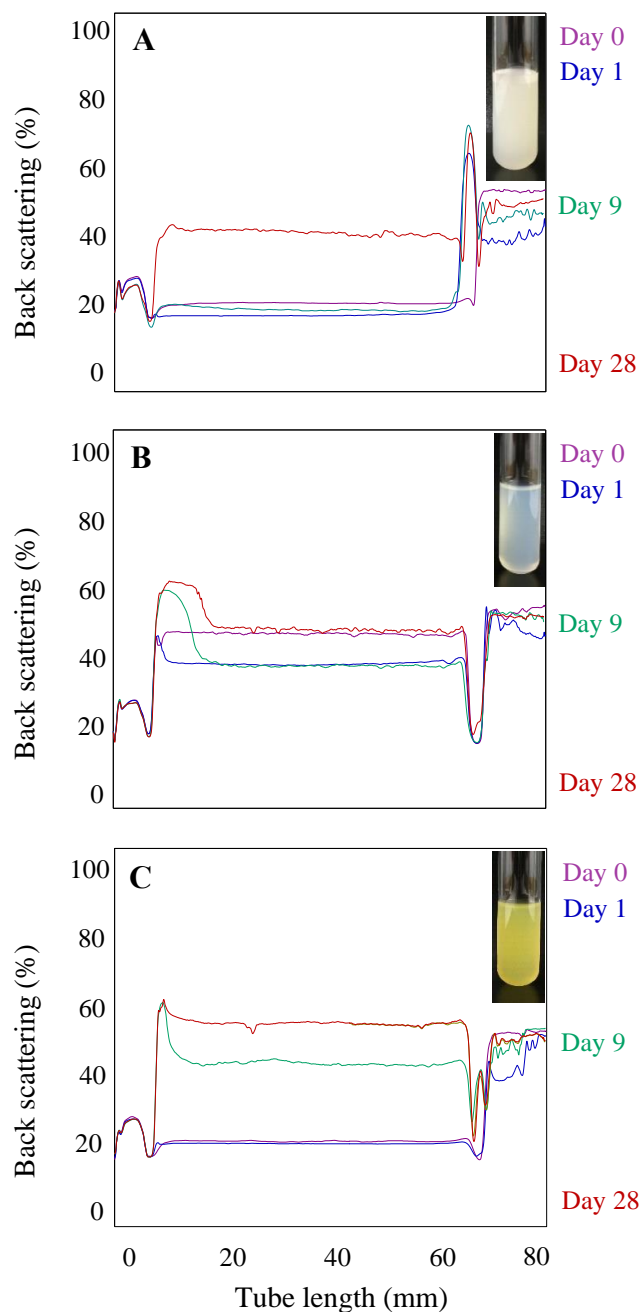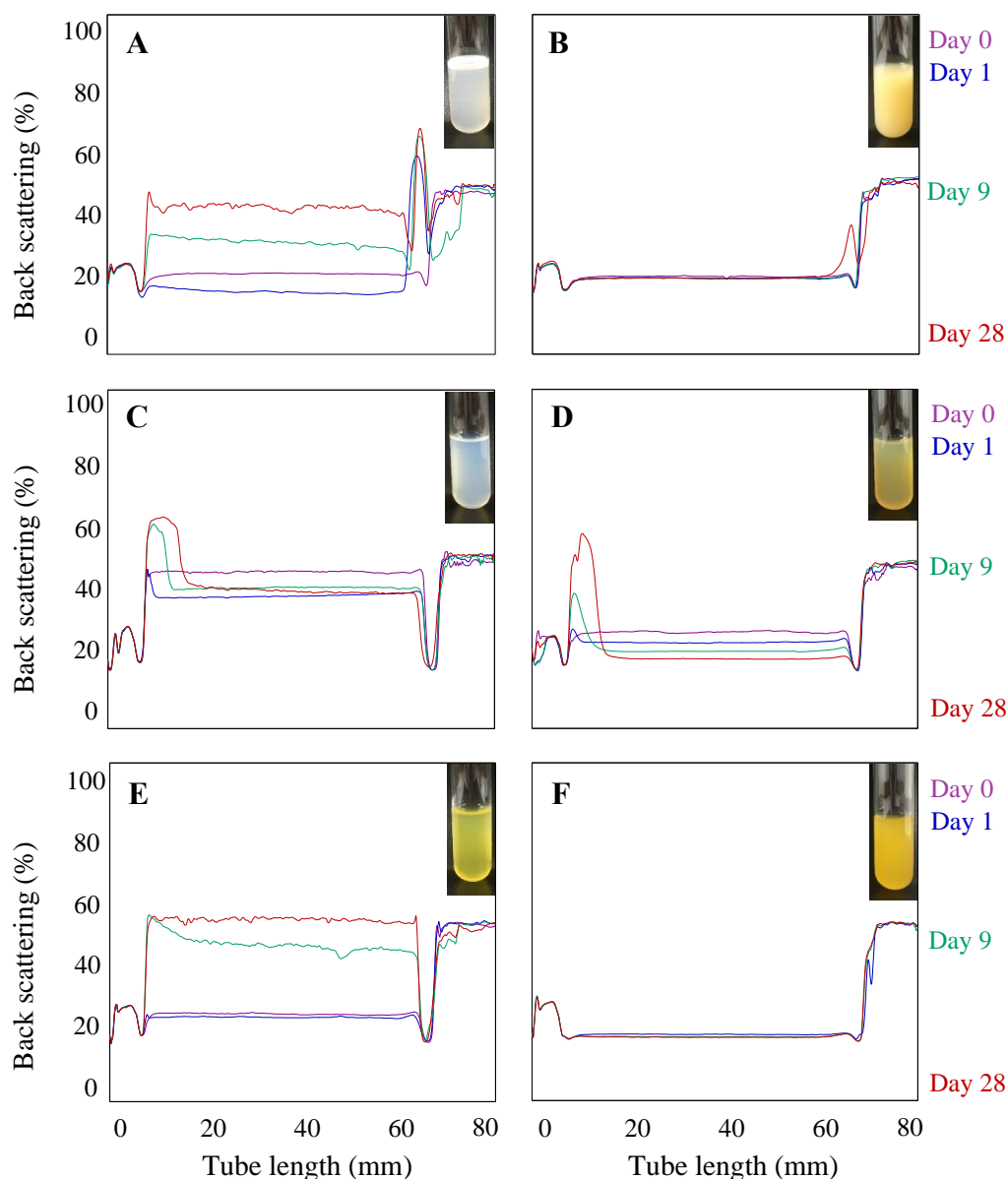

Figure 2. Backscattering distribution (%) of emulsions and nanoemulsions formulated with 1% (w/w) of corn oil (CO) (A), lemongrass essential oil (LEO) (B) or mandarin essential oil (MEO) (C). The aqueous phase consisted of water.

In the case of LEO-nanoemulsions, it seems that there was no creaming throughout storage as no serum layer was observed visually, neither had an increase in the BS at the top part of the tub (Fig. 2B). However, these nanoemulsions exhibited an increase in the BS at the bottom of the tube, which indicates clarification. This instability process is also related to the upward movement of droplets, suggesting the appearance of creaming. The cream layer was more pronounced in emulsions and nanoemulsions containing CO and MEO compared to LEO, which might be related to differences in the electrostatic repulsion between oil droplets. CO and MEO presented a weaker charge at the oil/water interface (see section 3.1.2), generating a strong electrostatic attraction between droplets and, as a consequence, a lower stability against creaming. Exceptionally, nanoemulsions containing LEO at 0.1% (w/w) exhibited a droplet size increase throughout storage (Fig. 3D, E and F), indicating that oil droplets coalesced.

Emulsions and nanoemulsions stability against creaming was also influenced by the continuous phase composition. BS distribution profiles of emulsions and nanoemulsions have shown that their formulation with the apple juice-based beverage had higher stability against creaming than using the apple juice model (Fig. 4). It has been reported that increasing the continuous phase viscosity may help to minimize the droplet movement in the fluid so retarding gravitational separation of lipid droplets (McClements, Decker, & Weiss, 2007). As mentioned in section 3.1.1.1, the apple juice-based beverage presented higher viscosity values than the apple juice model, explaining the stability differences. Besides this, the presence of not only fructose but also glucose and sucrose in the apple juice-based beverage can facilitate a complete coverage of the oil/water interface, avoiding creaming. The hydration number of fructose is lower (4.6) compared to glucose and sucrose (5.5 and 6.6, respectively), therefore, less water molecules might be present in the apple juice-based beverage (Ikeda et al, 2013). As a result, Tween 80 would have become more hydrophobic and consequently, its affinity with the oil/water interface would have been enhanced.
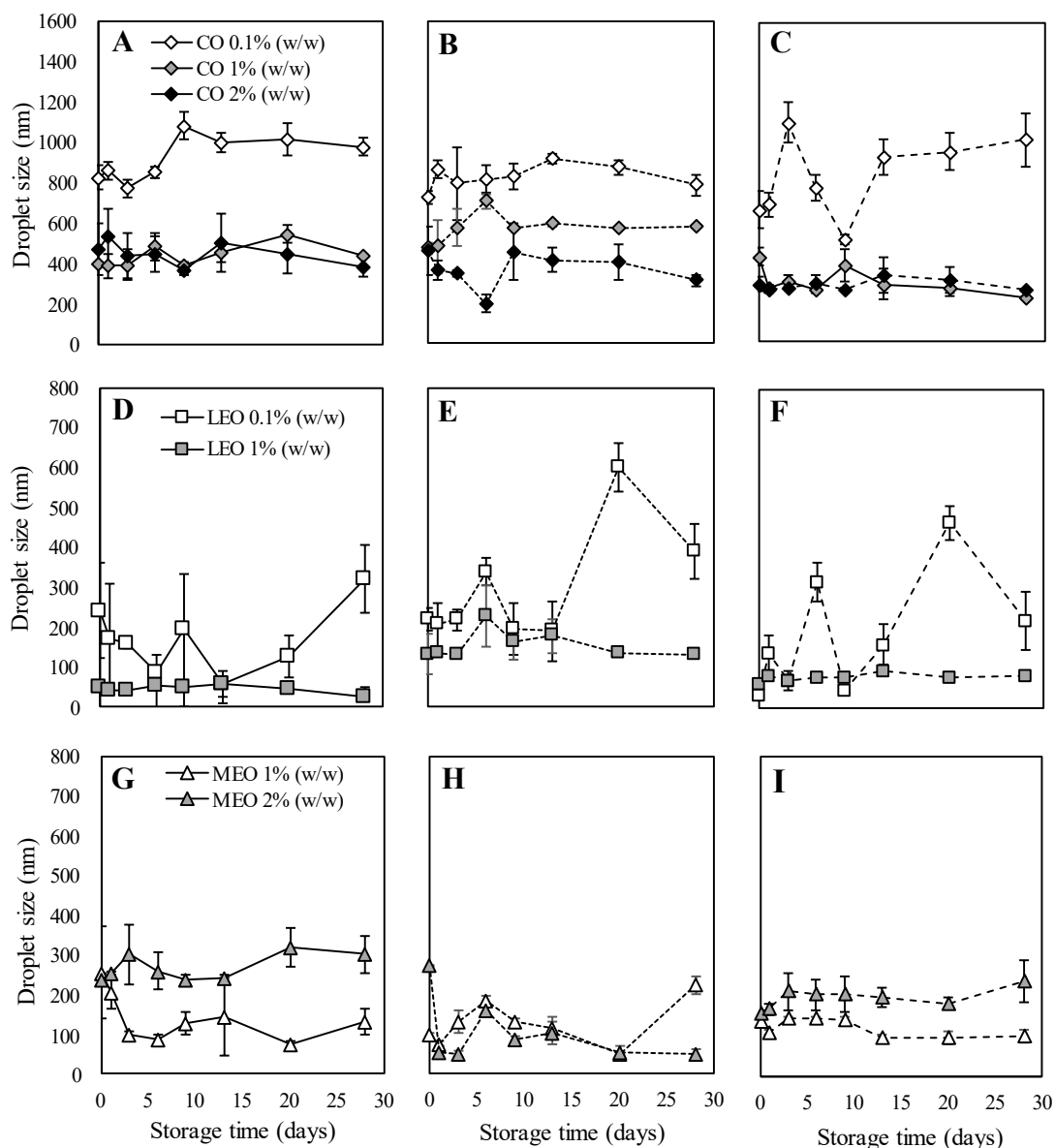
Figure 3. Droplet size (nm) throughout storage at 4 ºC of emulsions and nanoemulsions formulated with corn oil (CO) (A,B,C), lemongrass essential oil (LEO) (D,E,F) or mandarin essential oil (MEO) (G,H,I) at different concentrations (white symbols, 0.1% w/w; gray symbols, 1% w/w; black symbols, 2% w/w) during 28 days of storage. The lipid phase consisted of 0.1 or 1% (w/w) for LEO and 1 or 2% w/w for MEO. Additionally, CO (0.1, 1 or 2% w/w) emulsion was used as a control lipid phase. The continuous phase consisted of water (continuous line), apple juice model (dotted line) or apple juice-based beverage (hyphened line). Mean ± SD, n=2.

Figure 4. Backscattering distribution (%) of emulsions and nanoemulsions formulated with 1% (w/w) of corn oil (CO) (A,B), lemongrass essential oil (LEO) (C,D) or mandarin essential oil (MEO) (E,F). The aqueous phase consisted of an apple juice model (left panel) and apple juice-based beverage (right panel).
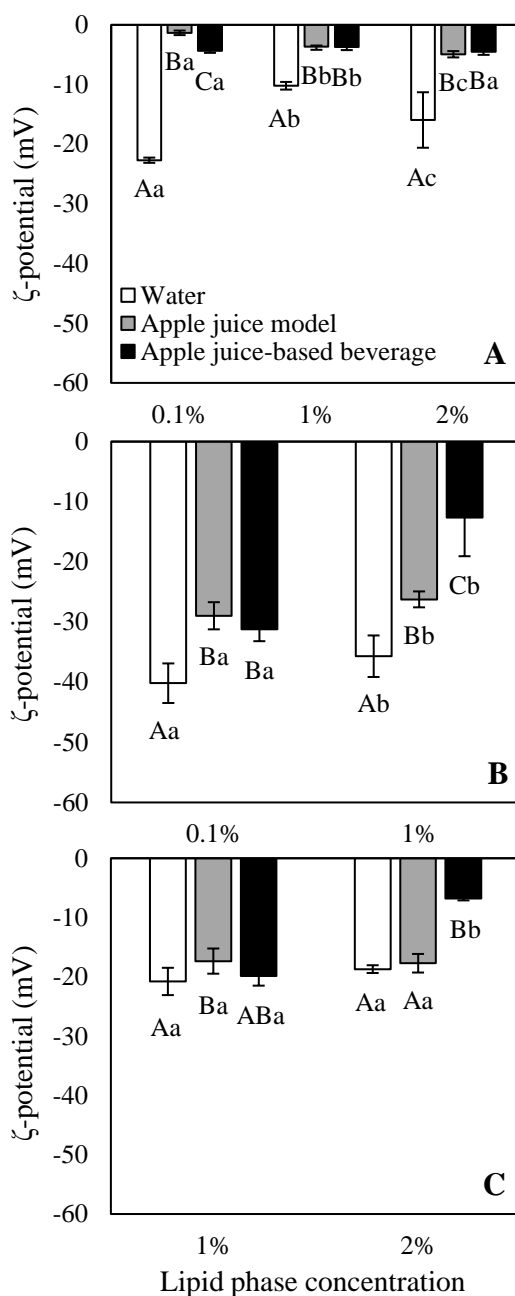
3.1.2 ζ-potential

In this study, despite using a non-ionic surfactant, all emulsions and nanoemulsions showed negative ζ-potential values ranging from -1.37 ± 0.42 to -40.17 ± 3.29 mV (Fig. 5). In fact, the ζ-potential of emulsions and nanoemulsions was highly related to the type of oil used. Nanoemulsions containing LEO presented strong negative charges, with values below -40 mV, while MEO-nanoemulsions and CO-emulsions had values less negative than -20 mV. The anionic nature of the oil droplets might be attributed to several

reasons. First, oil droplets naturally possess negative charge due to the presence of anionic hydroxyl groups (OH$^-$) in the water or oil used to prepare the emulsion (Marinova et al., 1996). Second, adsorption of polysorbate molecules to droplet surfaces has shown negative electrical charges when the pH of the emulsion is higher than 4 (Hsu & Nacu, 2003). And third, sodium alginate present in the aqueous phase of emulsions and nanoemulsions is anionic and might contribute to the overall negative charge of the oil droplets. Namely, Salvia-Trujillo, Rojas-Graü, Soliva-Fortuny, & Martín-Belloso (2013) observed strong negative electrical charges (-46.00 mV) in nanoemulsions formulated with Tween 80 and sodium alginate (1% w/w) in the aqueous phase. Thus, the final interface composition of the present emulsions and nanoemulsions may be determined by the competitive adsorption of Tween 80 and alginate (Gomes, Costa, & Cunha, 2018). In fact, Artiga-Artigas, Guerra-Rosas, Morales-Castro, Salvia-Trujillo, & Martín-Belloso (2018) reported that the competitive adsorption between alginate and Tween 80 was dependent on the EO type, since the higher the affinity between the hydrophilic part of the polymer and the EO, the more negative the ζ-potential values.

Additionally, the oil phase concentration highly influenced the ζ-potential, which decreased when increasing the oil phase concentration (Fig. 5). For instance, emulsions containing 0.1, 1 and 2% (w/w) of CO exhibited ζ-potential values of -22.68 ± 0.44, -10.20 ± 0.64 and -15.94 ± 4.65 mV, respectively. ζ-potential values determined by light scattering techniques are highly sensitive to the dispersed phase concentration. At high oil concentrations, the major component at the oil/water interface is oil (non-polar), generating a decrease in the available OH$^-$ groups from the aqueous phase that are oriented towards the oil/water interface, consequently leading to a reduction in the droplet electrical charge.

Moreover, there was a significant effect of the continuous phase composition on the ζ-potential of emulsions and nanoemulsions, showing a less negative electrical charge when increasing the complexity of the continuous phase. On the one hand, emulsions and nanoemulsions formulated with water exhibited negative electrical charges with values around -10, -35 and -18 mV for CO, LEO and MEO, respectively. On the other hand, emulsions and nanoemulsions formulated with the apple juice model or the apple juice-based beverage, exhibited a weaker surface charge with values up to -1.37 ± 0.42, -12.65 ± 6.41 and -6.80 ± 0.31 mV for CO, LEO and MEO, respectively. This might be attributed

to the fact that glucose and sucrose present in the apple juice-based beverage, show a great hydration ability and this would generate a lack of water molecules in the continuous phase. This, in turn, might contribute to the decrease in the ionized OH^- groups from water molecules, causing a reduction in the negative charge of the oil droplets.

Figure 5. ζ-potential (mV) of emulsions and nanoemulsions formulated with corn oil (CO) (A), lemongrass essential oil (LEO) (B) or mandarin essential oil (MEO) (C) at different concentrations. The continuous phase consisted of water (white bars), apple juice model (gray bars) or apple juice-based beverage (black bars). Different capital letters mean significant differences (p < 0.05) on the ζ-potential of each concentration. Different lowercase letters mean significant differences (p < 0.05) on the ζ-potential of each continuous phase. Mean $\pm$ SD, n=2.

Moreover, the presence of ionizable species such as mineral cations from dissolved salts might contribute in reducing the negative electrical charge due to a screening effect. These results evidence that the presence of water-soluble species in the surrounding aqueous phase of complex food systems might determine their droplet surface electrical charge.

3.2 Antioxidant capacity

The antioxidant activity of emulsions and nanoemulsions was determined by the oil type and concentration as well as by the continuous aqueous phase composition (Fig. 6). Nanoemulsions formulated with LEO showed higher antioxidant activity than CO and MEO (Fig. 6). In this regard, LEO-nanoemulsions at 1% (w/w) showed antioxidant values of 84.04 ± 0.62 µg Eq. Trolox/mL, while for CO or MEO-emulsions were 20.44 ± 0.51 and 15.63 ± 0.64 µg Eq. Trolox/mL, respectively. Therefore, the antioxidant activity of emulsions and nanoemulsions is mainly governed by the molecular structure of the main components of the lipid phase. The reducing power of molecular species determined by FRAP assay is generally associated with the presence of reductants able to donate a hydrogen atom and therefore, breaking the free radical chain (Olszowy & Dawidowicz, 2016). In this context, the presence of aldehyde groups as major constituents in LEO may have increased their reducing power, whereas MEO is mainly composed of hydrocarbon chains without reducing power.

The continuous phase composition mainly determined the antioxidant capacity of emulsions and nanoemulsions. In fact, the antioxidant activity values of nanoemulsions formulated within the apple juice-based beverage were at least two times higher as compared to the nanoemulsions formulated using water or an apple juice model (Fig. 6). For instance, the FRAP antioxidant activity of emulsions and nanoemulsions formulated using the apple juice-based beverage as continuous aqueous phase and with a lipid phase of 1% (w/w) CO, LEO or MEO was 188.66 ± 11.32, 211.14 ± 0.64 and 145.19 ± 5.70 µg Eq. Trolox/mL, respectively. Nevertheless, their antioxidant activity when formulated with water was below 100 µg Eq. Trolox/mL. These significantly higher values observed for the systems formulated with the apple juice-based beverage might be due to the fact that it is rich in polyphenolic compounds ($\sim$13 mg/L), including hydroxycinnamic acids, flavanols, and dihydrochalcones. They usually have high redox potentials, which allow them to act as reducing agents (Stracke, Rufer, Weibel, Bub, & Watzl, 2009; Suárez-Jacobo et al., 2011). In fact, even though there are no previously reported data about the

use of apple juice as a continuous phase for nanoemulsions formulation, there is strong evidence that would support the relationship between FRAP antioxidant capacity and the total polyphenolic content of apple juices (Suárez-Jacobo et al., 2011).
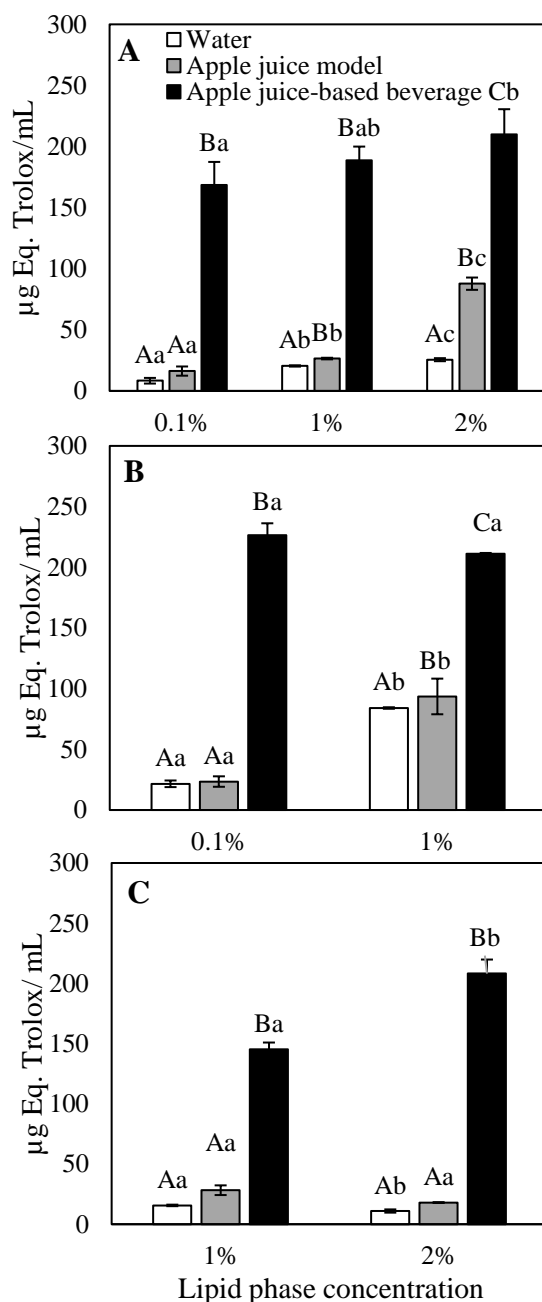

Figure 6. Trolox equivalent antioxidant capacity (µg/mL) of samples measured by the FRAP assay. Emulsions and nanoemulsions were formulated with corn oil (CO) (A), lemongrass essential oil (LEO) (B) or mandarin essential oil (MEO) (C) at different concentrations. The continuous phase consisted of water (white bars), apple juice model (gray bars) or apple juice-based beverage (black bars). Different capital letters mean significant differences ($p < 0.05$) on the Trolox equivalent antioxidant capacities of each concentration. Different lowercase letters mean significant differences ($p < 0.05$) on the Trolox equivalent antioxidant capacities of each continuous phase. Mean ± SD, n=2.

3.3   Antimicrobial activity

The antimicrobial activity of emulsions and nanoemulsions was assessed by determining the *E.coli* survival fraction during 28 days of storage (Fig. 7). The type of lipid phase and its concentration highly determined the bacterial killing potential of the antimicrobial nanoemulsions, being those formulated with EO the ones with higher antimicrobial activity in comparison to CO. In this regard, CO-emulsions (1% w/w) presented less than 2 log-reduction of *E. coli* after 28 days (Fig. 7A), which might account for the natural bacterial cell death during time. Nevertheless, nanoemulsions containing 1% (w/w) of either LEO or MEO were effective in reducing the *E.coli* population since they exhibited more than 5 log-reduction after being in contact for 28 days (Fig. 7B and C). The delivery mechanism of volatile compounds from nanoemulsions might be explained by the destabilization of the interfacial layer of small molecule non-ionic surfactants due to their interaction with the microbial cell since they tend to associate with some constituents of the biological membrane (Pérez-Conesa, Cao, Chen, McLandsborough, & Weiss, 2011). Nevertheless, nanoemulsions containing MEO showed a slower inactivation of the *E. coli* population in comparison with LEO, which evidences a slower release of the antimicrobial compounds present in the lipid core. In this sense, LEO-nanoemulsions presented identical *E. coli* population reduction immediately after being in contact with the microorganism and after 28 days with values of 7.20 ± 0.01 log-units, whereas MEO-nanoemulsions gradually increased the *E.coli* dead cells over time from values of 1.24 ± 0.03 to 5.89 ± 0.16 log-units. The differences in the bacterial killing performance of nanoemulsions are probably related to the intrinsic chemical composition of each EO (Friedman et al., 2002). As mentioned in section 3.2, LEO is mainly composed by components which have an aldehyde group conjugated to a carbon double bond, which is highly electronegative. Thus, implying an increase in the antimicrobial activity of the molecule as it may interfere in biological processes involving electron transfer and thus causing the death of the bacteria (Dorman, Deans, Merr, & Myrtaceae, 2000). On the contrary, cyclic hydrocarbons such as D-limonene, which can be found in MEO, do not have functional groups, exhibiting less efficacy against *E.coli* (Ling, Kormin, Abidin, & Anuar, 2019; Sokovicx́, Glamočlija, Marin, Brkić, & Van Griensven, 2010). Moreover, the differences in antimicrobial activity of LEO and MEO nanoemulsions might also be related to their droplet size. In fact, LEO presented smaller droplet sizes than MEO and therefore had a higher total surface area exposed to microbial cells, probably contributing

in the higher antimicrobial activity observed (Salvia-Trujillo, Rojas-Graü, Soliva-Fortuny, & Martín-Belloso, 2014).
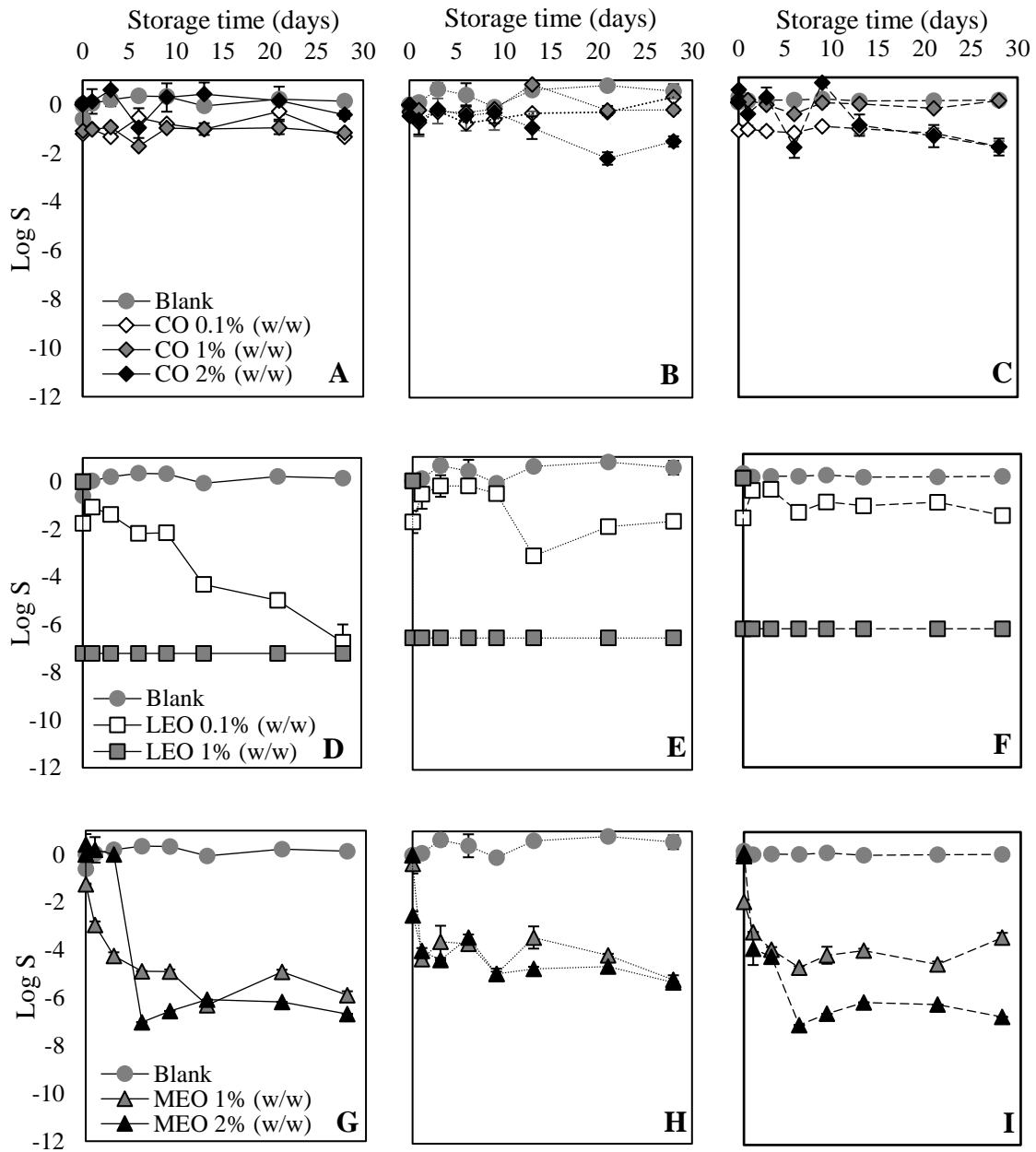
Figure 7. Survival fraction of *Escherichia coli* after contact with emulsions and nanoemulsions formulated with corn oil (CO) (A,B,C), lemongrass essential oil (LEO) (D,E,F) or mandarin essential oil (MEO) (G,H,I) at different concentrations (white symbols, 0.1% w/w; gray symbols, 1% w/w; black symbols, 2% w/w) during 28 days of storage. The lipid phase consisted of 0.1 or 1% (w/w) for LEO and 1 or 2% w/w for MEO. Additionally, CO (0.1, 1 or 2% w/w) emulsion was used as a control lipid phase. The aqueous phase consisted of an aqueous solution (continuous line), apple juice model (dotted line) or apple juice-based beverage (hyphened line). Data shown are a mean ± standard deviation. Mean ± SD, n=2.

Interestingly, the composition of the continuous aqueous phase also had a strong influence on the *E. coli* inactivation by the antimicrobial nanoemulsions. In fact, the more complex the continuous phase, the less efficiency against *E.coli* (Fig. 7). This behaviour was specifically noticeable in the case of LEO or MEO nanoemulsions. Nanoemulsions formulated with 0.1% (w/w) LEO and water as continuous phase showed a high bacterial reduction (6.74 ± 0.75 log-units), whereas those formed within the model or the apple juice-based beverage at the same LEO concentration exhibited only 1.67 ± 0.18 and 1.56 ± 0.20 log-units of reduction, respectively after 28 days of storage. On the one hand, the presence of nutrients, such as fructose, glucose and sucrose in food matrices may enable *E.coli* to repair damaged cells faster (Gill, Delaquis, Russo, & Holley, 2002). On the other hand, it has been previously observed by Skandamis, Tsigarida, & Nychas (2000) a restricted diffusion of EOs in complex food matrices, which was attributed to the increase in the medium viscosity and subsequently reducing their efficacy against pathogenic microorganisms. In this sense, the increase in viscosity caused by the presence of alginate at low pH in both the apple juice model and the apple juice-based beverage might have contributed to limitate the diffusion of EOs to the *E.coli* cell membrane.

4 Conclusions

In the present work, a significant influence of the oil type and concentration, as well as the continuous phase composition on the colloidal stability, antioxidant and antimicrobial activities of nanoemulsions containing EOs was evidenced. When nanoemulsions are formulated within complex food systems, they presented a higher colloidal stability and antioxidant activity in comparison to nanoemulsions in water, yet their bacterial killing efficacy against foodborne pathogenic microorganisms might be compromised. Specifically, the formation of antimicrobial nanoemulsions within complex food matrices, such as apple juice, led to smaller droplet sizes and contributed to the overall colloidal stability of the emulsified systems. This fact might be attributed to the decrease of water molecules in the continuous phase, enhancing the surfactant adsorption at the oil/water interface or due to the presence of surface-active molecules in vegetable-based foods, such as polyphenols. Moreover, even though using the apple juice-based beverage for nanoemulsions formulation showed less negatively charged oil droplets, and therefore less repulsion forces between them, they showed higher creaming stability, which reinforces the theory that a complex continuous phase might positively contribute to the

overall stability of the colloidal system. However, in the presence of a complex aqueous phase consisting on an apple juice-based beverage, EO nanoemulsions presented a lower antimicrobial capacity than nanoemulsions in water, thus evidencing the protective effect of the complex aqueous phase to the bacterial cell damage. This work significantly contributes to elucidate the role of food matrix complexity of nanoemulsions as delivery systems of food ingredients, such as antimicrobials, in order to establish dose-response mechanisms for bacterial inactivation and ultimately food preservation. Nonetheless, further studies regarding the effectivity of antimicrobial nanoemulsions against other microorganisms and in other fruit juices would be needed in order to fully understand their bacterial killing mechanism in complex food matrices.

5 Funding

The funding sources have no involvement on the design of this study; in the collection, analysis and interpretation of data; in the writing of the report; or in the decision to submit the article for publication.

6 CRediT authorship contribution statement

Anna Molet-Rodríguez: Methodology, Formal analysis, Investigation, Writing - original draft, Visualization. **Ana Turmo-Ibarz:** Investigation. **Laura Salvia-Trujillo:** Conceptualization, Formal analysis, Writing - review & editing, Visualization, Supervision, Funding acquisition, Project administration. **Olga Martín-Belloso:** Conceptualization, Writing - review & editing, Supervision, Funding acquisition, Project administration.

7 Declaration of competing interest

None.

8 Acknowledgements

9 References

Adorjan, B., & Buchbauer, G. (2010). Biological properties of essential oils: An updated review. *Flavour and Fragrance Journal*, *25*(6), 407–426.

Artiga-Artigas, M., Guerra-Rosas, M. I., Morales-Castro, J., Salvia-Trujillo, L., & Martín-Belloso, O. (2018). Influence of essential oils and pectin on nanoemulsion formulation: A ternary phase experimental approach. *Food Hydrocolloids*, *81*, 209–219.

Benzie, I.F. and Strain, J. (1996). The Ferric Reducing Ability of Plasma (FRAP) as a Measure of "Antioxidant Power": The FRAP Assay. *Analytical Biochemistry*, *239*(1), 70–76.

Burt, S. (2004). Essential oils: their antibacterial properties and potential applications in foods—a review. *International Journal of Food Microbiology*, *94*(3), 223–253.

Conner, D. E., & Kotrola, J. S. (1995). Growth and survival of Escherichia coli O157:H7 under acidic conditions. *Applied and Environmental Microbiology*, *61*(1), 382–385.

Di Mattia, C. D., Sacchetti, G., & Pittia, P. (2011). Interfacial Behavior and Antioxidant Efficiency of Olive Phenolic Compounds in O/W Olive oil Emulsions as Affected by Surface Active Agent Type. *Food Biophysics*, *6*(2), 295–302.

Dickinson, E. (2003). Hydrocolloids at interfaces and the influence on the properties of dispersed systems. *Food Hydrocolloids*, *17*(1), 25–39.

Donsì, F., Annunziata, M., Sessa, M., & Ferrari, G. (2011). Nanoencapsulation of essential oils to enhance their antimicrobial activity in foods. *LWT - Food Science and Technology*, *44*(9), 1908–1914.

Donsì, F., & Ferrari, G. (2016). Essential oil nanoemulsions as antimicrobial agents in food. *Journal of Biotechnology*, *233*, 106–120.

Dorman, H. J. D., Deans, S. G., Merr, L., & Myrtaceae, P. (2000). Antimicrobial agents from plants : antibacterial activity of plant volatile oils. *Journal of Applied Microbiology, 88*(2), 308–316.

Espina, L., Somolinos, M., Lorán, S., Conchello, P., García, D., & Pagán, R. (2011). Chemical composition of commercial citrus fruit essential oils and evaluation of their antimicrobial activity acting alone or in combined processes. *Food Control*, *22*(6), 896–902.

Ferreira, J. P., Alves, D., Neves, O., Silva, J., Gibbs, P. A., & Teixeira, P. C. (2010). Effects of the components of two antimicrobial emulsions on food-borne pathogens. *Food Control*, *21*(3), 227–230.

Friedman, M., Henika, P. R., & Mandrell, R. E. (2002). Bactericidal activities of plant essential oils and some of their isolated constituents against Campylobacter jejuni, Escherichia coli, Listeria monocytogenes, and Salmonella enterica. *Journal of Food Protection*, *65*(10), 1545–1560.

Gill, A. O., Delaquis, P., Russo, P., & Holley, R. A. (2002). Evaluation of antilisterial action of cilantro oil on vacuum packed ham. *International Journal of Food Microbiology*, *73*(1), 83–92.

Gomes, A., Costa, A. L. R., & Cunha, R. L. (2018). Impact of oil type and WPI/Tween 80 ratio at the oil-water interface: Adsorption, interfacial rheology and emulsion features. *Colloids and Surfaces B: Biointerfaces*, *164*, 272–280.

Guerra-Rosas, M. I., Morales-Castro, J., Ochoa-Martínez, L. A., Salvia-Trujillo, L., & Martín-Belloso, O. (2016). Long-term stability of food-grade nanoemulsions from high methoxyl pectin containing essential oils. *Food Hydrocolloids*, *52*, 438-446.

Hammer, K. A., Carson, C. F., & Riley, T. V. (1999). Antimicrobial activity of essential oils and other plant extracts. *Journal of Applied Microbiology*, *86*(6), 985–990.

Helander, I. M., Alakomi, H. L., Latva-Kala, K., Mattila-Sandholm, T., Pol, I., Smid, E. J., Gorris, L.G.M., Von Wright, A. (1998). Characterization of the Action of Selected Essential Oil Components on Gram-Negative Bacteria. *Journal of Agricultural and Food Chemistry*, *46*(9), 3590–3595.

Hsu, J. P., & Nacu, A. (2003). Behavior of soybean oil-in-water emulsion stabilized by nonionic surfactant. *Journal of Colloid and Interface Science*, *259*(2), 374–381.

Ikeda, S., Miyanoshita, M., & Gohtani, S. (2013). Effects of Sugars on the Formation of Nanometer-Sized Droplets of Vegetable Oil by an Isothermal Low-Energy Emulsification Method. *Journal of Food Science*, *78*(7), 1017–1021.

Jafari, S. M., He, Y., & Bhandari, B. (2007). Effectiveness of encapsulating biopolymers to produce sub-micron emulsions by high energy emulsification techniques. *Food Research International*, *40*(7), 862–873.

Jo, Y. J., Chun, J. Y., Kwon, Y. J., Min, S. G., Hong, G. P., & Choi, M. J. (2015). Physical and antimicrobial properties of trans-cinnamaldehyde nanoemulsions in water melon juice. *LWT - Food Science and Technology*, *60*(1), 444–451.

Klang, V., & Valenta, C. (2011). Lecithin-based nanoemulsions. *Journal of Drug Delivery Science and Technology*, *21*(1), 55–76.

Lambert, R. J. W., Skandamis, P. N., Coote, P. J., & Nychas, G. J. E. (2001). A study of the minimum inhibitory concentration and mode of action of oregano essential oil, thymol and carvacrol. *Journal of Applied Microbiology*, *91*(3), 453–462.

Ling, J. L. P., Kormin, F., Abidin, N. A. Z., & Anuar, N. A. F. M. (2019). Characterization and stability study of lemongrass oil blend microemulsion as natural preservative. *IOP Conference Series: Earth and Environmental Science*, *269*(1), 012026.

Marinova, K. G., Alargova, R. G., Denkov, N. D., Velev, O. D., Petsev, D. N., Ivanov, I. B., & Borwankar, R. P. (1996). Charging of Oil - Water Interfaces Due to Spontaneous Adsorption of Hydroxyl Ions. *Langmuir, 12*(8), 2045–2051.

Mazzotta, A. S. (2001). Thermal inactivation of stationary-phase and acid-adapted Escherichia coli O157:H7, Salmonella, and Listeria monocytogenes in fruit juices. *Journal of Food Protection*, *64*(3), 315–320.

McClements, D. J., Decker, E. A., & Weiss, J. (2007). Emulsion-based delivery systems for lipophilic bioactive components. *Journal of Food Science*, *72*(8), 109–124.

Nikolić, M., Marković, T., Mojović, M., Pejin, B., Savić, A., Perić, T., Marković, D., Stević, T., Soković, M. (2013). Chemical composition and biological activity of Gaultheria procumbens L. essential oil. *Industrial Crops and Products*, *49*, 561–567.

Olszowy, M., & Dawidowicz, A. L. (2016). Essential oils as antioxidants : their evaluation by DPPH , ABTS , FRAP , CUPRAC , and b -carotene bleaching methods. *Monatshefte Für Chemie - Chemical Monthly*, *147*(12), 2083–2091.

Oussalah, M., Phane, S., & Lacroix, M. (2006). Mechanism of Action of Spanish Oregano, Chinese Cinnamon, and Savory Essential Oils against Cell Membranes and Walls of Escherichia coli O157:H7 and Listeria monocytogenes. *Journal of Food Protection*, *69*(5), 1046–1055.

Pejin, B., Vujisic, L., Sabovljevic, M., Tesevic, V., & Vajs, V. (2011). Preliminary data on essential oil composition of the moss Rhodobryum ontariense (Kindb.) Kindb. *Cryptogamie, Bryologie*, *32*(2), 113–117.

Pérez-Conesa, D., Cao, J., Chen, L., McLandsborough, L., & Weiss, J. (2011). Inactivation of Listeria monocytogenes and Escherichia coli O157:H7 biofilms by micelle-encapsulated eugenol and carvacrol. *Journal of Food Protection*, *74*(1), 55–62.

Qian, C., & McClements, D. J. (2011). Formation of nanoemulsions stabilized by model food-grade emulsifiers using high-pressure homogenization: Factors affecting particle size. *Food Hydrocolloids*, *25*(5), 1000–1008.

Raut, J. S., & Karuppayil, S. M. (2014). A status review on the medicinal properties of essential oils. *Industrial Crops and Products*, *62*, 250–264.

Salvia-trujillo, L., Rojas-graü, A., Soliva-fortuny, R., & Martín-belloso, O. (2015). Physicochemical characterization and antimicrobial activity of food- grade emulsions and nanoemulsions incorporating essential oils. *Food Hydrocolloids*, *43*, 547–556.

Salvia-Trujillo, L., Rojas-Graü, A., Soliva-Fortuny, R., & Martín-Belloso, O. (2013). Physicochemical characterization of lemongrass essential oil-alginate anoemulsions: effect of ultrasound processing parameters. *Food and Bioprocess Technology*, *6*(9), 2439–2446.

Salvia-Trujillo, L., Rojas-Graü, M. A., Soliva-Fortuny, R., & Martín-Belloso, O. (2014). Impact of microfluidization or ultrasound processing on the antimicrobial activity against Escherichia coli of lemongrass oil-loaded nanoemulsions. *Food Control*, *37*(1), 292–297.

Sánchez-González, L., Vargas, M., González-Martínez, C., Chiralt, A., & Cháfer, M. (2011). Use of Essential Oils in Bioactive Edible Coatings: A Review. *Food Engineering Reviews*, *3*(1), 1–16.

Sell, C. (2010). Chemistry of Essential Oils. In K. H. Can Baser, & G. Buchbauer (2nd ed.), *Handbook of Essential oils. Science, Technology and Applications (pp. 165-194).* CRC Press, Taylor & Francis.

Skandamis, P., Tsigarida, E., & Nychas, G. J. E. (2000). Ecophysiological attributes of Salmonella typhimurium in liquid culture and within a gelatin gel with or without the addition of oregano essential oil. *World Journal of Microbiology and Biotechnology*, *16*(1), 31–35.

Sokovicх́, M., Glamočlija, J., Marin, P. D., Brkić, D., & Van Griensven, L. J. L. D. (2010). Antibacterial effects of the essential oils of commonly consumed medicinal herbs using an in vitro model. *Molecules*, *15*(11), 7532–7546.

Stracke, B. A., Rufer, C. E., Weibel, F. P., Bub, A., & Watzl, B. (2009). Three-year comparison of the polyphenol contents and antioxidant capacities in organically and conventionally produced apples (Malus domestica bork. cultivar 'golden delicious'). *Journal of Agricultural and Food Chemistry*, *57*(11), 4598–4605.

Suárez-Jacobo, Á., Rüfer, C. E., Gervilla, R., Guamis, B., Roig-Sagués, A. X., & Saldo, J. (2011). Influence of ultra-high pressure homogenisation on antioxidant capacity, polyphenol and vitamin content of clear apple juice. *Food Chemistry*, *127*(2), 447–454.

Teo, A., Goh, K. K. T., Wen, J., Oey, I., Ko, S., Kwak, H. S., & Lee, S. J. (2016). Physicochemical properties of whey protein, lactoferrin and Tween 20 stabilised nanoemulsions: Effect of temperature, pH and salt. *Food Chemistry*, *197(A)*, 297-306.

Urakami, A. M., Ukada, K. F., Amano, Y. Y., & Ohtani, S. G. (2005). Effects of Sucrose on Emulsification of Triglyceride by Polyglycerin Fatty Acid Ester. *Journal of Oleo Science*, *54*(6), 335–340.

Viuda-Martos, M., El Gendy, A. E. N. G. S., Sendra, E., Fernández-López, J., El Razik, K. A. A., Omer, E. A., & Pérez-Alvarezj, J. A. (2010). Chemical composition and antioxidant and anti-Listeria activities of essential oils obtained from some Egyptian plants. *Journal of Agricultural and Food Chemistry*, *58*(16), 9063–9070.

Walker, R. M., Gumus, C. E., Decker, E. A., & McClements, D. J. (2017). Improvements in the formation and stability of fish oil-in-water nanoemulsions using carrier oils: MCT, thyme oil, & lemon oil. *Journal of Food Engineering*, *211*, 60–68.

Ziani, K., Fang, Y., & McClements, D. J. (2012). Encapsulation of functional lipophilic components in surfactant-based colloidal delivery systems: Vitamin E, vitamin D, and lemon oil. *Food Chemistry*, 134(2), 1106-1112.

Chapter II

Impact of dairy matrices on O/W emulsions colloidal stability, lipid digestibility and β-carotene bioaccessibility

Anna Molet-Rodríguez, Olga Martín-Belloso, Laura Salvia-Trujillo*

Abstract

O/W emulsions have been proposed as delivery systems of lipophilic bioactive compounds into water-based food products. However, their colloidal stability and functionality can be compromised due to the physicochemical properties of food macromolecules and/or matrix characteristics. Thus, this work aimed to study the impact of the food macromolecules and matrix characteristics on the colloidal stability of β-carotene-loaded O/W emulsion into different dairy products (whole milk, whole yogurt, skimmed milk and skimmed yogurt) before and during *in vitro* gastrointestinal digestion. In addition, the relationship between the colloidal stability, lipolysis and β-carotene bioaccessibility was also evaluated. The colloidal stability of the O/W emulsion was maintained after its incorporation into dairy products and during GI conditions. Instead, dairy macromolecules experienced aggregation under acidic gastric conditions. The lipolysis of the O/W emulsion was faster and higher once co-ingested with dairy products, probably due to the higher and greater lipolysis of the dairy fat globules compared to O/W emulsion oil droplets. In addition, the O/W-skimmed yogurt presented the highest lipolysis, which was attributed to an easier contact between lipase and lipid phase. Nevertheless, although O/W-dairy products had higher free fatty acids release than O/W emulsion, they presented similar β-carotene bioaccessibility, which could be explained by the ability of proteins to hinder its micellization. Thus, this work provides valuable insight for designing food products fortified with bioactive compounds.

Keywords

Emulsions; food matrix; dairy products; milk; yogurt; *in vitro* digestion.

1 Introduction

Over the last decades, the food industry has shown a growing interest in fortifying food products with bioactive compounds, since they have been proved to have health benefits (Das, Bhaumik, Raychaudhuri, & Chakraborty, 2012; Granato et al., 2020; Kris-Etherton et al., 2002). Nevertheless, the incorporation of lipophilic bioactive compounds (*i.e.,* β-carotene) in water-based food products is limited due to their poor solubility in such medium and sensitivity to certain environments, like pH, temperature, oxygen and light (Boon, McClements, Weiss, & Decker, 2010; Gleeson, Ryan, & Brayden, 2016). In this regard, oil-in-water (O/W) emulsions, which consists of lipid droplets dispersed in a continuous aqueous phase, have great potential to carry and protect these lipophilic compounds as well as to enhance their bioaccessibility (McClements, Decker, & Weiss, 2007; McClements & Li, 2010). Nevertheless, they are thermodynamically unstable, so they will tend to breakdown over time by some physicochemical mechanisms, such as creaming, sedimentation, Ostwald ripening and flocculation, which normally ends with coalescence (McClements, 2015). In this sense, one of the main challenges of food fortification with O/W emulsions carrying lipophilic bioactive compounds is maintaining O/W emulsion physicochemical properties and colloidal stability before and during *in vitro* gastrointestinal (GI) digestion. Food products are generally composed of proteins, fats and carbohydrates, such as sugars that can interact with the oil droplets of O/W emulsions and alter their colloidal stability and consequently lipolysis and bioactive compound bioaccessibility. On the one hand, proteins are well-known to possess interfacial activity, being able to interact with the oil/water interface of the O/W emulsion (Dickinson, 2001). On the other hand, sugars could enhance O/W emulsion colloidal stability by binding water molecules in the aqueous phase and consequently, increasing the number of hydrophobic surfactant molecules able to adsorb at the oil/water interface (Ikeda, Miyanoshita, & Gohtani, 2013; Molet-Rodríguez, Turmo-Ibarz, Salvia-Trujillo, & Martín-Belloso, 2021). Nevertheless, foods are not simply the sum of individual macromolecules, but complex matrices with different characteristics and physicochemical properties (Hassan, Frank, Farmer, Schmidt, & Shalabi 1995).

Dairy products comprise milk and milk-derived products formed by milk processing. As a result, they present differences in macromolecular composition and organization as well as food matrix pH and physical state (Dalgleish & Corredig, 2012; Lee & Lucey, 2010).

Whole milk consists of fat globules and casein micelles dispersed in an aqueous phase containing globular proteins and lactose (Pereira, 2014). The process of whole yogurt formation, which consist of lactose milk fermentation by its incubation at low temperature with several bacterial cultures, results in the conversion of lactose into lactic acid, causing a decrease in the lactose content in whole yogurt (Lee & Lucey, 2010). Acid lactic production led to a lower pH in yogurt (pH 4.6) compared with milk (pH 6.7). In addition, yogurt processing led to the formation of casein aggregates and denatured whey protein-casein complexes, and consequently food matrix physical state changes, from liquid (milk) to semi-solid (yogurt) (Francis, Glover, Yu, Povey, Holmes, 2019). Other dairy products of interest are skimmed milk and skimmed yogurt from which fat has been removed (Lubary, Hofland, & ter Horst, 2011).

In this sense, this work aimed to study the physicochemical properties and colloidal stability of a β-carotene-loaded O/W emulsion incorporated into dairy products with different food macromolecular composition and matrix characteristics, before ingestion and during *in vitro* gastrointestinal digestion. Moreover, the colloidal stability upon gastric and small intestinal conditions was related to lipid digestibility and β-carotene bioaccessibility. First, the β-carotene-loaded O/W emulsion was formulated with corn oil and Tween 80 and then incorporated into solutions of sodium caseinate (SC), whey protein isolate (WPI) and lactose to study their individual effect. Then, the O/W emulsion was incorporated into a skimmed milk model and commercial dairy products (whole milk, whole yogurt, skimmed milk and skimmed yogurt). Their microstructure was analyzed before and during *in vitro* digestion stages in terms of droplet size, ζ-potential and optical microscopy. Finally, lipid digestibility and β-carotene bioaccessibility of each system were evaluated.

2 Material and methods

2.1 Materials

Corn oil (Koipesol Asua, Deoleo, Spain), β-carotene (C9750) of ≥ 93% purity and polyoxyethylene sorbitan monooleate (Tween 80) from Sigma Aldrich (St Louise, MO, USA) were the food-grade ingredients used in the formulation of the β-carotene-loaded O/W emulsion. Sodium caseinate (Acros Organics, Geel, Belgium), whey protein isolate kindly donated by El Pastoret de la Segarra (Lleida, Spain) and lactose 1-hydrate

(PanReac AppliChem, ITW Reagents, Barcelona, Spain) were the dairy macromolecules evaluated. Bovine whole milk and skimmed milk (Hacendado, Mercadona, Spain) as well as bovine whole yogurt and skimmed yogurt (Milsani, Aldi, Germany) were the selected dairy products, which composition is listed in Table 1. Pepsin from porcine gastric mucosa (77160), pancreatin from porcine pancreas (P1625) and bile bovine (B3883) were purchased from Sigma Aldrich. The fluorescence dye, fluorescein isothiocyanate (FitC) (46424) was purchased from Thermo Scientific (Germany). Dimethyl sulfoxide (DMSO) was used to solubilize Fit C. The chemicals used in the extraction analysis to quantify the β-carotene concentration were ethanol absolute and hexane (fraction from petroleum), both HPLC grade (Sharlab S.L, Sentmenat, Spain). The rest of the chemicals used were of analytical grade. All solutions were prepared with milli-Q water with a resistivity of 18.2 MΩ.cm at 25 °C (Milli-Q apparatus, Millipore, Bedford, UK).

Table 1. Fat, protein and sugar composition of the studied dairy food products.

Formulation	Fat (% w/w)	Protein (% w/w)	Sugar (% w/w)
Whole milk	3.6	3.1	4.6
Skimmed milk	0.3	3.1	4.7
Whole yogurt	2.5	4.1	4.6
Skimmed yogurt	0.5	3.9	5.4

2.2 Methods

2.2.1 Formation of the β-carotene-loaded O/W emulsion

Firstly, β-carotene was dispersed in corn oil (0.1 g/100 g) by heating (< 50 °C, 10 min) and sonicating (5 min) and it was repeated three consecutive times, to obtain the lipid phase. Then, a coarse oil-in-water (O/W) emulsion was prepared by pre-homogenizing 20% (w/w) of lipid phase, 10% (w/w) of Tween 80 and milli-Q water (70% w/w) using a laboratory T25 digital Ultra-Turrax mixer (IKA, Staufen, Germany), working at 7200 rpm for 3 min. Then, the oil droplet size of the coarse O/W emulsion was reduced to submicron range by passing it two times through a microfluidizer (M110P, Microfluidics, Massachusetts, USA) at a pressure of 150 MPa.

2.2.2 Formulation of the dairy macromolecule solutions or products fortified with the β-carotene-loaded O/W emulsion

2.2.2.1 Formulation of the fortified dairy macromolecule solutions

Individual aqueous solutions of SC (2.3% w/w), WPI (0.5% w/w) or lactose (4.7% w/w) were prepared by its dissolution in milli-Q water (pH 6.7) at the same concentration as in milk for 4 h at 750 rpm and 25 °C to allow its complete hydration. Then, 80% (w/w) of each solution was mixed with the O/W emulsion (20% w/w) to obtain the dairy macromolecule solutions fortified with the O/W emulsion, which contained 4 % w/w of lipid. These formulations are referred to as O/W-SC, O/W-WPI and O/W-lactose. Additionally, the O/W emulsion (20% w/w) was diluted and mixed with milli-Q water (80% w/w) to reach the same concentration of lipid as in the other formulations.

2.2.2.2 Formulation of the fortified skimmed milk model

A skimmed milk model solution was prepared by dissolving SC (2.3% w/w), WPI (0.5% w/w) and lactose (4.7% w/w) in milli-Q water (pH 6.7) and mixing during 4 h at 750 rpm and 25 °C. Later, 80% w/w of this solution was mixed with the O/W emulsion (20% w/w) to obtain the O/W-skimmed milk model. In addition, 20% (w/w) of milli-Q water was added to the skimmed milk model solution (80% w/w) (750 rpm, 5 min) as a control.

2.2.2.3 Formulation of the fortified dairy products

Commercial whole milk, skimmed milk, whole yogurt or skimmed yogurt (80% w/w) were mixed with the O/W emulsion (20% w/w) for 5 min at 750 (milk) and 1500 rpm (yogurt), to obtain the fortified dairy products, referred to as O/W-whole milk, O/W-skimmed milk, O/W-whole yogurt and O/W-skimmed yogurt. Whole milk, skimmed milk, whole yogurt or skimmed yogurt (80% w/w) mixed with (20% w/w) milli-Q water (750 or 1500 rpm, 5 min) were used as dairy products control.

2.2.3 In vitro gastrointestinal digestion

The static *in vitro* GI digestion of the O/W emulsion, O/W-dairy macromolecule solutions (SC, WPI, lactose), O/W-skimmed milk model and O/W-dairy products was conducted according to the INFOGEST international consensus with minor modifications (Minekus et al., 2014). In addition, skimmed milk model (without the O/W emulsions) was also

127

subjected to gastrointestinal digestion in order to know the contribution of protein hydrolysis to the pH-stat signal. Dairy products (whole milk, skimmed milk, whole yogurt and skimmed yogurt) were also digested to quantify the lipid digestibility percentage of the food matrix without O/W emulsion.

2.2.3.1 Gastric phase

The electrolyte simulated gastric fluid (eSGF) solution consisted of a mixture of electrolytes [0.5 M KCl, KH_2PO_4 0.5M, 1 M NaCl, 2M NaCl, 0.15 M $MgCl_2(H_2O)$ and 0.5 M $(NH_4)_2CO_3$] dissolved in milli-Q water. Then, the gastric mixture solution was prepared by dissolving pepsin (8.8 mg pepsin/ mL) in eSGF, followed by the addition of $CaCl_2(H_2O)_2$ 0.3 M, HCl 1 M and milli-Q water. The gastric digestion was performed by mixing each fortified dairy macromolecule solution, product or controls with the gastric mixture to a final ratio of 1:1. It was incubated under dark conditions for 2 h at 37 °C and continuous agitation using an orbital shaker working at 100 rpm. After the gastric phase, three aliquots, referred to as gastric chyme aliquots, were collected for microscopic, droplet size and ζ-potential analysis and the rest was used for the subsequent intestinal digestion.

2.2.3.2 Intestinal phase

To simulate the small intestinal phase, a 30 mL-aliquot of the gastric chyme was placed in a water bath at 37 °C. Subsequently, 3.5 mL of bile salts (54 mg/mL) diluted in a phosphate buffer (0.005 M, pH 7) and 1.5 mL of intestinal salts (10 mM of $CaCl_2$ and 160 mM of NaCl) were added to the sample, and the pH was adjusted to 7.0. Then, 2.5 mL of pancreatin solution (215 mg/mL) diluted in the phosphate buffer (0.005 M, pH 7) were added to initiate the lipid hydrolysis, which was monitored with a titration unit (pH-stat, Metrohm USA Inc., Riverview, FL, USA) maintaining the pH at 7. The percentage of free fatty acid (FFA) release was calculated according to equation (1):

$$Free\ fatty\ acid\ release\ (\%) = \frac{V_{NaOH} \times C_{NaOH} \times M_{lipid}}{2 \times m_{lipid}} \times 100 \tag{1}$$

where V_{NaOH} is NaOH volume (mL) used to compensate the FFAs released during the digestion, C_{NaOH} is NaOH molarity (0.25 M), M_{lipid} is lipid molecular weight, m_{lipid} is the total lipid weight in the 30-mL aliquot placed in the titration unit. The molecular weight

of corn oil, as well as milk and yogurt globules, were 867.30 g/mol, 709.25 g/mol and 813.63 g/mol, respectively.

After the small intestinal digestion, three aliquots of each digest were taken for microscopic, particle size and ζ-potential analysis. For the purpose of determining the β-carotene bioaccessibility, the digest was transferred into glass tubes and heat-shocked at 80 °C for 3 min in order to stop the lipolysis reaction and placed in an iced-water bath afterwards.

2.2.4 β-carotene bioaccessibility

The β-carotene bioaccessibility is defined as the fraction of β-carotene that can be incorporated into the mixed micelles and thus becomes available for absorption in the body. The β-carotene bioaccessibility from the O/W emulsion, O/W-dairy macromolecule solutions, O/W-skimmed milk model and O/W-dairy products after being subjected to the prior described *in vitro* GI digestion procedure, was evaluated. The digest was centrifuged (AVANTI J-25, Beckman Instruments Inc., Fullerton, CA, USA) at 4000 rpm for 40 min at a temperature of 8 °C. The supernatant, being the aqueous fraction containing the mixed micelles, was collected and considered as the micellar fraction in which the β-carotene is solubilized. The β-carotene quantification was conducted following the method reported by Liu, Wang, McClements, & Zou (2018), where 0.5 mL of each formulation before GI digestion or each micellar fraction were mixed with 2 mL of ethanol and 3 mL of hexane and vortexed for 10 s at 1800 rpm. Afterwards, the upper hexane phase containing the β-carotene was analyzed spectrophotometrically with a V-670 spectrophotometer (Jasco, Tokyo, Japan) at 450 nm. The concentration of β-carotene extracted from each formulation before GI digestion or each micellar fraction was determined from a calibration curve of absorbance versus β-carotene concentration in hexane. The β-carotene bioaccessibility was then calculated using the following equation (2):

$$\beta - carotene\ bioaccessibility\ (\%) = \frac{C_{micellar}}{C_{before\ digestion}} \times 100 \qquad (2)$$

where $C_{micelle}$ is the β-carotene concentration of the micelle fraction and $C_{before\ digestion}$ is the β-carotene concentration of the fortified dairy macromolecule solution, skimmed milk model or food product before GI digestion.

2.2.5 Physicochemical characterization

Aliquots of the O/W emulsion, O/W-dairy macromolecule solutions, O/W-skimmed milk model and O/W-dairy products before GI digestion, gastric chyme and digest were characterized in terms of droplet size, size distribution, ζ -potential and optical microscopy analysis to determine changes in their microstructure.

2.2.5.1 Droplet size and size distribution

Particle size and size distribution were measured using static light scattering (SLS) (Mastersizer 2000, Malvern Instruments Ltd, Worcestershire, UK). Samples were dispersed in distilled water at 2200 rpm and the average droplet size and size distribution were reported as surface-weighted average ($D_{[3;2]}$) and volume (%), respectively. The refractive indexes for corn oil and distilled water were 1.47 and 1.33, respectively.

2.2.5.2 ζ -potential

The ζ -potential (mV) of the oil droplets was determined by phase analysis light scattering (PALS) with a Zetasizer NanoZS laser diffractometer (Malvern Instruments Ltd., Worcestershire, UK). Samples were diluted in milli-Q water at neutral pH (in the case of O/W-whole yogurt and O/W-skimmed yogurt the pH of milli-Q water was 4.6) with a dilution factor of 1:9 aliquot-to-solvent and placed in a capillary cell to assess the electrophoretic mobility of the particles.

2.2.5.3 Optical Microscopy Analysis

Phase contrast microscopy images of the samples were taken with an optical microscope (BX41, Olympus, Göttingen, Germany) using a 100x oil immersion objective lens and equipped with UIS2 optical system. Additionally, O/Wemulsion incorporated into skimmed milk and skimmed yogurt were observed using fluorescence with a 40x oil lens and the same optical microscope. Protein was stained in green using a fluorescent agent named Fit C (1mg/mL DMSO) to see their location within the system. All images were processed using the instrument software (Olympus cellSense, Barcelona, Spain).

2.3 Statistical analysis

All experiments were assayed in duplicate and data was expressed as the mean with standard deviation. An analysis of variance was carried out and the Tukey HSD test was run to determine significant differences at a 5% significance level ($p < 0.05$) with statistical software JMP Pro 14 (SAS Institute Inc.).

3 Results and discussion

## 3.1 Droplet size, size distribution and microstructure

3.1.1 *Before in vitro gastrointestinal digestion*

The incorporation of the O/W emulsion into individual solutions of the main macromolecules present in the studied dairy products, being SC, WPI and lactose, did not significantly affect the O/W emulsion average particle size. O/W emulsion, O/W-SC, O/W-WPI and O/W-lactose had average particle sizes of 270 ± 10, 280 ± 10, 260 ± 2 and 260 ± 4 nm, respectively (Fig. 1A). In addition, they presented monomodal size distributions with particle populations around 500 nm (Fig. 2A) and their microscopy images showed submicron oil droplets homogeneously dispersed in the continuous phase (Supplementary material, Fig. S1). In this regard, even though SC, WPI and lactose are known to possess oil emulsification capacity (Dickinson, 2001; Luo et al., 2014), the absence of particle size changes between the O/W emulsion and O/W-SC, OW-WPI or O/W-lactose evidenced that the oil/water interface of the O/W emulsion was completely covered by Tween 80 molecules before being incorporated into the dairy macromolecule solutions (Gomes, Costa, & Cunha, 2018). As a consequence, the studied dairy macromolecule might be located in the bulk continuous aqueous phase instead of adsorbing at the oil/water interface. It is worth mentioning that upon neutral pH conditions, SC has a strong tendency to form small self-assembled soluble particles called casein sub-micelles (10-20 nm), which coexist in equilibrium with free casein molecule solubilized in aqueous solution (Dalgleish & Corredig, 2012; Pereira, 2014). Thus, the aqueous phase of the O/W-SC would contain oil droplets dispersed, but also casein sub-micelles, which would be expected to account for the overall particle size. In this regard, the absence of differences between the average particle size and size distribution of the O/W emulsion and O/W-SC might be attributed to the fact that casein sub-micelles size is close to the detection limit of the SLS technique (10 nm).
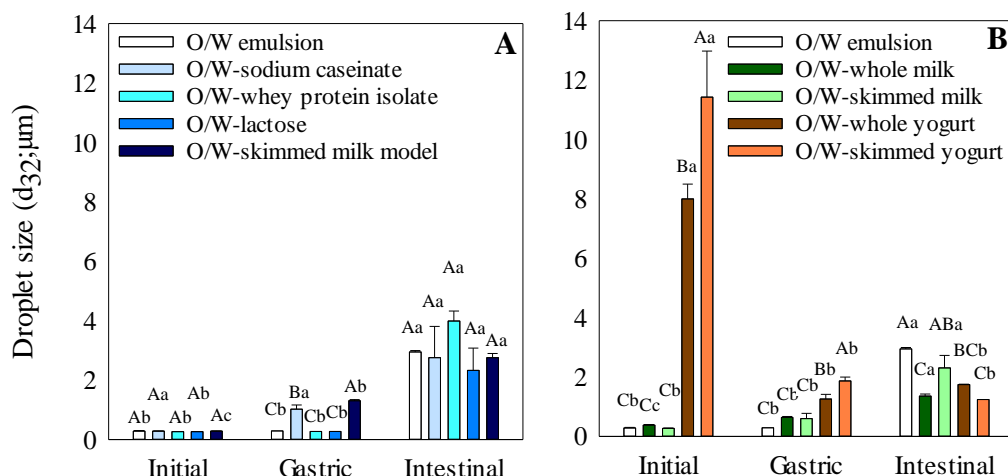
Figure 1. Surface-weight average droplet size (d32; µm) of the oil-in-water (O/W) emulsion incorporated into dairy macromolecule solutions (A) and dairy food products (B) before (initial) and after being submitted to simulated gastric and small intestinal conditions. Dairy macromolecule solutions: sodium caseinate, whey protein isolate, lactose as well as skimmed milk model. Dairy food products: whole milk, skimmed milk, whole yogurt and skimmed yogurt. Different upper-case letters mean significant differences between different formulations for the same gastrointestinal phase. Different lower-case letters indicate significant differences between different gastrointestinal phases for the same formulation.

The O/W emulsion droplet size was not affected by a more complex dairy solution since the O/W-skimmed milk model showed an average particle size of 280 ± 10 nm and a monomodal distribution. Thus, it showed a similar average particle size and size distribution than the O/W emulsion, evidencing that the co-existence of the studied dairy macromolecules in the skimmed milk model neither altered their individual structure and physicochemical properties nor the O/W emulsion particle size. Regarding the O/W-dairy products, the composition and physicochemical properties of the dairy matrix influenced their average particle size. O/W-skimmed milk presented similar particle size (270 ± 10 nm) than the O/W emulsion, which suggests that milk protein and lactose maintained their individual structure (Fig. 1B). Instead, the O/W-whole milk showed a slightly higher average particle size (380 ± 20 nm) than the O/W emulsion, probably due to the presence of fat globules in this food matrix (Fig. 1B). Both O/W-whole yogurt and O/W-skimmed yogurt had higher average lipid diameters (8.00 ± 0.5 and 11.43 ± 1.55 µm, respectively) in comparison with the O/W emulsion, O/W-whole milk and O/W-skimmed milk (Fig. 1B). The increase in the average particle size of both fortified yogurts was confirmed by their size distribution, which showed a particle population of micrometric size (> 10 µm).
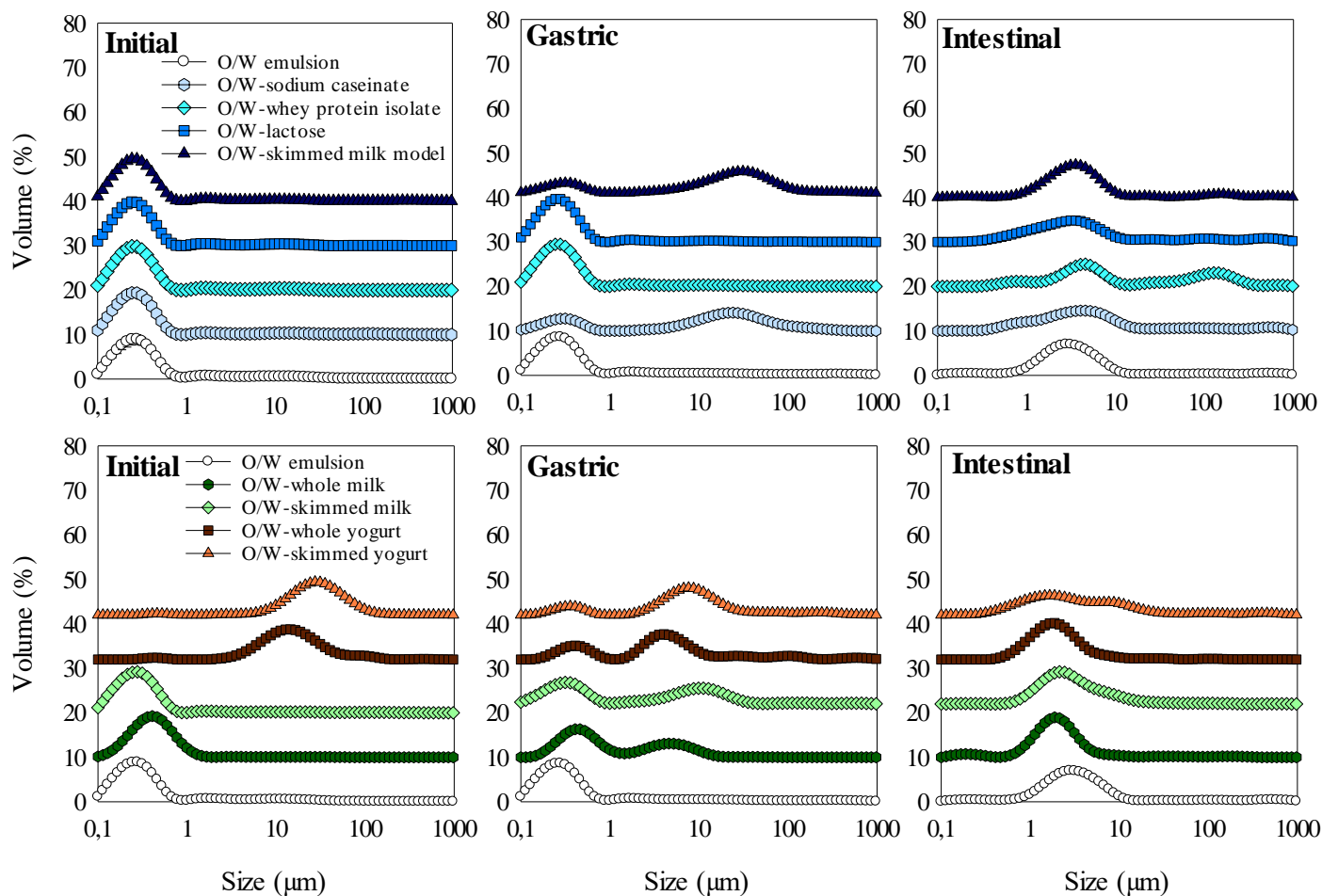
Figure 2. Droplet size distribution in volume (%) of the oil-in-water (O/W) emulsion incorporated into dairy macromolecule solutions (top panel) and dairy food products (bottom panel) before and after being submitted to simulated gastric and small intestinal conditions. Dairy macromolecule solution: sodium caseinate, whey protein isolate, lactose as well as skimmed milk model. Dairy food products: whole milk, skimmed milk, whole yogurt and skimmed yogurt.

The process of yogurt formation consists of milk lactose fermentation into lactic acid by the action of several bacterial cultures, which results in macromolecule structure changes (Lee & Lucey, 2010). Yogurt matrix acidification through lactic acid production causes casein micelles to deprotonate and form aggregates via hydrophobic attractions and van der Waals interactions (Francis et al., 2019). In addition, WPI denatures and unfolds, which led to its interaction with κ-casein forming a three-dimensional network, explaining the bigger average particle size of O/W-whole yogurt and O/W-skimmed yogurt in comparison with O/W-whole milk and O/W-skimmed milk (Hassan et al., 1995; Law & Leaver, 2000). Nevertheless, the microscopic images of O/W-whole yogurt and O/W-skimmed yogurt did not show an increase in the oil droplet size of the O/W emulsions, which would have maintained their stability after being incorporated into whole yogurt and skimmed yogurt.

3.1.2   *Gastric phase*

After simulated gastric conditions, the average particle size of the O/W emulsion remained stable (Fig. 1A). It has been previously reported that Tween 80 is a non-ionic surfactant, which is not sensitive to pH changes upon gastric conditions (pH 3), thus explaining the colloidal stability of the O/W emulsion (Teo et al., 2016; Zhu et al., 2019). The average particle size of O/W-WPI and O/W-lactose also remained stable upon gastric conditions, thus suggesting that the initial structure of WPI and lactose was not altered (Fig. 1A). Nevertheless, both O/W-SC and O/W-skimmed milk model showed an increase in particle size after gastric digestion (Fig. 1A). The average particle size of O/W-SC and O/W-skimmed milk model before gastric digestion was 280 ± 10 and 280 ± 10 nm, respectively, whereas it was 1.02 ± 0.14 and 1.30 ± 0.10 μm, respectively, after the gastric phase. This increase in particle size could be explained by the presence of SC in both solutions, which structure is susceptible to pH changes (Francis et al., 2019). The gastric phase pH may have caused casein sub-micelles to deprotonate and attract each other's, forming aggregates in the continuous aqueous phase that would be responsible for the bigger average particle size in the SC-containing systems. In fact, the presence of aggregated casein in both O/W-SC and O/W-skimmed milk model was confirmed by the apparition of a new population of big particles (> 10 μm) in their distribution graph after being subjected to the gastric phase (Fig. 2B). Nevertheless, the submicron peak corresponding to O/W emulsions was still present in both O/W-SC and O/W-skimmed

milk model after the gastric phase, assuming that O/W emulsions remain stable upon gastric conditions. Similarly, O/W-whole milk and O/W-skimmed milk presented slightly bigger particle size after the gastric phase (640 ± 30 and 600 ± 170 nm, respectively) than before gastric digestion (380 ± 20 and 270 ± 10 nm, respectively) (Fig. 1B), which correlates with the presence of protein aggregates in its microscopic image (Fig. 3).

In contrast, O/W-whole yogurt and O/W-skimmed yogurt experimented a decrease in the average particle size after the gastric phase (1.26 ± 0.16 and 1.87 ± 0.13 μm, respectively) in comparison with the particle size before gastric digestion (8.00 ± 0.5 and 11.43 ± 1.55 μm, respectively) (Fig. 1B). Differences in particle size before and after gastric phase of O/W-whole yogurt and O/W-skimmed yogurt were also observed in the distribution graph, which changed from monomodal with a peak above 10 μm to bimodal with one droplet population with diameters below 1 μm and another between 1 and 10 μm (Fig. 2D and E). The shift of the droplet size populations to a smaller size might be because there was less amount of aggregated protein after the gastric digestion than initially, as observed in the microscopy images (Fig. 3). In the gastric phase, denatured proteins, as found in yogurt, have been reported to be better digested than in their native state, which is the case of milk (Halabi, Croguennec, Bouhallab, Dupont, & Deglaire, 2020). For instance, Nguyen, Gathercole, Day, & Dalziel (2020) obtained a greater amount of bioactive peptides after *in vitro* gastrointestinal digestion of yogurt compared to milk. Therefore, this suggests that enhanced digestion of denatured protein in O/W-whole yogurt and O/W-skimmed yogurt might cause a reduction of the protein aggregates present in the aqueous phase and, consequently, a decrease of the average particle size of O/W-whole yogurt and O/W-skimmed yogurt. In addition, their microscopic images and distribution graph with populations of submicron size suggested that the O/W emulsions into whole and skimmed yogurt remained stable upon gastric conditions. Therefore, the decrease in the average particle size of O/W-whole yogurt and O/W-skimmed yogurt after the gastric phase would be attributed to a reduction of aggregates of protein in the continuous phase rather than the O/W emulsion destabilization phenomena.

	Initial	Gastric	Intestinal
O/W-whole milk			
O/W-skimmed milk			
O/W-whole yogurt			
O/W-skimmed yogurt			
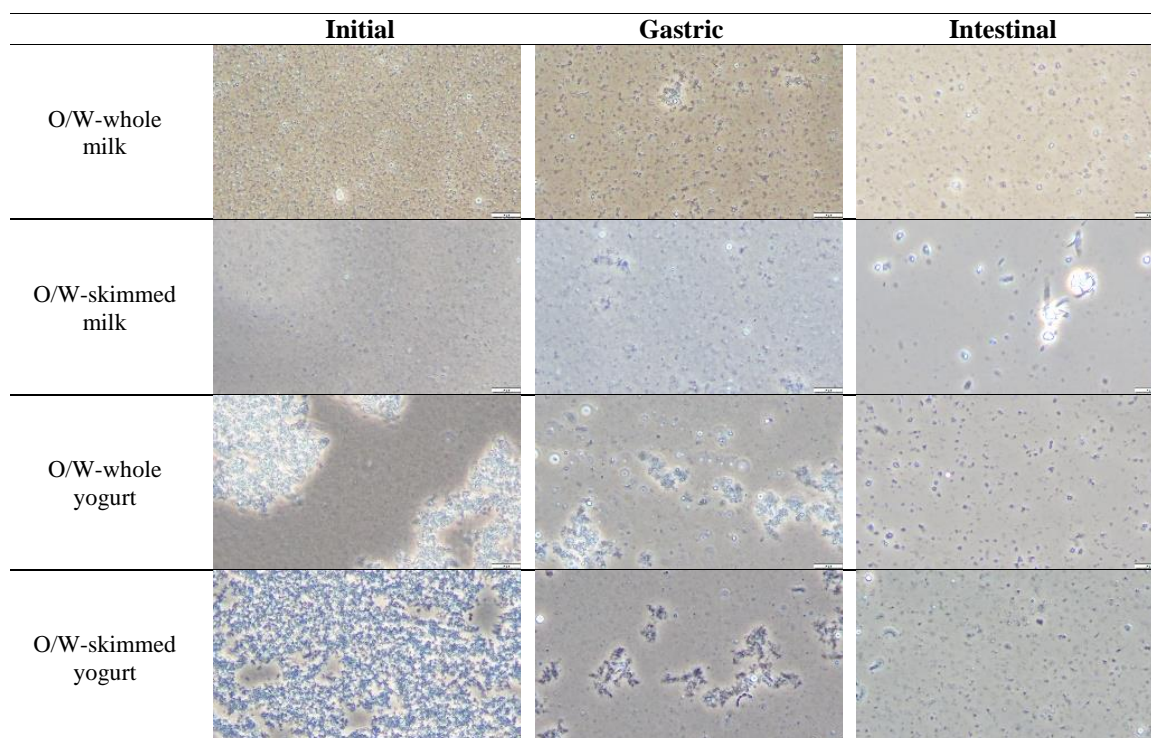
Figure 3. Optical microscopy images of the oil-in-water (O/W) emulsion incorporated into whole milk, skimmed milk, whole yogurt and skimmed yogurt. Scale bar: 10 µm.

3.1.3 *Small intestinal phase*

The average particle size of O/W emulsion, O/W-dairy macromolecule solutions and O/W-skimmed milk model incremented after the small intestinal phase (Fig. 1A and 2C). Large values of particle size obtained after the *in vitro* small intestinal digestion have been previously attributed to various reasons. Firstly, the presence of complex association colloids, such as mixed micelles, vesicles and lamellar structures, formed in the digestion medium as a result of the interactions of lipid digestion products, bile salts, phospholipids, and calcium micelles (Kossena, Boyd, Porter, & Charman, 2003). In fact, the microscopic images of the O/W-emulsion and O/W-dairy macromolecule solutions after the intestinal phase showed lamellar and amorphous particles of bigger size in comparison with the gastric ones (Supplementary material Fig. S1 and Fig. 3). Secondly, the partial displacement of emulsifier molecules from the droplet surfaces by the action of bile salts would have resulted in a single emulsifier molecule being attached to the surface of more than one droplet, provoking droplet flocculation and/or coalescence through charge neutralization and bridging effects (Borreani, Leonardi, Moraga, Quiles, & Hernando, 2019; Gasa-Falcon, Odriozola-Serrano, Oms-Oliu, & Martín-Belloso, 2019). Li & McClements (2010) obtained similar results with O/W emulsions stabilized with Tweens,

observing by confocal laser scanning microscopy that the droplets flocculated or coalesced when simulated intestinal fluids were added. Thirdly, bile salts may have adsorbed at the oil/water interface and altered their composition, thereby promoting interactions between droplets (Maldonado-Valderrama, Wilde, Macierzanka, & Mackie, 2011). Lastly, in those dairy macromolecule solutions or products containing proteins, the remaining non-digested SC and WPI could have aggregated, justifying the bigger droplet sizes obtained (Chang, Yaoguang & McClements, 2016).

Average particle size increase from gastric to intestinal phase was also observed in O/W-whole milk and O/W-skimmed milk (from 0.64 ± 0.03 to 1.36 ± 0.07 and from 0.60 ± 0.17 to 2.31 ± 0.42 μm, respectively) as well as in O/W-whole yogurt (from 1.26 ± 0.16 to 1.75 ± 0.01 μm). Nevertheless, it decreases in O/W-skimmed yogurt (from 1.87 ± 0.13 to 1.24 ± 0.01 μm). The smaller average particle size of the O/W-skimmed yogurt after small intestinal conditions in comparison with the other formulations can be attributed to its low content of un-digested lipid droplets (see section 3.3).

3.2 ζ-potential

3.2.1 *Before in vitro gastrointestinal digestion*

The ζ-potential values of the O/W emulsion, O/W-dairy macromolecule and O/W-skimmed milk model depended on the interfacial composition of the oil droplets. Before the gastric digestion, all of them showed negatively charged interfaces, with ζ-potential values ranging between -14.85 and -20.03 mV, without significant differences between them (Fig. 4A). Lipid droplets naturally possess a negative charge due to the presence of anionic hydroxyl groups (OH^-) in the water or oil used to prepare the O/W emulsion (Marinova et al., 1996). In addition, even though Tween 80 is non-ionic, it has been reported to form negatively charged oil droplets when the pH of the O/W emulsion is higher than 4 (Hsu & Nacu, 2003). Similarly, O/W-whole milk and O/W-skimmed milk presented negative oil/water interfaces with ζ-potential values of -16.63 ± 1.48 and -13.97 ± 0.98 mV, respectively (Fig. 4B). Contrarily, O/W-whole milk and O/W-skimmed yogurt presented almost neutral charges (0.70 ± 0.38 and 1.22 ± 0.25 mV, respectively), which could be attributed to the neutral electrical charge of the protein aggregates located in the aqueous phase.
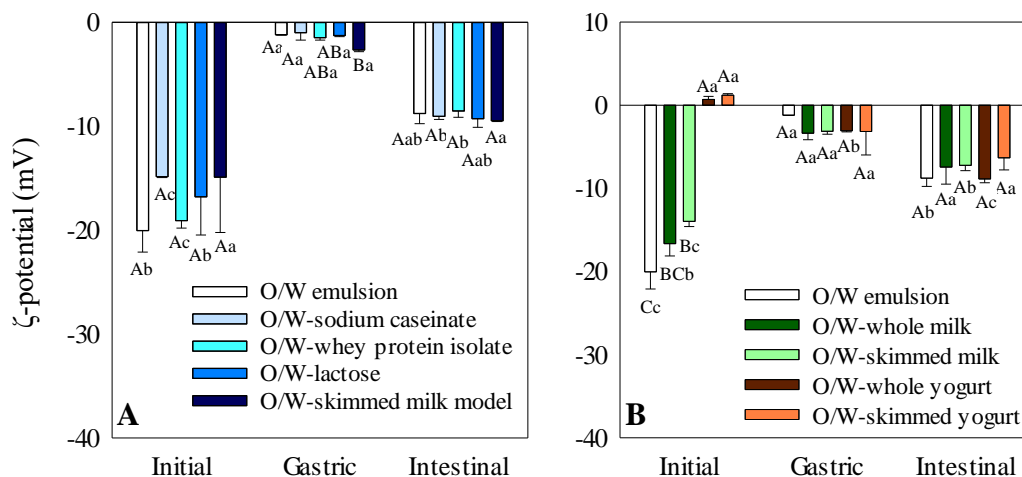
Figure 4. ζ-potential (mV) of the oil-in-water (O/W) emulsion incorporated into dairy macromolecule solutions (A) and dairy food products (B) before (initial) and after being submitted to simulated gastric and small intestinal conditions. Dairy macromolecule solutions: sodium caseinate, whey protein isolate, lactose as well as skimmed milk model. Dairy food products: whole milk, skimmed milk, whole yogurt and skimmed yogurt. Different upper-case letters mean significant differences between different formulations for the same gastrointestinal phase. Different lower-case letters indicate significant differences between different gastrointestinal phases for the same formulation.

3.2.2 Gastric phase

Salts from gastric fluids influenced the charge of the oil droplets in all the systems. After gastric conditions, the ζ-potential of O/W emulsion, O/W-dairy macromolecule solutions and O/W-skimmed milk model became less negative with values between -2.76 and -0.46, irrespective of the dairy macromolecule type (Fig. 4A). Moreover, O/W-dairy products also presented almost neutral charged oil/water interfaces (Fig. 4B). In this sense, the free ions present in the simulated gastric fluids would have attenuated the charges of the oil droplets, which is known as screening effect (Keowmaneechai & McClements, 2002).
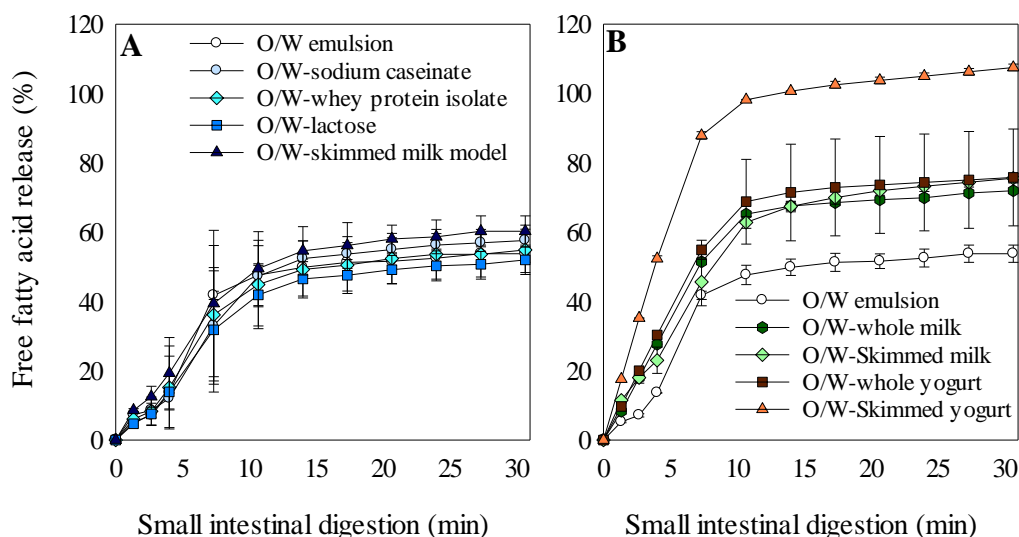
3.2.3 Small intestinal phase

The ζ-potential of all studied formulations became more negative after being subjected to intestinal conditions (Fig. 4A and B). The observed change in electrical charge between the gastric and the intestinal phases could be attributed to the adsorption at the oil/water interface of anionic digestion products (*e.g.,* free fatty acids) and/or components from the intestinal juices (*e.g.,* bile salts), which have surface-active properties (Hur, Decker, &

McClements, 2009; Pinheiro et al., 2013). Despite this, the neutral pH of the intestinal phase might be another reason why all studied formulations showed more negative ζ-potential values at the end of the small intestinal phase in comparison with the values obtained after the gastric phase.

3.3 Lipolysis rate during *in vitro* small intestinal digestion

The lipolysis reaction of the studied formulations was monitored during the *in vitro* small intestinal phase through the FFA release (%) to determine differences between their lipid digestibility (Fig. 5 and 6). In general, they showed a sigmoidal-shaped curve that first presented an exponential increase in the FFA release (Fig. 5). The start time of the lipolysis reaction, meaning the moment in which FFA started to be released, was dependent on the complexity of the dairy macromolecule solutions or products at which the O/W emulsion was incorporated. Indeed, O/W-dairy products showed a start of the lipolysis reaction immediately at the beginning of the small intestinal phase, whereas it was delayed for the O/W emulsion, O/W-dairy macromolecule solutions and O/W-skimmed milk model (Fig. 5A and B). Besides the oil from the O/W emulsion, O/W-dairy products also contained fat globules from the food matrix (Table 1), which hydrolysis could be responsible for the higher lipolysis observed at early moments of small intestinal digestion. In addition, the chain length of the fatty acids and their position within the triglyceride would also account for the higher lipid digestibility in O/W-dairy products at early moments. Triglycerides consist of a glycerol molecule having three fatty acids esterified at the hydroxyl residues, one in the central position of the glycerol molecule (sn-2) and the other two at the terminal positions sn-1 and sn-3. Dairy fat contains substantial quantities of short- and medium-chain fatty acids (C_4-C_{10}), which predominantly occupies the primary positions of the acylglycerol (sn-1 and sn-3) (Lubary et al., 2011). In turn, corn oil from O/W emulsion is mostly composed of long-chain fatty acids ($\geq C_{12}$), such as linoleic and oleic, that are mainly esterified in sn-2 and sn-3, respectively (Gao et al., 2017; Timm-Heinrich, Xu, Nielsen, & Jacobsen, 2003). In this context, it has been accepted that fatty acids on sn-2 carbon have higher bond energy and are harder to be lost than those at sn-1 and sn-3 positions, explaining the lower lipolysis in those samples without dairy fat (O/W emulsion, O/W-dairy macromolecule solutions and O/W-skimmed milk model) compared to O/W-dairy products, at early moments of small intestinal digestion (Karupaiah & Sundram, 2007). In addition, medium-chain

triglycerides (MCT) and short-chain triglycerides (SCT) are known to be digested by lipase more rapidly than long-chain triglycerides (LCT), which might also be contributing to the higher lipid digestibility observed for the O/W-dairy products in comparison with the other formulations (Salvia-Trujillo, Qian, Martín-Belloso, & McClements, 2013).

Figure 5. Lipid digestion rate expressed as free fatty acid release (%) up to 30 min of intestinal phase of the oil-in-water (O/W) emulsion incorporated into dairy macromolecule solutions (A) and dairy food products (B). Dairy macromolecule solutions: sodium caseinate, whey protein isolate, lactose as well as skimmed milk model. Dairy food products: whole milk, skimmed milk, whole yogurt and skimmed yogurt.

After the exponential phase of the FFA curve, a steady-state zone was reached in all the formulations, with a residual increase in the FFA until the end of the intestinal phase (Fig. 6A and B). There were non-significant differences in the FFA end-point between the O/W emulsion, O/W-dairy macromolecule solutions and O/W-skimmed milk model (FFA end-point ~ 60%), indicating that the individual solutions of SC, WPI and lactose or their mixture did not influence the lipolysis degree of the O/W emulsion (Fig. 6A). The uncomplete lipid digestion could be attributed to the fatty acids chain length of the triglyceride oil used to formulate the O/W emulsion. It has been previously reported that LCT oils, such as corn oil, tend to accumulate at the oil/water interface, thus hindering lipase activity (Li, Hu, & McClements, 2011).

Increasing the complexity of the fortified matrix using whole milk, skimmed milk, whole yogurt and skimmed yogurt, caused an increase in the FFA released at the end of the small intestinal phase. The O/W emulsion presented an FFA release of $64.58 \pm 2.75\%$, whereas it was 81.35 ± 0.54, 90.44 ± 2.05, 85.76 ± 14.58 and $121.48 \pm 2.75\%$ for the O/W-whole milk, O/W-skimmed milk, O/W-whole yogurt and O/W-skimmed yogurt, respectively (Fig. 6B).
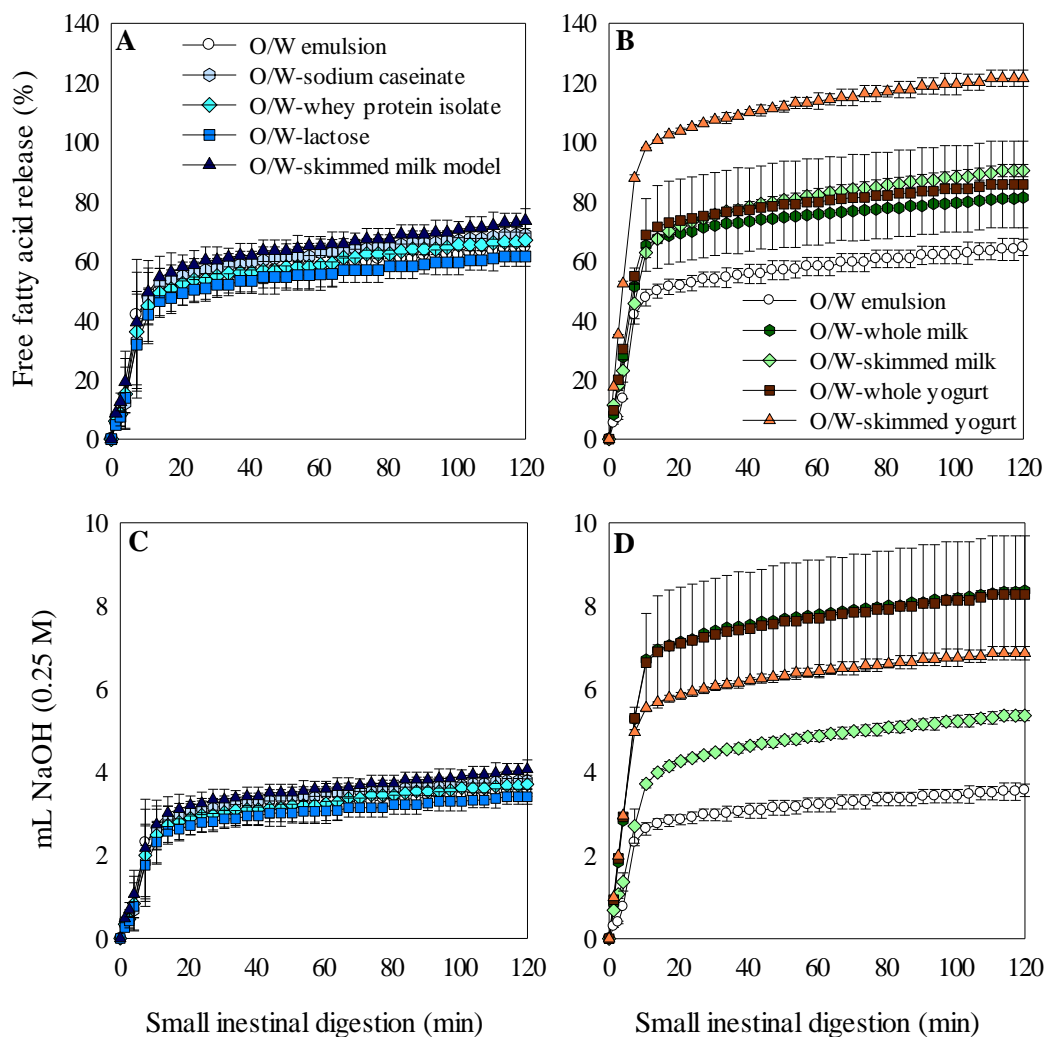
Figure 6. Lipid digestion rate and extent expressed as free fatty acid release (%) (A,C) and volume (mL) of NaOH needed during the small intestinal digestion (120 min) to maintain the pH to 7 (B,D) of the oil-in-water (O/W) emulsion incorporated into dairy macromolecule solutions (A, B) and dairy food products (C, D). Dairy macromolecule solutions: sodium caseinate, whey protein isolate, lactose as well as skimmed milk model. Dairy food products: whole milk, skimmed milk, whole yogurt and skimmed yogurt.

This high FFA release percentage obtained for the O/W-dairy products could be attributed to two reasons. On the one hand, the hydrolysis of the fat present in the dairy products might have incremented the total FFA release (Table 1). In this case, the small intestinal digestion of the whole milk, skimmed milk, whole yogurt and skimmed yogurt without the O/W emulsion, used as controls, needed 5.70 ± 0.65, 1.66 ± 0.31, 4.79 ± 0.62 and 1.36 ± 0.24 mL of NaOH, respectively, partly of which would correspond to the neutralization of the FFAs released from the dairy fat lipolysis (Supplementary material, Fig. S2). On the other hand, the release of free amino acids due to protein hydrolysis in the small intestinal phase could have contributed to the pH-stat signalling (Mat, Le Feunteun, Michon, & Souchon, 2016). In fact, the skimmed milk model needed 0.93 ± 0.05 mL of NaOH to neutralize the acid present in the small intestinal digestion, even in the absence of lipid (Supplementary material, Fig. S3). A possible explanation for the high FFA release at the end of the small intestinal digestion of the O/W-skimmed yogurt may be the presence of denaturized proteins at the oil/water interface of the oil droplets from the O/W emulsion, which would have facilitated the pancreatic lipase attack. Indeed, microscopic images of the coarse O/W-skimmed yogurt revealed part of the total protein deposited at the oil/water interface, whereas protein in the coarse O/W-skimmed milk remained in the bulk aqueous phase (Fig. 7). In agreement, other authors stated that protein heat treatment at 70 °C leads to a higher n-dodecane/water surface coverage in comparison with native protein (Dickinson & Hong, 1994; Roth, Murray, & Dickinson, 2000). In this context, it could be possible that part of the denatured protein absorbed at the oil/water interface of the O/W emulsion would have been previously hydrolysed, favouring lipase attack and consequently, leading to higher lipid digestibility compared to O/W-whole milk or skimmed milk.
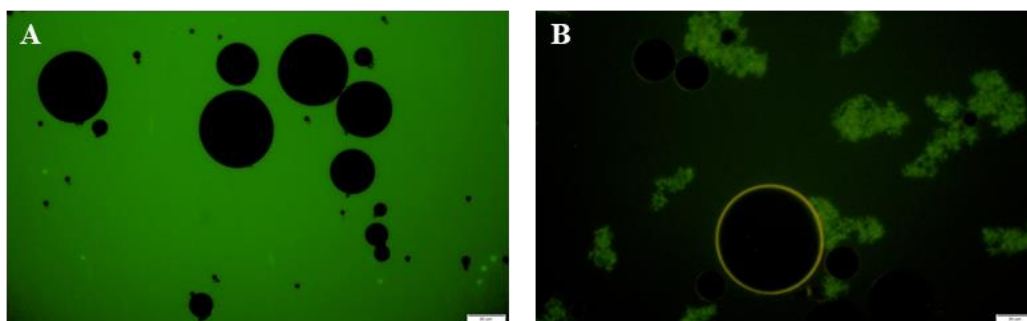
Figure 7. Optical microscopy images of the oil-in-water (O/W) emulsion incorporated into skimmed milk (A) and skimmed yogurt (B). Protein stained in green using fluorescein isothiocyanate (Fit C). Scale bar: 20 µm.
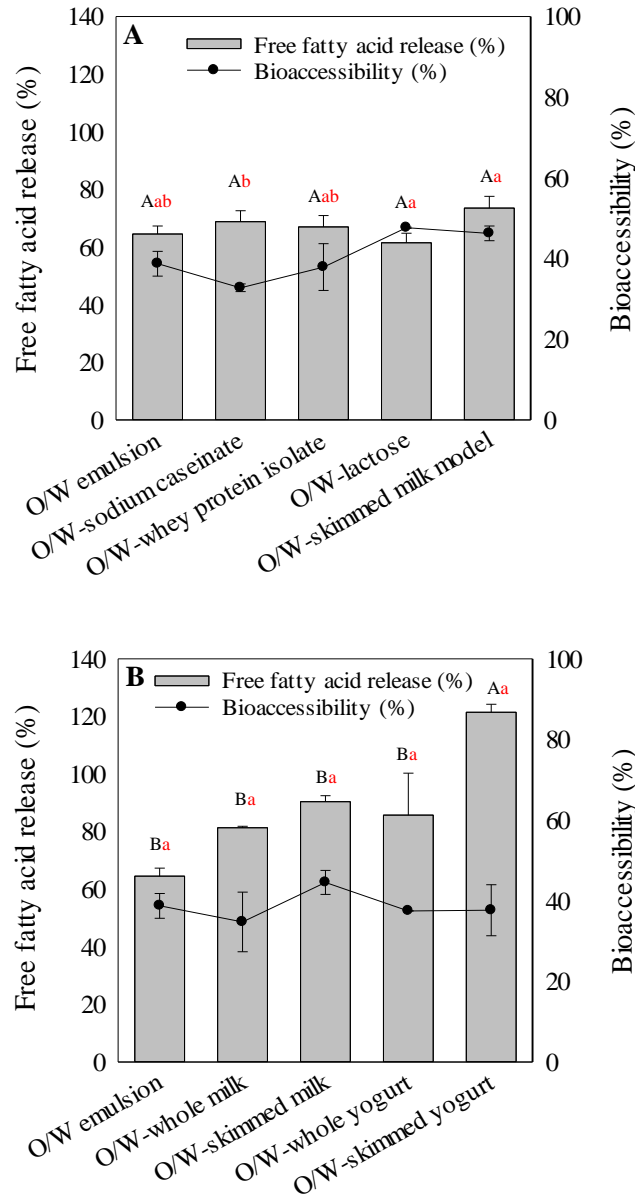
3.4 β-carotene bioaccessibility

The dairy solution or food product at which the O/W emulsion was incorporated had an impact on β-carotene bioaccessibility (Fig 8). O/W emulsion, O/W-SC and O/W-WPI presented values of 38.76 ± 3.06, 32.79 ± 0.95 and $37.92 \pm 5.81\%$, whereas it was slightly higher in the case of both O/W-lactose ($47.67 \pm 0.15\%$) and O/W-skimmed milk model ($46.27 \pm 1.82\%$) (Fig. 8A). In general, the low bioaccessibility values obtained for the O/W emulsion, O/W-SC and O/W-WPI may be due to two reasons. On the one hand, not all the FFA produced during the lipolysis participated in the formation of mixed micelles because of their interaction with other digestion products (Gasa-Falcon et al., 2019). On the other hand, mixed micelles formed during digestion may not have incorporated and solubilized β-carotene, which will further imply that β-carotene is not available to be absorbed. On the contrary, lactose could help in solubilizing β-carotene into the mixed micelles, explaining the higher values of O/W-lactose and O/W-skimmed milk model in comparison with the O/W emulsion.

This effect was not observed in the case of O/W-dairy products (Fig. 8B). Despite this, one would expect to obtain higher β-carotene bioaccessibility in both O/W-dairy products than in the O/W emulsion due to their higher FFA release percentage and consequently, the enhanced formation of mixed micelles. Nevertheless, they presented similar β-carotene bioaccessibility as the O/W emulsion (Fig. 8B). In this sense, it could be possible that part of the β-carotene present in the digest of the O/W-dairy products would have not been incorporated into mixed micelles formed during digestion due to its interaction with dairy macromolecules. Protein is known to form complexes with carotenoids *via* hydrophobic interactions and promote aggregation and precipitation of mixed micelles (Mun, Kim, Shin, & McClements, 2015; Wackerbarth, Stoll, Gebken, Pelters, & Bindrich, 2009). Thus, part of the solubilized β-carotene from the digested O/W-dairy products would have migrated to the pellet fraction during centrifugation, explaining the absence of differences in the β-carotene bioaccessibility between the O/W-dairy products and the O/W emulsion.

Figure 8. β-carotene bioaccessibility (%) (lines) in relation of the lipid digestibility in terms of free fatty acid release (%) (bars) at the end of the in vitro small intestinal phase (120 min) the of oil-in-water (O/W) emulsion incorporated into dairy macromolecule solutions (A) and dairy food products (B). Dairy macromolecule solutions: sodium caseinate, whey protein isolate, lactose as well as skimmed milk model. Dairy food products: whole milk, skimmed milk, whole yogurt and skimmed yogurt. Upper-case letters indicate significant differences between the free fatty acid release while different lower-case letters indicate significant differences between the β-carotene bioaccessibility values.

4 Conclusions

The present work contributes to understanding the effect of dairy matrices, being milk and yogurt, and their main macromolecules on the β-carotene-loaded O/W emulsions physicochemical properties and colloidal stability before and throughout the gastrointestinal *in vitro* digestion, as well as, their relationship with the lipid digestibility and β-carotene bioaccessibility. The physicochemical properties and colloidal stability of the O/W emulsion remain unaltered when incorporated into milk or yogurt. Moreover, the O/W emulsion colloidal stability during *in vitro* gastrointestinal conditions is not influenced by the dairy matrices. Even though the co-digestion of the O/W emulsion with dairy matrices does not compromise its colloidal stability, it results in faster and higher lipid digestibility. Actually, the amount and chain length of the lipid type, as well as, the specific conformation of the protein within each dairy matrix would determine the lipid digestibility. Dairy fat, which is mainly composed of short-chain fatty acids that occupy the primary positions of the acylglycerol, accelerates the lipolysis and enhances its extent. In addition, denatured proteins, as found in yogurt, could also enhance the lipolysis extent. Finally, β-carotene bioaccessibility is governed by the macromolecules within the dairy matrices, rather than by the lipolysis extent. Proteins could diminish the β-carotene present in the micellar fraction by interacting with mixed micelles and/or β-carotene itself, whereas lactose enhances its micellization. Hence, this work provides new insights into the potential use of O/W emulsions as carriers of bioactive compounds into food matrices throughout gastrointestinal digestion.

5 Acknowledgements

6 References

Boon, C. S., McClements, D. J., Weiss, J., & Decker, E. A. (2010). Factors influencing the chemical stability of carotenoids in foods. *Critical Reviews in Food Science and Nutrition*, *50*(6), 515–532.

Borreani, J., Leonardi, C., Moraga, G., Quiles, A., & Hernando, I. (2019). How do Different Types of Emulsifiers/Stabilizers Affect the In Vitro Intestinal Digestion of O/W Emulsions. *Food Biophysics*, *14*(3), 313–325.

Chang, Yaoguang, & McClements, D. J. (2016). Influence of emulsifier type on the in vitro digestion of fish oil-in-water emulsions in the presence of an anionic marine polysaccharide (fucoidan): Caseinate, whey protein, lecithin, or Tween 80. *Food Hydrocolloids*, *61*, 92–101.

Dalgleish, D. G., & Corredig, M. (2012). The structure of the casein micelle of milk and its changes during processing. *Annual Review of Food Science and Technology*, *3*(1), 449–467.

Das, L., Bhaumik, E., Raychaudhuri, U., & Chakraborty, R. (2012). Role of nutraceuticals in human health. *Journal of Food Science and Technology*, *49*(2), 173–183.

Dickinson, E. (2001). Milk protein adsorbed layers and the relationship to emulsion stability and rheology. *Studies in Surface Science and Catalysis*, *132*, 973–978.

Dickison, E., & Hong, S.T. (1994). Surface Coverage of β-Lactoglobulin at the Oil—Water Interface: Influence of Protein Heat Treatment and Various Emulsifiers. *Journal of Agricultural and Food Chemistry, 42*(8), 1602–1606.

Francis, M. J., Glover, Z. J., Yu, Q., Povey, M. J., & Holmes, M. J. (2019). Acoustic characterisation of pH dependant reversible micellar casein aggregation. *Colloids and Surfaces A: Physicochemical and Engineering Aspects*, *568*, 259–265.

Gao, B., Luo, Y., Lu, W., Liu, J., Zhang, Y., & Yu, L. (2017). Triacylglycerol compositions of sunflower, corn and soybean oils examined with supercritical CO2 ultra-performance convergence chromatography combined with quadrupole time-of-flight mass spectrometry. *Food Chemistry*, *218*, 569–574.

Gasa-Falcon, A., Odriozola-Serrano, I., Oms-Oliu, G., & Martín-Belloso, O. (2019). Impact of emulsifier nature and concentration on the stability of β-carotene enriched nanoemulsions during: In vitro digestion. *Food and Function*, *10*(2), 713–722.

Gleeson, J. P., Ryan, S. M., & Brayden, D. J. (2016). Oral delivery strategies for nutraceuticals: Delivery vehicles and absorption enhancers. *Trends in Food Science and Technology*, *53*, 90–101.

Gomes, A., Costa, A. L. R., & Cunha, R. L. (2018). Impact of oil type and WPI/Tween 80 ratio at the oil-water interface: Adsorption, interfacial rheology and emulsion features. *Colloids and Surfaces B: Biointerfaces*, *164*, 272–280.

Granato, D., Barba, F. J., Bursać Kovačević, D., Lorenzo, J. M., Cruz, A. G., & Putnik, P. (2020). Functional Foods: Product Development, Technological Trends, Efficacy Testing, and Safety. *Annual Review of Food Science and Technology*, *11*, 93–118.

Halabi, A., Croguennec, T., Bouhallab, S., Dupont, D., & Deglaire, A. (2020). Modification of protein structures by altering the whey protein profile and heat treatment affects: In vitro static digestion of model infant milk formulas. *Food and Function*, *11*(8), 6933–6945.

Hassan, A. N., Frank, J. F., Farmer, M. A., Schmidt, K. A., & Shalabi, S. I. (1995). Formation of Yogurt Microstructure and Three-Dimensional Visualization as Determined by Confocal Scanning Laser Microscopy. *Journal of Dairy Science*, *78*(12), 2629–2636.

Hsu, J. P., & Nacu, A. (2003). Behavior of soybean oil-in-water emulsion stabilized by nonionic surfactant. *Journal of Colloid and Interface Science*, *259*(2), 374–381.

Hur, S. J., Decker, E. A., & McClements, D. J. (2009). Influence of initial emulsifier type on microstructural changes occurring in emulsified lipids during in vitro digestion. *Food Chemistry*, *114*(1), 253–262.

Ikeda, S., Miyanoshita, M., & Gohtani, S. (2013). Effects of Sugars on the Formation of Nanometer-Sized Droplets of Vegetable Oil by an Isothermal Low-Energy Emulsification Method. *Journal of Food Science*, *78*(7), E1017–E1021.

Karupaiah, T., & Sundram, K. (2007). Effects of stereospecific positioning of fatty acids in triacylglycerol structures in native and randomized fats: A review of their nutritional implications. *Nutrition and Metabolism*, *4*(16), 1–17.

Keowmaneechai, E., & McClements, D. J. (2002). Effect of CaCl2 and KCl on Physiochemical Properties of Model Nutritional Beverages Based on Whey Protein Stabilized Oil-in-Water Emulsions. *Journal of Food Science, 67*(2), 665-671.

Kossena, G. A., Boyd, B. J., Porter, C. J. H., & Charman, W. N. (2003). Separation and characterization of the colloidal phases produced on digestion of common formulation lipids and assessment of their impact on the apparent solubility of selected poorly water-soluble drugs. *Journal of Pharmaceutical Sciences*, *92*(3), 634–648.

Kris-Etherton, P. M., Hecker, K. D., Bonanome, A., Coval, S. M., Binkoski, A. E., Hilpert, K. F., … Etherton, T. D. (2002). Bioactive compounds in foods: their role in the prevention of cardiovascular disease and cancer. *American Journal of Medicine*, *113*(9), Suppl 2, 71-88.

Law, A. J. R., & Leaver, J. (2000). Effect of pH on the thermal denaturation of whey proteins in milk. *Journal of Agricultural and Food Chemistry*, *48*(3), 672–679.

Lee, W. J., & Lucey, J. A. (2010). Formation and physical properties of yogurt. *Asian-Australasian Journal of Animal Sciences*, *23*(9), 1127–1136.

Li, Y., & Mcclements, D. J. (2010). New mathematical model for interpreting ph-stat digestion profiles: Impact of lipid droplet characteristics on in vitro digestibility. *Journal of Agricultural and Food Chemistry*, *58*(13), 8085–8092.

Li, Y., Hu, M., McClements, D.J. (2011). Factors affecting lipase digestibility of emulsified lipids using an in vitro digestion model: Proposal for a standardised pH-stat method. *Food Chemistry, 126*(2), 498-505.

Liu, W., Wang, J., McClements, D. J., & Zou, L. (2018). Encapsulation of β-carotene-loaded oil droplets in caseinate/alginate microparticles: Enhancement of carotenoid stability and bioaccessibility. *Journal of Functional Foods*, *40*(1), 527–535.

Lubary, M., Hofland, G. W., & ter Horst, J. H. (2011). The potential of milk fat for the synthesis of valuable derivatives. *European Food Research and Technology*, *232*(1), 1–8.

Luo, J., Wang, Z. W., Wang, F., Zhang, H., Lu, J., Guo, H. Y., & Ren, F. Z. (2014). Cryo-SEM images of native milk fat globule indicate small casein micelles are constituents of the membrane. *RSC Advances*, *4*(90), 48963–48966.

Maldonado-Valderrama, J., Wilde, P., MacIerzanka, A., & MacKie, A. (2011). The role of bile salts in digestion. *Advances in Colloid and Interface Science, 165*(1), 36–46.

Marinova, K. G., Alargova, R. G., Denkov, N. D., Velev, O. D., Petsev, D. N., Ivanov, I. B., & Borwankar, R. P. (1996). *Charging of Oil - Water Interfaces Due to Spontaneous Adsorption of Hydroxyl Ions*. *4*(18), 2045–2051.
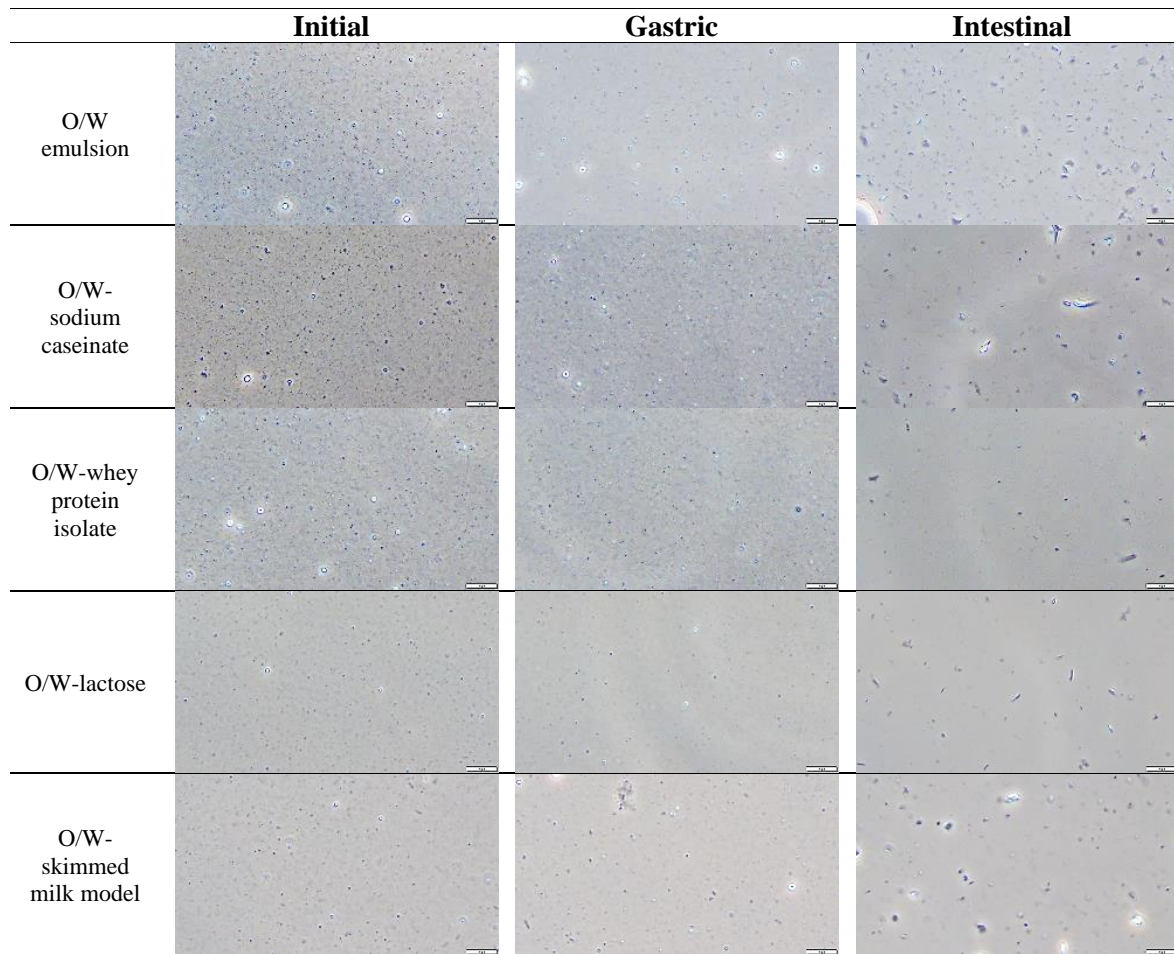
Mat, D. J. L., Le Feunteun, S., Michon, C., & Souchon, I. (2016). In vitro digestion of foods using pH-stat and the INFOGEST protocol: Impact of matrix structure on digestion kinetics of macronutrients, proteins and lipids. *Food Research International*, *88*(B), 226–233.

McClements, D. J., Decker, E. A., & Weiss, J. (2007). Emulsion-based delivery systems for lipophilic bioactive components. *Journal of Food Science*, *72*(8), 109–124.

McClements, D. J. & Li, Y. (2010). Structured emulsion-based delivery systems: Controlling the digestion and release of lipophilic food components. *Advances in Colloid and Interface Science.* 159 (2) 213–228.

McClements, D. J. (2015). *Food Emulsions: Principles, Practices, and Techniques* (3rd ed.). CRC Press, Taylor & Francis Group.

Minekus, M., Alminger, M., Alvito, P., Ballance, S., Bohn, T., Bourlieu, C., … Brodkorb, A. (2014). A standardised static in vitro digestion method suitable for food-an international consensus. *Food and Function*, *5*(6), 1113–1124. 1

Molet-Rodríguez, A., Turmo-Ibarz, A., Salvia-Trujillo, L., & Martín-Belloso, O. (2021). Incorporation of antimicrobial nanoemulsions into complex foods: A case study in an apple juice-based beverage. *LWT - Food Science and Technology*, *141*, 110926.

Mun, S., Kim, Y. R., Shin, M., & McClements, D. J. (2015). Control of lipid digestion and nutraceutical bioaccessibility using starch-based filled hydrogels: Influence of starch and surfactant type. *Food Hydrocolloids*, *44*, 380–389.

Nguyen, H. T. H., Gathercole, J. L., Day, L., & Dalziel, J. E. (2020). Differences in peptide generation following in vitro gastrointestinal digestion of yogurt and milk from cow, sheep and goat. *Food Chemistry*, *317*, 126419.

Pereira, P. C. (2014). Milk nutritional composition and its role in human health. *Nutrition*, *30*(6), 619–627.

Pinheiro, A. C., Lad, M., Silva, H. D., Coimbra, M. A., Boland, M., & Vicente, A. A. (2013). Unravelling the behaviour of curcumin nanoemulsions during in vitro digestion: Effect of the surface charge. *Soft Matter*, *9*(11), 3147–3154.

Roth, S., Murray, B. S., & Dickinson, E. (2000). Interfacial Shear Rheology of Aged and Heat-Treated β-Lactoglobulin Films: Displacement by Nonionic Surfactant. *Journal of Agricultural and Food Chemistry, 48*(5), 1491–1497.

Salvia-Trujillo, L., Qian, C., Martín-Belloso, O., & McClements, D. J. (2013). Modulating β-carotene bioaccessibility by controlling oil composition and concentration in edible nanoemulsions. *Food Chemistry*, *139*(1–4), 878–884.

Teo, A., Goh, K. K. T., Wen, J., Oey, I., Ko, S., Kwak, H. S., & Lee, S. J. (2016). Physicochemical properties of whey protein, lactoferrin and Tween 20 stabilised nanoemulsions: Effect of temperature, pH and salt. *Food Chemistry, 197*(A), 297-306.

Timm-Heinrich, M., Xu, X., Nielsen, N. S., & Jacobsen, C. (2003). Oxidative stability of structured lipids produced from sunflower oil and caprylic acid. *European Journal of Lipid Science and Technology*, *105*(8), 436–448.

Wackerbarth, H., Stoll, T., Gebken, S., Pelters, C., & Bindrich, U. (2009). Carotenoid-protein interaction as an approach for the formulation of functional food emulsions. *Food Research International*, *42*(9), 1254–1258.

Zhu, Z., Wen, Y., Yi, J., Cao, Y., Liu, F., & McClements, D. J. (2019). Comparison of natural and synthetic surfactants at forming and stabilizing nanoemulsions: Tea saponin, Quillaja saponin, and Tween 80. *Journal of Colloid and Interface Science*, *536*, 80–87.
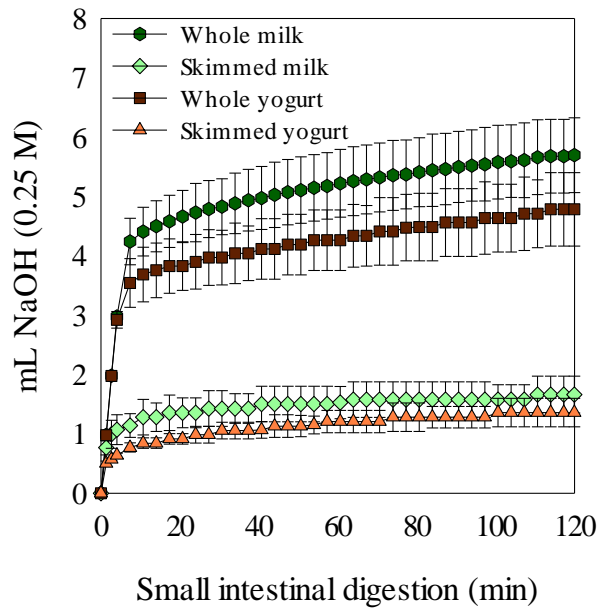
Supplementary material

|	Initial	Gastric	Intestinal
O/W emulsion			
O/W-sodium caseinate			
O/W-whey protein isolate			
O/W-lactose			
O/W-skimmed milk model			

Figure S1. Optical microscopy images of the oil-in-water (O/W) emulsion incorporated into dairy macromolecule solutions: sodium caseinate, whey protein isolate, lactose as well skimmed milk model. Scale bar: 10 μm.

Figure S2. Volume (mL) of NaOH needed during the small intestinal digestion (120 min) to maintain the pH to 7 of the dairy food products: whole milk, skimmed milk, whole yogurt and skimmed yogurt.
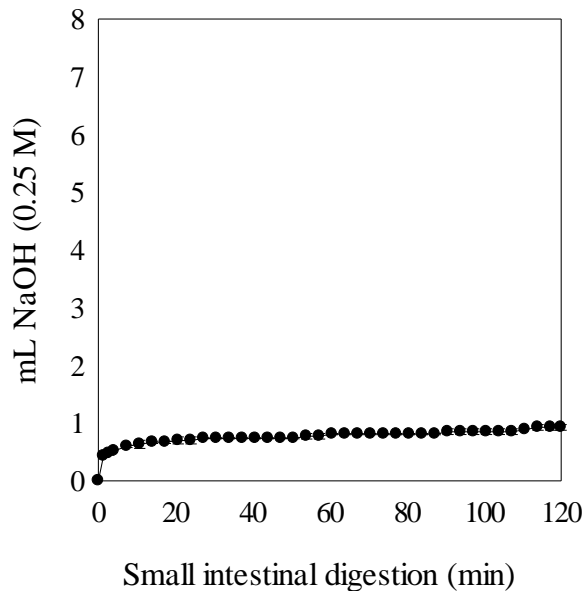
Figure S3. Volume (mL) of NaOH needed during the small intestinal digestion (120 min) to maintain the pH to 7 of the skimmed milk model.

Chapter III

In vitro digestibility of O/W emulsions co-ingested with complex meals: Influence of the food matrix

Anna Molet-Rodríguez, Amelia Torcello-Gómez, Laura Salvia-Trujillo, Olga Martín-Belloso, Alan Mackie*

Abstract

Oil-in-water (O/W) emulsions are promising delivery systems of lipophilic bioactive compounds into water-based meals. Colloidal stability of β-carotene-loaded O/W emulsion incorporated into whole milk, oatmeal and whole milk-oatmeal, and their subsequent emptying rate, lipid digestibility and β-carotene retention during *in vitro* gastrointestinal digestion were evaluated using a semi-dynamic gastric model and a static small intestinal model. Incorporating the O/W emulsion into oatmeal and whole milk-oatmeal resulted in aggregates of either β-glucan and/or protein, as well as coalesced lipid droplets. Semi-dynamic gastric digestion of O/W-whole milk showed lipid droplets embedded into a protein network, which might be located at the bottom of the vessel and emptied at earlier times in comparison with the O/W emulsion. Contrarily, O/W-oatmeal and O/W-whole milk-oatmeal had a delayed lipid emptying, probably because of their increased viscosity due to the β-glucan presence in oats. Regarding the lipid digestibility during *in vitro* small intestinal digestion, O/W-whole milk and O/W whole milk-oatmeal presented a higher percentage of free fatty acids release (> 63 %) compared to O/W emulsion and O/W-oatmeal (< 58 %), which could be attributed to faster and greater digestibility of milk fat globules. Finally, β-carotene retention during *in vitro* gastrointestinal digestion was higher in O/W-meals (> 20 %) than in O/W emulsion (< 16 %), probably due to the antioxidant properties of milk protein and oat β-glucan. Hence, this work provides valuable insight for developing functional meals by using emulsion-based delivery systems carrying active compounds.

Graphical abstract
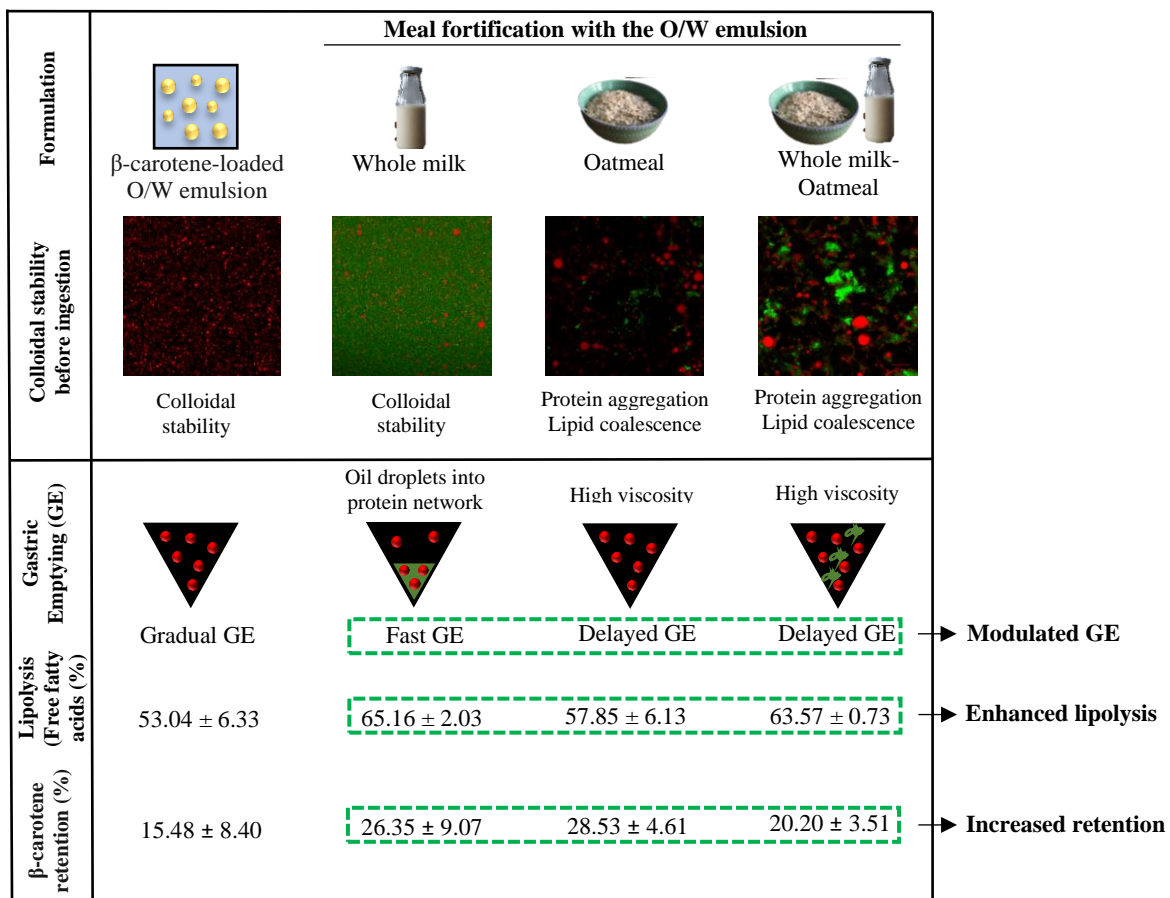
Keywords

Emulsions; fortified meals; food matrix; semi-dynamic digestion; whole milk; oatmeal.

Highlights

- Microstructural changes of dairy protein and oatmeal fibre impact the colloidal stability.
- The physicochemical properties of dairy and oatmeal matrices modulate the lipid emptying rate.
- The amount and type of fat within meals influence lipid digestibility.
- Dairy and oatmeal matrices enhance the β-carotene retention in O/W emulsions.

1   Introduction

The consumption of a diet rich in carotenoids, such as β-carotene, is well-known to have a positive impact on human health as they have been associated with functional properties, such as provitamin A activity, antioxidant capacity and enhancement of the immune system response (Maiani et al., 2009; Saini, Nile, & Park, 2015). Therefore, there is a growing interest in developing food products enriched with β-carotene to increase their functionality. Nevertheless, since β-carotene has a very low water-solubility, its incorporation into water-based food matrices is limited (Saini et al., 2015). In addition, its susceptibility to chemical degradation upon pH and temperature conditions like those found during gastrointestinal (GI) digestion, results in the loss of its functional properties (Boon, McClements, Weiss, & Decker, 2010). The use of oil-in-water (O/W) emulsions, consisting of dispersed oil droplets (from 100 nm to 10 μm) in a continuous aqueous phase, may facilitate the dispersion of β-carotene in water-based food matrices as well as its protection from degradation processes (Zhang et al., 2017). Nevertheless, there is very little information available about O/W emulsions colloidal stability once incorporated into water-based food matrices and their subsequent stability during their passage through the different phases of GI digestion. Physicochemical properties of food macromolecules may be detrimental to O/W emulsions colloidal stability by interacting with oil droplets interface and/or increasing the viscosity of the continuous phase (Gasa-Falcon, Odriozola-Serrano, Oms-Oliu, & Martín-Belloso, 2017; Thongngam & McClements, 2005). Moreover, the colloidal stability of the O/W emulsions incorporated into food matrices is related to their subsequent gastric emptying rate, as well as lipid digestion rate and extent during small intestinal digestion. In addition, β-carotene may be exposed, thus losing its functional properties upon GI conditions. Semi-dynamic *in vitro* digestion model allows mimicking the behaviour of O/W emulsions or food matrices during gastric digestion by adding acid, gastric fluids and enzymes gradually, as well as simulating the gastric emptying (GE) (Mulet-Cabero, 2020a). In fact, the behaviour of O/W emulsions or food matrices during the gastric digestion process using an *in vitro* semi-dynamic model were previously assessed (Ferreira-Lazarte et al., 2017; Mulet-Cabero, Mackie, Wilde, Fenelon, & Brodkorb, 2019; Mulet-Cabero, Rigby, Brodkorb, & Mackie, 2017). Nevertheless, to our knowledge, an understanding of O/W emulsions behaviour once co-digested with complex meals using an *in vitro* semi-dynamic model is lacking.

Therefore, the aim of this work was to investigate the influence of the food matrix components, such as dairy protein, fat and vegetable fibre, on the colloidal stability of β-carotene-loaded O/W emulsions co-ingested with complex meals before ingestion and throughout simulated gastric digestion. Moreover, the colloidal stability of the different formulations during simulated gastric digestion was related to their subsequent lipid digestibility during simulated small intestinal digestion. For this, β-carotene-loaded O/W emulsions stabilized with Tween 80 were incorporated into whole milk, oatmeal or whole milk-oatmeal and were submitted to a semi-dynamic *in vitro* digestion. After simulating the oral phase, the meals containing the β-carotene-loaded O/W emulsion were submitted to a semi-dynamic *in vitro* gastric phase, with aliquots of the bolus taken after 5-time intervals, simulating the GE. The gastric chyme emptied at different times was then subjected to static *in vitro* small intestinal phase in order to evaluate lipid digestibility. The colloidal stability in terms of particle size, particle size distribution and microstructure of the meals containing the β-carotene-loaded O/W emulsion was determined before *in vitro* oral digestion and after the different gastric emptying times. Moreover, the β-carotene retention after the small intestinal phase of each GE was determined.

2   Material and methods

2.1   Materials

Sunflower oil from a local supermarket (Tesco, Ireland), β-carotene (C9750) of ≥ 93% purity and polyoxyethylene sorbitan monooleate (Tween 80) from Sigma Aldrich (St Louise, MO, USA) were the ingredients used in the formulation of the β-carotene-loaded O/W emulsion. Whole milk and Scottish oat flakes, used to prepare the meals in which the O/W emulsion was incorporated, were purchased from a local supermarket (Tesco, Ireland). α-amylase from human saliva (A1031), pepsin from porcine gastric mucosa (P7012), pancreatin from porcine pancreas (P7545) and bile bovine (B3883) were purchased from Sigma Aldrich (St Louise, MO, USA). The α-amylase activity reported by Sigma Aldrich was 97.80 U/mg solid. The activities of pepsin and pancreatin were measured according to the assays detailed in Brodkorb et al. (2019). Pepsin had an activity of 3940 U/mg solid and pancreatin had an activity of 6.48 U/mg solid. The fluorescence dyes, Nile red (N3013), fast green (F7252) and methyl blue (95290), were purchased from Sigma Aldrich. The chemicals used in the extraction analysis to quantify the β-carotene

concentration were ethanol absolute and hexane (fraction from petroleum), both HPLC grade (Sharlab S.L, Sentmenat, Spain). The rest of the chemicals used were of analytical grade. All solutions were prepared with milli-Q water with a resistivity of 18.2 MΩ.cm at 25 °C (Milli-Q apparatus, Millipore, Bedford, UK).

2.2   Methods

2.2.1   *Formulation of the β-carotene-loaded O/W emulsion and incorporation into complex meals*

2.2.1.1   Formation of the β-carotene-loaded O/W emulsion

Firstly, β-carotene was dispersed in sunflower oil (0.1 g/100 g) by sonicating (5 min) and heating (< 50 °C, 10 min) three consecutive times, to obtain the lipid phase. Then, a coarse O/W emulsion was prepared by pre-homogenizing 20 % (w/w) of lipid phase, Tween 80 (2 % w/w) and milli-Q water (78 % w/w) using a high shear laboratory mixer, T-25 digital Ultra-Turrax (IKA, Staufen, Germany), working at 7200 rpm for 3 min. An O/W emulsion with oil droplets in the submicron range was obtained by passing the coarse O/W emulsion two times through a Jet Homogenizer (a two-chamber homogenizer developed in the School of Food Science and Nutrition, University of Leeds, Leeds, UK) at a pressure of ~300 bar.

2.2.1.2   Incorporation of the β-carotene-loaded O/W emulsion into complex meals

Three different meals, being whole milk, oatmeal and whole milk-oatmeal, were fortified with the O/W emulsion (O/W-meals). Oatmeal (*Avena sativa* L.) was chosen as a food matrix due to the rich β-glucan content, which has been suggested to have an impact on lipid digestibility (Grundy et al., 2017).

First, two preliminary blends were prepared by mixing (750 rpm; 5 min) the O/W emulsion (20 % w/w) with 80 % w/w of milli-Q water (O/W emulsion:water) or whole milk (O/W emulsion:whole milk). Then, 87 % (w/w) of the O/W emulsion:water or O/W emulsion:whole milk was diluted in milli-Q water (13 % w/w) and subsequently, mixed and boiled (750 rpm; 5 min). These two systems are referred in the manuscript as the O/W emulsion and O/W-whole milk. In addition, oat flakes were added to the O/W emulsion:water or O/W emulsion:whole milk to a final ratio of 13/87 and oatmeals were prepared by boiling and mixing at 750 rpm for 5 min. These two systems are referred in

the manuscript as O/W-oatmeal and O/W-whole milk-oatmeal. Afterwards, they were allowed to cool down to room temperature before the *in vitro* GI digestion. Lipid, protein and carbohydrate content, as well as the total solids of O/W emulsion and O/W-meals are listed in Table 1.

Table 1. Compositional description of the β-carotene-loaded oil-in-water (O/W) emulsion and after incorporation into whole milk, oatmeal and whole milk-oatmeal.

Formulation	Lipid % (w/w)	Protein % (w/w)	Fibre % (w/w)	Total solids (g)
O/W emulsion	3.48	0	0	1.04
O/W-whole milk	6.06	2.44	3.27	3.53
O/W-oatmeal	4.39	1.34	7.87	4.08
O/W-whole mil-oatmeal	6.97	3.78	11.14	6.57

2.2.2 In vitro gastrointestinal digestion

The O/W emulsion and O/W-meals were submitted to simulated GI digestion. Oral and intestinal *in vitro* digestions were performed following the INFOGEST static protocol (Brodkorb et al., 2019). A semi-dynamic *in vitro* model recently described by Mulet-Cabero et al. (2020a) was used to mimic gastric digestion.

2.2.2.1 Stock solutions of simulated digestive fluids

The electrolyte stock solutions of digestion fluids (x1.25 concentrated), including electrolyte simulated salivary fluid (eSSF: KCl, KH_2PO_4, $NaHCO_3$, $MgCl_2(H_2O)_6$, $(NH_4)_2CO_3$, HCl), electrolyte simulated gastric fluid (eSGF: KCl, KH_2PO_4, $NaHCO_3$, NaCl, $MgCl_2(H_2O)_6$, $(NH_4)_2CO_3$) and electrolyte simulated intestinal fluid (eSIF: KCl, KH_2PO_4, NaCl, $MgCl_2(H_2O)_6$) were prepared according to Brodkorb et al. (2019), adjusted to pH 7 and stored at −20 °C. The authors of this method have stated that the use of carbonate salts in the electrolyte solutions requires the use of sealed containers with limited headspace. In open vessels, as in the case of the small intestine digestion of the present study, CO_2 would be released and the pH would progressively increase with time. Following their suggestions, in eSIF, sodium bicarbonate ($NaHCO_3$), the main source of carbonates, was replaced with NaCl at the same molar ratio to maintain the ionic strength of the electrolyte solutions.

2.2.2.2   Static *in vitro* oral digestion

In the reaction vessel, which was a v-form vessel (Yorlab, UK) with a thermostat jacket (37°C), 30 g of O/W emulsion or O/W-meals were mixed with the oral mixture solution consisting of eSSF, $CaCl_2(H_2O)_2$ (0.3 M) and milli-Q water to a final ratio of 1:1 with the dry weight of food (Supplementary material Table S1). The volume of oral mixture solution added varied slightly between meals, ranging from 1.04 to 6.57 mL (Table 1 and Supplementary material Table S1). In addition, α-amylase (150 U/mL oral mixture solution) was added to the gastric mixture solution for the meals containing starch (O/W-oatmeal and O/W-whole milk-oatmeal). Then, the pH of the mixture was adjusted to 7 and incubated at 37 ºC for 2 min with continuous agitation at 150 rpm using an overhead stirrer (Hei-TORQUE Value 100, Heidolph, Germany) with a 3D printed stirrer paddle.

2.2.2.3   Semi-dynamic *in vitro* gastric digestion

A gastric mixture solution was prepared to have a final ratio of 1:1 with the oral bolus. The gastric mixture solution consisted of SGF (eSGF, $CaCl_2(H_2O)_2$ (0.3 M) and milli-Q water), HCl (1 M) and pepsin solution (Supplementary material Table S2). The pH of the oral bolus was decreased to simulate the fasted state in the stomach by adding 10% of the SGF solution and HCl until reaching pH 2. During the gastric digestion, three solutions were added: (1) the remaining 90% of SGF solution at pH 7, (2) pepsin solution (4000 U/mL of gastric mixture solution) and (3) HCl (1 M). The volume of acid needed to decrease the pH of the tested O/W emulsion and O/W-meals to 2 was determined previously, following the pH test protocol described in Mulet-Cabero et al. (2020a). A dosing device (800 Dosino, Metrohm, Switzerland) with an automatic titrator (902 Titrando, Metrohm, Switzerland) was used to deliver both the gastric mixture solution and HCl. The enzyme solution was delivered by a syringe pump (Legato, Kd Scientific, USA). The rate at which these solutions were delivered was dependent on the total gastric digestion time of O/W emulsion or O/W-meals (Supplementary material Table S3 and S4). The gastric content was mixed at 10 rpm (using the same overhead stirrer as in the oral phase) and 37°C during the total gastric phase time determined for each sample.

The simulation of the GE was determined considering the composition of each fortified meal (Table 1) and calculating their caloric content (kcal/g of meal) based on the standard Atwater factors (1 g of lipid yields 9 kcal, 1 g of protein yields 4 kcal and 1 g of

carbohydrates yields 4 kcal). The emptying rate used was constant and based on the caloric content of the studied meals and scaled-down from 2 kcal/min/mL of the realistic meal that would be digested *in vivo*, being 180 mL for the O/W emulsion and O/W-whole milk and 207 mL for the O/W-oatmeal and O/W-whole milk-oatmeal. Thus, the volume and time of each GE point differed between the fortified meals (Supplementary material Table S4). GE was simulated by taking five aliquots, referred to as GE1-5 in the text, corresponding to the portion of O/W emulsion or O/W-meals that would be delivered into the duodenum. Aliquots were taken from the bottom of the vessel using a 10 mL pipette tip, the aperture of which had a 2 mm diameter because it approximates the upper limit of particle size that has been seen to pass through the pyloric opening into the duodenum (Thomas, 2006). To inhibit pepsin activity, NaOH (2 M) was added to each GE sample to increase the pH above 7. Aliquots of GEs were collected for immediate analysis of particle size and particle size distribution (GE1 and GE5) as well as confocal microscopy (GE1, GE3 and GE5) and the rest was snap-frozen in liquid nitrogen and stored at -80 °C for subsequent *in vitro* small intestinal digestion.

2.2.2.4 Static *in vitro* small intestinal digestion

Each GE sample was placed in a water bath at 37 °C and their *in vitro* small intestinal digestion (Brodkorb et al., 2019) was simulated using a pH-stat (Metrohm USA Inc., Riverview, FL, USA). The intestinal mixture was prepared using 42.5 % (v/v) of eSIF, 0.2 % (v/v) of $CaCl_2(H_2O)_2$ (0.3 M) and 19.8 % (v/v) of Milli-Q water was added to each GE sample followed by an adjustment of pH to 7. Afterwards, 12.5 % (v/v) of bile bovine solution (20 mM intestinal mixture) and 25 % (v/v) of pancreatin solution (200 U of trypsin/mL intestinal mixture) were also added. To compensate for the free fatty acids (FFAs) that were released during the lipid digestion, the pH was constantly maintained at 7 by adding dropwise a NaOH solution (0.25 M). After 120 min, the digest collected was transferred into a glass tube and heat-shocked at 85 °C for 5 min in order to stop the lipolysis reaction and placed in an iced-water bath afterwards.

The volume of NaOH recorded during 120 min of small intestinal digestion was employed to calculate the lipid digestibility defined by the percentage of free fatty acids (FFAs) release, using equation (1):

$$Free\ fatty\ acids\ release\ (\%) = \frac{V_{NaOH} \times C_{NaOH} \times M_{lipid}}{2 \times m_{lipid}} \times 100 \tag{1}$$

where V_{NaOH} is NaOH volume (mL) used to compensate the FFAs released during the digestion, C_{NaOH} is NaOH molarity (0.25 M), M_{lipid} is lipid molecular weight and m_{lipid} is lipid total weight present in the O/W emulsion or O/W-meals before starting the small intestinal digestion. The molecular weight was 872, 700 and 867 g/mol for sunflower oil, whole milk and oat flakes lipid, respectively. The m_{lipid} of the O/W emulsion, O/W-whole milk, O/W-oatmeal and O/W-whole milk-oatmeal was 0.95, 1.58, 1.15 and 1.84 g, respectively.

The total lipid digestibility of O/W emulsion or O/W-meals was calculated as the sum of the FFAs release (%) in each individual GE.

2.2.3 *Characterization of the β-carotene-loaded O/W emulsion and incorporated into meals*

Particle size, size distribution and confocal microscopy images were taken to determine structural changes that occurred once the O/W emulsion was incorporated in the studied meals and during their subsequent semi-dynamic *in vitro* gastric digestion, that is, in the GE aliquots.

2.2.3.1 Particle size and particle size distribution

Particle size and size distribution of initial (before *in vitro* oral digestion), GE1 and GE5 aliquots from O/W emulsion and O/W-meals were measured using static light scattering (SLS) (Mastersizer 2000, Malvern Instruments Ltd, Worcestershire, UK). Aliquots from O/W-oatmeal and O/W-whole milk-oatmeal were centrifuged at 3000 rpm for 5 min and the upper part was collected for its subsequent particle size measurement (Eppendorf 5702, Hamburg, Germany). Initial, GE1 and GE5 aliquots were diluted in milli-Q water and stirred in the dispersion unit with a speed of 2200 rpm.

Particle size was reported as surface-weighted average (D$_{[3;2]}$) (data shown in the text). The refractive index of sunflower oil and water were 1.47 and 1.33, respectively.

2.2.3.2 Confocal laser scanning microscopy (CLSM)

Confocal microscopy images of initial, GE1, GE3 and GE5 aliquots from O/W emulsion and O/W-meals were taken. A stock solution of Nile Red (1 mg/mL in dimethyl sulfoxide) was used to stain the lipid, Fast Green (1 mg/mL in milli-Q water) was used to stain the protein and Methyl Blue (1 mg/mL in milli-Q water) was used to stain the β-glucan. Aliquots were dyed with the stock solutions of Nile red and Fast Green or Methyl blue and excited at wavelengths of 488, 633 and 665 nm, respectively. The emission filters were set at 555–620 nm for Nile Red, 660–710 nm for Fast Green and 550-700 nm for Methyl Blue. A Zeiss LSM 880 inverted confocal microscope (Carl Zeiss MicroImaging GmbH, Jena, Germany) with an oil immersion 63× lens and the pinhole diameter maintained at 1 Airy Unit to filter out the majority of the scattered light was used to capture the confocal images. All images were processed using the instrument software Zen.

2.2.4 β-carotene retention after gastrointestinal digestion

The capacity of O/W emulsion and O/W-meals to retain β-carotene after being subjected to the prior described *in vitro* GI digestion was determined by the method reported by Liu, Wang, McClements, & Zou (2018) with minor modifications. A 1 mL-aliquot of the initial O/W emulsion or each GE digest was mixed with 1 mL of ethanol and 1.5 mL of hexane, vortexed for 10 s and centrifuged at 9000 rpm for 10 min at 4 °C (Universal 320R, Andreas Hettich GmbH & Co. KG, Tuttlingen, Germany). The hexane fraction was analyzed spectrophotometrically (CECIL CE 2021; Cecil Instruments Ltd, Cambridge, UK) at 450 nm. The concentration of β-carotene extracted from the initial O/W emulsion or each GE digest was determined from a calibration curve of absorbance versus β-carotene concentration in hexane. The β-carotene retention was then calculated using equation (2):

$$\beta - carotene\ retention(\%) = \frac{C_{digest}}{C_{initial}} \times 100 \qquad (2)$$

where C$_{digest}$ and C$_{initial}$ are the β-carotene concentration in each GE digest and in the

initial O/W emulsion, respectively. The total β-carotene retention of O/W emulsion or O/W-meals was calculated as the sum of the β-carotene retention in each of their individual GE samples after *in vitro* small intestinal digestion.

2.3   Statistical analysis

All experiments were assayed in duplicate and data was expressed as the mean with standard deviation. An analysis of variance was carried out and the Tukey HSD test was run to determine significant differences at a 5% significance level ($p < 0.05$) with statistical software JMP Pro 14 (SAS Institute Inc.).

3   Results and discussion

## 3.1   Initial microstructure of the β-carotene-loaded O/W emulsion and after incorporation into complex meals

Initial O/W emulsion had an average oil particle size of 0.56 ± 0.03 μm with a monomodal size distribution (Fig. 1A), and homogeneous dispersion of submicron oil droplets according to its initial CLSM image (Fig. 2). Incorporating the O/W emulsion into the studied complex meals resulted in submicron oil droplets from the O/W emulsion and colloidal particles from the meals co-dispersed in the aqueous phase (Fig. 2 and 3). In the case of the O/W-whole milk, its initial CLSM image clearly showed lipid (red) and protein (green) particles dispersed in the aqueous phase (Fig. 2). Lipid particles probably correspond to O/W emulsion oil droplets and milk fat globules, whereas protein particles were presumably casein micelles. Despite this, O/W-whole milk also presented submicron average particle size (0.44 ± 0.04 μm) and monomodal size distribution (Fig. 1B). Before commercialization, whole milk is normally homogenized to reduce particle size (from 3-5 μm to below 1 μm) and increase the colloidal stability of native fat globules. In addition, it is well-known that casein micelles have particle sizes in the range of 50-500 nm (Fox & Brodkorb, 2008). In the present study, the reduced particle size of whole milk colloidal particles made it difficult to distinguish between them and submicron oil droplets from O/W emulsion by SLS, thus observing no differences in the average particle size and size distribution of O/W emulsion and O/W-whole milk.
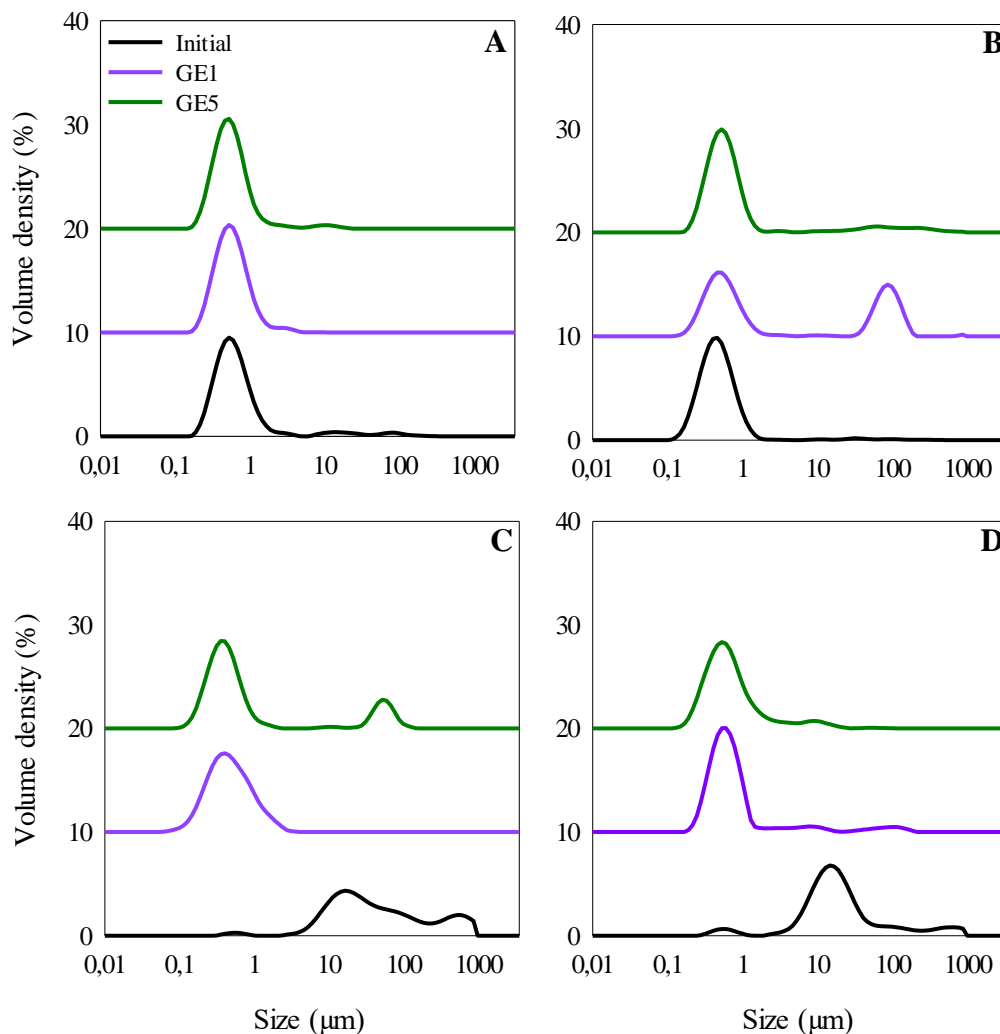
Figure 1. Droplet size distribution in volume density (%) of the β-carotene-loaded oil-in-water (O/W) emulsion (A) and after incorporation into whole milk (B), oatmeal (C) and whole milk-oatmeal (D) initially (before *in vitro* oral digestion) and at gastric emptied (GE) aliquots 1 and 5 of the semi-dynamic *in vitro* gastric digestion.

Regarding O/W-oatmeal and O/W-whole milk-oatmeal, they presented significantly larger initial average particle sizes (13.07 ± 1.81 and 7.60 ± 1.21 μm, respectively) than O/W-whole milk, which correlated with the existence of particle populations in the micro-range in the particle size distribution graph (Fig. 1C and D). In this regard, CLSM images of both oatmeal and whole milk-oatmeal (without O/W emulsion) evidenced large lipid particles as well clusters of β-glucan (blue) and/or protein (green) (Supplementary material, Fig. S1). Thus, the microstructure of oatmeal and whole milk-oatmeal would be responsible for the larger average particle sizes and size distributions observed in the O/W-oatmeal and O/W-whole milk-oatmeal compared to the O/W-whole milk.
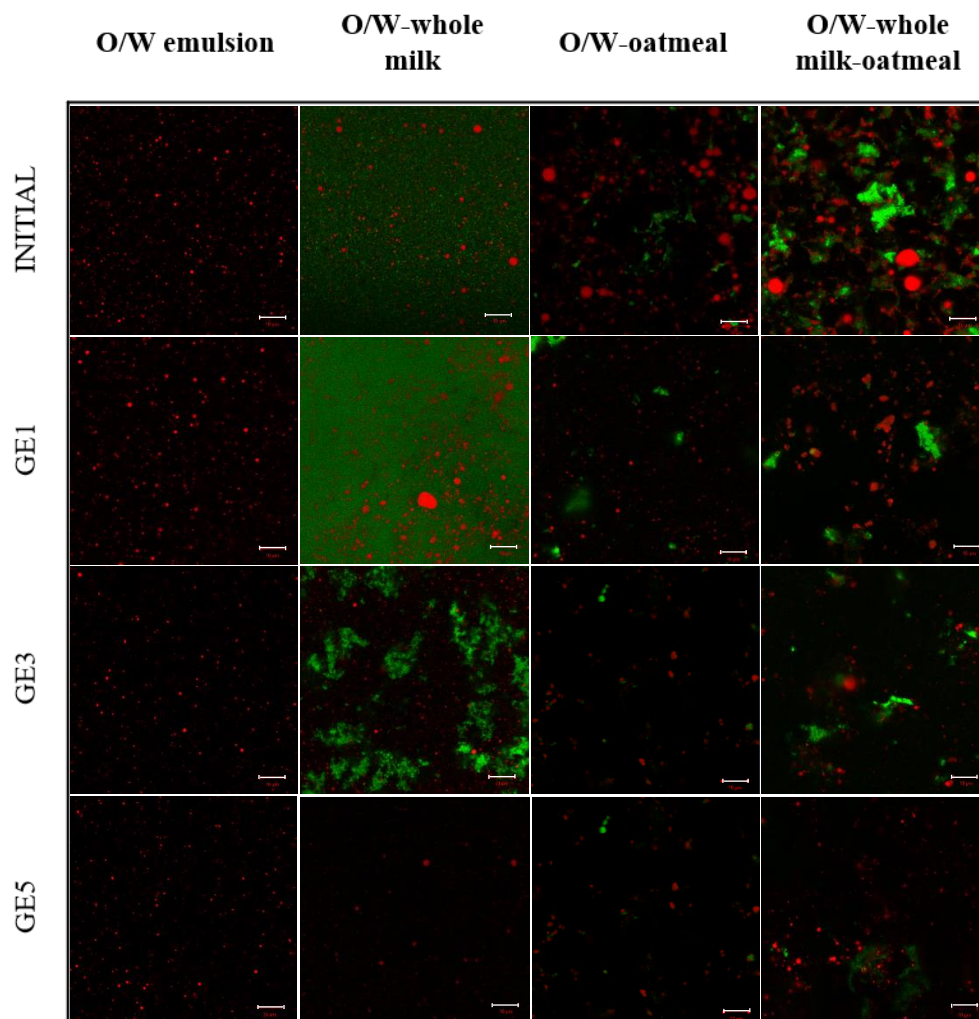
Figure 2. Confocal microscopy images of the β-carotene-loaded oil-in-water (O/W) emulsion and after incorporation into whole milk, oatmeal and whole milk-oatmeal initially (before *in vitro* oral digestion) and at gastric emptied (GE) aliquots 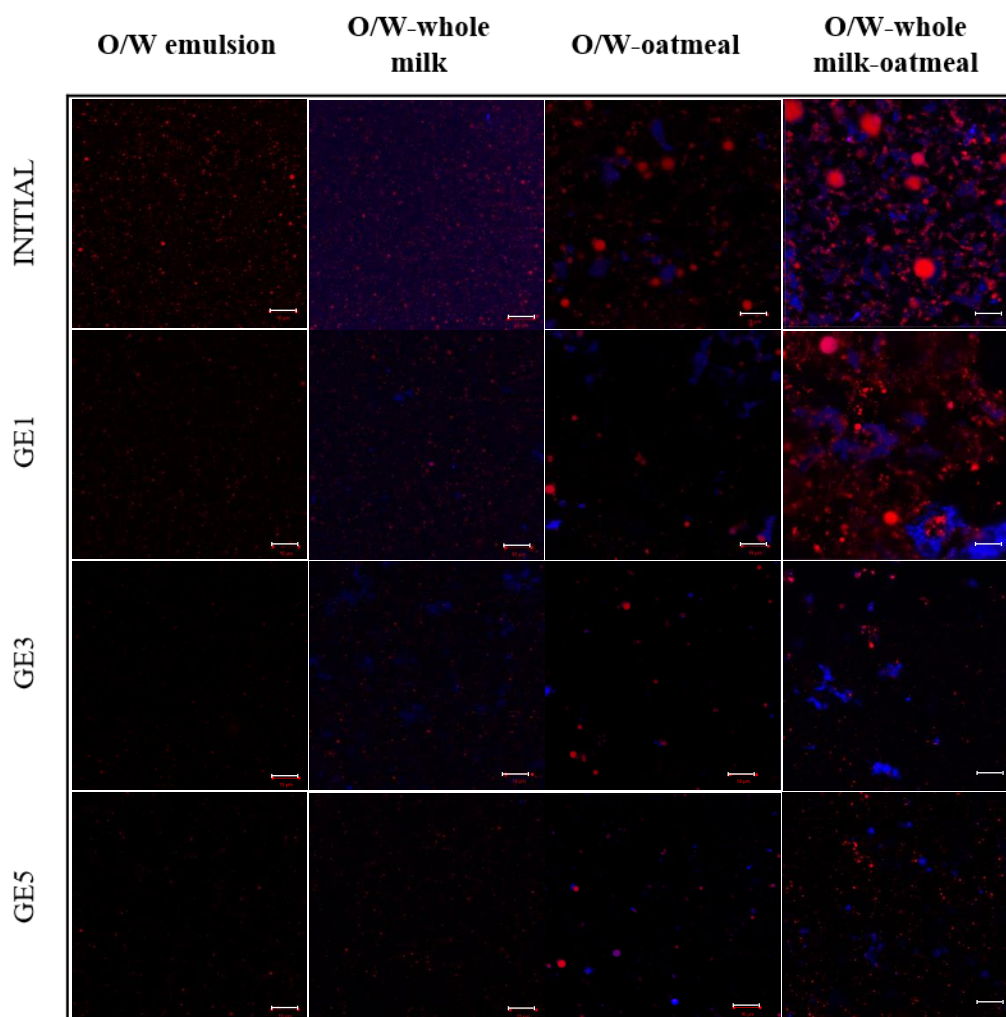1, 3 and 5 of the semi-dynamic *in vitro* gastric digestion. Protein and lipid in green (dye: Fast Green) and red (dye: Nile Red), respectively. The scale bar corresponds to 10 µm.

Oat flakes are good sources of β-glucan fibre, which is a linear unbranched polysaccharide composed of consecutive β-D-glucopyranosyl units linked by β(1-3) and β(1-4) glycosidic bonds (White, Fisk, & Gray, 2006). On the one hand, repeated units of three (cellotriosyl) or four (cellotetraosyl) sequences separated by single β(1-3) linkages in the polysaccharide chain are known to favour auto-aggregation through hydrogen bonds, explaining the observed β-glucan aggregates and the increased particle size in O/W-oatmeal and O/W-whole milk-oatmeal (Tosh, Brummer, Wood, Wang, & Weisz, 2004; Wu et al., 2006). On the other hand, studies on the stability of casein micelles in contact with β-glucan have demonstrated limited compatibility between them (De Bont,

Van Kempen, & Vreeker, 2002; Goh, Sarkar, & Singh, 2014). In particular, these authors have stated that the exclusion of β-glucan from the casein micelles surface area may cause osmotic attraction of casein micelles and consequently their aggregation. In agreement with this, in the present study, aggregates of protein were observed in the CLSM image of the O/W-whole milk-oatmeal (Fig. 2).

Figure 3. Confocal microscopy images of the β-carotene-loaded oil-in-water (O/W) emulsion and after incorporation into whole milk, oatmeal and whole milk-oatmeal initially (before *in vitro* oral digestion) and at gastric emptied (GE) aliquots 1, 3 and 5 of the semi-dynamic *in vitro* gastric digestion. β-glucan and lipid in blue (dye: Methyl blue) and red (dye: Nile Red), respectively. The scale bar corresponds to 10 μm.

3.2   *In vitro* gastrointestinal digestion of the β-carotene-loaded O/W emulsion and after incorporation into complex meals

3.2.1   Semi-dynamic in vitro gastric digestion

During semi-dynamic *in vitro* gastric digestion, O/W emulsion or O/W-meals were mixed with gastric fluids containing pepsin and HCl. As a consequence of this acidification, meal microstructure could be altered due to protein precipitation and the formation of aggregates (Francis, Glover, Yu, Povey, & Holmes, 2019). In addition, gastric samples were taken after 5-time intervals, simulating GE. Hence, changes in both the gastric pH and meal microstructure in each GE aliquot will be discussed in the following sections.

3.2.1.1   Gastric pH

Before the gastric digestion, the gastric mixture showed pH values of 2, simulating the fasted state (Fig. 4A and B). Once the O/W emulsion or O/W-meals were added to the reaction vessel, the pH increased to around 6 due to the buffering capacity of some of their components (Salaün, Mietton, & Gaucheron, 2005). During gastric digestion, this pH decreased back to the basal conditions due to both the addition of HCl and the emptying of nutrients with buffering capacity to the subsequent static small intestinal phase (Mulet-Cabero et al., 2020a). Nevertheless, significant differences in pH at the initial stages of gastric digestion (GE1 and GE2) were observed between the tested formulations. In particular, after GE1 time of gastric digestion, the O/W emulsion had a pH of 2.10, that is to say, it rapidly reached the basal pH. Contrarily, the gastric pH of the O/W-whole milk, O/W-oatmeal and O/W-whole milk-oatmeal at the same emptying point was 5.20, 2.90 and 4.00, respectively (Fig. 4A and B). Thus, the incorporation of milk with the O/W emulsion led to higher resistance to pH changes upon gastric acid addition. In this sense, it is well-known that, in foods, buffering capacity is primarily influenced by protein, which has the ability to act as a buffer (Mennah-Govela & Bornhorst, 2021). For instance, acidic amino acids present in protein (*e.g.,* aspartic and glutamic acids) have the ability to resist the changes of the gastric pH by neutralizing the H^+ added to the vessel (Mennah-Govela, Singh, & Bornhorst, 2019).
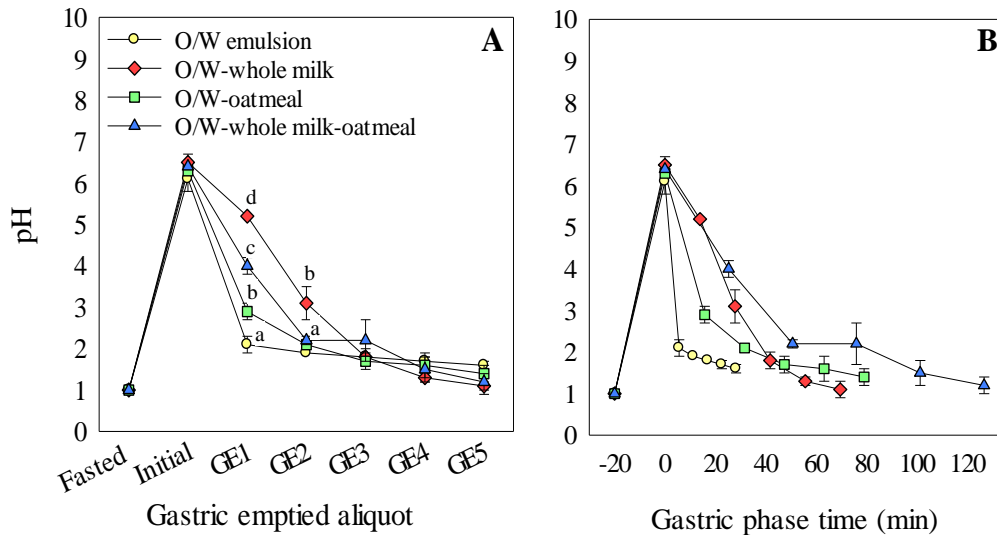
Figure 4. Gastric pH changes of the β-carotene-loaded oil-in-water (O/W) emulsion (○) and after incorporation into whole milk (◊), oatmeal (□) and whole milk-oatmeal (Δ) during *in vitro* gastric semi-dynamic digestion, expressed as function of gastric emptying (GE) points (A) and as function of the digestion time (B). Fasted state (before gastric digestion), initial (meals including oral phase and basal volume) and different GE aliquots (GE1-GE5).

In addition, a recent study dealing with the buffering capacity of several protein-based model food systems have reported a much higher buffering capacity in those food models with higher protein content (Mennah-Govela et al., 2019). In this context, pH differences in GE1 between O/W-whole milk and O/W-oatmeal might be attributed to the higher protein content in whole milk (2.44% w/w) in comparison with oatmeal (1.34% w/w) (Table 1). Nevertheless, even though the O/W-whole milk-oatmeal contained the highest protein content (3.78% w/w), it exhibited lower pH values in GE1 than the O/W-whole milk. The lower buffering capacity of the O/W-whole milk-oatmeal compared to O/W-whole milk might have been caused by the previously mentioned casein aggregation due to the presence of β-glucan (see section 3.1). In O/W-whole milk-oatmeal, aggregation of casein micelles induced by the presence of β-glucan might have led to the reduction of exposed acidic amino acid groups located in the surface, explaining its lower buffering capacity in comparison with the O/W-whole milk (Francis et al., 2019; Mennah-Govela & Bornhorst, 2021). The same tendency was observed at subsequent gastric digestion time points (GE2), with the O/W-whole milk presenting significantly higher pH compared to the other studied meals fortified with O/W emulsion. From GE3 until the end of the gastric digestion (GE5), all the O/W-meals reached the basal pH without statistically significant differences among them, which might be due to a reduction of the buffering

capacity in advanced gastric digestion time. This was confirmed by the CLSM images of all O/W-meals in GE3 and GE5 (Fig. 2), which showed low protein content, presumably because of its earlier emptying.

3.2.1.2 Microstructure changes

The particle size distribution of the O/W emulsion in GE1 and GE5 was not significantly different from the initial one, showing that it remained stable during its passage through gastric digestion (Fig. 1A). In contrast, the particle size distribution of the studied O/W-meals varied during the gastric digestion time due to pH changes and/or proteolysis occurring during gastric digestion (Fig. 1B, C and D). On the one hand, the initial monomodal distribution observed for the O/W-whole milk become multimodal in GE1. It presented one peak in the submicron range, which may belong to O/W emulsion oil droplets, milk fat globules and casein micelles, and another around 114 μm. This population of bigger droplets could correspond to the network of aggregated protein observed by CLSM in GE1 (Fig. 2). Casein micelles at pH close to their isoelectric point (pH 4.5-4.8) are known to precipitate (Francis et al., 2019). However, GE1 of O/W-whole milk had higher pH (5.20 ± 0.01) than the isoelectric point of casein micelles (Fig. 4A). Thus, other factors might also have caused the aggregation of casein molecules in GE1. In fact, it has been previously reported that pepsin favours the hydrolysis of κ-caseins, which leads to a reduction of the steric repulsion between casein micelles and consequently their aggregation at higher pH values than their isoelectric point (Mulet-Cabero et al., 2020b; Tam & Whitaker, 1972). Nevertheless, the size distribution of O/W-whole milk in GE5 was monomodal again, which could be explained by an absence of protein in this GE aliquot because of its earlier emptying (Fig. 1B). This was confirmed by CLSM images that showed the presence of protein molecules in all the GE aliquots except in GE5 (Fig. 2). On the other hand, the initial multimodal distributions of the O/W-oatmeal and O/W-whole milk-oatmeal, which were attributed to the protein and β-glucan aggregates from meal matrices, became monomodal in GE1 (Fig. 1C and D). This could be due to the re-dissolution of protein and β-glucan aggregates by the secretion of gastric fluids during the gastric digestion time (Fig. 2 and 3). In GE5, O/W-oatmeal presented a multimodal size distribution with one population of particles in the submicron range and another between 10 and 100 μm. Instead, O/W-whole milk-oatmeal size distribution was monomodal. The population of micrometric particles in O/W-oatmeal could be explained

by the re-aggregation of β-glucan in GE5 because of the increase in the ionic strength by SGF (Sarantis, Eren, Kowalcyk, Jimenez–Flores, & Alvarez, 2021). Nevertheless, the re-aggregation of β-glucan due to the increase in the ionic strength would not occur in presence of milk protein as observed in O/W-whole milk oatmeal.

3.2.2 *Static in vitro small intestinal digestion*
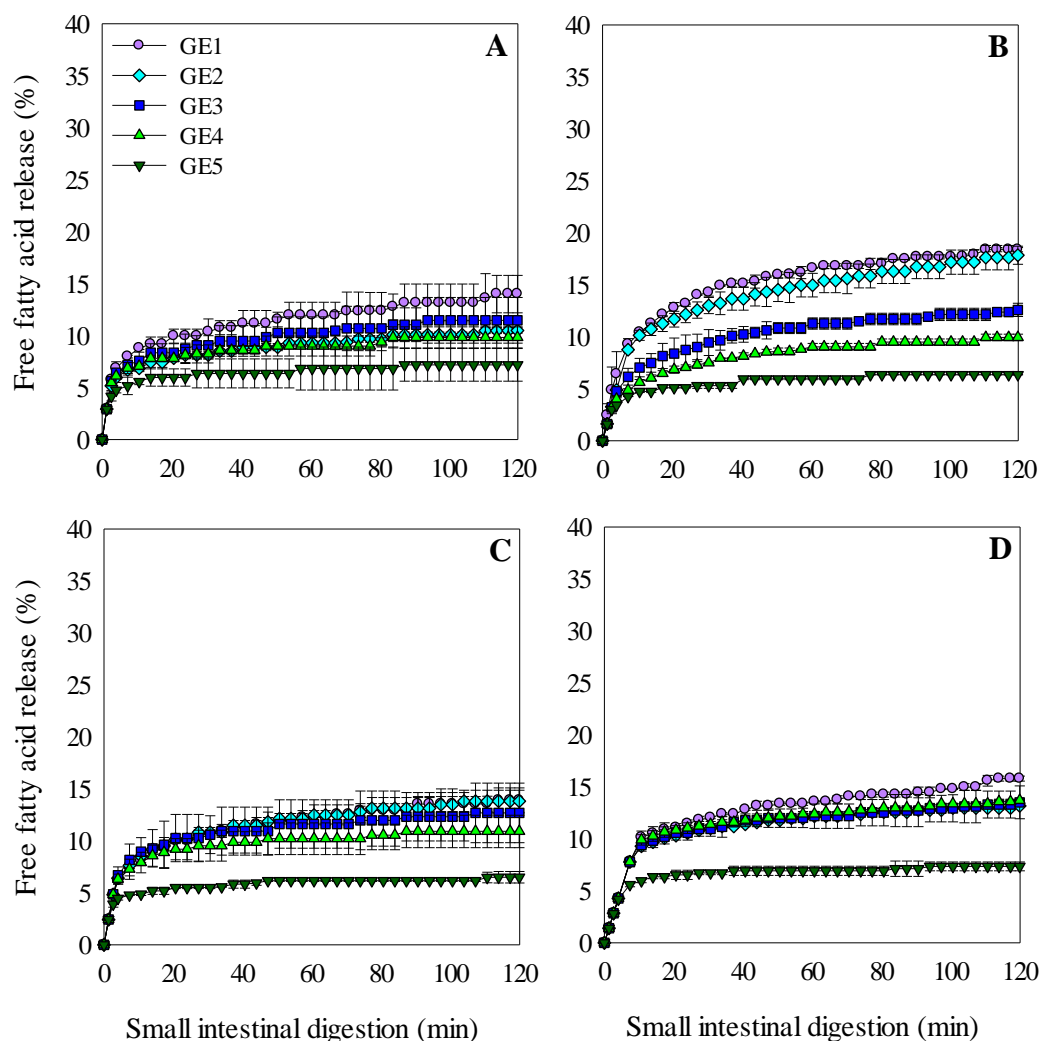
3.2.2.1 Lipid digestibility in each gastric emptying

The *in vitro* lipid digestibility during the static small intestinal phase of the different GEs, measured as the percentage of FFA release, is related to the lipid content of the samples taken at different gastric digestion moments. In this regard, O/W emulsion showed a gradual decrease in FFA release along the different GEs, from 14.01 ± 1.80 (GE1) to $7.20 \pm 1.57\%$ (GE5) (Fig. 5 and 6A). This can be related to the dilution that occurs during the gastric phase, subsequently decreasing the concentration of lipids in the gastric vessel during time. Hence, O/W emulsion at GE1 presented a higher oil concentration than at GE2, and it decreased progressively in subsequent GE points. This suggests that the O/W emulsion presents high colloidal stability in the gastric phase, as seen in CLSM images (Fig. 2), since the dilution factor during the gastric phase determines the lipid digestibility in the small intestinal phase. In fact, it has been widely reported that Tween 80 renders highly stable emulsions under gastric conditions, in contrast with other surfactants (Verkempinck et al., 2018). In this sense, other authors have reported a gradual decrease of the FFA release along the gastric emptying of O/W emulsions when subjected to semi-dynamic *in vitro* digestion and a sudden increase at the final GE, which is attributed to the emptying of the creamed lipid layer of unstable emulsions (Mulet-Cabero et al., 2020b). Hence, the FFA release in the small intestine after the semi-dynamic gastric phase may not only indicate the amount of lipid that is delivered into the small intestinal phase but also may be related to the stability of the O/W emulsion under gastric conditions when incorporated into different meals. For instance, the gradual decrease in FFA release from GE1 to GE2 points of the O/W emulsion was no longer observed for the O/W-whole milk. In fact, similar FFA release was observed in both GE1 ($18.39 \pm 0.20\%$) and GE2 ($17.85 \pm 0.87\%$) of O/W-whole milk, showing that the presence of whole milk led to a greater amount of lipid emptied at early times of the gastric digestion in comparison with the O/W emulsion (Fig. 5 and 6B). CLSM images of the O/W-whole milk at GE1 showed lipid droplets entrapped in a network of protein formed by their precipitation due to the

174

action of pepsin (section 3.2.1.2) (Fig. 2). Hence, the larger amount of lipid in GE1 and GE2 of O/W-whole milk could be explained by migration of the protein network to the bottom of the vessel (sedimentation), thus emptying the lipid droplets entrapped in the protein network at early gastric times (GE1 and GE2) (Mulet-Cabero et al., 2019). In the subsequent GE samples, FFA release percentage decreased gradually from 12.60 ± 0.63 (GE3) to $6.37 \pm 0.03\%$ (GE5), thus behaving as the O/W emulsions (Fig. 5 and 6B). This behaviour could be attributed to the low protein content present in these GE samples, as observed in the CLSM images of GE3 and GE5.
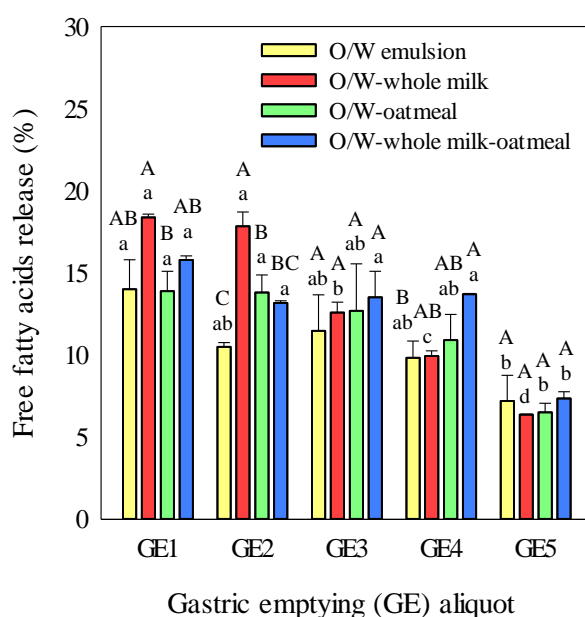
Figure 5. Lipid digestibility of the different gastric emptying (GE) samples from the β-carotene-loaded oil-in-water (O/W) emulsion (yellow) and after incorporation into whole milk (red), oatmeal (green) and whole milk-oatmeal (blue) at the end of *in vitro* small intestinal digestion expressed as the percentage of free fatty acid release. Different upper-case letters mean significant differences between formulations for the same GE. Different lower-case letters indicate significant differences between GE aliquots for the same formulation.

Figure 6. Lipid digestibility rate of the gastric emptied samples (GE1-5) from the β-carotene oil-in-water (O/W) emulsion (A) and after incorporation into whole milk (B), oatmeal (C) and whole milk-oatmeal (D) during *in vitro* small intestinal digestion, expressed as the percentage of free fatty acid release.

Regarding the O/W-whole milk-oatmeal, it presented a lower FFA release percentage at GE1 ($15.80 \pm 0.24\%$) than the O/W-whole milk ($18.39 \pm 0.20\%$), even though having a larger amount of lipid initially (Fig. 5 and Table 1). In addition, it is important to notice that FFA release percentages in GE aliquots 1 to 4 of O/W-oatmeal and O/W-whole milk-oatmeal remained practically constant and decreased at GE5 (Fig 5, 6C and 6D). For instance, O/W-whole milk-oatmeal between GE1 and GE4 presented end-point FFA release values from 15.80 to 13.71%, whereas it was $7.36 \pm 0.42\%$ in GE5 (Fig. 5 and 6D). This suggests higher gastric retention in both O/W-oatmeal and O/W-whole milk-oatmeal compared to O/W emulsion and O/W-whole milk, which might be attributed to the physicochemical properties of the oat flakes. Similarly, other authors have also reported increased gastric retention of semi-solid meals compared to liquid ones due to

their elevated viscosity (Mackie, Rafiee, Malcolm, Salt, & van Aken, 2013). In the present study, the β-glucan within oat flakes could have possibly altered the physicochemical properties of the food systems by either increasing their viscosity and/or forming a gel depending on their molecular weight, explaining the delay in the lipid emptying observed when the O/W emulsion was incorporated in meals containing oat flakes (Brummer et al., 2014; Regand, Tosh, Wolever, & Wood, 2009; Tosh et al., 2004). This was confirmed by the presence of solubilized β-glucan in the aqueous phase of O/W-oatmeal and O/W-whole milk-oatmeal at GE1 and GE3, as observed in their CLSM images (Fig. 3). In addition, the initial visual images of the meals showed that both O/W-oatmeal and O/W-whole milk-oatmeal had a gel-like appearance, while the O/W emulsion and O/W-whole milk were liquid (Fig. 7).
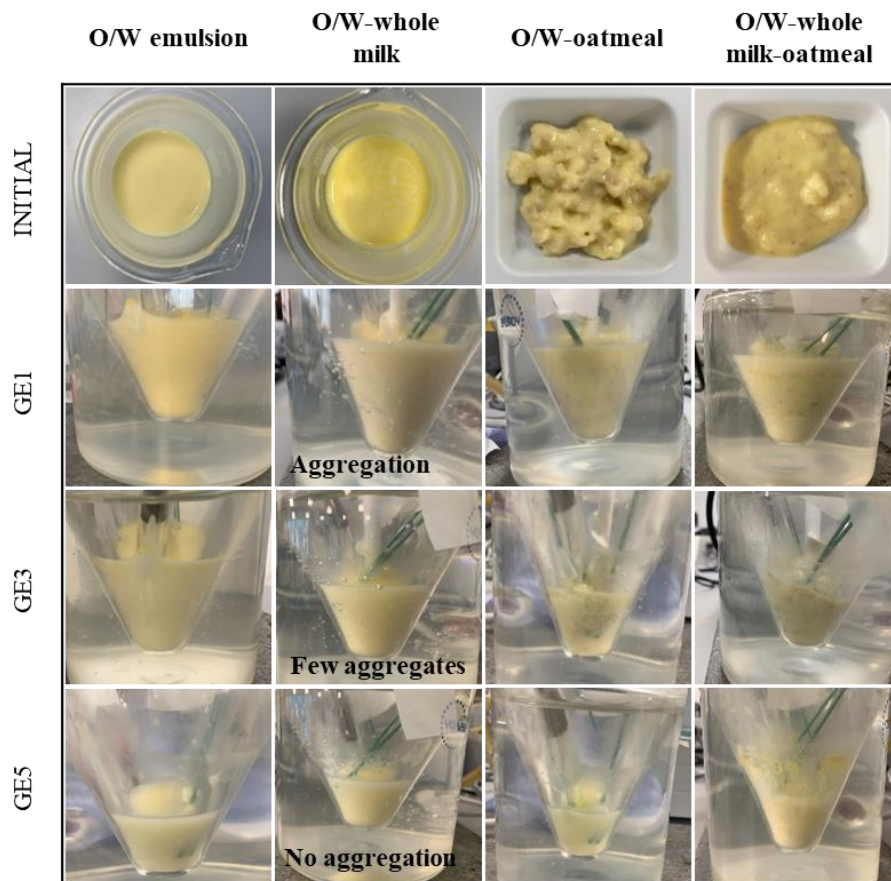
Figure 7. Visual appearance of the β-carotene-loaded oil-in-water (O/W) emulsion and after incorporation into whole milk, oatmeal and whole milk-oatmeal initially (before *in vitro* oral digestion) and at gastric emptying (GE) points 1, 3 and 5 of *in vitro* gastric semi-dynamic digestion.

3.2.2.2 Total lipid digestibility of β-carotene-loaded O/W emulsion and after incorporation into complex meals

The total lipid digestibility of O/W emulsion at the end of the *in vitro* small intestinal digestion, measured as the total percentage of FFA release, was 53.04 ± 6.33% (Table 2). The uncomplete lipid digestion could be attributed to the fatty acids chain length of the triglyceride oil used to formulate the O/W emulsion. It has been previously reported that long-chain triglyceride (LCT) oil, like sunflower oil, tend to accumulate at the oil/water interface, thus hindering lipase activity (Li, Hu, & McClements, 2011).

Table 2. Total lipid digestibility of the β-carotene-loaded oil-in-water emulsion (O/W) and after incorporation into whole milk, oatmeal and whole milk-oatmeal at the end of the *in vitro* small intestinal digestion, expressed as the percentage of free fatty acids release.

Formulation	Total free fatty acid release (%)
O/W emulsion	53.04 ± 6.33[A]
O/W-whole milk	65.16 ± 2.03[A]
O/W-oatmeal	57.85 ± 6.13[A]
O/W-whole milk-oatmeal	63.57 ± 0.73[A]

The lipid digestibility of O/W-whole milk (65.16 ± 2.03%), O/W-oatmeal (57.85 ± 6.13%) and O/W-whole milk-oatmeal (63.57 ± 0.73%) tended to be greater compared to the O/W emulsion, although no significant differences were observed between them (Table 2). One possible explanation for this increase is that milk fat globules may have demonstrated a larger extent of hydrolysis in comparison with sunflower oil droplets from the O/W emulsion. Triglycerides consist of a glycerol molecule having three fatty acids esterified at the hydroxyl residues, one in the central position of the glycerol molecule (sn-2) and the other two at the terminal positions sn-1 and sn-3. It has been accepted that fatty acids on sn-2 carbon have greater bond energy and are more difficult to be lost than those at sn-1 and sn-3 positions (Karupaiah & Sundram, 2007). Whole milk contains substantial quantities of short- and medium-chain fatty acids (C_4-C_{10}), which predominantly occupies the primary positions of the acylglycerol (sn-1 and sn-3) (Lubary, Hofland, & ter Horst, 2011). In turn, sunflower oil is mostly composed of long-chain fatty acids ($\geq C_{12}$), such as linoleic and oleic, that are mainly esterified in sn-2 and sn-3,

respectively (Gao et al., 2017; Timm-Heinrich, Xu, Nielsen, & Jacobsen, 2003). Medium- (MCT) and short-chain triglycerides (SCT) are known to be digested by lipase more rapidly than LCT, which might be related to a greater digestibility of the milk fat in comparison with the oil droplets (Salvia-Trujillo, Qian, Martín-Belloso, & McClements, 2013).

3.3 β-carotene retention after *in vitro* gastrointestinal digestion of the O/W emulsion and after incorporation into complex meals

The concentration of β-carotene in each GE sample after the *in vitro* small intestinal digestion of the O/W emulsion or O/W-meals was determined, and the percentage of β-carotene retained was calculated based on its initial concentration in O/W emulsion. In general, as gastric digestion progressed (from GE1 to GE5), the β-carotene retention tended to decrease, although no significant differences were observed (Fig. 8). The total β-carotene retention at the end of the small intestinal digestion of the O/W emulsion was $15.48 \pm 8.40\%$ (Table 3). Due to its unsaturated structure, β-carotene is highly susceptible to degradation during digestion. However, the incorporation of β-carotene into emulsions is known to reduce its degradation even when exposed to environmental stresses such as the pH and temperature of the digestion process (Mao et al., 2009). In fact, other authors have reported β-carotene retention values above 50% after *in vitro* digestion of O/W emulsions of similar droplet size (Liu et al., 2018). The differences between the results observed in the present work and previously reported data may rely on the surfactant used to stabilize the oil/water interface. In fact, several authors reported that β-carotene degradation in Tween-stabilized O/W emulsions was significantly faster than in protein-stabilized ones, which might be explained by several reasons (Jo & Kwon, 2014; Mao et al., 2009; Qian, Decker, Xiao, & McClements, 2012). First, protein-stabilized O/W emulsions have more negatively charged oil droplets than Tween-stabilized ones, favouring their repulsion. Second, milk protein is known to have antioxidant properties due to its ability to scavenge free radicals and chelate pro-oxidant transition metals, avoiding β-carotene oxidation. And third, it has been also suggested that protein forms relatively thicker membranes than Tween around lipid droplets acting as a physical barrier that separated the hydrophilic bioactive compound from the aqueous phase pro-oxidants.
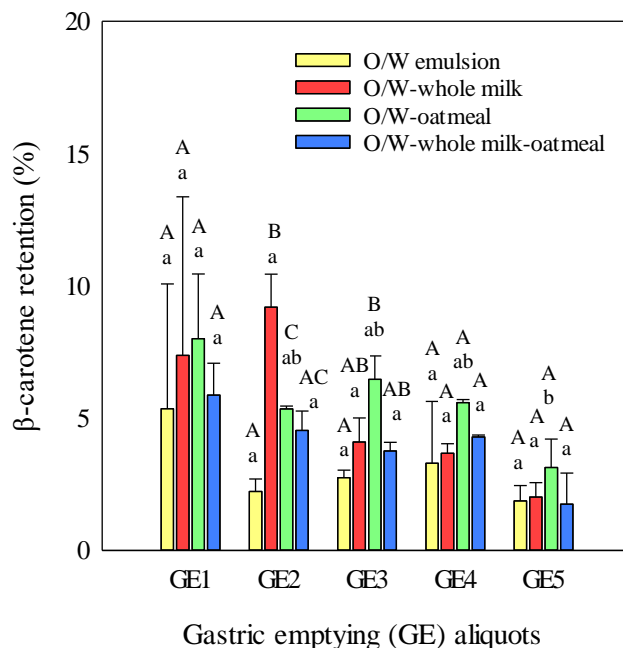
Figure 8. β-carotene retention (%) after *in vitro* gastrointestinal digestion of the different gastric emptying (GE) samples from the β-carotene O/W emulsion (yellow) and after incorporation into whole milk (red), oatmeal (green) and whole milk-oatmeal (blue). Different upper-case letters mean significant differences between formulations for the same GE. Different lower-case letters indicate significant differences between GE aliquots for the same formulation.

In addition, the macromolecules present in each meal affected the total β-carotene retention, which was 26.35 ± 9.07, 28.53 ± 4.61 and $20.20 \pm 3.51\%$ for O/W-whole milk, O/W-oatmeal and O/W-whole milk-oatmeal, respectively (Table 3). This fact has also been observed by other researchers, who hypothesized that enhanced protection of β-carotene encapsulated in O/W emulsions incorporated in milk in comparison with water can be explained by the presence of protein and polysaccharides in these food systems (Chuacharoen & Sabliov, 2016). Other authors have stated that polysaccharides are capable of retarding carotenoid oxidation in O/W emulsions by *(i)* slowing down the diffusion of prooxidants to oil droplet surface because of the viscosity increase and *(ii)* metal ion chelation and hydrogen donation, through which polysaccharides function as radical chain breakers (Sun, Gunasekaran, & Richards, 2007).

Table 3. Total β-carotene retained (%) after *in vitro* gastrointestinal digestion of the oil-in-water (O/W) emulsion and after incorporation into whole milk, oatmeal and whole milk-oatmeal.

Formulation	Total β-carotene retained (%)
O/W emulsion	15.48 ± 8.40^A
O/W-whole milk	26.35 ± 9.07^A
O/W-oatmeal	28.53 ± 4.61^A
O/W-whole milk-oatmeal	20.20 ± 3.51^A

4 Conclusions

The present study provides useful information about the influence of the food matrix components, such as dairy protein and fat, as well as vegetable fibre, on the colloidal stability of β-carotene-loaded O/W emulsions once incorporated into complex meals and their subsequent colloidal stability, lipid emptying rate, lipid digestibility and β-carotene retention throughout a semi-dynamic *in vitro* digestion model and subsequent static small intestine model. The particle size of the O/W emulsion incorporated into a meal consisting of a combination of milk and oat flakes fibre was determined by the limited compatibility between casein micelles and β-glucan, which translated into bigger particle sizes than O/W emulsion. During semi-dynamic *in vitro* gastric digestion, it was evident that microstructural changes of meal matrices as a result of macromolecule interactions influence the lipid emptying rate. Casein precipitation during the gastric phase led to a faster lipid emptying in O/W-whole milk, whereas it was delayed in both O/W-oatmeal and O/W-whole milk-oatmeal probably due to viscosity increase by the presence of β-glucan. The addition of the O/W emulsion into meals containing whole milk presented the highest total lipid digestibility, showing faster and more extensive digestion of milk fat globules compared to sunflower oil droplets. Finally, the intrinsic antioxidant activity of milk and oat flakes components demonstrate their ability to protect against degradation of the β-carotene loaded into O/W emulsions that were subsequently incorporated into meals. Hence, this work elucidates the contribution of whole milk and/or oat flakes within complex food matrices, on the formation and digestibility of meals fortified with O/W emulsions as carriers of lipophilic bioactive compounds.

5   Author contributions

Anna Molet-Rodríguez: Conceptualization, Methodology, Formal analysis, Investigation, Visualization, Writing - original draft. **Amelia Torcello-Gómez:** Conceptualization, Methodology, Visualization, Resources, Writing - review & editing. **Laura Salvia-Trujillo:** Formal analysis, Visualization, Supervision, Funding acquisition, Project administration, Writing - review & editing. **Olga Martín-Belloso:** Supervision, Funding acquisition, Project administration, Writing - review & editing. **Alan Mackie:** Conceptualization, Methodology, Visualization, Resources, Writing - review & editing, Supervision, Funding acquisition, Project administration.

6   Acknowledgements

7   References

Boon, C.S., McClements, D.J., Weiss, J., Decker, E.A. (2010). Factors Influencing the Chemical Stability of Carotenoids in Foods. *Critical Reviews in Food Science and Nutrition, 50*(6), 515-532.

Brodkorb, A., Egger, L., Alminger, M., Alvito, P., Assunção, R., Ballance, S., … Recio, I. (2019). INFOGEST static in vitro simulation of gastrointestinal food digestion. *Nature Protocols*, *14*(4), 991–1014.

Brummer, Y., Defelice, C., Wu, Y., Kwong, M., Wood, P. J., & Tosh, S. M. (2014). Textural and rheological properties of oat beta-glucan gels with varying molecular weight composition. *Journal of Agricultural and Food Chemistry*, *62*(14), 3160–3167.

Chuacharoen, T., & Sabliov, C. M. (2016). The potential of zein nanoparticles to protect entrapped b -carotene in the presence of milk under simulated gastrointestinal (GI) conditions. *LWT - Food Science and Technology*, *72*, 302–309.

De Bont, P. W., Van Kempen, G. M. P., & Vreeker, R. (2002). Phase separation in milk protein and amylopectin mixtures. *Food Hydrocolloids*, *16*(2), 127–138.

Ferreira-Lazarte, A., Montilla, A., Mulet-Cabero, A. I., Rigby, N., Olano, A., Mackie, A., & Villamiel, M. (2017). Study on the digestion of milk with prebiotic carbohydrates in a simulated gastrointestinal model. *Journal of Functional Foods*, *33*, 149–154.

Fox, P. F., & Brodkorb, A. (2008). The casein micelle: Historical aspects, current concepts and significance. *International Dairy Journal*, *18*(7), 677–684.

Francis, M. J., Glover, Z. J., Yu, Q., Povey, M. J., & Holmes, M. J. (2019). Acoustic characterisation of pH dependant reversible micellar casein aggregation. *Colloids and Surfaces A: Physicochemical and Engineering Aspects*, *568*, 259–265.

Gao, B., Luo, Y., Lu, W., Liu, J., Zhang, Y., & Yu, L. (2017). Triacylglycerol compositions of sunflower, corn and soybean oils examined with supercritical CO_2 ultra-performance convergence chromatography combined with quadrupole time-of-flight mass spectrometry. *Food Chemistry*, *218*, 569–574.

Gasa-Falcon, A., Odriozola-Serrano, I., Oms-Oliu, G., & Martín-Belloso, O. (2017). Influence of mandarin fiber addition on physico-chemical properties of nanoemulsions containing β-carotene under simulated gastrointestinal digestion conditions. *LWT - Food Science and Technology*, *84*, 331–337.

Goh, K. K. T., Sarkar, A., & Singh, H. (2014). Milk Protein–Polysaccharide Interactions. In Singh, Boland, & Thompson (2nd ed.), *Milk Proteins* (pp. 387-419). Academic Press.

Grundy, M. M. L., Quint, J., Rieder, A., Ballance, S., Dreiss, C. A., Cross, K. L., … Wilde, P. J. (2017). The impact of oat structure and b-glucan on in vitro lipid digestion. *Journal of Functional Foods*, *38*(A), 378–388.

Jo, Y. J., & Kwon, Y. J. (2014). Characterization of β-carotene nanoemulsions prepared by microfluidization technique. *Food Science and Biotechnology*, *23*(1), 107–113.

Karupaiah, T., & Sundram, K. (2007). Effects of stereospecific positioning of fatty acids in triacylglycerol structures in native and randomized fats: A review of their nutritional implications. *Nutrition and Metabolism*, *4*(16), 1–17.

Li, Y., Hu, M., McClements, D.J. (2011). Factors affecting lipase digestibility of emulsified lipids using an in vitro digestion model: Proposal for a standardised pH-stat method. *Food Chemistry, 126*(2), 498-505.

Liu, W., Wang, J., McClements, D. J., & Zou, L. (2018). Encapsulation of β-carotene-loaded oil droplets in caseinate/alginate microparticles: Enhancement of carotenoid stability and bioaccessibility. *Journal of Functional Foods*, *40*, 527–535.

Lubary, M., Hofland, G. W., & ter Horst, J. H. (2011). The potential of milk fat for the synthesis of valuable derivatives. *European Food Research and Technology*, *232*(1), 1–8.

Mackie, A. R., Rafiee, H., Malcolm, P., Salt, L., & van Aken, G. (2013). Specific food structures supress appetite through reduced gastric emptying rate. *American Journal of Physiology - Gastrointestinal and Liver Physiology*, *304*(11), 1038–1043.

Maiani, G., Castón, M. J., Catasta, G., Toti, E., Cambrodón, I. G., Bysted, A., Granado-Lorencio, F., Olmedilla-Alonso, B., Knuthsen, P., Valoti, M., Böhm, V., Mayer-Miebach, E., Behsnilian, D., & Schlemmer, U. (2009). Carotenoids: actual knowledge on food sources, intakes, stability and bioavailability and their protective role in humans. *Molecular Nutrition & Food Research*, *53*(2), S194–S218.

Mao, L., Xu, D., Yang, J., Yuan, F., Gao, Y., & Zhao, J. (2009). Effects of small and large molecule emulsifiers on the characteristics of β-carotene nanoemulsions prepared by high pressure homogenization. *Food Technology and Biotechnology*, *47*(3), 336–342.

Mennah-Govela, Y. A., & Bornhorst, G. M. (2021). Food buffering capacity: quantification methods and its importance in digestion and health. *Food and Function*, *12*(2), 543–563.

Mennah-Govela, Y. A., Singh, R. P., & Bornhorst, G. M. (2019). Buffering capacity of protein-based model food systems in the context of gastric digestion. *Food and Function*, *10*(9), 6074–6087.

Mulet-Cabero, A. I., Egger, L., Portmann, R., Ménard, O., Marze, S., Minekus, M., … Mackie, A. (2020a). A standardised semi-dynamic: in vitro digestion method suitable for food-an international consensus. *Food and Function*, *11*(2), 1702–1720.

Mulet-Cabero, A. I., Mackie, A. R., Wilde, P. J., Fenelon, M. A., & Brodkorb, A. (2019). Structural mechanism and kinetics of in vitro gastric digestion are affected by process-induced changes in bovine milk. *Food Hydrocolloids*, *86*, 172–183.

Mulet-Cabero, A. I., Rigby, N. M., Brodkorb, A., & Mackie, A. R. (2017). Dairy food structures influence the rates of nutrient digestion through different in vitro gastric behaviour. *Food Hydrocolloids*, *67*, 63–73.

Mulet-Cabero, A. I., Torcello-Gómez, A., Saha, S., Mackie, A. R., Wilde, P. J., & Brodkorb, A. (2020b). Impact of caseins and whey proteins ratio and lipid content on in vitro digestion and ex vivo absorption. *Food Chemistry*, *319*, 126514.

Qian, C., Decker, E. A., Xiao, H., & McClements, D. J. (2012). Inhibition of β-carotene degradation in oil-in-water nanoemulsions: Influence of oil-soluble and water-soluble antioxidants. *Food Chemistry*, *135*(3), 1036–1043.

Regand, A., Tosh, S. M., Wolever, T. M. S., & Wood, P. J. (2009). Physicochemical properties of glucan in differently processed oat foods influence glycemie response. *Journal of Agricultural and Food Chemistry*, *57*(19), 8831–8838.

Saini, R.K., Nile, S.H., & Park, S.W. (2015). Carotenoids from fruits and vegetables: Chemistry, analysis, occurrence, bioavailability and biological activities. *Food Research International journal, 76,* 735–750.

Salaün, F., Mietton, B., & Gaucheron, F. (2005). Buffering capacity of dairy products. *International Dairy Journal*, *15*(2), 95–109.

Salvia-Trujillo, L., Qian, C., Martín-Belloso, O., & McClements, D. J. (2013). Modulating β-carotene bioaccessibility by controlling oil composition and concentration in edible nanoemulsions. *Food Chemistry*, *139*(1–4), 878–884.

Sarantis, S. D., Eren, N. M., Kowalcyk, B., Jimenez–Flores, R., & Alvarez, V. B. (2021). Thermodynamic interactions of micellar casein and oat β-glucan in a model food system. *Food Hydrocolloids*, *115*, 106559.

Sun, C., Gunasekaran, S., & Richards, M. P. (2007). Effect of xanthan gum on physicochemical properties of whey protein isolate stabilized oil-in-water emulsions. *Food Hydrocolloids*, *21*(4), 555–564.

Tam, J. J., & Whitaker, J. R. (1972). Rates and Extents of Hydrolysis of Several Caseins by Pepsin, Rennin, Endothia parasitica Protease and Mucor pusillus Protease. *Journal of Dairy Science*, *55*(11), 1523–1531.

Thomas, A. (2006). Gut motility, sphincters and reflex control. *Anaesthesia and Intensive Care Medicine*, *7*(2), 57–58.

Thongngam, M., & McClements, D. J. (2005). Isothermal titration calorimetry study of the interactions between chitosan and a bile salt (sodium taurocholate). *Food Hydrocolloids*, *19*(5), 813–819.

Timm-Heinrich, M., Xu, X., Nielsen, N. S., & Jacobsen, C. (2003). Oxidative stability of structured lipids produced from sunflower oil and caprylic acid. *European Journal of Lipid Science and Technology*, *105*(8), 436–448.

Tosh, S. M., Brummer, Y., Wood, P. J., Wang, Q., & Weisz, J. (2004). Evaluation of structure in the formation of gels by structurally diverse (1 → 3)(1 → 4)-β-D-glucans from four cereal and one lichen species. *Carbohydrate Polymers*, *57*(3), 249–259.

Verkempinck, S. H. E., Salvia-Trujillo, L., Moens, L. G., Charleer, L., Van Loey, A. M., Hendrickx, M. E., & Grauwet, T. (2018). Emulsion stability during gastrointestinal conditions effects lipid digestion kinetics. *Food Chemistry*, *246*, 179–191.

White, D. A., Fisk, I. D., & Gray, D. A. (2006). Characterisation of oat (Avena sativa L.) oil bodies and intrinsically associated E-vitamers. *Journal of Cereal Science*, *43*(2), 244–249.

Wu, J., Zhang, Y., Wang, L., Xie, B., Wang, H., & Deng, S. (2006). Visualization of Single and Aggregated Hulless Oat (Avena nuda L.) (1→3),(1→4)-β- d -Glucan Molecules by Atomic Force Microscopy and Confocal Scanning Laser Microscopy . *Journal of Agricultural and Food Chemistry*, *54*(3), 925–934.

Zhang, R., Zhang, Z., Zou, L., Xiao, H., Zhang, G., Decker, E.A., & McClements, D.J. (2016). Enhancement of carotenoid bioaccessibility from carrots using excipient emulsions: influence of particle size of digestible lipid droplets. *Food and Function, 7*(1), 93-103.

Supplementary material

Table S1. Volume and compositional description of oral mixture solution used in the static *in vitro* oral digestion of oil-in-water (O/W) emulsion and after incorporation into whole milk, oatmeal and whole milk-oatmeal.

Formulation	Oral mixture volume[a] (mL)	Oral mixture composition			
		eSSF % (v/v)	$CaCl_2(H_2O)_2$[b] % (v/v)	α-amlylase solution[c] % (v/v)	Milli-Q water[d] % (v/v)
O/W emulsion	1.04	80	0.5	0	19.5
O/W-whole milk	3.53	80	0.5	0	19.5
O/W-oatmeal	4.08	80	0.5	5	14.5
O/W-whole milk-oatmeal	6.57	80	0.5	5	14.5

[a]Ratio of oral mixture volume to total solids of the formulations was 1:1.

[b]$CaCl_2(H_2O)_2$ (0.3 M) to achive a final concentration of 1.5 mM in the oral mixture solution.

[c]α-amylase solution (150 U/mL oral mixture solution) was added to those formulations containing starch, that is O/W-oatmeal and O/W-whole milk oatmeal.

[d]Required volume of milli-Q water to reach the total oral mixture volume

Table S2. Volume and compositional description of gastric mixture solution used in the semi-dynamic *in vitro* gastric digestion of oil-in-water (O/W) emulsion and after incorporation into whole milk, oatmeal and whole milk-oatmeal.

Formulation	Gastric mixture volume[a] (mL)	Gastric mixture composition				
		eSGF % (v/v)	HCl[b] % (v/v)	$CaCl_2(H_2O)_2$[c] % (v/v)	Pepsin solution[d] % (v/v)	Milli-Q water[e] % (v/v)
O/W emulsion	31.04	76.67	4.37	0.05	3.33	15.58
O/W-whole milk	33.53	76.67	11.76	0.05	3.33	8.19
O/W-oatmeal	34.08	76.67	6.86	0.05	3.33	13.09
O/W-whole milk-oatmeal	36.57	76.67	13.02	0.05	3.33	6.93

[a]Ratio of gastric mixture volume to oral bolus of the formulations was 1:1.

[b]HCl content in each meal was determined in a previous test, which determine the volume and concentration of HCl (1 M) needed to decrease the pH of the tested formulations to pH 2.

[c]$CaCl_2(H_2O)_2$ (0.3 M) to achive a final concentration of 0.15 mM in the gastric mixture solution.

[d]Pepsin solution (4000 U/mL in the gastric mixture solution).

[e]Required volume of milli-Q water to reach the total gastric mixture volume.

Table S3. Rate of gastric secretions used in semi-dynamic *in vitr*o gastric digestion of oil-in-water (O/W) emulsion and after incorporation into whole milk, oatmeal and whole milk-oatmeal.

Formulation	Gastric secretions		
	Rate of gastric mixture (mL/min)	Rate of pepsin solution (µL/min)	Rate of HCl solution (1M) (µL/min)
O/W emulsion	0.96	36.7	43.4
O/W-whole milk	0.42	16.0	51.0
O/W-oatmeal	0.38	14.4	26.6
O/W-whole milk-oatmeal	0.25	9.6	33.8

Table S4. Gatric emptying (GE) volume (mL) and time (min) for oil-in-water (O/W) emulsion and after incorporation into whole milk, oatmeal and whole milk-oatmeal. Five emptying points were done.

Formulation	Gastric emptying volume (mL)	Gastric emptying time (min)				
		GE1	GE2	GE3	GE4	GE5
O/W emulsion	12.42	5.64	11.28	16.91	22.55	28.19
O/W-whole milk	13.41	13.93	27.86	41.79	55.71	69.64
O/W-oatmeal	13.63	15.80	31.60	47.40	63.20	79.00
O/W-whole milk-oatmeal	14.63	25.34	50.68	76.02	101.36	126.69
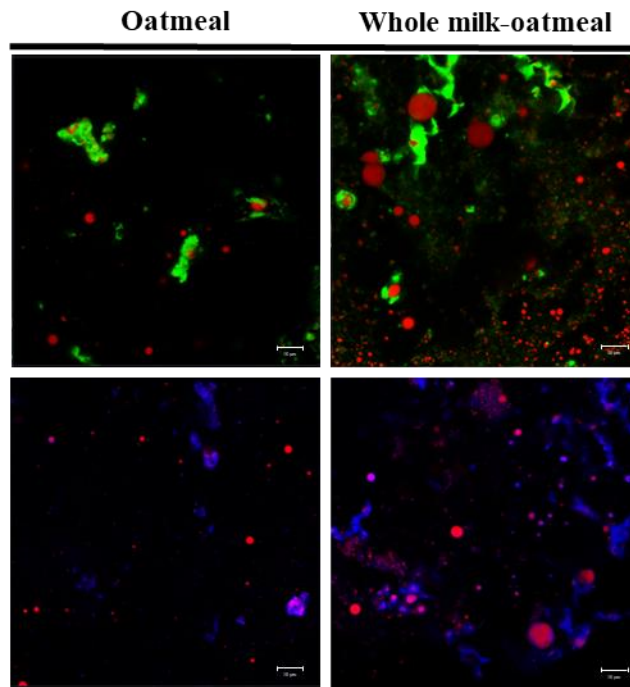
Figure S1. Confocal microscopy images of oatmeal and whole-milk oatmeal. Protein, β-glucan and lipid are green (dye: Fast green), blue (dye: Methyl blue) and red (dye: Nile red), respectively. The scale bar corresponds to 10 μm.

PUBLICATIONS

Section II

Chapter IV

Formation and stabilization of W₁/O/W₂ emulsions with gelled lipid phases

Anna Molet-Rodríguez, Olga Martín-Belloso, Laura Salvia-Trujillo*

Abstract

Water-in-oil-in-water ($W_1/O/W_2$) emulsions are emulsion-based systems where the dispersed phase is an emulsion itself, offering great potential for the encapsulation of hydrophilic bioactive compounds. However, their formation and stabilization is still a challenge mainly due to water migration, which could be reduced by lipid phase gelation. This study aimed to assess the impact of lipid phase state being liquid or gelled using glyceryl stearate (GS) at 1% (w/w) as well as the hydrophilic emulsifier (T80: Tween 80 or lecithin) and the oil type (MCT:medium-chain triglyceride or corn oil (CO) as long-chain triglyceride) on the formation and stabilization of chlorophyllin $W_1/O/W_2$ emulsions. Their colloidal stability against temperature and light exposure conditions was evaluated. Gelling both lipid phases (MCT and CO) rendered smaller W_1 droplets during the first emulsification step, followed by the formation of $W_1/O/W_2$ emulsions with smaller W_1/O droplet size and more stable against clarification. The stability of $W_1/O/W_2$ emulsions was sensitive to a temperature increase, which might be related to the lower gelling degree of the lipid phase at higher temperatures. This study provides valuable insight into the formation and stabilization of $W_1/O/W_2$ emulsions with gelled lipid phases as delivery systems of hydrophilic bioactive compounds under common food storage conditions.

Keywords

1   Introduction

Water-in-oil-in-water ($W_1/O/W_2$) emulsions consist of a water-in-oil (W_1/O) emulsion dispersed in an outer aqueous phase. The most common method to fabricate $W_1/O/W_2$ emulsions consists of a two-step process in which an initial step of making the W_1/O emulsion is followed by its dispersion in another aqueous phase (Muschiolik & Dickinson, 2017). Due to the compartmentalized internal structure, $W_1/O/W_2$ emulsions offer great potential for the encapsulation and controlled release of hydrophilic bioactive compounds (Aditya et al., 2015; Artiga-Artigas, Molet-Rodríguez, Salvia'Trujillo, & Martín-Belloso, 2018a). However, in these systems, multiple instability mechanisms can occur during their production and storage, such as coalescence of the lipid droplets and/or inner water droplets, and the coalescence of the inner water droplets with the outer water phase, which leads to water migration between both water phases. Also, inner water droplets may shrink or swell as a result of the water transfer between the inner and the outer water phases (Dickinson, 2011). In addition, it is well known that the temperature and light during storage can also affect the stability of emulsion-based systems (Chen & Zhong, 2015; Liang, Shoemaker, Yang, Zhong, & Huang, 2013; Teo et al., 2016). However, there is still scarce scientific evidence about the impact of the storage conditions on the stability of $W_1/O/W_2$ emulsions (Bou, Cofrades, & Jiménez-Colmenero, 2014). In principle, in order to form a $W_1/O/W_2$ emulsion, an initial lipophilic emulsifier is used for the stabilization of the inner interface. Polyglycerol polyricinoleate (PGPR) has been demonstrated to be highly effective as W_1/O stabilizer, due to its ability to form small W_1 droplets, and because it forms a physical barrier around these droplets preventing their coalescence (Artiga-Artigas et al., 2018a; Matos, Gutiérrez, Coca, & Pazos, 2014). To stabilize the second interface, it is necessary to use a hydrophilic emulsifier. In this case, it has been reported that polysorbates, lecithin and proteins can be effective stabilizers of this secondary interface (Dickinson, 2011; Jo & Kwon, 2014; Lamba, Sathish, & Sabikhi, 2015). In $W_1/O/W_2$ emulsions, the lipid phase is filled with nanometric inner water droplets, implying that the size of the lipid droplets is typically larger than 1 μm, which in turn renders highly unstable emulsions (Mason, Wilking, Meleson, Chang, & Graves, 2006). Therefore, strategies for improving the colloidal stability of $W_1/O/W_2$ emulsions are necessary, which require modifying the properties of both the lipid and aqueous phases. On the one hand, through adding biopolymers in the outer aqueous phase to increase its viscosity, the oil droplet mobility can be reduced and

subsequently the colloidal stability of $W_1/O/W_2$ emulsions may be enhanced (Dickinson, 2011). On the other hand, increasing the viscosity of the lipid phase by formulating solid, semi-solid or gelled lipid phases, as well as decreasing its polarity, may minimize the diffusion rates between the two aqueous phases avoiding the destabilization of the inner water phase both during the emulsion formation and during their storage (Bonnet et al., 2009; Fernández-Martín et al., 2017). For instance, glyceryl monostearate (GS), a monoacylglycerol mainly composed of stearic acid (C18:0), has been recently used as an ingredient to gel lipid phases of O/W nanoemulsions through the formation of a crystal network (Abreu-Martins, Artiga-Artigas, Hilsdorf Piccoli, Martín-Belloso, Salvia-Trujillo, 2020; Wang, Decker, Rao, & Chen, 2019). However, to the best of our knowledge, the use of GS to formulate gelled lipid phases in order to improve the colloidal stability of $W_1/O/W_2$ emulsions has not been studied.

Therefore, the aim of the present work was to study the impact of the lipid phase composition and lipid phase state (liquid vs. gelled) on the formation and stabilization of $W_1/O/W_2$ emulsions. Specifically, they were formulated with two oil types with different triglyceride chain lengths, being medium-chain triglyceride (MCT) and a long-chain triglyceride oil being corn oil (CO). In addition, the formulation of gelled lipid phases of both oils was conducted by adding 1% (w/w) of glyceryl stearate (GS) in the lipid phase. Moreover, the use of different hydrophilic emulsifiers (Tween 80, T80; or lecithin) was also studied for the formation of $W_1/O/W_2$ emulsions. Droplet size and microscopy characterization of the inner W_1 droplets and the W_1/O droplets was measured. The stability of the formulated $W_1/O/W_2$ emulsions against storage under different environmental stresses, namely temperature (4, 25 or 35 °C) or light exposure, were also evaluated. Finally, chlorophyllin (CHL) was used as model hydrophilic compound for the evaluation of the formulated $W_1/O/W_2$ emulsions as delivery systems. Encapsulation efficiency (EE) immediately after the formulation of $W_1/O/W_2$ emulsions and during storage was determined.

2   Material and methods

2.1   Materials

MCT (Myglyol, Oxi-med expres) (99.9% of purity) and CO (Koipesol Asua, Deoleo, Spain) were used as a lipid phase. Sunflower oil, which was kindly donated by Borges (Lleida, Spain), was the dispersant in droplet size measurements. GS (Imwitor® 491) with a purity of 96.7% (0.8% free glycerol and 95.9% monoglycerides) was used to formulate the gelled lipid phases. Polyglycerol polyricinoleate (PGPR) from castor oil (Grinsted®, DuPont Danisco NHIB Iberica S. L, Barcelona, Spain) was utilized as lipophilic emulsifier. Polyoxyethylene sorbitan monooleate (Tween 80) (Lab Scharlab, Barcelona, Spain) and L-α-soybean lecithin (lecithin), acquired from Alfa Aesar (Thermo Fisher Scientific, GmbH, Karlsruhe, Germany), were used as food-grade hydrophilic emulsifiers. CHL (coppered trisodium salt) with a molecular weight of 724.15 g/mol, copper contains 3.5–6.5% and a purity of $\geq 95\%$ was purchased from Alfa Aesar (Thermo Fisher Scientific, GmbH, Karlsruhe, Germany). Sodium alginate (MANUCOL®DH) was obtained from FMC Biopolymer Ltd. (Scotland, UK). NaCl POCH S.A. (Gliwice, Poland) was added to both the inner and outer aqueous phases of the system, in order to adjust the osmotic pressure balance between the aqueous phases. Ultrapure Milli-Q water obtained from a Millipore filtration system (Merck, Darmstadt, Germany) was used for the preparation of all $W_1/O/W_2$ and solutions.

2.2   Formation of $W_1/O/W_2$ Emulsions
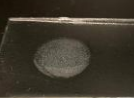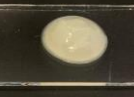
$W_1/O/W_2$ were prepared according to a two-step emulsification method previously used by Artiga-Artigas et al. (2018a) with some modifications, consisting of the formation of the W_1/O emulsion followed by its dispersion in an outer aqueous phase.

2.2.1   *Formation of the W_1/O Emulsions*

W_1/O emulsions with liquid and gelled lipid phases were formulated using pure MCT or CO as the lipid phase and GS (1% w/w) as oleogelator. The lipid phase of the W_1/O emulsions was prepared by dissolving PGPR (6% w/w) in the lipid phase (MCT or CO) using a magnetic stirrer (450 rpm) for 5 min at 50 °C. To form the gelled lipid W_1/O emulsions, GS was firstly melted by increasing the temperature at 50 °C and subsequently mixed with each of the previously prepared lipid phases containing PGPR. The visual

appearance of the lipid phases being liquid or gelled at 4, 25 or 35 °C is presented in Table 1. W_1/O emulsions were formed by mixing the lipid phase with an aqueous phase consisting of 112.5 ppm CHL, 0.05 M NaCl and 2% (w/w) sodium alginate by using a laboratory T25 digital Ultra-Turrax mixer (IKA, Staufen, Germany) working at 11000 rpm for 5 min. The temperature during the first emulsification step was kept at 50 °C in order to maintain the lipid phase in liquid state. Once the W_1/O emulsions were formed, one aliquot was taken for its subsequent characterization, which temperature was reduced down to 4 °C for 2 h in order to allow lipid gelation in those emulsions with GS. The rest was maintained at 50 ºC for the formation of the W_1/O/W_2 emulsions.

Table 1. Visual appearance at 4, 25 and 35 °C of the gelled lipid phases consisting of blends of medium-chain triglyceride (MCT) or corn oil (CO), GS (1% w/w) and PGPR (6% w/w).

Lipid type	4 °C	25 °C	35 °C
MCT			
CO			

2.2.2 *Formation of the W_1/O/W_2 Emulsions*

The second step was the dispersion of the previously prepared W_1/O emulsions in the outer aqueous phase using a laboratory T25 digital Ultra-Turrax mixer (IKA, Staufen, Germany) working at 4000 rpm for 2 min. From each W_1/O emulsion, two different W_1/O/W_2 emulsions were formed. On the one hand, the W_1/O emulsion (20% w/w) was dispersed in an outer aqueous phase (80% w/w) containing NaCl 0.05 M, sodium alginate (2% w/w) and T80 (2% w/w). On the other hand, a percentage of 2% w/w of lecithin was previously mixed with the W_1/O emulsion (18% w/w) using a magnetic stirrer at 750 rpm during 5 min followed by its dispersion in an outer aqueous phase (80% w/w) containing NaCl 0.05 M and sodium alginate (2% w/w).

2.3 Initial Characterization of W$_1$/O Emulsions and W$_1$/O/W$_2$ Emulsions

2.3.1 Droplet size

The mean droplet diameter (nm) of the W$_1$ droplets in W$_1$/O emulsions were measured by dynamic light scattering (DLS) using a Zetasizer Nano-ZS laser diffractometer (Malvern Instruments Ltd., Worcestershire, UK) working at 633 nm and 25 °C, equipped with a backscatter detector (173°). Refractive indexes (RIs) of MCT and CO were 1.48 and 1.47, respectively. Samples were prior diluted in hexane, whose RI was 1.38, using a dilution factor of 1:9 sample-to-solvent. The inner W$_1$ droplet size was characterized by average droplet size (nm). The droplet size of W$_1$/O/W$_2$ emulsions was measured by the static light scattering (SLS) technique with a Mastersizer 3000™ (Malvern Instruments Ltd., Worcestershire, UK). Samples were dispersed in distilled water (RI = 1.33) at 2200 rpm and the oil droplet size was reported as volume-weighted average (D$_{[4;3]}$).

2.3.2 Optical Microscopy Analysis

Phase contrast microscopy images of the W$_1$/O/W$_2$ emulsions were taken with an optical microscope (BX41, Olympus, Göttingen, Germany) using a ×100 oil immersion objective lens and equipped with UIS2 optical system. All images were processed using the instrument software (Olympus cellSense, Barcelona, Spain).

2.3.3 ζ-potential

The ζ-potential (mV) of the oil droplets in W$_1$/O/W$_2$ emulsions was measured by phase-analysis light scattering (PALS) with a Zetasizer NanoZS laser diffractometer (Malvern Instruments Ltd., Worcestershire, UK). Samples were prior diluted in ultrapure water using a dilution ratio of 1:9 sample-to-solvent.

2.3.4 Apparent Viscosity

Viscosity measurements (mPa·s) of the different lipid phases and W$_1$/O were performed by using a vibro-viscometer (SV-10, A&D Company, Tokyo, Japan) vibrating at 30 Hz, with constant amplitude (0.4 mm) and working at 50 °C. Aliquots of 10 mL of each sample were used for determinations.

2.4 Colloidal Stability of W_1/O/W_2 Emulsions

The stability of the prepared W_1/O/W_2 emulsions was measured by SLS during 12 days of dark storage at 4 °C as explained in section 2.3.1. In addition, their stability was also performed by multiple light scattering with a Turbiscan ™Classic MA 2000 (Formulation, Toulouse, France). The turbidity measurement allows the detection of the destabilization phenomenon by multiple light scattering. Stability analysis was carried out as a variation of backscattering (BS) during storage of W_1/O/W_2 emulsions. The equation (1) was applied in order to calculate the BS:

$$BS = 1/\sqrt{\lambda *} \tag{1}$$

where λ was the photon transport mean free path in the analyzed dispersion. From the physical point of view, the $\lambda*(\Phi,d)$ value in the analyzed dispersion was evaluated by using equation (2):

$$\lambda * (\Phi, d) = \left[\frac{2d}{3\Phi\,(1-g)Qs} \right] \tag{2}$$

where Φ is the volume fraction of particles, d is the mean diameter of particles and g(d) and QS (d) are the optical parameters given by the Mie theory (Peng et al., 2016).

Each backscattering (BS) profile obtained can be split in three zones corresponding to the bottom (on the left), the intermediate part (in the middle) and the top of the tube (on the right) where an aliquot of approximately 7 mL of the sample was placed. Emulsions destabilization mechanisms can be easily identified as BS variations in the different parts of the BS profile. Variations in particle size (flocculation or coalescence) is shown as displacement of the horizontal lines from the intermediate part of the BS profile. Whereas, gravitational separation can show up peaks either on the left part (sedimentation) or on the right (creaming). Both sedimentation and creaming can cause clarification of the emulsions. In this study, all samples showed a decrease of the BS signal on the left part of the BS profile (approx. from 0 to 50 mm), which means clarification due to gravitational movement of oil droplets to the top of the sample. Therefore, focus will be put on the analysis of BS variations on left zone of the graphs, which corresponds to the bottom of the tubes.

Data analysis of the BS values are represented as BS variation (ΔBS), which refers to the BS of each storage day relative to the initial storage day.

The stability of the $W_1/O/W_2$ emulsions as determined by the BS variation was also evaluated under common storage conditions, visible light (λ = 350–700 nm) and two different storage temperatures (25 and 35 °C).

2.5 Encapsulation Efficiency of CHL in $W_1/O/W_2$ Emulsions

The percentage of CHL entrapped in the inner aqueous phase over 12 days of refrigerated storage (4 °C) was determined according to the methods described by Aditya et al. (2015) and Teixé-Roig, Oms-Oliu, Velderrain-Rodríguez, Odriozola-Serrano, Martín-Belloso (2018) with modifications. Briefly, 10 mL of the $W_1/O/W_2$ emulsion was placed in a Falcon™ tube and centrifuged (AVANTI J-25, Beckman Instruments Inc., Fullerton, CA, USA) at 4500 rpm for 10 min at 4 °C. The outer aqueous phase at the bottom of the Falcon tube (which contained the unentrapped CHL) was collected using a syringe and centrifuged at 7500 rpm for 15 min at 4 °C, prior dilution at 1:4 with methanol. The process was repeated twice in order to extract all the unentrapped CHL. The methanol fraction containing the CHL was analyzed spectrophotometrically (V-670 spectrophotometer, Jasco, Tokyo, Japan) at 405 nm. Encapsulation efficiency (EE) was calculated using the following equation (3):

$$EE(\%) = \frac{N_{w1} - N_{w2}}{N_{w1}} \times 100 \qquad\qquad (3)$$

where N_{W2} is the amount of CHL in the methanol phase and N_{W1} is the amount of CHL initially added to the inner aqueous phase.

2.6 Statistical Analysis

All experiments were assayed in duplicate and three replicate analyzes were carried out on each parameter in order to obtain mean values. An analysis of variance was carried out and the Tukey HSD test was run to determine significant differences at a 5% significance level ($p < 0.05$) with statistical software JMP Pro 14 (SAS Institute Inc., Cary, NC, USA).

3 Results and Discussion

3.1 Initial Characterization of the W_1/O Emulsions

Within liquid lipid phases, the fatty acid chain length of the lipid phase had a significant impact on the droplet size of the internal W_1 droplets. CO-W_1/O emulsions, formulated with a lipid phase with long-chain fatty acids, exhibited significantly smaller average W_1 droplet sizes in comparison with MCT-W_1/O emulsions, which averaged 475.90 ± 63.22 and 587.47 ± 52.77 nm, respectively (Table 2).

Table 2. Droplet size (nm) and apparent viscosity (mPa·s) of chlorophyllin-loaded W_1/O emulsions formulated with different lipid phases consisting of medium-chain triglyceride (MCT) or corn oil (CO) and without or with glyceryl stearate (GS). Different upper-case letters (A, B) indicate significant differences between lipid type. Different lower-case letters (a, b) indicate significant differences between different lipid states.

		W_1/O emulsions	
	Lipid type	Droplet size (nm)	Apparent viscosity (mPa·s)[1]
Liquid lipids	MCT	$587.47 \pm 52.77^{A,a}$	$68.7 \pm 1.5^{A,a}$
	CO	$475.90 \pm 63.22^{B,a}$	$150.3 \pm 1.5^{B,a}$
Solid lipids	MCT-GS	$447.10 \pm 120.80^{A,b}$	$116.0 \pm 2.6^{A,b}$
	CO-GS	$433.53 \pm 235.80^{A,a}$	$308.5 \pm 14.4^{B,b}$

The differences in the W_1 droplet size observed in the different lipid phases might be attributed to several reasons. On the one hand, it has been reported that the efficiency of the droplet size reduction during emulsification increases as the ratio of the dispersed phase to the continuous phase viscosities decrease (Tabibiazar & Hamishehkar, 2015; Weiss & Muschiolik, 2007). This might be attributed to higher mechanical forces created during homogenization. Since the same aqueous phase composition (W_1) was used for all the formulated systems, the viscosity of the lipid continuous phase might be related to the water droplet disruption efficiency. Accordingly, it was observed that CO had a higher viscosity than MCT, being 20.5 and 9.8 mPa.s, respectively. On the other hand, the oil hydrophobicity seems to also play an important role in the W_1 droplet size of W_1/O emulsions stabilized with PGPR. Tabibiazar & Hamishehkar (2015) observed a more compact molecular arrangement and a stronger interaction of PGPR at the water/oil interface of W_1/O emulsions formulated with CO, which is more lipophilic, in comparison

to MCT, which is less lipophilic (Tabibiazar & Hamishehkar, 2015). Therefore, it is possible that the W_1 droplet size in the present work is both dependent on the viscosity and/or the hydrophobicity of the oil used as continuous phase.

Moreover, the lipid phase state, being liquid or gelled also determined the size of the W_1 droplets. The W_1 droplet size in W_1/O emulsions with a gelled lipid phase was smaller than in the respective emulsions with liquid lipid phases. W_1 droplets with a gelled lipid phase formulated with MCT+GS presented significantly smaller W_1 droplets, with values of 447.10 ± 120.80 nm, while in those formulated with MCT were 587.47 ± 52.77 nm (Table 2). This might be attributed to a number of reasons. On the one hand, the addition of GS in the lipid phase significantly increases its viscosity (Table 2), which might increase the emulsification efficiency due to an increase of the mechanical forces during emulsification. On the other hand, GS is a monoglyceride with interfacial activity that might present adsorption at the surface of the W_1 droplets, thus contributing to a certain extent to the droplet size reduction during emulsification (Zhao et al., 2018). Nonetheless, this effect was less pronounced in the case of the lipid phases containing CO, with and without GS. These results can be explained by the stronger interaction of CO with the surfactant to stabilize the inner W_1 droplets, which might favour the total covering of the water/oil interface by PGPR. As a result, GS would remain in the bulk lipid phase forming a network of crystals rather than to adsorb at the water/oil interface (Ghosh, Tran, & Rousseau, 2011). In fact, this hypothesis is supported by the results reported by Weiss & Muschiolik (2007), who observed differences in the interfacial tension of MCT/fat–crystallized W_1/O emulsions depending on the interaction between the lipid components and PGPR. In concordance with the droplet size results measured by DLS, it was also possible to identify homogeneous nanometric droplets in all W_1/O emulsions in the microscopy images (Table 3). Nevertheless, due to the limit of detection of the optic microscopy, it was not possible to visually observe differences in their droplet size when varying the lipid phase formulation.

Table 3. Optical microscopy images of chlorophyllin-loaded W_1/O emulsions (day 0) and $W_1/O/W_2$ (day 0 and 12) formulated with different lipid phases consisting of medium-chain triglyceride (MCT) or corn oil (CO) and without or with glyceryl stearate (GS) as well as different hydrophilic surfactants (Tween 80 (T80) or Lecithin). Scale bar: 10 μm.

Lipid type	W_1/O emulsions	$W_1/O/W_2$ emulsions – day 0		$W_1/O/W_2$ emulsions – day 12	
	PGPR	T80	Lecithin	T80	Lecithin
MCT					
CO					
MCT-GS					
CO-GS					

3.2 Formation of $W_1/O/W_2$ Emulsions

The influence of the surfactant type (T80 or lecithin) and the state (liquid vs. gelled) of the lipid phase on the formation of $W_1/O/W_2$ emulsions will be addressed in terms of their structure as determined by optical microscopy as well as droplet size and ζ-potential.

3.2.1 Optical Microscopy

The capability of forming $W_1/O/W_2$ emulsions mainly depended on the type of hydrophilic emulsifier used to disperse the W_1/O droplets into the W_2 phase (Table 3), being T80 capable of forming double emulsions regardless of the lipid type or state, while lecithin did not form $W_1/O/W_2$ emulsions for all the lipid types. Nevertheless, gelling the lipid phase allowed the formation of $W_1/O/W_2$ emulsions when lecithin was used as surfactant, for both lipid types (MCT and CO). In those emulsions with a liquid lipid phase, the use of T80 led to the formation of $W_1/O/W_2$ emulsions with MCT or CO, since in both cases oil droplets filled with water droplets were observed (Table 3). T80 has a high proportion of polar groups and consequently, it strongly adsorbs at the oil/water interface, which explains the results obtained (Jo & Known, 2014). On the contrary, lecithin was only able to form initially stable $W_1/O/W_2$ emulsions when CO was used as

a lipid phase, while single O/W emulsions were formed when using MCT as lipid phase, evidencing a clear destabilization of the dispersed inner W_1 droplets when MCT was used. This might be related to the lower polarity of MCT in comparison to CO (Schmidts, Dobler, Guldan, Paulus, & Runkel, 2010), hence MCT being less efficient than CO in preventing the water migration from the inner to the outer aqueous phase during the emulsification process. In addition to this, lecithin presents a strong amphiphilic nature and is preferably adsorbed in highly lipophilic interfaces, such as in CO rather than in MCT. Hence, in those emulsions formulated with MCT as lipid phase, lecithin would have been preferably located in the bulk phase, causing an osmotic imbalance between the two aqueous phases, and ultimately the destabilization of the W_1 dispersed droplets. When GS was used to gel the lipid phase, initially stable $W_1/O/W_2$ emulsions were obtained irrespective of the hydrophilic emulsifier and oil used (Table 3). This might be attributed to a decrease in water migration between aqueous phases due to the physical barrier formed by the presence of a GS crystal network in the gelled lipid phase. These results are consistent with recent studies on the impact of the lipid phase solidification on the resistance of $W_1/O/W_2$ emulsions to osmotic stress (Herzi & Essafi, 2018; Liu et al., 2020; Nelis et al., 2019). For instance, Liu et al. (2020) reported that under an external applied osmotic gradient, $W_1/O/W_2$ emulsions containing soybean oil experimented swelling or shrinkage, whereas semi-solid hydrogenated soybean oil $W_1/O/W_2$ emulsions remained without changes and thereby retarded the leakage of the W_1 phase components (Liu et al., 2020).

3.2.2 *Droplet Size*

Since the objective of this work was to study the formation and stability of $W_1/O/W_2$ emulsions, in the following sections, only those formulations rendering the formation of $W_1/O/W_2$ emulsions will be discussed, being liquid lipid $W_1/O/W_2$ emulsions formulated with lipid phases consisting on MCT or CO and stabilized with T80, and CO stabilized with lecithin. $W_1/O/W_2$ emulsions with gelled liquid phases formulated with MCT or CO mixed with GS as lipid phases and stabilized with T80 or lecithin were also included. On the one hand, the type of oil used in order to formulate $W_1/O/W_2$ emulsions had a significant impact on the droplet size of the W_1/O droplets stabilized with T80 (Table 4), being significantly smaller when using MCT (9.90 ± 0.15 µm) as compared to CO (13.14 ± 1.51 µm). Other authors have reported a relationship between the dispersed phase

viscosity and the final emulsion droplet size, obtaining smaller droplet sizes when using a low viscosity dispersed phase (Qian & McClements, 2011; Weiss & Muschiolik, 2007). This might be also applicable when the dispersed phase is a water-in-oil emulsion, such as the case of the present work. In this regard, the viscosity values of the W_1/O emulsions formulated with MCT, were significantly lower (68.7 ± 1.5 mPa·s) than the ones with CO (150.3 ± 1.5 mPa·s) (Table 2). Hence, it is reasonable to assume a relationship between the dispersed phase viscosity and the oil droplet size on the formation of W_1/O/W_2 emulsions. On the other hand, the surfactant type (T80 or lecithin) used to stabilize the CO-W1/O droplets dispersed in the W_2 phase did not cause a significant effect on their droplet size, which ranged between 13.14 and 14.54 µm (Table 4). Both emulsifiers are classified as small-molecule emulsifiers, thus occupying the same space at the oil/water interface and consequently leading to the formation of droplets with similar sizes (Kralova & Sjöblom, 2009).

Table 4. Droplet size ($D_{[4;3]}$) and ζ-potential (mV) of chlorophyllin-loaded W_1/O/W_2 emulsions formulated with different lipid phases consisting of medium-chain triglyceride (MCT) or corn oil (CO) and without or with glyceryl stearate (GS) as well as different hydrophilic surfactants (Tween 80 (T80) or Lecithin). A, B indicates significant differences between the lipid type. a, b indicates significant differences between the used surfactants. x, y indicates significant differences between the lipid phase state.

	W_1/O/W_2 emulsions		
	Lipid-emulsifier type	**$D_{[4;3]}$ (µm)**	**ζ-potential (mV)**
Liquid lipids	MCT-T80	$9.90 \pm 0.15^{A,a,x}$	$-24.65 \pm 3.44^{A,a,x}$
	CO-T80	$13.14 \pm 1.51^{B,a,x}$	$-26.92 \pm 5.02^{A,a,x}$
	CO-Lecithin	$14.54 \pm 0.14^{B,a,x}$	$-70.95 \pm 4.81^{B,b,x}$
Solid lipids	MCT-GS-T80	$11.09 \pm 5.71^{A,a,x}$	$-25.06 \pm 1.64^{A,a,x}$
	CO-GS-T80	$9.06 \pm 1.96^{A,a,y}$	$-30.01 \pm 5.72^{B,a,x}$
	MCT-GS-Lecithin	$7.35 \pm 0.68^{A,b,y}$	$-63.52 \pm 2.90^{A,b,y}$
	CO-GS-Lecithin	$7.64 \pm 0.45^{A,b,y}$	$-57.52 \pm 7.61^{B,b,y}$

Regarding the lipid phase state, non-significant differences in the average oil droplet size of the W_1/O/W_2 emulsions formulated with MCT and GS were observed in comparison to their respective liquid emulsions (Table 4). On the contrary, CO-W_1/O/W_2 emulsions showed a significantly smaller average oil droplet size with a gelled (7.64–9.06 µm) than with a liquid (13.14–14.54 µm) lipid phase, regardless of the emulsifier used. In a

previous study of O/W emulsions, it was also observed that when the lipid phase was crystallized with GS, there was a reduction in the average oil droplet size, which was attributed to the GS surface-active properties and adsorption to the oil/water interface (Abreu-Martins et al., 2020).

3.2.3   ζ-potential

The ζ-potential of the $W_1/O/W_2$ emulsions is detailed in Table 4. There were no significant differences between the electrical charge (ζ-potential) of the T80-stabilized $W_1/O/W_2$ emulsions formulated with MCT or CO oil, with values ranging between −24.65 and −26.92 mV. On the contrary, the emulsifier type affected the electrical charge of the oil droplets, presenting more negative values when lecithin was used as emulsifier (−70.95 ± 4.81 mV) in comparison to T80. The lower ζ-potential values of $W_1/O/W_2$ emulsions stabilized with lecithin might be due to the anionic nature of this emulsifier, which is rich in phosphate groups (PO_3^{-4}) (Artiga-Artigas, Lanjari-Pérez, Martín-Belloso, 2018b; Zhang et al., 2012). On the contrary, T80 is a non-ionic emulsifier, meaning it does not give a charge when adsorbed at the interface. However, it is known that anionic hydroxyl groups (OH^-) present in the water or oil used to prepare the $W_1/O/W_2$ emulsion can give small negative charges (McClements, 2015). On the one hand, lecithin led to less negatively charged dispersed droplets when the lipid phase was gelled in comparison to the respective liquid phase. In this regard, ζ-potential values were −70.95 ± 4.81 and −57.52 ± 7.61 mV for CO-$W_1/O/W_2$ emulsions with liquid and gelled lipid phases, respectively (Table 4). This might be attributed to the ability of GS to displace a certain amount of anionic lecithin molecules from the oil droplet surface (Gaonkar & Borwankar, 1991), thus contributing to the overall increase in the ζ-potential values becoming less negatively charged. On the other hand, $W_1/O/W_2$ emulsions stabilized with T80, showed similar ζ-potential values when formulated with either MCT or CO, regardless of the lipid state (Table 4). This might be due to the fact that T80 strongly adsorbs at the oil/water interface, which prevents its displacement by GS molecules, hence maintaining its interfacial electrostatic characteristics (Nash & Erk, 2017).

## 3.3 Colloidal Stability of $W_1/O/W_2$ Emulsions

The colloidal stability of $W_1/O/W_2$ emulsions was characterized in terms of optical microscopy, as well as static and multiple light scattering during 12 days of dark storage at 4 °C in order to simulate common storage conditions. As visually observed by phase contrast optical microscopy (Table 3), gelling the lipid phase with GS rendered $W_1/O/W_2$ emulsions with smaller droplet sizes after 12 days of storage regardless of the type of lipid (MCT or CO) or emulsifier (T80 or lecithin) used. Nonetheless, gelling the lipid phase led to higher droplet size variations of the W_1/O droplets dispersed in the W_2 phase during storage time as indicated by the large droplet size deviations as measured by SLS, while the droplet size of the $W_1/O/W_2$ emulsions with liquid lipid phases remained constant with small standard deviations (Fig. 1). It has been reported that O/W nanoemulsions with a liquid lipid phase have spherical shape, while solid lipid ones tend to be non-spherical due to the formation of crystals on the lipid phase (Mehnert & Mäder, 2012). If we consider that in the present study the droplet size was expressed as volume mean diameter, which assumes spherical droplets, a possible non-spherical shape of the W_1/O droplets with GS may be detected as bigger oil droplets (Abreu-Martins et al., 2020).
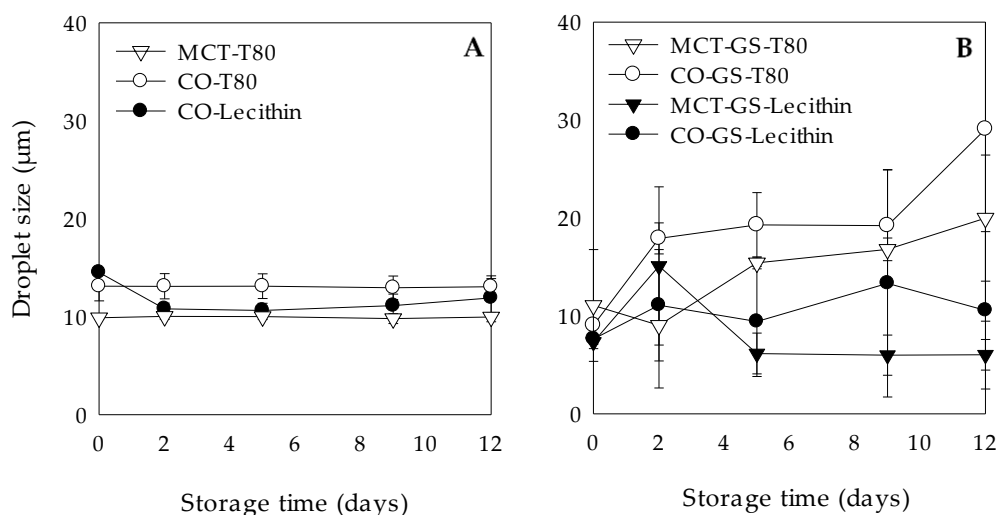
Figure 1. Droplet size ($D_{[4;3]}$) during 12 days of dark storage at 4 °C of chlorophyllin-loaded $W_1/O/W_2$ emulsions formulated with different lipid phases consisting of medium-chain triglyceride (MCT) or corn oil (CO) and without (A) or with (B) glyceryl stearate (GS) as well as different hydrophilic surfactants (Tween 80 (T80) or Lecithin).

In addition, the increase in droplet size may also be attributed to oil droplets aggregation due to changes in the crystal morphology. Numerous studies have observed that lipid crystals rearrange in a more stable form (from α to β) after emulsion formation (Fredrick, Walstra, & Dewettinck, 2010; Helgason, Salminen, Kristbergsson, McClements, & Weiss, 2015; Qian, Decker, Xiao, & McClements, 2013). As a consequence, these β-form crystals could lead to an increase in the surface-area of the oil droplets, enhancing the attraction forces between them. In the case of lecithin, droplet aggregation might have been inhibited by the high electrostatic repulsion between oil droplets (section 3.2.3).

Clarification, measured as ΔBS at the bottom of the tube, was also influenced by the lipid phase state. In general, $W_1/O/W_2$ emulsions with a liquid lipid phase showed a significant increase in BS values during storage time, whereas their respective $W_1/O/W_2$ emulsions with a gelled lipid phase remained without changes, which evidenced their higher stability against clarification (Fig. 2). According to Fernández-Martín et al. (2017) the crystallization of a lipid phase would increase its viscosity offering a higher resistance to a viscous flow. Regarding the BS changes in the $W_1/O/W_2$ emulsions with liquid lipid phases, they presented ΔBS values below 5 during the first 2 days of storage, but experimented an increase after 5 days (Fig. 2A). At that point, clarification rather depended on the type of hydrophilic emulsifier used to disperse the W_1/O droplets into the W_2 phase, than on the lipid phase composition, with ΔBS values of around 20 and below 15 for lecithin and T80, respectively. Nevertheless, at the end of the storage time, differences in the ΔBS were predominantly due to the lipid phase composition. For instance, $W_1/O/W_2$ emulsions stabilized with T80 presented ΔBS values of 11.64 ± 1.08 and 23.88 ± 0.74 for MCT and CO, respectively (Fig. 2A). This might be due to the reduced initial oil droplet size of the $W_1/O/W_2$ emulsions formulated with MCT as compared to CO, which is known to cause droplets to be closely packed, retarding their migration to the upper part of the tube (McClements, Decker, Weiss, 2007).
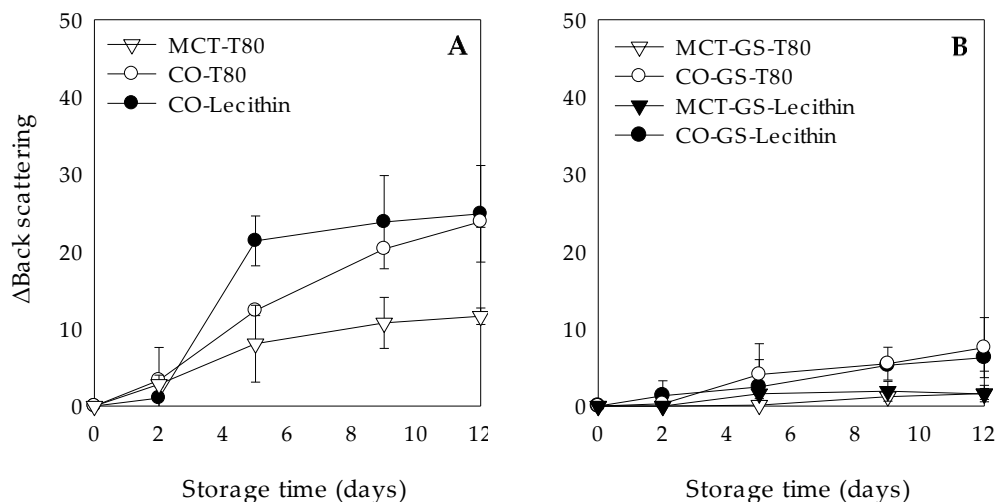
Figure 2. Clarification, expressed as variation of backscattering (ΔBS), at 4 °C during 12 days of dark storage of chlorophyllin-loaded $W_1/O/W_2$ emulsions formulated with different lipid phases consisting of medium-chain triglyceride (MCT) or corn oil (CO) and without (A) or with (B) glyceryl stearate (GS) as well as different hydrophilic surfactants (Tween 80 (T80) or Lecithin).

3.3.1 Effect of Temperature

The stability of the $W_1/O/W_2$ emulsions with liquid or gelled lipid phases stored at different temperatures (4 °C, 25 and 35 °C) against clarification is shown in Fig. 3. In general, when they were stored at 25 and 35 °C, the ΔBS values obtained were higher compared to those at 4 °C, which evidenced a decrease in $W_1/O/W_2$ emulsions stability. The extent of the liquid lipid $W_1/O/W_2$ emulsions instability stored at 25 and 35 °C was mainly dependent on the type of hydrophilic emulsifier used. After 2 days of storage, $W_1/O/W_2$ emulsions stabilized with T80 presented a noticeable increase of the ΔBS values when stored at 25 °C (ΔBS > 18) and 35 °C (ΔBS > 25) in comparison with those at 4 °C (ΔBS < 4) (Fig. 2A and Fig. 3A,B). This might be attributed to an increase in the free energy of the system due to the higher temperature which might result in a higher number of oil droplet collisions ultimately leading to destabilization. In contrast, lecithin-stabilized $W_1/O/W_2$ emulsions showed no significant differences in the ΔBS values at 4 and 25 °C, remaining stable against clarification (Fig. 2A and Fig. 3A). As mentioned before, lecithin-stabilized $W_1/O/W_2$ emulsions showed highly negative initial ζ-potential values (Table 4), suggesting that even at 25 °C, the electrostatic repulsion between the droplets may be high enough to inhibit droplet aggregation (Ozturk, Argin, Ozilgen, & McClements, 2015).
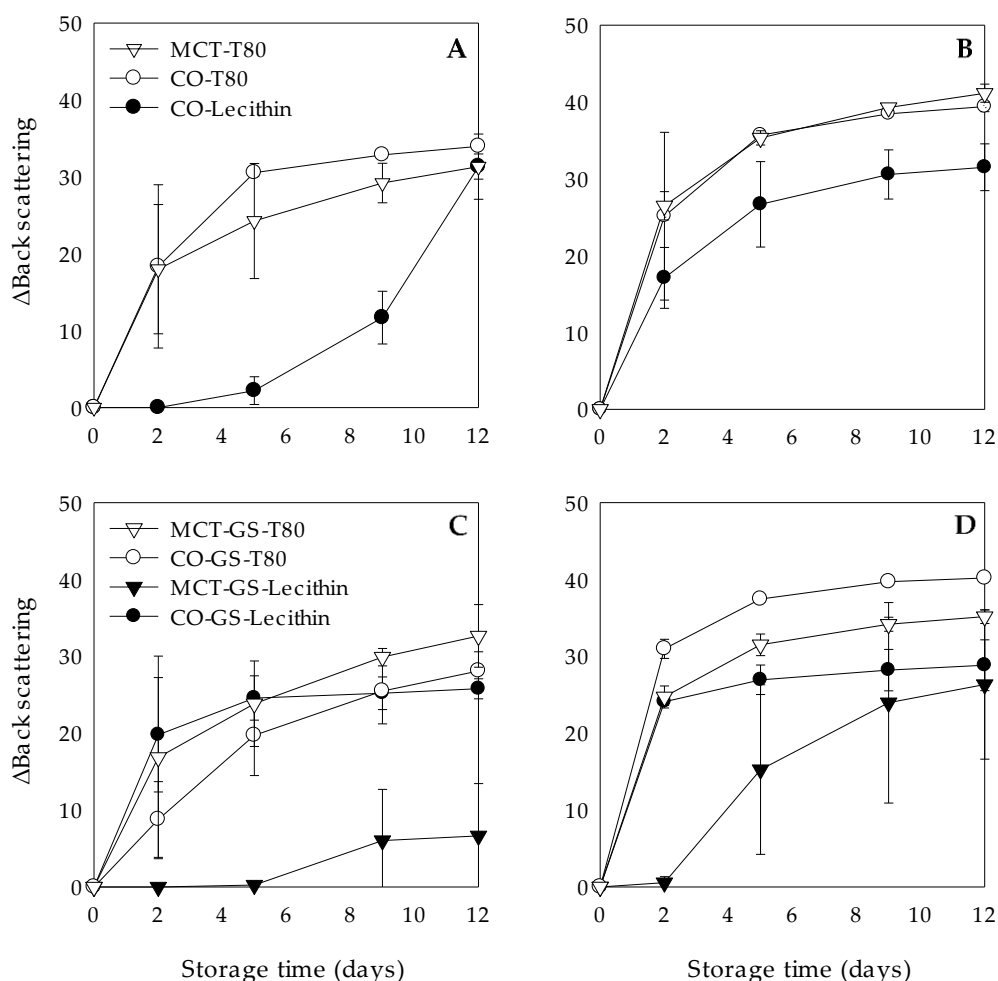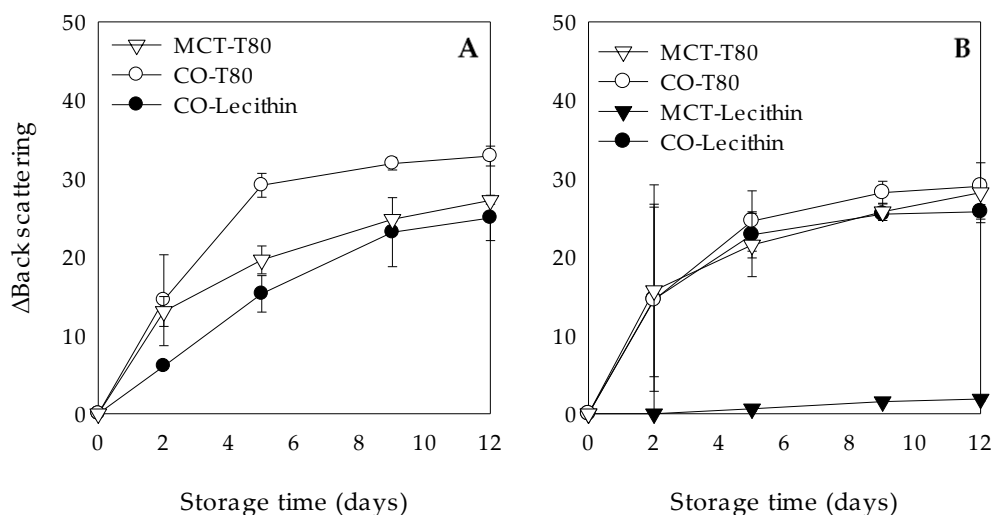
Figure 3. Clarification, expressed as variation of backscattering (ΔBS), at 25 °C (A,C) and 35 °C (B,D) during 12 days of dark storage of chlorophyllin-loaded $W_1/O/W_2$ emulsions formulated with different lipid phases consisting of medium-chain triglyceride (MCT) or corn oil (CO) and without (A,B) or with (C,D) glyceryl stearate (GS) as well as different hydrophilic emulsifiers (Tween 80 (T80) or Lecithin).

When the storage temperature was 35 °C, an increase of ΔBS values up to 17.12 ± 3.96 was observed after 2 days of storage, suggesting that the electrostatic forces might not have been enough to overcome the attraction between the oil droplets (Fig. 3B). At the end of the storage time, all liquid lipid $W_1/O/W_2$ emulsions stored at 25 and 35 °C showed phase separation due to clarification phenomenon (Fig. 3A,B). Clarification phenomenon of the $W_1/O/W_2$ emulsions with gelled lipid phase at 25 and 35 °C was more pronounced than in their respective emulsions with liquid lipid phases. Indeed, they presented ΔBS values above 8 already from day 2 of storage at both 25 and 35 °C, regardless of the type of lipid or emulsifier (Fig. 3C,D). This might be attributed to changes in the lipid phase state when increasing the storage temperature from 4 to 25 and 35 °C (Kharat, Zhang, &

McClements, 2018; Weiss et al., 2008) (Table 1). At 4 °C, gelation and/or partial crystallization of the dispersed phase significantly increases its viscosity, and consequently the stability of the $W_1/O/W_2$ emulsions (section 3.3). At higher storage temperatures, especially at 35 °C, visual observations of the lipid phase showed a loss of structural consistency, which might be caused by its lower gelling and/or crystallization degree (Table 1). As a consequence, $W_1/O/W_2$ emulsions with gelled lipid phase at 25 and 35 °C, would behave as liquid lipid emulsions, explaining the observed instabilities. Interestingly, gelling the MCT lipid phase allowed the formation of highly stable $W_1/O/W_2$ emulsions at all the studied temperatures, in fact, they had no significant differences in the ΔBS values during the first 5 days of storage (Fig. 2B and Fig. 3C,D). Instead, their respective liquid lipid $W_1/O/W_2$ emulsions could not even be formed (section 3.2.1).

3.3.2 *Effect of Light Exposure*

$W_1/O/W_2$ emulsions stability against clarification was also evaluated when subjected to light exposure during 12 days of storage at 25 °C (Fig. 4). At the end of the storage time, all $W_1/O/W_2$ emulsions (gelled and liquid lipid phase) showed no significant changes in the ΔBS values when exposed to light (Fig. 4A,B) as compared to those stored in the dark (Fig. 3A,C). Based on a previous research, where the effect of light exposure on the stability of emulsions with a lipid solidified phase was studied, it would have been expected to observe an increase in clarification due to an accelerated droplet growth (Freitas & Müller, 1998). These authors reported that high energetic radiations caused droplet collisions, leading to droplet aggregation and destabilization of the emulsion systems. However, in the present study, a low intensity light was used, which has been reported to have no negative effects on emulsion stability (Genuino et al., 2012).

Figure 4. Clarification, expressed as variation of backscattering (ΔBS), at 25 °C during 12 days of light exposure of chlorophyllin-loaded $W_1/O/W_2$ emulsions formulated with different lipid phases consisting of medium-chain triglyceride (MCT) or corn oil (CO) and without (A) or with (B) glyceryl stearate (GS) as well as different hydrophilic surfactants (Tween 80 (T80) or Lecithin).

3.4 Encapsulation Efficiency of CHL in $W_1/O/W_2$ Emulsions

Finally, the ability of the fresh $W_1/O/W_2$ emulsions to encapsulate CHL in the inner aqueous phase was evaluated (Fig. 5). $W_1/O/W_2$ emulsions both with gelled and liquid lipid phases showed CHL EE values higher than 98%. Our results are in agreement with a previous study where the CHL EE values in liquid lipid $W_1/O/W_2$ emulsions were around 91% (Artiga-Artigas et al., 2018a). Interestingly, in this study, emulsions containing lecithin had the highest CHL EE, which might be due to a possible interaction between the phosphate ions of lecithin and the hydroxyl groups of the encapsulated compound, being capable of forming H-bonds with the CHL. It is worth mentioning that this is the first study in which $W_1/O/W_2$ emulsions with a gelled lipid phase are used for CHL encapsulation.
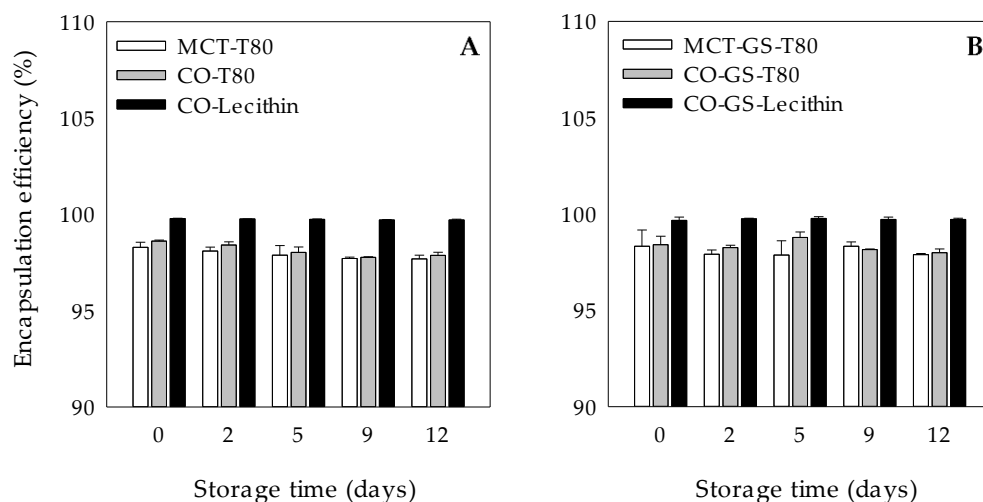
Figure 5. Encapsulation efficiency (%) during 12 days of dark storage at 4 °C of chlorophyllin-loaded $W_1/O/W_2$ emulsions formulated with different lipid phases consisting of medium-chain triglyceride (MCT) or corn oil (CO) and without (A) or with (B) glyceryl stearate (GS) as well as different hydrophilic surfactants (Tween 80 (T80) or Lecithin).

4 Conclusions

The present work evidenced that the formation and stabilization of double $W_1/O/W_2$ emulsions can be enhanced with the use of gelled lipid phases. When liquid phases were used, only T80 was able to form $W_1/O/W_2$ emulsions both with CO or MCT liquid oils, while lecithin only rendered double emulsions with CO. With gelled lipid phases containing 1% (w/w) GS, $W_1/O/W_2$ emulsions were successfully formed regardless of the lipid and surfactant type, showing also smaller inner water droplets (W_1) and smaller lipid (W_1/O) droplets in comparison to the respective formulations with liquid oils. This may be attributed to a decrease in the migration of water from the inner to the outer aqueous phase by the gelled lipid phase. Additionally, it was evidenced that their long-term stability under different storage temperatures was dependent on the lipid phase state. At 4 °C, the gelled and/or crystallized lipid phase contributed to a higher $W_1/O/W_2$ emulsions stability in comparison to liquid lipid emulsions. Hence this work contributes in elucidating the role of the lipid phase state, being liquid or gelled, on the formation and stabilization of $W_1/O/W_2$ emulsions that may act as carriers of hydrophilic bioactive compounds.

5 Author Contributions

6 Funding

7 Data Availability Statement

Data sharing not applicable.

8 Acknowledgments

9 Conflicts of Interest

The authors declare no conflict of interest. The funders had no role in the design of the study; in the collection, analyzes, or interpretation of data; in the writing of the manuscript, or in the decision to publish the results.

10 Sample Availability

Samples of the compounds are not available from the authors.

11 References

Abreu-Martins, H., Artiga-Artigas, M., Hilsdorf Piccoli, R., Martín-Belloso, O., & Salvia-Trujillo, L. (2020). The lipid type affects the in vitro digestibility and β-carotene bioaccessibility of liquid or solid lipid nanoparticles. *Food Chemistry*, *311*, 126024.

Aditya, N. P., Aditya, S., Yang, H., Kim, H. W., Park, S. O., & Ko, S. (2015). Co-delivery of hydrophobic curcumin and hydrophilic catechin by a water-in-oil-in-water double emulsion. *Food Chemistry, 173,* 7-13.

Artiga-Artigas, M., Molet-Rodríguez, A., Salvia-Trujillo, L., & Martín-Belloso, O. (2018a). Formation of Double (W1/O/W2) Emulsions as Carriers of Hydrophilic and Lipophilic Active Compounds. *Food and Bioprocess Technology*, *12*, 422–435.

Artiga-Artigas, María, Lanjari-Pérez, Y., & Martín-Belloso, O. (2018b). Curcumin-loaded nanoemulsions stability as affected by the nature and concentration of surfactant. *Food Chemistry*, *266*, 466–474.

Bonnet, M., Cansell, M., Berkaoui, A., Ropers, M. H., Anton, M., & Leal-Calderon, F. (2009). Release rate profiles of magnesium from multiple W/O/W emulsions. *Food Hydrocolloids*, *23*(1), 92–101.

Bou, R., Cofrades, S., & Jiménez-Colmenero, F. (2014). Physicochemical properties and riboflavin encapsulation in double emulsions with different lipid sources. *LWT - Food Science and Technology*, *59*(2), 621–628.

Chen, H., & Zhong, Q. (2015). Thermal and UV stability of β-carotene dissolved in peppermint oil microemulsified by sunflower lecithin and Tween 20 blend. *Food Chemistry, 174,* 630-636.

Dickinson, E. (2011). Double Emulsions Stabilized by Food Biopolymers. *Food Biophysics*, *6*(1), 1–11.

Fernández-Martín, F., Freire, M., Bou, R., Cofrades, S., & Jiménez-Colmenero, F. (2017). Olive oil based edible W/O/W emulsions stability as affected by addition of some acylglycerides. *Journal of Food Engineering*, *196*, 18–26.

Fredrick, E., Walstra, P., & Dewettinck, K. (2010). Factors governing partial coalescence in oil-in-water emulsions. *Advances in Colloid and Interface Science*, *153*(1–2), 30–42.

Freitas, C., & Müller, R. H. (1998). Effect of light and temperature on zeta potential and physical stability in solid lipid nanoparticle (SLN®) dispersions. *International Journal of Pharmaceutics*, *168*(2), 221–229.

Gaonkar, A. G., & Borwankar, R. P. (1991). Competitive adsorption of monoglycerides and lecithin at the vegetable oil-water interface. *Colloids and Surfaces*, *59*, 331–343.

Genuino, H. C., Horvath, D. T., King'Ondu, C. K., Hoag, G. E., Collins, J. B., & Suib, S. L. (2012). Effects of visible and UV light on the characteristics and properties of crude oil-in-water (O/W) emulsions. *Photochemical and Photobiological Sciences*, *11*(4), 692–702.

Ghosh, S., Tran, T., & Rousseau, D. (2011). Comparison of pickering and network stabilization in water-in-oil emulsions. *Langmuir*, *27*(11), 6589–6597.

Helgason, T., Salminen, H., Kristbergsson, K., McClements, D. J., & Weiss, J. (2015). Formation of transparent solid lipid nanoparticles by microfluidization: Influence of lipid physical state on appearance. *Journal of Colloid and Interface Science*, *448*, 114–122.

Herzi, S., & Essafi, W. (2018). Different magnesium release profiles from W/O/W emulsions based on crystallized oils. *Journal of Colloid and Interface Science*, *509*(2018), 178–188.

Jo, Y. J., & Kwon, Y. J. (2014). Characterization of β-carotene nanoemulsions prepared by microfluidization technique. *Food Science and Biotechnology*, *23*(1), 107–113.

Kharat, M., Zhang, G., & McClements, D. J. (2018). Stability of curcumin in oil-in-water emulsions: Impact of emulsifier type and concentration on chemical degradation. *Food Research International*, *111*, 178–186.

Kralova, I., & Sjöblom, J. (2009). Surfactants used in food industry: A review. *Journal of Dispersion Science and Technology*, *30*(9), 1363–1383.

Lamba, H., Sathish, K., Sabikhi, L. (2015). Double Emulsions: Emerging Delivery System for Plant Bioactives. *Food and Bioprocess Technology, 8,* 709–728.

Liang, R., Shoemaker, C. F., Yang, X., Zhong, F., & Huang, Q. (2013). Stability and bioaccessibility of β-carotene in nanoemulsions stabilized by modified starches. *Journal of Agricultural and Food Chemistry*, *61*(6), 1249–1257.

Liu, J., Kharat, M., Tan, Y., Zhou, H., Muriel Mundo, J. L., & McClements, D. J. (2020). Impact of fat crystallization on the resistance of W/O/W emulsions to osmotic stress: Potential for temperature-triggered release. *Food Research International*, *134*, 109273.

Mason, T. G., Wilking, J. N., Meleson, K., Chang, C. B., & Graves, S. M. (2006). Nanoemulsions: formation, structure, and physical properties. *Journal of Physics: Condensed Matter*, *18*(41), R635–R666.

Matos, M., Gutiérrez, G., Coca, J., & Pazos, C. (2014). Preparation of water-in-oil-in-water (W1/O/W2) double emulsions containing trans-resveratrol. *Colloids and Surfaces A: Physicochemical and Engineering Aspects*, *442*, 69–79.

McClements, D. J., Decker, E. A., & Weiss, J. (2007). Emulsion-based delivery systems for lipophilic bioactive components. *Journal of Food Science*, *72*(8), 109–124.

McClements, D. J. (2015). *Food Emulsions: Principles, Practices, and Techniques* (3rd ed.). CRC Press, Taylor & Francis Group.

Mehnert, W., & Mäder, K. (2012). Solid lipid nanoparticles: Production, characterization and applications. *Advanced Drug Delivery Reviews*, *47*(2-3), 165-196.

Muschiolik, G., & Dickinson, E. (2017). Double Emulsions Relevant to Food Systems: Preparation, Stability, and Applications. *Comprehensive Reviews in Food Science and Food Safety*, *16*(3), 532–555.

Nash, J. J., & Erk, K. A. (2017). Stability and interfacial viscoelasticity of oil-water nanoemulsions stabilized by soy lecithin and Tween 20 for the encapsulation of bioactive carvacrol. *Colloids and Surfaces A: Physicochemical and Engineering Aspects*, *517*, 1–11.

Nelis, V., Declerck, A., Vermeir, L., Balcaen, M., Dewettinck, K., & Van der Meeren, P. (2019). Fat crystals: A tool to inhibit molecular transport in W/O/W double emulsions. *Magnetic Resonance in Chemistry*, *57*(9), 707–718.

Ozturk, B., Argin, S., Ozilgen, M., & McClements, D. J. (2015). Formation and stabilization of nanoemulsion-based vitamin E delivery systems using natural biopolymers: Whey protein isolate and gum arabic. *Food Chemistry*, *188*, 256–263.

Peng, K., Wang, X., Lu, L., Liu, J., Guan, X., & Huang, X. (2016). Insights into the Evolution of an Emulsion with Demulsifying Bacteria Based on Turbiscan. *Industrial and Engineering Chemistry Research*, *55*(25), 7021–7029.

Qian, C, & McClements, D. J. (2011). Formation of nanoemulsions stabilized by model food-grade emulsifiers using high-pressure homogenization: Factors affecting particle size. *Food Hydrocolloids*, *25*(5), 1000–1008.

Qian, C, Decker, E. A., Xiao, H., & McClements, D. J. (2013). Impact of lipid nanoparticle physical state on particle aggregation and β-carotene degradation: Potential limitations of solid lipid nanoparticles. *Food Research International*, *52*(1), 342–349.

Schmidts, T., Dobler, D., Guldan, A. C., Paulus, N., & Runkel, F. (2010). Multiple W/O/W emulsions-Using the required HLB for emulsifier evaluation. *Colloids and Surfaces A: Physicochemical and Engineering Aspects*, *372*(1–3), 48–54.

Tabibiazar, M., & Hamishehkar, H. (2015). Formulation of a Food Grade Water-In-Oil Nanoemulsion: Factors Affecting on Stability. *Pharmaceutical Sciences*, *21*(4), 220–224.

Teixé-Roig, J., Oms-Oliu, G., Velderrain-Rodríguez, G. R., Odriozola-Serrano, I., & Martín-Belloso, O. (2018). The Effect of Sodium Carboxymethylcellulose on the Stability and Bioaccessibility of Anthocyanin Water-in-Oil-in-Water Emulsions. *Food and Bioprocess Technology*, *11,* 2229–2241.

Teo, A., Goh, K. K. T., Wen, J., Oey, I., Ko, S., Kwak, H. S., & Lee, S. J. (2016). Physicochemical properties of whey protein, lactoferrin and Tween 20 stabilised nanoemulsions: Effect of temperature, pH and salt. *Food Chemistry, 197*(A), 297-306.

Wang, Q., Decker, E. A., Rao, J., & Chen, B. (2019). A combination of monoacylglycerol crystalline network and hydrophilic antioxidants synergistically enhances the oxidative stability of gelled algae oil. *Food and Function*, *10*(1), 315–324.

Weiss, J., Decker, E. A., McClements, D. J., Kristbergsson, K., Helgason, T., & Awad, T. (2008). Solid lipid nanoparticles as delivery systems for bioactive food components. *Food Biophysics*, *3*(2), 146–154.

Weiss, J., & Muschiolik, G. (2007). Factors affecting the droplet size of water-in-oil emulsions (W/O) and the oil globule size in Water-in-oil-in-water emulsions (W/O/W). *Journal of Dispersion Science and Technology*, *28*(5), 703–716.

Zhang, H. Y., Tehrany, E. A., Kahn, C. J. F., Ponc, M., Linder, M., & Cleymand, F. (2012). Effects of nanoliposomes based on soya, rapeseed and fish lecithins on chitosan thin films designed for tissue engineering. *Carbohydrate Polymers, 88*(2), 618–627.

Zhao, B., Gu, S., Du, Y., Shen, M., Liu, X., & Shen, Y. (2018). Solid lipid nanoparticles as carriers for oral delivery of hydroxysafflor yellow A. *International Journal of Pharmaceutics*, *535*(1–2), 164–171.

Chapter V

Food matrix effect on the *in vitro* lipid digestibility and chlorophyllin bioaccessibility of $W_1/O/W_2$ emulsions with gelled lipid phases into whole milk

Anna Molet-Rodríguez, Mohsen Ramezani, Laura Salvia-Trujillo, Olga Martín-Belloso*
In preparation

Abstract

Gelling the lipid phase of $W_1/O/W_2$ emulsions has been proposed as a strategy to enhance their colloidal stability as well as modulate lipid digestibility and chlorophyllin (CHL) bioaccessibility. This work aimed to study the impact of lipid phase gelation using different lipid phase compositions and states, being medium-chain triglyceride oil (MCT) as liquid phase and MCT with glyceryl stearate (GS) and hydrogenated palm oil (HPO) as gelled lipid phase, on the colloidal stability, lipid digestion and CHL bioaccessibility of $W_1/O/W_2$ emulsions before and after incorporated into whole milk. $W_1/O/W_2$ emulsions with gelled lipid phase formulated with MCT-GS were successfully formed and proved to be more stable than liquid ones upon gastric conditions. In contrast, the use of HPO as gelled lipid phase led to phase separation with an upper cream layer and a lower serum phase, which was maintained during the gastric phase. Non-significant differences in the lipolysis rate were observed between $W_1/O/W_2$ emulsions with gelled lipid phase (MCT-GS or HPO) and liquid ones (MCT), suggesting the melting of the lipid phase at intestinal conditions. $W_1/O/W_2$ emulsions formulated with MCT or MCT-GS led to complete lipid digestion, whereas using HPO only 40% of lipid was digested, thus it depended on the lipid phase composition rather than the state. In accordance, the CHL bioaccessibility was higher using MCT and MCT-GS than HPO. The co-ingestion of $W_1/O/W_2$ emulsions with gelled lipid phase with whole milk did not alter their colloidal stability, lipid digestibility and CHL bioaccessibility. Hence, it provides valuable information for the design of complex foods incorporating $W_1/O/W_2$ emulsions with gelled lipid phase as delivery systems of functional ingredients.

Keywords: $W_1/O/W_2$ emulsions; gelled lipid phase; lipolysis; bioaccessibility; food matrix; whole milk.

1 Introduction

There is a growing interest in the use of emulsion-based systems to encapsulate and deliver bioactive compounds into water-based foods. In this regard, the use of water-in-oil-in-water ($W_1/O/W_2$) emulsions presents important advantages over conventional oil-in-water (O/W) nanoemulsions, due to their compartmentalized internal structure (Lamba, Sathish, Sabikhi, 2015). $W_1/O/W_2$ emulsions consist of a water-in-oil (W_1/O) emulsion dispersed in an outer aqueous phase (Muschiolik & Dickinson, 2017). Thus, they allow the encapsulation of hydrophilic bioactive ingredients, such as chlorophyllin (CHL) in the inner W_1 droplets as well as protect and release in a controlled manner the encapsulated compounds during gastrointestinal (GI) digestion (Artiga-Artigas, Molet-Rodríguez, Salvia-Trujillo, & Martín-Belloso, 2018; Muschiolik & Dickinson, 2017). However, regardless of their high potential, several destabilization mechanisms have been described for $W_1/O/W_2$ emulsions, being coalescence of the lipid droplets and/or inner water droplets, and the coalescence of the inner water droplets with the outer water phase, which leads to water migration between both water phases (Dickinson, 2011). Also, inner water droplets may shrink or swell as a result of the water transfer between the inner and the outer water phases (Herzi & Essafi, 2018; Tamnak et al., 2016). In this context, the successful delivery of the encapsulated hydrophilic bioactive compound might depend on several factors, including the susceptibility of these emulsion-based delivery systems to physical alteration when they are incorporated into food products or subjected to an *in vitro* GI digestion. Food macromolecules, such as protein, are known to possess interfacial activity, which enables them to interact with oil droplets interface either initially or during the digestion process (Artiga-Artigas et al., 2020). As a consequence, the co-ingestion of $W_1/O/W_2$ emulsions with complex food matrices can compromise their initial physicochemical properties, their colloidal stability during *in vitro* digestion and the bioactive compound functionality. In addition, GI conditions, such as pH, ionic strength and temperature, may compromise $W_1/O/W_2$ emulsions colloidal stability, lipid digestibility and consequently, hydrophilic compound bioaccessibility (Frank et al., 2012; Liu et al., 2020; Teixé-Roig, Oms-Oliu, Velderrain-Rodríguez, Odriozola-Serrano, & Martín-Belloso, 2018). To overcome these instabilities, the increase of the lipid phase viscosity by formulating gelled and/or solid lipid phases, has been proposed as it can minimize the diffusion rates between the two aqueous phases of $W_1/O/W_2$ emulsions (Andrade, Wright, & Corredig, 2018; Bonnet et al., 2009; Bou, Cofrades, & Jiménez-

Colmenero, 2014; Molet-Rodríguez, Martín-Belloso, & Salvia-trujillo, 2021). Nevertheless, there is very little information available about the behaviour of $W_1/O/W_2$ emulsions with gelled lipid phase during *in vitro* gastrointestinal before and after incorporated into food matrices.

Hence, the purpose of the present work was to study the impact of the lipid phase composition and state (liquid vs. gelled) of $W_1/O/W_2$ emulsions containing CHL on the *in vitro* lipid digestibility rate and extent. Specifically, the $W_1/O/W_2$ emulsion with a liquid lipid phase was formulated with MCT. The $W_1/O/W_2$ emulsions with gelled lipid phases consisted of a blend of MCT with 5% (w/w) GS and pure HPO. Moreover, the interactions between the previously studied $W_1/O/W_2$ emulsions and whole milk macromolecules, being mostly proteins, were also addressed. Their physicochemical stability under *in vitro* GI digestion was analyzed by measuring changes in droplet size and distribution as well as in morphology. The *in vitro* lipid digestibility was assessed in terms of free fatty acids (FFAs) release percentage and the bioaccessibility of CHL after the *in vitro* digestion was determined.

2 Material and methods

2.1 Materials

MCT oil (Mygliol® 812 N) and GS (Imwitor® 491) with a purity of 99.9% and 96.7% (0.8% free glycerol and 95.9% monoglycerides), respectively, according to their certificate of analysis were purchased from IOI Oleochemical GmbH (Hamburg, Germany) and organic HPO containing ≤ 0.1 free fatty acids was acquired from Mystic Moments (Hants, UK). Polyglycerol polyricinoleate (PGPR) from castor oil (Grinsted®, DuPont Danisco NHIB Iberica S.L, Barcelona, Spain) was utilized as a lipophilic emulsifier. Polyoxyethylene sorbitan monooleate (Tween 80) from Lab Scharlab (Sentmenat, Spain) was used as a food-grade hydrophilic emulsifier. CHL (coppered trisodium salt) with a molecular weight of 724.15 g/mol, copper contains 3.5–6.5% and a purity of $\geq 95\%$ was purchased from Alfa Aesar (Thermo Fisher Scientific, GmbH, Karlsruhe, Germany). Sodium alginate (MANUCOL®DH) was obtained from FMC Biopolymer Ltd. (Scotland, UK). NaCl from POCH S.A. (Gliwice, Poland) was added to both the inner and outer aqueous phases of the system, to adjust the osmotic pressure balance between the aqueous phases. $W_1/O/W_2$ emulsions were formulated with ultrapure

milli-Q water obtained from a Millipore filtration system (18.2 mΩ.cm, Merck Millipore, Madrid, Spain). Whole milk (Hacendado, Mercadona, Spain) was the food in which the $W_1/O/W_2$ emulsions were incorporated. Pepsin from porcine gastric mucosa (77160), pancreatin from porcine pancreas (P1625) and bile bovine (B3883) were purchased from Sigma Aldrich (St Louise, MO, USA). The chemical used in the extraction analysis to quantify the CHL concentration was hexane (fraction from petroleum) HPLC grade (Sharlab S.L, Sentmenat, Spain). The rest of the chemicals used were of analytical grade.

2.2   Methods

2.2.1   *Formation of chlorophyllin-loaded $W_1/O/W_2$ emulsions and incorporation in whole milk*

$W_1/O/W_2$ emulsions were prepared using a two-stage emulsification procedure, consisting of the formation of the W_1/O emulsion followed by its dispersion in an outer aqueous phase (Molet-Rodríguez et al., 2021).

2.2.1.1   Formation of the chlorophyllin-loaded W_1/O emulsions

Liquid phase W_1/O emulsion with pure MCT or gelled lipid W_1/O emulsions with lipid phases consisting of (*i*) a blend of MCT with 5% (w/w) of GS and (*ii*) pure HPO were formulated. GS or HPO were firstly melted by increasing the temperature to 60 °C. The development of a gelled MCT lipid phase involved the aggregation of GS through its self-assembly and/or crystallization. Specifically, the lipid phase containing a blend of MCT and GS was formulated with 5% (w/w) of GS and the rest MCT, by mixing for 5 min using a magnetic stirrer working at 450 rpm and 60 ºC. The melting properties of the lipid blends were characterized by differential scanning calorimetry (DSC) from −20 to 80 °C at 1 K/min in a previous study of our group (Abreu-Martins, Artiga-Artigas, Hilsdorf Piccoli, Martín-Belloso, & Salvia-Trujillo, 2020). Then, lipid phases (94% w/w) were mixed with PGPR (6% w/w) at 450 rpm and 60 °C for 5 min. Afterwards, W_1/O emulsions were formed by mixing each lipid phase:PGPR mixture (70% w/w) with an aqueous phase (30% w/w) consisting of 7500 ppm CHL, 0.05 M NaCl and 2% (w/w) sodium alginate by using a laboratory T25 digital Ultra-Turrax mixer (IKA, Staufen, Germany), working at 11000 rpm for 5 min. The temperature during the first emulsification step was kept at 60 °C in order to maintain the lipid phases containing GS and HPO in liquid state.

2.2.1.2   Formation of the chlorophyllin-loaded $W_1/O/W_2$ emulsions

The second step was the dispersion of the previously prepared W_1/O emulsions (20% w/w) in an outer aqueous phase (80% w/w) containing NaCl 0.05 M, sodium alginate (2% w/w) and Tween 80 (2.5% w/w), using a laboratory T25 digital Ultra-Turrax mixer working at 4000 rpm for 3 min. Once the $W_1/O/W_2$ emulsions were formed, their temperature was reduced down to 4 °C for 2 h in order to allow lipid gelation in those emulsions with GS and HPO.

2.2.1.3   Incorporation of chlorophyllin-loaded $W_1/O/W_2$ emulsions into whole milk

The previously prepared $W_1/O/W_2$ emulsions (30.4% w/w), formulated with pure MCT, a blend of MCT and GS (5% w/w) and pure HPO were incorporated into whole milk (69.6% w/w) and subsequently mixed at 900 rpm for 5 min, referred in the manuscript as $W_1/O/W_2$ emulsions in whole milk. In addition, $W_1/O/W_2$ emulsions (30.4% w/w) were also diluted in milli-Q water (69.6% w/w) and mixed at 450 rpm for 5 min, to reach the same final concentration as when incorporated in whole milk. They are referred to as $W_1/O/W_2$ emulsions. Two aliquots of each initial formulation were collected for droplet size and microscopic analysis.

2.2.2   *In vitro gastrointestinal digestion of chlorophyllin-loaded $W_1/O/W_2$ emulsions and into whole milk*

The *in vitro* digestibility of the $W_1/O/W_2$ emulsions and $W_1/O/W_2$ emulsions in whole milk was conducted according to the INFOGEST international consensus (Minekus et al., 2014), consisting of a gastric and intestinal phase.

2.2.2.1   Gastric phase

The electrolyte simulated gastric fluid (eSGF) solution consisted of a mixture of electrolytes [0.5 M KCl, KH_2PO_4 0.5M, 1 M NaCl, 2M NaCl, 0.15 M $MgCl_2(H_2O)$ and 0.5 M $(NH_4)_2CO_3$] dissolved in milli-Q water. Then, the gastric mixture solution was prepared by dissolving pepsin (8.8 mg pepsin/ mL) in eSGF, followed by the addition of $CaCl_2(H_2O)_2$ 0.3 M, HCl 1 M and milli-Q water. The gastric digestion was performed by mixing each $W_1/O/W_2$ emulsion or $W_1/O/W_2$ emulsion in whole milk with the gastric mixture to a final ratio of 1:1. It was incubated under dark conditions for 2 h at 37 °C and

continuous agitation using an orbital shaker working at 100 rpm. After the gastric phase, two aliquots, referred to as gastric chyme, were collected for droplet size and microscopic analysis.

2.2.2.2   Intestinal phase

To simulate the small intestinal phase, a 30 mL-aliquot of the gastric chyme was placed in a water bath at 37 °C. Subsequently, 3.5 mL of bile salts (54 mg/mL) diluted in a phosphate buffer (0.005 M, pH 7) and 1.5 mL of intestinal salts (10 mM of $CaCl_2$ and 160 mM of NaCl) were added to the sample, and the pH was adjusted to 7.0. Then, 2.5 mL of pancreatin solution (215 mg/mL) diluted in phosphate buffer were added to initiate the lipid hydrolysis. The lipolysis reaction was monitored with a titration unit (pH-stat, Metrohm USA Inc., Riverview, FL, USA), which maintained the pH at 7. After this, the digest was transferred into glass tubes and heat-shocked at 80 °C for 3 min in order to stop the lipolysis reaction and placed in an iced-water bath afterwards. Two aliquots of each digest collected after the small intestine phase were taken for droplet size and microscopic analysis and the rest was used for CHL bioaccessibility measurements.

The percentage of free fatty acids (FFAs) released was calculated according to equation (1):

$$Free\ fatty\ acids\ released\ (\%) = \frac{V_{NaOH} \times C_{NaOH} \times M_{lipid}}{2 \times m_{lipid}} \times 100 \tag{1}$$

where V_{NaOH} is NaOH volume (mL) used to compensate the FFAs released during the digestion, C_{NaOH} is NaOH molarity (0.25 M), M_{lipid} is lipid molecular weight, m_{lipid} is the total lipid weight in the 30-mL aliquot placed in the titration unit. The molecular weight was 509, 1704, 839 and 709 g/mol for MCT, GS, HPO and milk fat respectively.

2.2.3   *Physical characterization of chlorophyllin-loaded $W_1/O/W_2$ emulsions and into whole milk*

Initial, gastric chyme and digest aliquots of each $W_1/O/W_2$ emulsion (MCT, MCT-GS and HPO) were characterized in terms of droplet size, size distribution and microscopy to determine microstructural changes of their main components (*i.e.,* lipid droplets). The same characterization procedures were used for $W_1/O/W_2$ emulsions (MCT, MCT-GS and

HPO) in whole milk, in order to detect microstructural changes in $W_1/O/W_2$ emulsions and whole milk macromolecules when co-ingested together.

2.2.3.1 Droplet size

The droplet size and size distribution were measured using static light scattering (SLS) (Mastersizer 2000, Malvern Instruments Ltd, Worcestershire, UK). The initial, gastric chyme and digest aliquots were dispersed in distilled water at 2200 rpm and the average W_1/O droplet size and size distribution were reported as surface-weighted average ($D_{[3;2]}$) and volume (%), respectively.

2.2.3.2 Optical Microscopy Analysis

Phase contrast microscopy images of the initial, gastric chyme and digest aliquots were taken with an optical microscope (BX41, Olympus, Göttingen, Germany) using a 100x oil immersion objective lens and equipped with UIS2 optical system. All images were processed using the instrument software (Olympus cellSense, Barcelona, Spain).

2.2.4 *Bioaccessibility of chlorophyllin at the end of the small intestine of $W_1/O/W_2$ emulsions and into whole milk*

The CHL bioaccessibility of the $W_1/O/W_2$ emulsions and $W_1/O/W_2$ emulsion in whole milk after being subjected to the prior described *in vitro* GI digestion procedure was evaluated. The digest was centrifuged (AVANTI J-25, Beckman Instruments Inc., Fullerton, CA, USA) at 4000 rpm for 40 min at a temperature of 8 °C. The supernatant, being the aqueous fraction was collected and was considered to be the fraction in which CHL is solubilized. CHL quantification was conducted by a method in which a 0.5 mL-aliquot of the supernatant was mixed with 3 mL of Milli-Q water and 2 mL of hexane and vortexed for 10 s. The lower fraction containing the CHL was collected and filtered with a nonsterile nylon syringe filter, pore: 0.45 μm, ⌀13 mm (Branchia, Labbox labware, Barcelona, Spain) in order to remove the larger particles than 0.45 μm that cannot be absorbed by epithelium cells. Afterwards, the absorbance of the CHL in the filtrate was measured with a V-670 spectrophotometer (Jasco, Tokyo, Japan) at 405 nm. The concentration of CHL extracted from the digest was determined from a calibration curve of absorbance versus CHL concentration in milli-Q water.

The CHL bioaccessibility was then calculated using equation (2):

$$CHL\ bioaccessibility\ (\%) = \frac{C_{digest}}{C_{theoretic}} \times 100 \tag{2}$$

where C_{digest} and $C_{theoretic}$ are the concentration measured in the aqueous fraction of the centrifuged digest and the CHL concentration used in the formulation of $W_1/O/W_2$ emulsions, respectively.

2.3 Statistical analysis

All experiments were assayed in duplicate and data was expressed as the mean with standard deviation. An analysis of variance was carried out and the Tukey HSD test was run to determine significant differences at a 5% significance level ($p < 0.05$) with statistical software JMP Pro 14 (SAS Institute Inc.).

3 Results and discussion

3.1 Formation of the chlorophyllin-loaded $W_1/O/W_2$ emulsions with gelled lipid phase

The capability of forming $W_1/O/W_2$ emulsions with gelled lipid phase mainly depended on the lipid phase composition (Fig. 1). The $W_1/O/W_2$ emulsion with gelled lipid phase formulated using MCT-GS was successfully formed as observed in its visual appearance immediately after preparation. Instead, the $W_1/O/W_2$ emulsions with gelled lipid phase using HPO showed phase separation, a lower serum phase and an upper cream layer (Fig. 1). It could be attributed to the location of lipid crystals in the bulk lipid phase, which has been previously reported to form less stable $W_1/O/W_2$ emulsions than using lipid phases with surface-active properties, such as GS.

A:W$_1$/O/W$_2$ emulsion			B:W$_1$/O/W$_2$ emulsion + Whole milk		
MCT	MCT+GS (5%)	HPO	MCT	MCT+GS (5%)	HPO

a.   Lower serum phase
b.   Upper cream layer
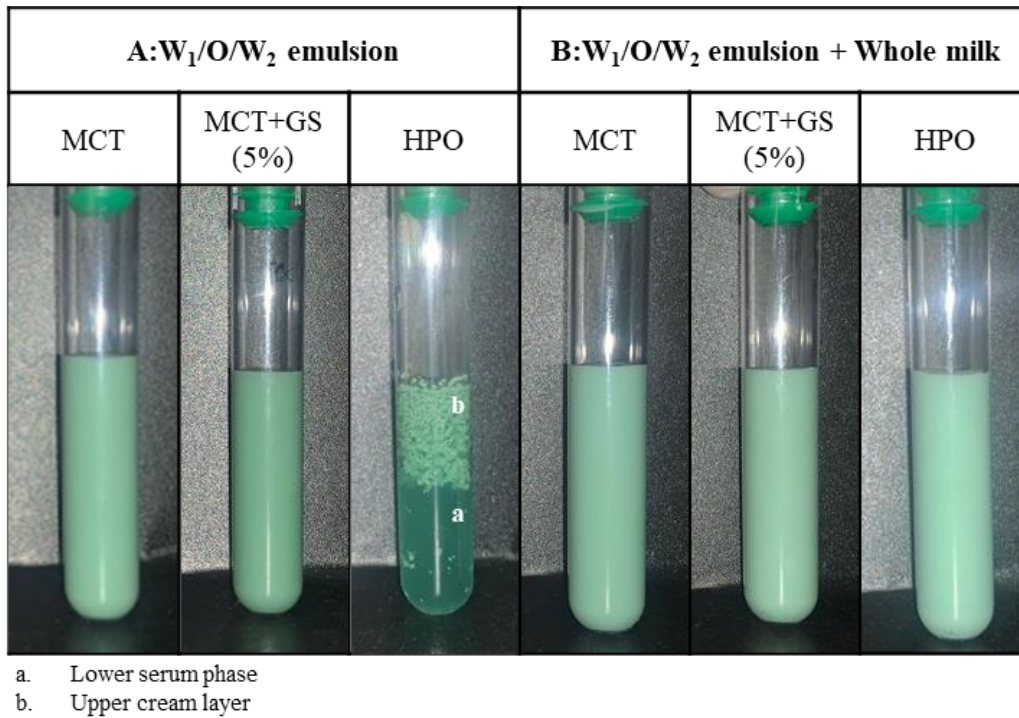
Figure 1. Visual appearance immediately after preparation of W$_1$/O/W$_2$ emulsions formulated with different lipid phases (A) and incorporated into whole milk (B). Lipid phases: pure medium-chain triglyceride oil (MCT), a blend of MCT and 5% (w/w) glyceryl stearate (GS) and pure hydrogenated palm oil (HPO).

3.2   Initial physical characterization of chlorophyllin-loaded W$_1$/O/W$_2$ emulsions

3.2.1   Influence of the lipid phase composition and state

The initial particle size of the W$_1$/O/W$_2$ emulsion formulated with pure MCT was 7.88 ± 0.15 μm and presented a narrow monomodal distribution with an intensity peak slightly below 10 μm (Fig. 2A and 3). Instead, the W$_1$/O/W$_2$ emulsion with a gelled lipid phase consisting of MCT-GS (5% w/w) presented a smaller size, with an average value of 4.30 ± 0.63 μm (Fig. 2A). GS is a monoglyceride presenting interfacial activity that might adsorb at the oil/water interface, thus contributing to a certain extent of W$_1$/O droplet size reduction during emulsification (Abreu-Martins et al., 2020; Molet-Rodríguez et al., 2021). Indeed, the monomodal size distribution of MCT-GS with an intensity peak of around 5 μm confirmed the presence of smaller droplets when the lipid phase contained GS in comparison with pure MCT (Fig. 3A).
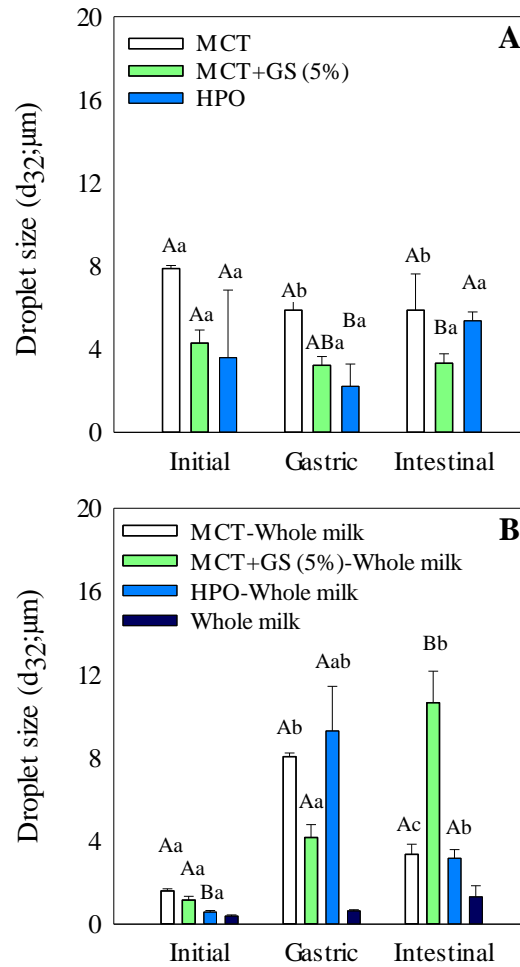
Figure 2. Surface-weight average droplet size (d_{32}; μm) of $W_1/O/W_2$ emulsions formulated with different lipid phases (A) and incorporated into whole milk (B) initially and after being subjected to simulated gastric and small intestinal conditions. Lipid phases: pure medium-chain triglyceride oil (MCT), a blend of MCT and 5% (w/w) glyceryl stearate (GS) and pure hydrogenated palm oil (HPO). Whole milk was used as a food matrix. Different upper-case letters mean significant differences ($p < 0.05$) between samples in the same phase, whereas different lower-case letters mean significant differences ($p < 0.05$) of each sample in the different phases. Mean ± SD, n=2.
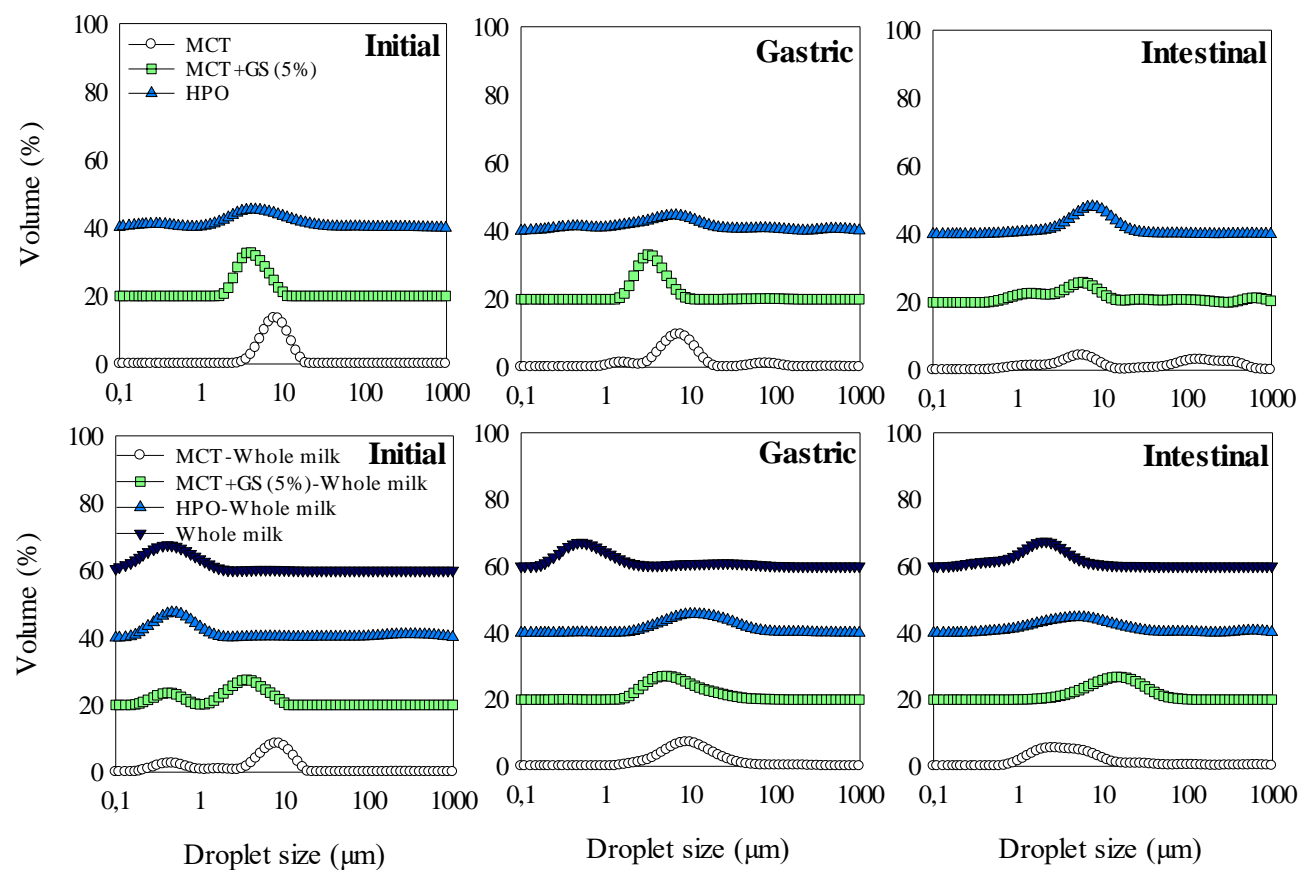
Figure 3. Droplet size distribution in volume (%) of $W_1/O/W_2$ emulsions formulated with different lipid phases (top panel) and incorporated into whole milk (bottom panel) initially and after being subjected to simulated gastric and small intestinal conditions. Lipid phases: pure medium-chain triglyceride oil (MCT), a blend of MCT and 5% (w/w) glyceryl stearate (GS) and pure hydrogenated palm oil (HPO).

However, the microscopy images of the initial $W_1/O/W_2$ emulsions formulated MCT or MCT-GS evidenced oil droplet aggregation (Fig. 4). It can be attributed to the ability of alginate molecules present in the outer aqueous phase to promote droplet flocculation in emulsions through a bridging or depletion mechanism. Bridging flocculation occurs when a biopolymer simultaneously binds to the surfaces of two or more droplets, whereas depletion flocculation occurs due to the presence of sufficiently high levels of non-adsorbed biopolymer molecules in the aqueous phase surrounding the droplets (Dickinson, 2003).

Lipid phase	Initial	Gastric	Intestinal
MCT			
MCT+GS (5%)			
HPO	A | B	A | B	

A. Lower serum phase
B. Upper cream layer
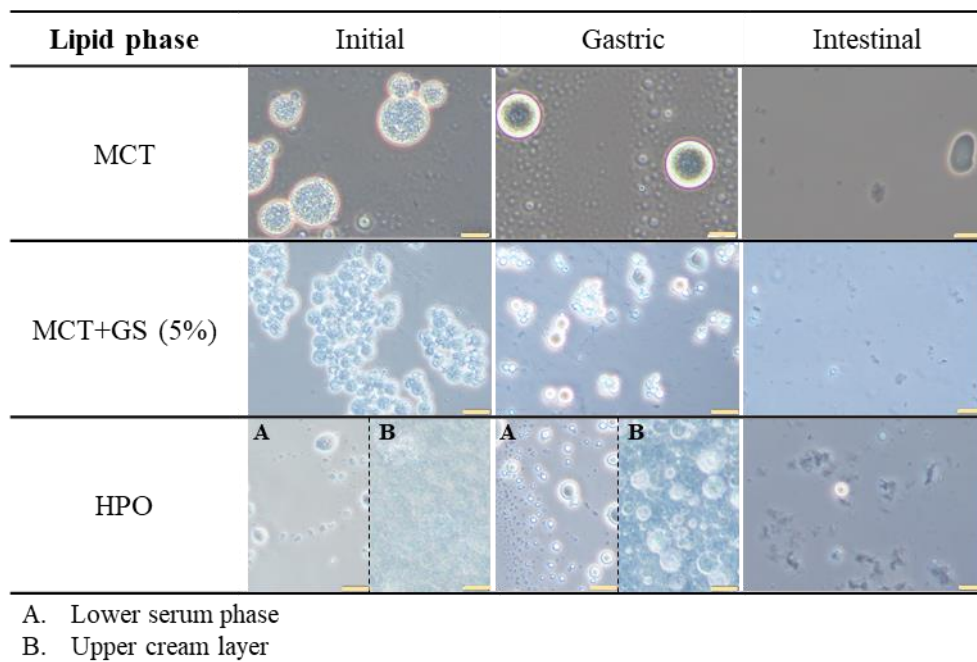
Figure 4. Optical microscopy images of $W_1/O/W_2$ emulsions formulated with different lipid phases, initially and after being subjected to simulated gastric and small intestinal conditions. Lipid phases: pure medium-chain triglyceride oil (MCT), a blend of MCT and 5% (w/w) glyceryl stearate (GS) and pure hydrogenated palm oil (HPO). Scale bar: 10 μm.

In addition, Frasch-Melnik, Spyropoulos, & Norton (2010) have stated that the existence of free fat crystals in the lipid phase of $W_1/O/W_2$ emulsions might cause W_1/O droplets aggregation. They argued that even though lipid crystals with surface-active properties are preferably located at the W_1/O interface, as GS in the present study, some crystals would be located in the bulk lipid phase, therefore being able to interact with neighbouring W_1/O droplets interface, resulting in W_1/O droplets aggregation. In this regard, both the presence of alginate molecules in the external aqueous phase and lipid

crystals in the bulk lipid phase might be responsible for the W_1/O particle aggregation observed in the $W_1/O/W_2$ emulsion (MCT-GS).

The $W_1/O/W_2$ emulsion with a gelled lipid phase consisting of pure HPO showed the smallest average particle size (3.60 ± 3.25 µm) (Fig. 2A). Nevertheless, its size distribution graph presented also a population of bigger particles (between 1 and 10 µm), which would be due to its heterogeneity (Fig. 1 and 3).

3.2.2 Influence of whole milk matrix

$W_1/O/W_2$ emulsions into whole milk presented a smaller average particle size than their respective $W_1/O/W_2$ emulsions (Fig. 2A and B). The average particle sizes of $W_1/O/W_2$ emulsions formulated with pure MCT, a blend of MCT and GS (5% w/w), and pure HPO were 7.88 ± 0.15, 4.30 ± 0.63 and 3.60 ± 3.25 µm, respectively (Fig 2A) whereas after their incorporation into whole milk average particle sizes of 1.60 ± 0.10, 1.16 ± 0.18 and 0.59 ± 0.07 µm, were observed, respectively (Fig. 2B). Nevertheless, microscopic images of the $W_1/O/W_2$ emulsions before and after incorporated into whole milk showed similar W_1/O droplets size (Fig. 4 and 5). In the case of both $W_1/O/W_2$ emulsion (MCT) and $W_1/O/W_2$ emulsion (MCT-GS), their monomodal distribution changed to bimodal when whole milk was present. For instance, in $W_1/O/W_2$ emulsion (MCT)-whole milk, a population of particles remained to have a size slightly below 10 µm, but it showed a new population corresponding to particles of smaller sizes (<1 µm) (Fig. 3). Whole milk fat globules had an average droplet size of 0.39 ± 0.06 µm (Fig. 2B and 6), giving the possibility to distinguish between the W_1/O particles from the $W_1/O/W_2$ emulsion and the fat globules from whole milk. In addition, it is well-known that casein micelles in milk have particle sizes in the range of 50-500 nm (Fox & Brodkorb, 2008). Thus, the population of nanometric particles observed in the size distribution graph of $W_1/O/W_2$ emulsion (MCT or MCT-GS)-whole milk might be due to the presence of fat globules and casein micelles dispersed in their outer aqueous phases.

A. Lower serum phase
B. Upper cream layer

Figure 5. Optical microscopy images of $W_1/O/W_2$ emulsions formulated with different lipid phases and incorporated into whole milk, initially and after being subjected to simulated gastric and small intestinal conditions. Lipid phases: pure medium-chain triglyceride oil (MCT), a blend of MCT and 5% (w/w) glyceryl stearate (GS) and pure hydrogenated palm oil (HPO). Scale bar: 10 μm.
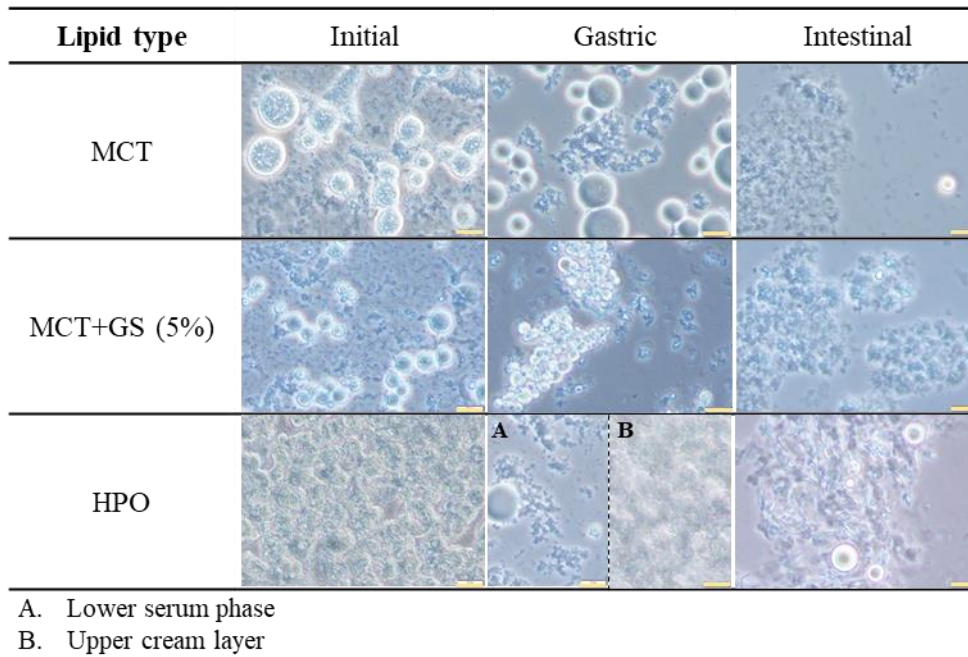
Regarding the HPO-$W_1/O/W_2$ emulsion into whole milk, its particle size distribution graph presented a single peak below 1 μm, while its respective $W_1/O/W_2$ emulsion presented a bimodal distribution, with a main peak above 5 μm (Fig. 3). It can be attributed to the improved stability of the HPO-$W_1/O/W_2$ emulsion when incorporated into whole milk, as observed in its homogeneous visual appearance in comparison with the HPO-$W_1/O/W_2$ emulsion that presented two phases (Fig. 1). In this context, it might be possible that the oil/water interface of the $W_1/O/W_2$ emulsion with HPO had not been fully saturated by Tween 80 during emulsion formation (Molet-Rodríguez et al., 2021). As a consequence, milk proteins, which are known to have surface-active properties, could have been absorbed at the oil/water interface, obtaining smaller droplets with improved stability (Gomes, Costa, & Cunha, 2018) (Fig. 2B).

Food matrix	Initial	Gastric	Intestinal
Whole milk			
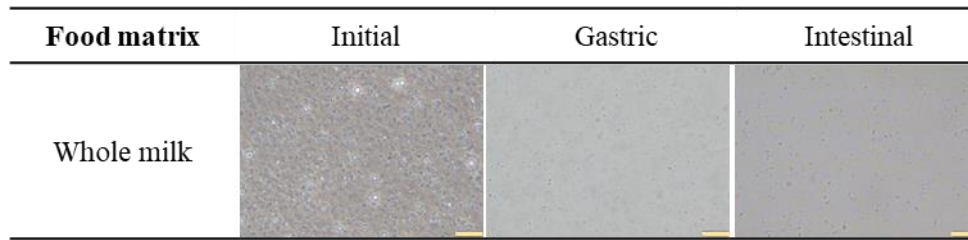
Figure 6. Optical microscopy images of whole milk, initially and after being subjected to simulated gastric and small intestinal conditions. Scale bar: 10 μm.

3.3 Physical characterization of chlorophyllin-loaded $W_1/O/W_2$ emulsions after static *in vitro* gastric digestion

3.3.1 Influence of the lipid phase composition and state

After simulated gastric conditions, the average particle size of the $W_1/O/W_2$ emulsion with liquid lipid phase (MCT) was significantly smaller (5.88 ± 0.43 μm) than that of the initial emulsion (7.88 ± 0.15 μm) (Fig. 2A). In addition, the monomodal size distribution observed initially for the $W_1/O/W_2$ emulsion (MCT), with a peak around 10 μm, became multimodal after the gastric *in vitro* digestion, which also presented two populations of droplets with sizes around 1 and 100 μm (Fig. 3). It is well established that $W_1/O/W_2$ emulsions are susceptible to osmotic pressure changes. For instance, Liu et al. (2020) have reported that under an external applied osmotic gradient, W_1/O droplets in $W_1/O/W_2$ emulsions might experience swelling or shrinkage. These instability mechanisms could be explained by considering the osmolarity difference between the inner water droplets and the outer aqueous phase. In the present study, salts present in SGF solution could promote the partial migration of water from the inner (W_1) to the outer aqueous phase (W_2) of the $W_1/O/W_2$ emulsion with MCT, and consequently, the shrinkage of its W_1/O droplets. In contrast, the droplet size of $W_1/O/W_2$ emulsions with gelled lipid phase formulated with a blend of MCT and GS or pure HPO did not change significantly from their initial size (Fig. 2A). This could be explained by the ability of the gelled lipid phases to act as a barrier and avoid water migration between aqueous phases (Herzi & Essafi, 2018; Liu et al., 2020; Molet-Rodríguez et al., 2021; Weiss & Muschiolik, 2007). Despite this, it is important to notice that the W_1/O droplets aggregation observed initially for the $W_1/O/W_2$ emulsion (MCT), was not present after the gastric phase, whereas it was maintained for the $W_1/O/W_2$ emulsion (MCT-GS). W_1/O droplets aggregation observed before gastric digestion was attributed to the presence of alginate in the external aqueous

phase for $W_1/O/W_2$ emulsion (MCT) and/or free GS crystals in the bulk lipid phase for $W_1/O/W_2$ emulsion (MCT-GS) (see section 3.2.1). In this regard, the absence of aggregation in $W_1/O/W_2$ emulsion (MCT) after the gastric phase might be attributed to the dilution of alginate molecules by the gastric mixture, therefore reducing their ability to promote bridging or depletion flocculation. In the case of $W_1/O/W_2$ emulsion with HPO, although it did not present an increase in the average particle size, it continued showing phase separation after gastric conditions.

3.3.2 *Influence of whole milk matrix*

The average particle size of W_1/O in $W_1/O/W_2$ emulsions into whole milk experienced a significant increase after the gastric phase, regardless of the lipid phase state (Fig. 2B). For instance, the initial average particle sizes of the $W_1/O/W_2$ emulsions into whole milk formulated with pure MCT, a blend of MCT and GS (5% w/w) and pure HPO were 1.60 ± 0.10, 1.16 ± 0.18 and 0.59 ± 0.07 μm, respectively, whereas after the gastric phase they showed average sizes of 8.06 ± 0.18, 4.17 ± 0.62 and 9.30 ± 2.14 μm, respectively (Fig. 2B). In concordance, $W_1/O/W_2$ emulsions into whole milk formulated with MCT, MCT-GS and HPO presented monomodal particle size distributions with intensity peaks around 10, 5 and 10 μm, respectively (Fig. 3). Nevertheless, microscopy images of $W_1/O/W_2$ emulsions into whole milk formulated with MCT and MCT-GS after the gastric phase showed lipid droplets of similar size to the initial ones. In addition, it also presented protein aggregates in the outer aqueous phase, which were probably responsible for the increased average droplet size of $W_1/O/W_2$ emulsion into whole milk after the gastric phase rather than lipid droplets instability. Indeed, casein micelles are known to deprotonate and form aggregates via hydrophobic attractions and van der Waals interactions at pH close to their isoelectric point (pH 4.5-4.8), that is, upon gastric pH conditions. In addition, the gastric aliquot of HPO-$W_1/O/W_2$ emulsion into whole milk, presented two phases (cream and serum), thus suggesting that oil droplets suffer destabilization and further phase separation has occurred (Fig. 1). Based on the results in section 3.2.2 (initial phase), the $W_1/O/W_2$ emulsion (HPO) showed enhanced stability when mixed with whole milk, which was attributed to the possible absorption of milk proteins at the oil/water interface. In this sense, the gastric phase pH of 3 may have caused absorbed proteins to deprotonate and subsequently oil droplets to attract each other's, explaining the observed $W_1/O/W_2$ emulsion phase separation.

3.4 Physical characterization of chlorophyllin-loaded $W_1/O/W_2$ emulsions after static *in vitro* small intestinal digestion

3.4.1 *Influence of the lipid phase composition and state*

The average W_1/O particle size of $W_1/O/W_2$ emulsions at the end of the small intestinal phase depended on the lipid phase composition. $W_1/O/W_2$ emulsions with lipid phases consisting of MCT or MCT-GS presented no significant variations after the small intestinal digestion compared to the end of the gastric phase (Fig. 2A). Despite that the average particle size of $W_1/O/W_2$ emulsions (MCT and MCT-GS) remained without changes, variations were observed in their distribution graphs, which had three peak intensities ranging from 1 μm to more than 100 μm (Fig. 3). It is well-known that lipid phase hydrolysis during small intestinal digestion of emulsion-based delivery systems leads to lipid droplets break-up. Both $W_1/O/W_2$ emulsions (MCT and MCT-GS) had complete lipid hydrolysis (see section 3.5.1), suggesting that the particle size after the small intestinal digestion would correspond to lipolysis subproducts in the digest rather than W_1/O particles from the $W_1/O/W_2$ emulsions. Hence, the smallest particle population around 1 μm could correspond to mixed micelles and monoacylglycerols generated by lipid digestion (Zhang, Zhang, Zhang, Decker, & McClements, 2015). Regarding particle populations of larger sizes (above 10 μm) observed in the distribution graph after small intestinal digestion (Fig. 3), they could be attributed to the presence of complex association colloids, such as vesicles and lamellar structures, formed in the digestion medium as a result of the interactions of lipid digestion products, bile salts, phospholipids, and calcium micelles (Gasa-Falcon, Odriozola-Serrano, Oms-Oliu, & Martín-Belloso, 2017). In the case of the $W_1/O/W_2$ emulsion with HPO, it had an increase in the average particle size after being subjected to small intestinal digestion (from 2.22 ± 1.07 to 5.37 ± 0.43 μm) and monomodal size distribution. It might be attributed to the presence of both digested products or non-digested lipid particles in the digest, as observed in its microscopy image after the small intestinal phase (Fig. 3 and 4). In concordance, $W_1/O/W_2$ emulsions with HPO showed an uncomplete lipid digestibility (see section 3.5.1).

3.4.2 *Influence of whole milk matrix*

The small intestinal digestion of $W_1/O/W_2$ emulsions into whole milk led to particle size variations. $W_1/O/W_2$ emulsion (MCT) incorporated into whole milk showed average particle size reduction from gastric phase (8.06 ± 0.18 µm) to small intestinal phase (3.36 ± 0.49 µm). Its size distribution was monomodal, but with a peak that comprised a wide range of sizes, thus evidencing the presence of dispersed particles from different nature such as digestion products (Fig. 3). Similarly, $W_1/O/W_2$ emulsion (HPO) into whole milk showed a particle size reduction from 9.30 ± 2.14 to 3.17 ± 0.42 µm. It is important to notice that the lipolysis of $W_1/O/W_2$ emulsion (HPO) was higher when it was incorporated in whole milk (see section 3.5.2). As a result, it can be expected that the digest of the $W_1/O/W_2$ emulsion (HPO) into whole milk contained a higher amount of digestion products and less content of non-digested emulsion compared to the $W_1/O/W_2$ emulsion (HPO) itself. In contrast, the average particle size of $W_1/O/W_2$ emulsions (MCT-GS) into whole milk from gastric to intestinal phase, increased from around 4.17 ± 0.62 to 10.66 ± 1.51 µm (Fig. 2B). This increase in particle size could be due to oil droplets aggregation (Salvia-Trujillo, Qian, Martín-Belloso, & McClements, 2013a). Indeed, Marwah, Magarkar, Ray, Aswal, & Bunker (2018) have shown that one-tailed amphiphile molecules such as GS, can form large aggregates in an aqueous medium containing hydrophilic/lipophilic molecules. In addition, the remaining non-digested SC and WPI could have aggregated, justifying the bigger droplet sizes obtained (Chang & McClements, 2016).

3.5 Lipolysis rate of chlorophyllin-loaded $W_1/O/W_2$ emulsions during *in vitro* small intestinal phase

3.5.1 *Influence of the lipid phase composition and state*

In general, the lipid digestion reaction of the $W_1/O/W_2$ emulsions, measured as the percentage of FFAs release, started immediately at the beginning of the intestinal phase with an exponential increase in the FFAs released (Fig. 7A). This evidences that the gelling of the lipid phase by adding GS to MCT or with pure HPO did not affect the lipid digestibility rate of $W_1/O/W_2$ emulsions, which could be behaving as liquid lipid $W_1/O/W_2$ emulsions due to the potential melting of the lipid phase at the intestinal conditions (Molet-Rodríguez et al., 2021). Similar to our findings, Abreu-Martins et al. (2020) have observed no significant differences between the lipid digestibility kinetics of

O/W nanoemulsions stabilized with MCT and blends of MCT and GS. Nevertheless, these authors have observed a delay in the lipolysis initiation of O/W nanoemulsions formulated with HPO, which was attributed to its higher melting temperature in comparison with the blend of MCT-GS. Other authors have also reported a delay in the lipolysis initiation of solid lipid O/W nanoemulsions formulated with tripalmitin, fully hydrogenated soybean oil and cocoa butter (Bonnaire et al., 2008; Guo, Bellissimo, & Rousseau, 2017; Hart, Lin, Thilakarathna, & Wright, 2018). Thus, the lipolysis kinetics of solid lipid O/W nanoemulsions have been observed to be highly related to the specific crystalline state of the solid fat used at the intestinal temperature conditions (Abreu-Martins et al., 2020). In the present study, the absence of differences in the lipid digestibility rate of $W_1/O/W_2$ emulsions formulated with MCT-GS or HPO may suggest that the presence of W_1 droplets within the oil droplets could have affected the type of HPO crystals formed and consequently, their crystalline state during the intestinal phase. Accordingly, Andrade et al. (2018) have observed no significant differences in the initiation time of the lipolysis reaction between $W_1/O/W_2$ emulsions with liquid (soybean oil) or gelled lipid phases (soybean oil + trimyristin).

After 20 min, all the systems reached a steady-state zone, with a slight increase in the FFA until the end of the intestinal phase, yet presenting different end-point values depending on the lipid phase composition (Fig. 7A). The observed differences depended on the fatty acid composition of each lipid phase used. $W_1/O/W_2$ emulsions with pure MCT and a blend of MCT and GS presented FFAs values of 115.46 ± 1.35% and 110.49 ± 7.39%, respectively (Fig. 7A). Their final amount of FFA released greater than 100% can be explained by the conversion of monoacylglycerols into glycerol and FFAs, which was not taken into account in the calculations (Carey, Small & Bliss, 1983). In the case of the $W_1/O/W_2$ emulsion with HPO, it showed a final FFA release of 33.40 ± 0.52% (Fig. 7A). MCT is known to be digested by lipase more rapidly than long-chain triglycerides (LCT) such as those present in HPO, explaining the lower FFA released of the $W_1/O/W_2$ emulsion with HPO compared to the ones with MCT or MCT-GS (Salvia-Trujillo, Qian, Martín-Belloso, & McClements, 2013b). This has been attributed to the ability of medium-chain fatty acids to migrate more rapidly to the aqueous phase, while long-chain fatty acids tend to accumulate at the oil/water interface, thus hindering the lipase activity (Li, Hu, & McClements, 2011). Despite the lower lipolysis of lipid droplets formed mainly by LCT, other authors have observed higher FFAs release values than the ones

obtained in the present study. As mentioned in section 3.1.1, the visual appearance of the $W_1/O/W_2$ emulsion formulated with HPO showed an upper cream layer of non-emulsified oil (Fig. 4), which has been reported to have a slower digestibility by lipase than emulsified oils (Zhang et al., 2016).
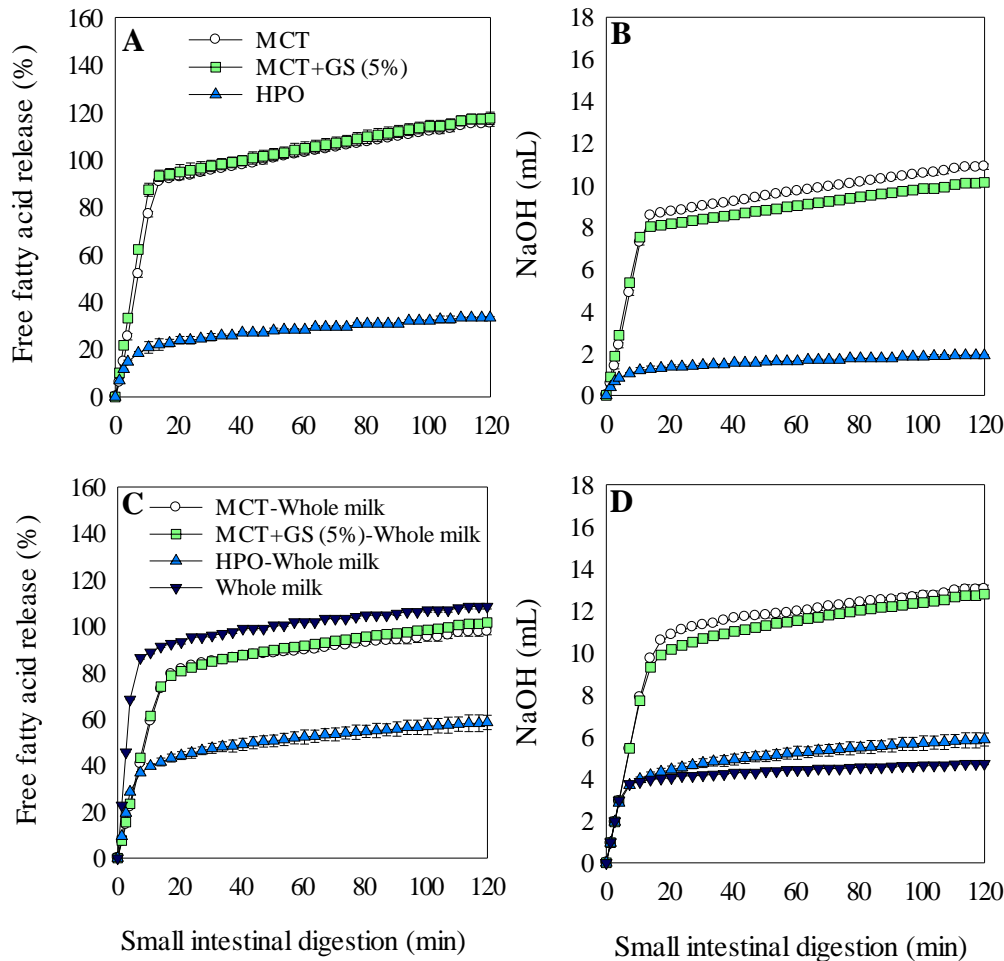
Figure 7. Lipid digestion rate and extent expressed as free fatty acid release (%) during small intestinal time (min) (A,C) and volume (mL) of NaOH used to maintain the pH to 7 (B,D) of $W_1/O/W_2$ emulsions formulated with different lipid phases (A,B) and incorporated into whole milk (C, D). Lipid phases: pure medium-chain triglyceride oil (MCT), a blend of MCT and 5% (w/w) glyceryl stearate (GS) and pure hydrogenated palm oil (HPO).

3.5.2 Influence of whole milk matrix

The $W_1/O/W_2$ emulsions formulated with MCT and MCT-GS into whole milk presented a final percentage of FFAs release $\geq$ 96%, suggesting that all triglycerides had been hydrolysed (Fig. 7C). For example, $W_1/O/W_2$ emulsions with MCT and MCT-GS into

whole milk had FFA release values of 96.02 ± 1.40 and 99.94 ± 1.34%, respectively (Fig 7C). Therefore, the co-digestion of both $W_1/O/W_2$ emulsions (MCT and MCT-GS) with whole milk do not interfere with the almost complete hydrolysis of triglycerides into FFAs. In the case of the $W_1/O/W_2$ emulsion formulated with HPO, its co-digestion with whole milk led to higher percentages of FFA release (57.71 ± 3.06%) compared to the $W_1/O/W_2$ emulsion itself (33.40 ± 0.52%) (Fig. 7A and C). One possible explanation for the higher FFA release percentage obtained for the $W_1/O/W_2$ emulsion formulated with HPO after their incorporation into whole milk would be the digestion of milk fat globules, thus contributing to the overall FFA release percentage. In fact, the small intestinal digestion of the whole milk without the $W_1/O/W_2$ emulsion, used as control, has a FFA release of 104.55 ± 0.97% (Fig. 7C). In addition, there may have been other components in the systems, such as milk proteins, that were hydrolyzed and contributed to the mL of NaOH needed to neutralize the acid released (Mat, Le Feunteun, Michon, & Souchon, 2016). Milk proteins could also have contributed to the observed increased lipid digestibility by (*i*) improving the $W_1/O/W_2$ emulsion stability and/or (*ii*) enhancing the access of lipase to the lipid droplets as a result of their smaller size. On the one hand, emulsified oils are well known to present a faster lipid digestibility than non-emulsified oils (Zhang et al., 2016). In this sense, the emulsifying properties of milk proteins (see section 3.1.2) and consequently the higher stability of the $W_1/O/W_2$ emulsion in whole milk might explain the higher digestibility. On the other hand, the reduction of the W_1/O droplet size observed in Fig. 1B, and consequently, the increase of the surface area would have favoured lipase activity (Salvia-Trujillo et al., 2013a).

3.6 Chlorophyllin bioaccessibility after *in vitro* gastrointestinal digestion of $W_1/O/W_2$ emulsions

3.6.1 *Influence of the lipid phase composition and state*

The hydrophilic nature of CHL allows its solubilization in water-based solutions, thus CHL bioaccessibility (the fraction that is available for absorption in the small intestine) is based on its direct solubilization into the aqueous phase of the digest obtained after GI digestion. In this study, the concentration of CHL in the aqueous phase of the digest was determined and related to the initial concentration used in $W_1/O/W_2$ emulsions formulation, being referred to as CHL bioaccessibility (Fig. 8A).
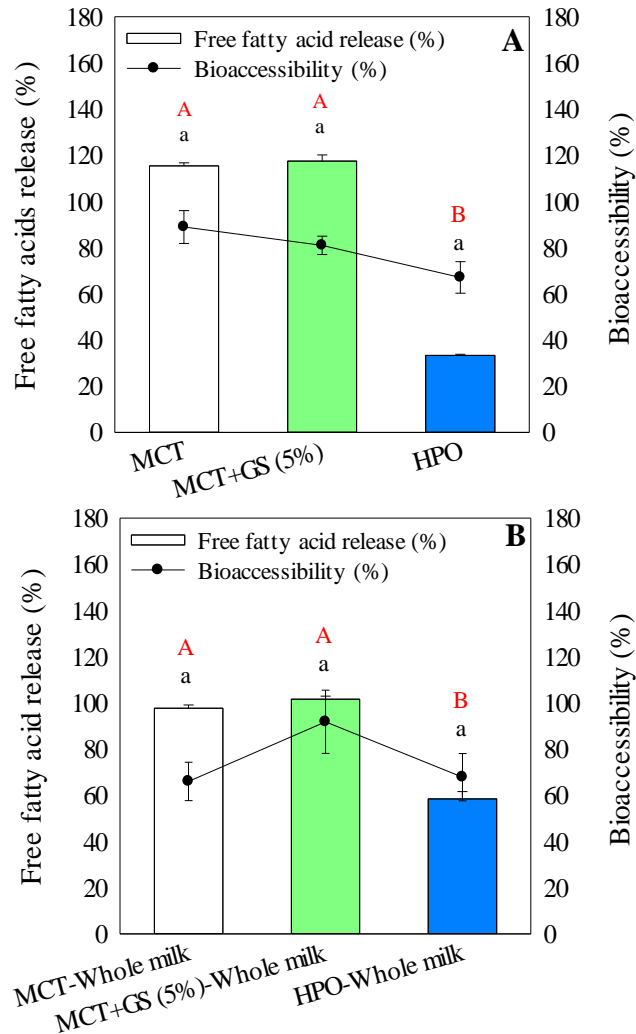
Figure 8. Chlorophyllin (CHL) bioaccessibility (%) (lines) in relation of the lipid digestibility in terms of free fatty acid release (%) (bars) at the end of the in vitro small intestinal phase (120 min) of $W_1/O/W_2$ emulsions formulated with different lipid phases (A) and incorporated into whole milk (B). Lipid phases: pure medium-chain triglyceride oil (MCT), a blend of MCT and 5% (w/w) glyceryl stearate (GS) and pure hydrogenated palm oil (HPO). Different upper-case letters indicate significant differences between the free fatty acid release. Lower-case letters indicate significant differences between the CHL bioaccessibility value.

The CHL bioaccessibility of all $W_1/O/W_2$ emulsions studied presented values above 67%. Nevertheless, higher CHL bioaccessibility values were obtained for $W_1/O/W_2$ emulsions formulated with MCT ($88.97 \pm 7.12\%$) and MCT-GS ($81.05 \pm 3.99\%$) than HPO ($67.12 \pm 6.82\%$) (Fig. 8A). The CHL bioaccessibility of $W_1/O/W_2$ emulsions was directly related with their respective lipid digestion extent at the end of the intestinal phase, which was higher for $W_1/O/W_2$ emulsions formulated with MCT ($115.46 \pm 1.35\%$) and MCT-GS ($110.49 \pm 7.39\%$) than HPO ($33.40 \pm 0.52\%$) (Fig. 8A). In this context, the low lipid

digestibility of $W_1/O/W_2$ emulsions formulated with HPO would hamper the release of CHL encapsulated in the inner aqueous phase, explaining its low bioaccessibility. Thus, our results suggest that the lipid phase composition determines the lipid digestibility extent of $W_1/O/W_2$ emulsions and consequently, the release of the hydrophilic compound and its bioaccessibility.

3.6.2   *Influence of whole milk matrix*

The CHL bioaccessibility after the *in vitro* small intestinal digestion of $W_1/O/W_2$ emulsion (MCT) co-digested with whole milk was lower (66.07 ± 8.29%) compared to its respective $W_1/O/W_2$ emulsion (88.97 ± 7.12%). Instead, $W_1/O/W_2$ emulsion with gelled lipid phases (MCT-GS and HPO) co-digested with whole milk showed non-significant differences in the CHL bioaccessibility (91.87 ± 13.64 and 67.88 ± 10.26%, respectively) with their respective $W_1/O/W_2$ emulsion with gelled lipid phase (81.05 ± 3.99 and 67.12 ± 6.82%, respectively). It could be possible that the CHL in the digest of the $W_1/O/W_2$ emulsion (MCT) would have interacted with milk macromolecules, thus hindering the adsorption of CHL in the small intestine.

4   Conclusions

The results of the present research contribute to understanding the role of the lipid type and state on the colloidal stability, lipid digestion rate and CHL bioaccessibility of $W_1/O/W_2$ emulsions with gelled lipid phase as carriers of hydrophilic bioactive compounds before and after co-ingestion with whole milk. The lipid phase composition dictated the successful formation of $W_1/O/W_2$ emulsions with gelled lipid phase, with MCT-GS forming stable $W_1/O/W_2$ emulsions, whereas HPO led to an upper cream layer and a lower serum phase. Gelling the lipid phase of $W_1/O/W_2$ emulsions prevents the destabilization of W_1/O droplets upon gastric conditions. Nevertheless, the lipolysis rate during the intestinal phase was not affected by the lipid phase gellation, probably due to its melting at small intestinal conditions. Indeed, the lipolysis extent of $W_1/O/W_2$ emulsions with gelled lipid phase was determined by the lipid phase type rather than the state. $W_1/O/W_2$ emulsions formulated with MCT (liquid lipid phase) and MCT-GS (gelled lipid phase) resulted in complete lipid digestion, whereas it was 40% in the case of using HPO. The incorporation of $W_1/O/W_2$ emulsions formulated with HPO into whole milk helped in enhancing its colloidal stability. Nevertheless, the lipid digestibility and CHL

bioaccessibility of W_1/O/W_2 emulsions with gelled lipid phase was not affected when co-ingested with whole milk. CHL bioaccessibility is negatively affected by the presence of proteins. The present work contributes to elucidating the lipolysis of W_1/O/W_2 emulsions with gelled lipid phase before and after incorporation into whole milk. Nevertheless, further studies with gelled lipid phases with higher melting temperatures than the ones used in the present study are needed to understand the lipolysis of W_1/O/W_2 emulsions with gelled lipid phase.

5 Acknowledgements

6 References

Abreu-Martins, H., Artiga-Artigas, M., Hilsdorf Piccoli, R., Martín-Belloso, O., & Salvia-Trujillo, L. (2020). The lipid type affects the in vitro digestibility and β-carotene bioaccessibility of liquid or solid lipid nanoparticles. *Food Chemistry*, *311*, 126024.

Andrade, J., Wright, A. J., & Corredig, M. (2018). In vitro digestion behavior of water-in-oil-in-water emulsions with gelled oil-water inner phases. *Food Research International*, *105*, 41–51.

Artiga-Artigas, M., Molet-Rodríguez, A., Salvia-Trujillo, L., & Martín-Belloso, O. (2018). Formation of Double (W1/O/W2) Emulsions as Carriers of Hydrophilic and Lipophilic Active Compounds. *Food and Bioprocess Technology*, *12*, 422–435.

Artiga-Artigas, Abreu-Martins, H. H., Zeeb, B., Piccoli, R. H., Martín-Belloso, O., & Salvia-Trujillo, L. (2020). Antimicrobial Kinetics of Nanoemulsions Stabilized with Protein:Pectin Electrostatic Complexes. *Food and Bioprocess Technology*, *13*(11), 1893–1907.

Bonnaire, L., Sandra, S., Helgason, T., Decker, E. A., Weiss, J., & McClements, D. J. (2008). Influence of lipid physical state on the in vitro digestibility of emulsified lipids. *Journal of Agricultural and Food Chemistry*, *56*(10), 3791–3797.

Bonnet, M., Cansell, M., Berkaoui, A., Ropers, M. H., Anton, M., & Leal-Calderon, F. (2009). Release rate profiles of magnesium from multiple W/O/W emulsions. *Food Hydrocolloids*, *23*(1), 92–101.

Bou, R., Cofrades, S., & Jiménez-Colmenero, F. (2014). Physicochemical properties and riboflavin encapsulation in double emulsions with different lipid sources. *LWT - Food Science and Technology*, *59*(2), 621–628.

Carey, M. C., Small, D. M., & Bliss, C. M. (1983). Lipid digestion and absorption. *Annual Review of Physiology, 45*, 651–677.

Chang, Y., McClements, D.J. (2016). Influence of emulsifier type on the in vitro digestion of fish oil-in- water emulsions in the presence of an anionic marine polysaccharide (fucoidan): Caseinate, whey protein, lecithin, or Tween 80. *Food Hydrocolloids, 61,* 92-101.

Dickinson, E. (2011). Double Emulsions Stabilized by Food Biopolymers. *Food Biophysics*, *6*(1), 1–11.

Dickinson, E. (2003). Hydrocolloids at interfaces and the influence on the properties of dispersed systems. *Food Hydrocolloids*, *17*(1), 25–39.

Fox, P. F., & Brodkorb, A. (2008). The casein micelle: Historical aspects, current concepts and significance. *International Dairy Journal*, *18*(7), 677–684.

Frank, K., Walz, E., Gräf, V., Greiner, R., Köhler, K., & Schuchmann, H. P. (2012). Stability of Anthocyanin-Rich W/O/W-Emulsions Designed for Intestinal Release in Gastrointestinal Environment. *Journal of Food Science*, *77*(12), N50-N57.

Frasch-Melnik, S., Spyropoulos, F., & Norton, I. T. (2010). W1/O/W2 double emulsions stabilised by fat crystals – Formulation , stability and salt release. *Journal of Colloid and Interface Science, 350*(1), 178–185.

Gasa-Falcon, A., Odriozola-Serrano, I., Oms-Oliu, G., & Martín-Belloso, O. (2017). Influence of mandarin fiber addition on physico-chemical properties of nanoemulsions containing β-carotene under simulated gastrointestinal digestion conditions. *LWT - Food Science and Technology*, *84*, 331–337.

Gomes, A., Costa, A. L. R., & Cunha, R. L. (2018). Impact of oil type and WPI/Tween 80 ratio at the oil-water interface: Adsorption, interfacial rheology and emulsion features. *Colloids and Surfaces B: Biointerfaces*, *164*, 272–280.

Guo, Q., Bellissimo, N., & Rousseau, D. (2017). The Physical State of Emulsified Edible Oil Modulates Its in Vitro Digestion. *Journal of Agricultural and Food Chemistry*, *65*(41), 9120–9127.

Hart, S. M., Lin, X. (Lois), Thilakarathna, S. H., & Wright, A. J. (2018). Emulsion droplet crystallinity attenuates early in vitro digestive lipolysis and beta-carotene bioaccessibility. *Food Chemistry*, *260*, 145–151.

Herzi, S., & Essafi, W. (2018). Different magnesium release profiles from W/O/W emulsions based on crystallized oils. *Journal of Colloid and Interface Science*, *509*, 178–188.

Lamba, H., Sathish, K., & Sabikhi, L. (2015). Double Emulsions: Emerging Delivery System for Plant Bioactives. *Food and Bioprocess Technology, 8,* 709-728.

Li, Y., Hu, M., & McClements, D. J. (2011). Factors affecting lipase digestibility of emulsified lipids using an in vitro digestion model: Proposal for a standardised pH-stat method. *Food Chemistry*, *126*(2), 498–505.

Liu, J., Kharat, M., Tan, Y., Zhou, H., Muriel Mundo, J. L., & McClements, D. J. (2020). Impact of fat crystallization on the resistance of W/O/W emulsions to osmotic stress: Potential for temperature-triggered release. *Food Research International*, *134*, 109273.

Marwah, M., Magarkar, A., Ray, D., Aswal, V., & Bunker, A. (2018). Glyceryl Monostearate : Probing the Self Assembly of a Lipid Amenable To Surface Modi fi cation for Hepatic Targeting. *J. Phys. Chem.*, *122*(38), 22160–22169.

Mat, D. J. L., Le Feunteun, S., Michon, C., & Souchon, I. (2016). In vitro digestion of foods using pH-stat and the INFOGEST protocol: Impact of matrix structure on digestion kinetics of macronutrients, proteins and lipids. *Food Research International*, *88*(B), 226–233.

Minekus, M., Alminger, M., Alvito, P., Ballance, S., Bohn, T., Bourlieu, C., … Brodkorb, A. (2014). A standardised static in vitro digestion method suitable for food-an international consensus. *Food and Function*, *5*(6), 1113–1124.

Molet-Rodríguez, A., Martín-Belloso, O., & Salvia-trujillo, L. (2021). Formation and Stabilization of W1/O/W2 Emulsions with Gelled Lipid Phases. *Molecules*, *26*(2), 312.

Muschiolik, G., & Dickinson, E. (2017). Double Emulsions Relevant to Food Systems: Preparation, Stability, and Applications. *Comprehensive Reviews in Food Science and Food Safety*, *16*(3), 532–555.

Salvia-Trujillo, L., Qian, C., Martín-Belloso, O., & McClements, D. J. (2013a). Influence of particle size on lipid digestion and β-carotene bioaccessibility in emulsions and nanoemulsions. *Food Chemistry*, *141*(2), 1472–1480. 1

Salvia-Trujillo, L., Qian, C., Martín-Belloso, O., & McClements, D. J. (2013b). Modulating β-carotene bioaccessibility by controlling oil composition and concentration in edible nanoemulsions. *Food Chemistry*, *139*(1–4), 878–884.

Tamnak, S., Mirhosseini, H., Tan, C. P., Tabatabaee Amid, B., Kazemi, M., & Hedayatnia, S. (2016). Encapsulation properties, release behavior and physicochemical characteristics of water-in-oil-in-water (W/O/W) emulsion stabilized with pectin-pea protein isolate conjugate and Tween 80. *Food Hydrocolloids, 61*, 599-608.

Teixé-Roig, J., Oms-Oliu, G., Velderrain-Rodríguez, G. R., Odriozola-Serrano, I., & Martín-Belloso, O. (2018). The Effect of Sodium Carboxymethylcellulose on the Stability and Bioaccessibility of Anthocyanin Water-in-Oil-in-Water Emulsions. *Food and Bioprocess Technology*, *11*, 2229–2241.

Weiss, J., & Muschiolik, G. (2007). Factors affecting the droplet size of water-in-oil emulsions (W/O) and the oil globule size in Water-in-oil-in-water emulsions (W/O/W). *Journal of Dispersion Science and Technology*, *28*(5), 703–716.

Zhang, R., Zhang, Z., Zhang, H., Decker, E. A., & McClements, D. J. (2015). Influence of emulsifier type on gastrointestinal fate of oil-in-water emulsions containing anionic dietary fiber (pectin). *Food Hydrocolloids*, *45*, 175–185.

Zhang, R., Zhang, Z., Zou, L., Xiao, H., Zhang, G., Decker, E. A., & McClements, D. J. (2016). Enhancement of carotenoid bioaccessibility from carrots using excipient emulsions: Influence of particle size of digestible lipid droplets. *Food and Function*, *7*(1), 93–103.

GENERAL DISCUSSION

SECTION I: O/W emulsions and nanoemulsions

Essential oils (EOs)-O/W nanoemulsions into apple juice-based beverage being a clear fruit juice from concentrate (chapter I) and β-carotene-loaded O/W emulsions into dairy products (chapters II and III) or dairy and oatmeal-based products combination (chapter III), focusing on the influence of food matrix composition and characteristics on O/W emulsion and nanoemulsion physicochemical properties, colloidal stability and functionality.

1   Apple juice-based beverage

Three different formulations with increasing levels of complexity, being water, an apple juice model and an apple juice-based beverage were used as a continuous phase of the O/W nanoemulsions. The apple juice-based beverage was mostly composed of sugars (*i.e.,* fructose, glucose and sucrose), which are found dissolved in an aqueous solution. In addition, in a lesser concentration, it can also contain active compounds (*i.e.,* polyphenols) and minerals, which impairs it with biological, physical and chemical properties. Apple juice model consisted of an aqueous solution of fructose. Thus, in chapter I, the potential of incorporating Tween 80 stabilized-O/W nanoemulsions containing 0.1 or 1% (w/w) of lemongrass essential oil (LEO) or 1 or 2% (w/w) of mandarin essential oil (MEO) into an apple juice-based beverage was assessed in terms of physicochemical properties, colloidal stability and functionality (*i.e.,* antioxidant and antimicrobial activity) using water, apple juice model and apple juice-based beverage as continuous aqueous phase.

1.1   Physicochemical properties of EOs-O/W nanoemulsions once incorporated into apple juice-based beverage

The physicochemical properties of EOs-O/W nanoemulsions within water, apple juice model or apple juice-based beverage were assessed in terms of droplet size and ζ-potential. Irrespective of the EO type and concentration, increasing the complexity of the continuous aqueous phase led to smaller oil droplet sizes. For instance, the average droplet sizes of the O/W nanoemulsion containing 0.1% (w/w) of LEO within water, apple juice model and apple juice-based beverage were 241.01 ± 119.38, 149.97 ± 32.57 and 26.74 ± 13.39 nm, respectively. The continuous aqueous phase viscosity incremented

when its complexity increased, having values of 22.10 ± 0.62, 28.01 ± 1.14 and 56.87 ± 1.96 mPa·s for water, apple juice model and apple juice-based beverage, respectively. Thus, there could be a relationship between the viscosity of the food matrix used as a continuous phase and the oil droplet size. Accordingly, it is well established that increasing the continuous phase viscosity led to smaller oil droplets, due to increased shear stress in high energy homogenizers (Qian & McClements, 2011). Nevertheless, other authors have observed that the presence of sugar in the aqueous phase might render smaller oil droplets (Urakami, Ukada, Amano, & Ohtani, 2005). They hypothesized that a sugar molecule in the continuous phase might bind with water molecules contributing to a higher emulsifier hydrophobicity, thereby facilitating its deposition at the oil/water interface. Besides the presence of sugars in the apple juice-based beverage, surface-active compounds such as polyphenols have also been related with a reduction of O/W nanoemulsions droplet size, since they might have adsorbed at the oil/water interface, contributing to the oil droplet size decrease during emulsification (Di Mattia, Sacchetti, & Pittia, 2011). Hence, these results evidence that apple juice-based beverages might influence the EOs-O/W nanoemulsions oil droplet size by either increasing the continuous phase viscosity and/or modifying the oil/water interface composition.

There was also a significant effect of the continuous phase complexity on the ζ-potential of EOs-O/W nanoemulsions. The use of the apple juice model or apple juice-based beverage resulted in EOs-O/W nanoemulsions with oil droplets that had weaker negative electrical charges (between -31.20 and -6.80 mV) than using water (between -40.17 and -18.69 mV), regardless of the type and concentration of EOs. This could be attributed to the presence of sugar in the apple juice model and the apple juice-based beverage. Lipid droplets naturally possess negative charges due to the presence of anionic hydroxyl groups (OH^-) in the water or oil used to prepare the O/W nanoemulsion (Marinova et al., 1996). It has been previously reported that the hydration ability of sugars can generate a lack of water molecules in the continuous phase (Urakami et al., 2005). Thus, in the present study, sugars from the food matrix might have contributed to decreasing the OH^- groups from water molecules located at the oil/water interface, explaining the reduction in the negative charge of the oil droplets. Moreover, the presence of ionizable species in the apple juice-based beverage, such as mineral cations from dissolved salts, might also contribute to reducing the negative electrical charge due to a screening effect.

1.2 Colloidal stability of EOs-O/W emulsions and nanoemulsions once incorporated into apple juice-based beverage

The influence of the continuous aqueous phase (water, apple juice model or apple juice-based beverage) on the colloidal stability of EOs-O/W nanoemulsions was analyzed by monitoring their backscattering (BS) and measuring their oil droplet size variation during 28 days of storage at room temperature. BS distribution profiles of EOs-O/W nanoemulsions have shown that their formulation with the apple juice-based beverage had higher stability against creaming than using water or the apple juice model, regardless of the EO type and concentration. In addition, the average droplet size of EOs-O/W nanoemulsions within the apple juice-based beverage did not change over 28 days of storage. It has been stated that increasing the continuous phase viscosity may help to minimize the droplet movement in the fluid, thus retarding the gravitational separation of oil droplets (McClements, Decker, & Weiss, 2007). As mentioned before, the apple juice-based beverage presented higher viscosity values than water and apple juice model, which could explain the stability differences. Besides this, this fact could be explained by the smaller oil droplet sizes observed in presence of apple juice-based beverage compared to water and apple juice model, which have been reported to be more stable than oil droplets of bigger size (Mason, Wilking, Meleson, Chang, & Graves, 2006). In the case of the O/W nanoemulsion containing LEO at 0.1% (w/w), it exhibited a droplet size increase during storage time, regardless of the continuous phase composition. Some EOs present a relatively high water-solubility due to the presence of monoterpenes in their composition and therefore, they are prone to suffer Ostwald ripening. It consists of the diffusion of lipid material from small droplets into larger ones, explaining the oil droplet size increase of 0.1% (w/w) LEO-O/W nanoemulsions during storage.

1.3 Functionality of EOs-O/W nanoemulsions once incorporated into apple juice-based beverage

1.3.1 Antioxidant activity

The antioxidant activity of EOs-O/W nanoemulsions formulated with water, apple juice model or apple juice-based beverage as continuous phase was determined by the ferric reducing antioxidant power (FRAP) assay, which measures their ability to reduce ferric ion (Fe^{3+}) to ferrous ion (Fe^{2+}). Irrespective of the EO type and concentration, the antioxidant activity values obtained for the O/W nanoemulsions formulated with the apple

juice-based beverage were at least two times higher, reaching values of 211.14 µg Eq. Trolox/mL, as compared to the ones formulated using water or apple juice model that presented maximum antioxidant activity values of 93.56 µg Eq. Trolox/mL. Even though there is no previously reported data using apple juice as a continuous phase of O/W nanoemulsions, there is evidence supporting the relationship between the total polyphenolic content of apple juices and their antioxidant capacity (Maragò et al., 2015; Schempp, Christof, Mayr, & Treutter, 2016). In this sense, the high antioxidant values observed for the EOs-O/W nanoemulsions when formulated with the apple juice-based beverage were attributed to the fact that this food matrix is rich in polyphenolic compounds. In addition, vitamins have also been demonstrated to contribute to the antioxidant activity of fruit juices (Zulueta, Esteve, Frasquet, & Frígola, 2007).

1.3.2 *Antimicrobial activity*

The antimicrobial activity of EOs-O/W nanoemulsions formulated with water, apple juice model or apple juice-based beverage as continuous phase was assessed by evaluating the inactivation of inoculated *Escherichia coli (E.coli)* during 28 days storage. *E.coli* population was reduced up to undetectable levels (> 5 log-units) after 28 days of contact with EOs-O/W nanoemulsions formulated with water as a continuous phase, regardless of the type and concentration of EO. Instead, EOs-O/W nanoemulsions efficacy against *E.coli* was compromised when the continuous phase consisted of an apple juice model or an apple juice-based beverage*,* showing a lower reduction of the *E.coli* population compared to water. This behaviour was specifically noticeable in the case of 0.1% (w/w) LEO and 1% (w/w) MEO-O/W nanoemulsions. For instance, O/W nanoemulsions formulated with 0.1% (w/w) LEO and water as continuous phase showed a high bacterial reduction (6.74 ± 0.75 log-units) after 28 days of storage, whereas those formed within the apple juice model and the apple juice-based beverage at the same LEO concentration exhibited only 1.68 ± 0.18 and 1.56 ± 0.20 log-units of reduction, respectively. The presence of nutrients, such as fructose, glucose and sucrose in food matrices has been observed to repair damaged bacterial cells (Gill, Delaquis, Russo, & Holley, 2002). In addition, restricted diffusion of EOs in complex food matrices has been previously reported by Skandamis, Tsigarida, & Nychas (2000), which was attributed to an increase in the medium viscosity, such as in the case of the apple juice-based beverage. Thus, the results from the present study support the already reported negative relationship between

the presence of sugars or the aqueous phase viscosity and the antimicrobial activity of EOs, even when they are encapsulated in an O/W nanoemulsion.

2   Dairy products

The macromolecular composition of milk consists mainly of fat globules, protein (SC, sodium caseinate and WPI, whey protein isolate) and simple carbohydrates (lactose). Yogurt has a similar composition to that of milk, except for the absence of lactose. In addition, yogurt and milk differ in macromolecule organization as well as food matrix physicochemical properties. In chapters II and III, the behaviour of β-carotene-loaded O/W emulsions formulated with long-chain triglyceride (LCT) oils and stabilized with Tween 80 incorporated into dairy products during *in vitro* gastrointestinal digestion was evaluated. Particularly, in chapter II, whole milk, skimmed milk, whole yogurt and skimmed yogurt were the selected dairy products, whereas only whole milk was used in chapter III. Firstly, the physicochemical properties of β-carotene-loaded O/W emulsions once incorporated into dairy products were studied. Secondly, the colloidal stability of β-carotene-loaded O/W emulsion incorporated into dairy products during semi-dynamic *in vitro* gastric digestion (chapter III) and after static *in vitro* gastric digestion (chapter II) was assessed. Moreover, in chapter III, the colloidal stability of the β-carotene-loaded O/W emulsions into dairy products during simulated gastric digestion was related to their emptying rate. Thirdly, the lipid digestibility of the β-carotene-loaded O/W emulsions co-digested with dairy products during static *in vitro* small intestinal digestion was studied. Lastly, the functionality in terms of β-carotene retention (chapter III) and bioaccessibility (chapter II) during and after *in vitro* gastrointestinal digestion was also evaluated.

2.1   Physicochemical properties of β-carotene-loaded O/W emulsions once incorporated into dairy products

2.1.1   Milk

First, the individual effect of the main macromolecules present in dairy products on the particle size of β-carotene-loaded O/W emulsions was studied in chapter II. The incorporation of the O/W emulsion (0.28 ± 0.02 μm) into individual solutions of SC, WPI and lactose (O/W-dairy macromolecule solutions) did not affect its average particle size (between 0.26 to 0.28 μm), droplet size distribution (monomodal) or microstructure (homogeneously dispersed oil droplets). Similarly, the co-existence of the three

macromolecules in the skimmed milk model neither altered their individual behaviour and structure nor the O/W emulsion oil droplet size, since the O/W emulsion into the skimmed milk model (O/W-skimmed milk model) showed an average particle size of 0.28 ± 0.01 μm and a monomodal distribution. Thus, even though SC, WPI and lactose are known to possess oil emulsification capacity (Dickinson, 2001; Luo et al., 2014), the absence of particle size changes between the O/W emulsion, O/W-dairy macromolecule solutions and O/W-skimmed milk model evidenced that the oil/water interface of O/W emulsion was already completely covered by Tween 80 molecules before being incorporated into milk macromolecule solutions (Gomes, Costa, & Cunha, 2018). As a consequence, SC, WPI and lactose might locate at the bulk continuous aqueous phase instead of adsorbing at the oil/water interface. The average particle size of β-carotene-loaded O/W emulsions was not even influenced when incorporated into complex food matrices, being whole milk or skimmed milk, as corroborated in both chapters II and III. For instance, in chapter II, the particle size of the O/W emulsion, O/W emulsions into whole milk (O/W-whole milk) and O/W emulsions into skimmed milk (O/W-skimmed milk) were 0.28 ± 0.02, 0.38 ± 0.02 and 0.27 ± 0.01 μm, respectively. The small increase in the average particle size of O/W emulsions into whole milk would probably correspond to the presence of milk fat globules dispersed in the continuous aqueous phase since the particle size of the whole milk (without O/W emulsions) averaged 0.35 ± 0.01 μm. In chapter III, O/W emulsion and O/W-whole milk had average particle sizes of 0.56 ± 0.03 and 0.44 ± 0.04 μm. In addition, they presented monomodal particle size distribution into the range of 0.1–1 μm and their microscopy images showed homogeneous submicron lipid droplets dispersed in the continuous aqueous phase, which evidence that the milk matrix did not affect the microstructure of the O/W emulsion. Variations in the particle size of O/W emulsions between chapters II and III were due to differences in the fabrication method and processing parameters used for their formation.

The electrical charge (ζ-potential) of the β-carotene-loaded O/W emulsion was neither influenced by its incorporation into dairy macromolecule solutions nor whole milk and skimmed milk. In chapter II, the O/W emulsion showed negatively charged interfaces, with ζ-potential values of -20.03 ± 2.07 mV. Even though the emulsifier used in this study (Tween 80) was non-ionic, it has been reported to form negatively charged oil droplets when the pH of the O/W emulsion is higher than 4 (Hsu & Nacu, 2003). In addition, oil droplets naturally possess a negative charge due to the presence of OH⁻ groups in the

water or oil used to prepare the O/W emulsion (Marinova et al., 1996). The ζ-potential values of O/W-dairy macromolecule solutions (between -17.85 and -19.08 mV), as well as O/W-whole milk and O/W-skimmed milk (-16.63 ± 1.48 and -13.97 ± 0.61 mV, respectively), were similar to the ones of the O/W emulsion.

2.1.2 Yogurt

In chapter II, it has been shown that yogurt did not affect the O/W emulsions oil droplet size. Although the O/W-whole yogurt and O/W-skimmed yogurt had higher average particle sizes (8.00 ± 0.50 and 11.43 ± 1.55 μm, respectively) compared to the O/W emulsion (0.28 ± 0.02 μm), it was attributed to the presence of protein aggregates in yogurt matrices rather than O/W emulsion destabilization phenomena. O/W-whole and skimmed yogurt microscopy images showed aggregates of dairy protein, yet the microstructure of the O/W emulsion did not present any variation. Yogurt is the result of the milk lactose fermentation into lactic acid by incubating it with several bacteria at low temperatures. This process results in aggregation of casein micelles and denatured WPI-casein complex formation (Francis, Glover, Yu, Povey, & Holmes, 2019; Law & Leaver, 2000; Vasbinder, Alting, & De Kruif, 2003). These interactions are responsible for the formation of a three-dimensional network in the whole or skimmed yogurt, explaining the bigger average particle size of O/W-whole and skimmed yogurt compared to the O/W emulsion (Hassan, Frank, Farmer, Schmidt, & Shalabi, 1995).

The incorporation of the O/W emulsion (-20.03 ± 2.07 mV) into whole yogurt or skimmed yogurt led to neutral electrical charges (0.70 ± 0.38 and 1.22 ± 0.17 mV, respectively). It could be attributed to the neutral electrical charge of the protein aggregates located in the aqueous phase of O/W-whole or skimmed yogurt rather than changes in the electrical charge of oil droplets from the O/W emulsion.

2.2 Colloidal stability during gastric conditions of β-carotene-loaded O/W emulsions co-digested with dairy products

2.2.1 Milk

Changes in particle size and size distribution of O/W emulsion, O/W-whole milk or O/W-skimmed milk during and after *in vitro* gastric digestion were studied using semi-dynamic and static *in vitro* gastric digestion methods. Irrespective of the *in vitro* gastric digestion

method used, the average particle size and size distribution of the O/W emulsions remained constant throughout the gastric phase, thus maintaining their colloidal stability. Nevertheless, the average particle size and size distribution of O/W-whole milk or O/W-skimmed milk presented variations upon *in vitro* gastric conditions. Using the semi-dynamic *in vitro* digestion method (chapter III), it was observed that the initial monomodal distribution that had been observed for the O/W-whole milk (see section 2.1.1) changed to multimodal after 14 min of gastric digestion (first gastric emptying, GE1). It presented one peak in the submicron range, which may correspond to the O/W emulsions and milk fat globules, and another around 114 µm. These bigger droplets might correspond to the network of proteins observed by confocal microscopy. Even though the effect of protein within whole milk on the Tween 80-stabilized O/W emulsions was not previously studied, it is well-known that at pH close to their isoelectric point (pH 4.5-4.7), casein micelles are known to precipitate and consequently form a network of insoluble proteins (Francis et al., 2019). Nevertheless, the size distribution at the end of the gastric phase (last GE, GE5) was monomodal again, which was explained by an absence of proteins in this GE, which had been emptied previously. It was opposite to the results obtained after the static *in vitro* gastric digestion method, in which there was an increase in the particle size of O/W-whole milk (from 0.38 ± 0.02 to 0.64 ± 0.03 µm) and O/W-skimmed milk (from 0.27 ± 0.01 to 0.60 ± 0.17 µm) after the gastric phase. Nevertheless, their microscopy images after the static *in vitro* gastric digestion showed aggregates of protein, yet the O/W emulsion remained without microstructural changes. In fact, the macromolecule solutions containing SC and fortified with the O/W emulsion (O/W-SC and O/W-skimmed milk model) also presented an increased average particle size compared to the O/W emulsion, with a new population of particles of bigger size (> 10 µm) in their distribution graph and the presence of aggregated casein micelles after being submitted to the gastric phase conditions. Thus, complementary results from the static and semi-dynamic *in vitro* gastric digestion methods allow understanding the behaviour of O/W-whole milk and O/W-skimmed milk during and after gastric digestion.

2.2.2 Yogurt

O/W-whole yogurt and O/W-skimmed yogurt experimented a decrease in their initial average particle size (8.00 ± 0.50 and 11.43 ± 1.55 µm, respectively) after being subjected to static *in vitro* gastric conditions (1.26 ± 0.16 and 1.87 ± 0.13 µm, respectively). This

may be because there was less amount of aggregated protein after the gastric digestion than initially, as observed in the microscopy images. In the gastric phase, denatured proteins, as found in yogurt, have been reported to be digested higher than in their native state, which could explain the observed reduction of protein aggregates and consequently the average particle size decrease (Halabi, Croguennec, Bouhallab, Dupont, & Deglaire, 2020; Nguyen, Gathercole, Day, & Dalziel, 2020). Accordingly, Nguyen et al. (2020) obtained a greater number of bioactive peptides after *in vitro* gastrointestinal digestion of yogurt compared to milk.

O/W emulsion, O/W-whole yogurt and O/W-skimmed yogurt presented almost neutral ζ-potential values after the static *in vitro* gastric phase. In this sense, the free ions present in the simulated gastric fluids would have attenuated the charges of the oil droplets (Keowmaneechai & McClements, 2002).

2.3 Colloidal stability during small intestine conditions of β-carotene-loaded O/W emulsions co-digested with dairy products

O/W emulsion, O/W-whole milk, O/W-skimmed milk and O/W-whole yogurt experienced a particle size increase after static *in vitro* small intestinal conditions. Several reasons have been previously attributed to the increase in particle size of O/W emulsions after the small intestinal digestion. Firstly, the presence of complex association colloids, such as mixed micelles, vesicles and lamellar structures, formed in the digestion medium as a result of the interactions of lipid digestion products, bile salts, phospholipids, and calcium micelles (Kossena, Boyd, Porter, & Charman, 2003). Secondly, the partial displacement of emulsifier molecules from the droplet surfaces by the action of bile salts would have resulted in a single emulsifier molecule being attached to the surface of more than one droplet, provoking droplet flocculation and coalescence through charge neutralization and bridging effects (Borreani, Leonardi, Moraga, Quiles, & Hernando, 2019; Gasa-Falcon, Odriozola-Serrano, Oms-Oliu, & Martín-Belloso, 2019). Chang, McLandsborough, & McClements (2012) and Li & McClements (2010) obtained similar results with O/W emulsions stabilized with Tweens, observing by confocal laser scanning microscopy that the droplets flocculated and coalesced when simulated intestinal fluids were added. Lastly, bile salts may have adsorbed at the oil/water interface and altered their composition, thereby promoting interactions between oil droplets (Maldonado-Valderrama, Wilde, Macierzanka, & Mackie, 2011). In the case of O/W-skimmed yogurt,

particle size decreases from 1.87 ± 0.13 to 1.24 ± 0.01 µm after small intestinal digestion. This smaller average particle size for the O/W-skimmed yogurt after small intestinal conditions in comparison with the other formulations can be attributed to its lower content of un-digested lipid droplets (see section 2.4.2).

O/W emulsion and O/W-dairy products presented negative ζ-potential values after the small intestinal phase. It could be attributed to the adsorption at the oil/water interface of surface-active anionic digestion products (*e.g.,* free fatty acids) and/or components present from the intestinal juices (*e.g.,* bile salts) (Hur, Decker, & McClements, 2009; Pinheiro et al., 2013). Despite this, the neutral pH of the intestinal phase might be another reason why more negative values of ζ-potential were obtained in comparison with the almost neutral charge of the gastric phase.

2.4 Functionality during *in vitro* small intestinal digestion of β-carotene-loaded O/W emulsions co-digested with dairy products

2.4.1 Lipid digestion in each gastric emptying

In chapter III, the lipolysis reaction of the GE samples from the O/W emulsion or O/W-whole milk was monitored during the *in vitro* small intestinal phase through the FFA release (%). It is related to the lipid content of the samples taken at different gastric digestion moments and so, provided relevant information about the lipid content that had been emptied in each GE. O/W emulsion showed a gradual decrease in FFA release along the different GEs, from $14.01 \pm 1.80\%$ (GE1) to $7.20 \pm 1.57\%$ (GE5), thus the O/W emulsion at GE1 presented a higher oil concentration than at GE2, and it decreased progressively in subsequent GE points. This can be related to the dilution that occurs during the gastric phase, subsequently decreasing the concentration of lipids in the gastric vessel during time. It suggests that the O/W emulsion presents high colloidal stability in the gastric phase, as seen in confocal microscopy images. In fact, it has been widely reported that Tween 80 renders highly stable emulsions under gastric conditions, in contrast with other emulsifiers (Verkempinck et al., 2018). In this sense, other authors have reported a gradual decrease of the FFA release along with the gastric emptying of O/W emulsions when subjected to semi-dynamic *in vitro* digestion and a sudden increase at the final GE, which is attributed to the emptying of the creamed lipid layer of unstable emulsions (Mulet-Cabero et al., 2020). Hence, the FFA release in the small intestine after the semi-dynamic gastric phase may not only indicate the amount of lipid that is delivered

into the small intestinal phase but also may be related to the stability of the O/W emulsion under gastric conditions when incorporated into different food matrices. For instance, the gradual decrease in FFA released from GE1 to GE2 points of the O/W emulsion was no longer observed for the O/W-whole milk. In fact, similar FFA release was observed in either GE1 (18.71 ± 0.65%) or GE2 (17.85 ± 0.65%) of O/W-whole milk, evidencing that the presence of whole milk led to a higher amount of lipid emptied at early times of the gastric digestion in comparison with the O/W emulsion. Confocal microscopy images of the O/W-whole milk at GE1 showed lipid droplets entrapped in a network of protein formed by its precipitation due to the action of pepsin. Hence, the higher amount of lipid in GE1 and GE2 of O/W-whole milk was due to the sedimentation of the protein network to the bottom of the vessel, thus emptying the lipid droplets entrapped in the protein network at early gastric times (GE1 and GE2) (Mulet-Cabero, Mackie, Wilde, Fenelon, & Brodkorb, 2019).

2.4.2 *Total lipid digestion*

In chapters II and III, the lipolysis reaction of the O/W emulsion and O/W-dairy products was monitored during static *in vitro* small intestinal phase through the free fatty acid (FFA) release (%) to determine differences between their lipid digestibility rate and extent. The lipolysis rate at earlier moments of the intestinal phase (0-5 min) depended on the complexity of the food matrix. All O/W-dairy products studied showed faster lipolysis at earlier moments of the intestinal phase compared to the O/W emulsions. Besides the oil from the O/W emulsion, O/W-dairy products also contained a proportion of fat from the dairy matrix, which could be responsible for the rapid lipolysis observed. Triglycerides consist of a glycerol molecule having three fatty acids esterified at the hydroxyl residues, one in the central position of the glycerol molecule (sn-2) and the other two at the terminal positions sn-1 and sn-3. Dairy fats contain substantial quantities of short- and medium-chain fatty acids (C_4-C_{10}), which predominantly occupies the primary positions of the acylglycerol (sn-1 and sn-3) (Lubary, Hofland, & ter Horst, 2011). In turn, vegetable oils, such as CO or sunflower oil from O/W emulsion are mostly composed of long-chain fatty acids ($\geq C_{12}$) that are mainly esterified in sn-2 and sn-3, respectively (Gao et al., 2017; Timm-Heinrich, Xu, Nielsen, & Jacobsen, 2003). In this context, it has been accepted that fatty acids on sn-2 carbon have higher bond energy and are harder to be lost than those at sn-1 and sn-3 positions, explaining the slower lipolysis initiation in O/W

emulsion (Karupaiah & Sundram, 2007). In addition, short-chain triglycerides (SCT) and medium-chain triglycerides (MCT) are known to be digested by lipase more rapidly than LCT, which might also be contributing to the faster lipid digestibility observed for the O/W-dairy products in comparison with the O/W emulsion (Salvia-Trujillo, Qian, Martín-Belloso, & McClements, 2013a). In fact, other studies have reported a higher digestibility of MCT compared to LCT when they are incorporated in O/W emulsions (Ahmed, Li, McClements, & Xiao, 2012; Li, Hu, & McClements, 2011).

Besides this, the O/W emulsions presented FFA release end-point values of 64.58 ± 3.57% (chapter II) and 53.04 ± 6.33% (chapter III), meaning that the lipolysis was uncompleted. As mentioned early in this section, it could be attributed to the free fatty acid chain length of the triglyceride oils used for the O/W emulsion formulation, being LCT oils in both chapter II and chapter III. In this sense, it has been stated that LCT tends to accumulate at the oil/water interface, thus hindering lipase activity (Li et al., 2011). In the case of the O/W-dairy products, the FFA release values at the end of the small intestinal phase were higher compared to O/W emulsions. For instance, in chapter II, O/W-dairy products showed FFA end-point values above 81.35%, whereas for the O/W emulsion it was 53.04 ± 6.33%. On the one hand, the hydrolysis of the fat present in the whole milk might have incremented the total FFA release percentage. On the other hand, the release of free amino acids due to protein hydrolysis in the small intestinal phase could have contributed to increasing the amount of NaOH needed to neutralize the acid released (Mat, Le Feunteun, Michon, & Souchon, 2016). In fact, the skimmed milk model needed 0.93 ± 0.05 mL of NaOH to neutralize the acid present in the small intestine digestion, even in the absence of lipid. Particularly, O/W-skimmed yogurt presented the highest FFA release percentage at the end of the small intestinal digestion. A possible explanation for the higher lipolysis extent of the O/W-skimmed yogurt compared to the other O/W-dairy products might be the presence of denaturized proteins at the oil/water interface of oil droplets, which would have facilitated its interaction with pancreatic lipase. Microscopic images of the coarse O/W-skimmed yogurt revealed part of the total protein deposited at the oil/water interface, whereas the protein in the coarse O/W-skimmed milk remained in the bulk aqueous phase. In agreement, other authors stated that protein heat treatment at 70 °C leads to a higher n-dodecane/water surface coverage in comparison with native protein (Dickinson & Hong, 1994; Roth, Murray, & Dickinson, 2000). In this context, it could be possible that part of the yogurt denatured protein absorbed at the oil/water interface of the O/W emulsion

would have been hydrolysed during the gastric phase, favouring lipase attack and consequently, leading to higher lipid digestibility compared to O/W-whole or skimmed milk.

2.4.3 β-carotene retention

In chapter III, the concentration of β-carotene in the GE samples after the small intestinal digestion of O/W emulsion and O/W-whole milk was determined, and the percentage of β-carotene retained under simulated GI conditions was calculated based on their initial concentration in O/W emulsion. In general, as gastric digestion progressed (from GE1 to GE5), the β-carotene retention tended to decrease, although no significant differences were observed within the different GE samples. In addition, the total β-carotene retention at the end of the *in vitro* small intestinal digestion of the O/W emulsion was 15.48 ± 8.40%, whereas it was 26.35 ± 9.07% after incorporated into whole milk. This fact has also been observed by other researchers, who hypothesized that enhanced protection of β-carotene encapsulated in O/W emulsions incorporated in milk in comparison with water can be explained by the presence of protein in the food matrix (Chuacharoen & Sabliov, 2016). Protein is known to act as an antioxidant because of its ability to chelate iron and/or be a free radical scavenger (Pihlanto, 2006).

2.4.4 β-carotene bioaccessibility

The β-carotene bioaccessibility is defined as the fraction of β-carotene that can be incorporated into the mixed micelles and thus becomes available for absorption in the body. In chapter II, O/W emulsion presented a β-carotene bioaccessibility of 38.76 ± 3.06%. Similar to our findings, Verkempinck et al. (2018) have reported β-carotene bioaccessibility of 33% after the *in vitro* GI digestion of O/W emulsions that were also formulated with LCT and stabilized with Tween 80. Nevertheless, other authors have reported a much higher β-carotene bioaccessibility (> 66%) of O/W emulsions using similar components in the formulation of O/W emulsions (Qian, Decker, Xiao, & McClements, 2012; Salvia-Trujillo et al., 2017). This is probably due to the incomplete lipolysis observed in the present study, with a maximum of 64.58 ± 3.57% of the FFA being released. Consequently, a lower number of mixed micelles able to solubilize β-carotene could be formed, explaining the lower bioaccessibility values in comparison with the ones obtained for other researchers.

Regarding the β-carotene bioaccessibility of O/W-dairy products (between 34.78 and 44.57%), it was similar to that of the O/W emulsion (38.76 ± 3.06%). Nevertheless, O/W-dairy products presented a higher FFA release percentage (>81.35%) compared to the O/W emulsion (64.58 ± 2.75%). A higher FFA release after small intestinal digestion has been related to a larger quantity of mixed micelles formed, resulting in a higher amount of β-carotene solubilized in mixed micelles, meaning a higher β-carotene bioaccessibility (Salvia-Trujillo, Qian, Martín-Belloso, & McClements et al., 2013b). In this sense, it could be possible that part of the β-carotene present in the digest of the O/W-dairy products would have not been incorporated into mixed micelles formed during digestion due to its interaction with dairy macromolecules. Accordingly, Mun, Kim, Shin, & McClements (2015) and Wackerbarth, Stoll, Gebken, Pelters, & Bindrich (2009) have observed that protein might hinder β-carotene micellization by forming complexes with carotenoids and/or promoting aggregation and precipitation of mixed micelles.

3   Dairy and oatmeal products

The chemical composition of oat grains is characterized by a high content of complex carbohydrates (66–76%), including starch and dietary fibre, and in minor proportion simple sugars. In particular, oat grains contain a high content of β-glucan, a water-soluble dietary fibre able to absorb water and form highly viscous solutions, which has been reported to delay nutrient emptying from the stomach to the duodenum (Knudsen, 2014; Mackie, Rafiee, Malcolm, Salt, & van Aken, 2013; Roye et al., 2020). Oat grains are commonly eaten in oatmeal, which consists of oat grains boiled in water (oatmeal) or milk (whole milk-oatmeal). In chapter III, the complexity of the food matrix was increased in comparison with chapters I and II, using a meal consisting of a food product combination (*i.e.,* whole milk-oatmeal). Colloidal stability of β-carotene-loaded O/W emulsion stabilized with Tween 80 and incorporated into oatmeal and whole milk-oatmeal, and their subsequent emptying rate, lipid digestibility and β-carotene retention during *in vitro* gastrointestinal digestion were evaluated using a semi-dynamic *in vitro* gastric model and static *in vitro* small intestinal model.

3.1 Physicochemical properties of β-carotene-loaded O/W emulsions once incorporated into whole milk-oatmeal

The average particle size of the O/W-oatmeal (13.07 ± 1.81 μm) and O/W-whole milk-oatmeal (7.60 ± 1.21 μm) was higher than the one of the O/W emulsion (0.56 ± 0.03 μm), which correlated with the existence of particle populations in the micro-range in the particle size distribution graph of O/W oatmeal and O/W- whole milk-oatmeal. The meal microstructure was responsible for the bigger particle sizes observed in both O/W-oatmeal and O/W-whole milk-oatmeal compared to the O/W emulsion since confocal images of the oatmeal and whole milk-oatmeal either with or without O/W emulsions clearly showed lipid droplets of micrometric size (≈10 μm) and also aggregates of β-glucan and/or protein. It has been previously demonstrated that β-glucan fibre from oat grains can auto-aggregate through hydrogen bonds (Tosh, Brummer, Wood, Wang, & Weisz, 2004; Wu et al., 2006). In addition, studies on the stability of casein micelles in contact with polysaccharides, such as β-glucan, have demonstrated limited compatibility between them (De Bont, Van Kempen, & Vreeker, 2002; Goh, Sarkar, & Singh, 2014). In this context, the exclusion of β-glucan from the casein micelles surface area may have caused the osmotic attraction of casein micelles and consequently their aggregation in O/W-whole milk-oatmeal.

3.2 Colloidal stability during *in vitro* gastric conditions of β-carotene-loaded O/W emulsions co-digested with whole milk-oatmeal

The particle size distribution of O/W emulsion in the different GE aliquots had no significant differences from the initial one, evidencing that it remained stable during its passage through gastric digestion. Instead, the microstructure of the O/W-oatmeal and O/W-whole milk-oatmeal was affected by the acidic conditions in this digestion phase. Their initial multimodal distribution due to protein and β-glucan aggregates changed to monomodal in GE1 as the aggregates were probably re-diluted by gastric fluids. In GE5, O/W-oatmeal presented a multimodal size distribution with one population of particles in the submicron range and another between 10 and 100 μm. Instead, O/W-whole milk-oatmeal size distribution was monomodal. The population of micrometric particles in O/W-oatmeal could be explained by the re-aggregation of β-glucan in GE5 because of the increase in the ionic strength due to the high volume of SGF added (Sarantis, Eren, Kowalcyk, Jimenez–Flores, & Alvarez, 2021). Nevertheless, the re-aggregation of β-

glucan due to the increase in the ionic strength would not occur in presence of milk protein as observed in O/W-whole milk oatmeal.

3.3 Functionality during *in vitro* small intestinal digestion of β-carotene-loaded O/W emulsions co-digested with whole milk-oatmeal

3.3.1 *Lipid digestion in each gastric emptying*

The lipolysis reaction of the GE samples from the O/W emulsion, O/W-oatmeal and O/W-whole milk-oatmeal was monitored during the *in vitro* small intestinal phase through the FFA release (%). It is related to the lipid content of the samples taken at different gastric digestion moments and so, provided relevant information about the lipid content that had been emptied in each GE. As mentioned earlier (see section 2.4.1), O/W emulsion at GE1 presented a higher oil concentration (14.01 ± 1.80% of FFA released) than at GE2 (10.51 ± 0.26% of FFA released), and it decreased progressively in subsequent GE points, suggesting that the O/W emulsion presents high colloidal stability in the gastric phase. Instead, the FFA release percentages in GE aliquots 1 to 4 of O/W-oatmeal and O/W-whole milk-oatmeal remained practically constant and decreased at GE5, thus the lipid emptying was delayed in these fortified products. For instance, O/W-whole milk-oatmeal between GE1 and GE4 presented end-point FFA release values from 15.80 ± 0.24 to 13.71 ± 0.05%, whereas it was 7.36 ± 0.42% in GE5. β-glucan within oat grains could have possibly altered the rheological properties of the food matrices by either increasing their viscosity and/or forming a gel depending on its molecular weight, explaining the delay in the lipid emptying observed when the O/W emulsion was incorporated in meals containing oat grains (Brummer et al., 2014; Regand, Tosh, Wolever, & Wood, 2009). This was confirmed by the presence of solubilized β-glucan in the aqueous phase of O/W-oatmeal and O/W-whole milk-oatmeal at GE1 and GE3. In addition, the initial visual images of the meals showed that both O/W-oatmeal and O/W-whole milk-oatmeal had a gel-like appearance, while the O/W emulsion was liquid. Similarly, other authors have also reported increased gastric retention of semi-solid meals compared to liquid ones due to their elevated viscosity (Mackie et al., 2013). Thus, our results suggest that highly viscous meal matrices could modulate the gastric emptying rate of O/W emulsions when co-ingested together.

3.3.2 Total lipid digestion

The total lipid digestion at the end of the small intestinal digestion of the O/W emulsion, O/W-oatmeal and O/W-whole milk-oatmeal was 53.04 ± 6.33, 57.85 ± 6.13 and $63.57 \pm 0.73\%$, respectively. Thus, the lipid digestibility of the meal containing whole milk had higher FFA end-point values, although no significant differences were observed with respect to the O/W emulsion. One possible explanation for this increase is that the fat globules from the milk experienced higher and faster hydrolysis in comparison with oil droplets from vegetable oil such as sunflower oil. These results are in agreement with the ones obtained for O/W-whole milk and O/W-whole yogurt in chapter II, which had higher lipid digestibility than the O/W emulsion.

3.3.3 β-carotene retention

The total β-carotene retention at the end of the small intestinal digestion of the O/W emulsion was $15.48 \pm 8.40\%$, whereas it was 28.53 ± 4.61 and $20.20 \pm 3.51\%$ after its incorporation into oatmeal and whole milk-oatmeal, respectively. In agreement, other studies have shown that polysaccharide is capable of retarding carotenoid oxidation in O/W emulsions by (*i*) slowing down the diffusion of prooxidants to oil droplet surface because of the viscosity increase and (*ii*) metal ion chelation and hydrogen donation, through which polysaccharide functions as radical chain breakers (Sun, Gunasekaran, & Richards, 2007).

SECTION II: $W_1/O/W_2$ emulsions

The effect of lipid phase composition and state as well as hydrophilic emulsifier on chlorophyllin (CHL)-loaded $W_1/O/W_2$ emulsions formation and physicochemical properties as well as colloidal stability and functionality during storage and *in vitro* gastrointestinal digestion were assessed (Chapter IV and V). In addition, the behaviour of $W_1/O/W_2$ emulsions with liquid and gelled lipid phase once co-digested with whole milk was also studied (Chapter V).

4 Chlorophyllin-loaded $W_1/O/W_2$ emulsions with liquid or gelled lipid phase

4.1 Physicochemical properties of chlorophyllin-loaded $W_1/O/W_2$ emulsions

4.1.1 Formation

The capability of forming $W_1/O/W_2$ emulsions with liquid lipid phase mainly depended on the affinity between lipid phase and hydrophilic emulsifier used to disperse the W_1/O droplets into the outer aqueous phase (W_2). Tween 80 was able of forming $W_1/O/W_2$ emulsions, regardless of the lipid phase composition, while lecithin did not form $W_1/O/W_2$ emulsions for all the lipid phases. Tween 80 has a high proportion of polar groups and consequently, it strongly adsorbs at the oil/water interface (Jo & Kwon, 2014). On the contrary, lecithin was only able to form initially stable $W_1/O/W_2$ emulsions when CO was used as a lipid phase, while single O/W emulsions were formed when using MCT, evidencing a clear destabilization of the dispersed W_1 droplets when MCT was used. Lecithin presents a strong amphiphilic nature and is preferably adsorbed in highly lipophilic interfaces, such as in CO rather than in MCT. In this regard, in those emulsions formulated with MCT as lipid phase, lecithin would have been preferably located in the bulk outer aqueous phase, causing an osmotic imbalance between the two aqueous phases, and ultimately the destabilization of the W_1 dispersed droplets. In addition to this, MCT could be less efficient than CO in preventing the water migration from the inner to the outer aqueous phase during the emulsification process, due to its higher polarity in comparison to CO (Schmidts, Dobler, Guldan, Paulus, & Runkel, 2010).

The formation of $W_1/O/W_2$ emulsions with gelled lipid phase depended on the lipid phase composition. $W_1/O/W_2$ emulsions with gelled lipid phases consisting of CO or MCT with 1 or 5% (w/w) of glyceryl stearate (GS) were successfully formed, whereas phase separation was observed when the gelled lipid phase consisted of hydrogenated palm oil (HPO). GS is a monoglyceride presenting interfacial activity that might adsorb at both the water/oil and oil/water interfaces, whereas HPO would probably remain at the bulk lipid phase (Abreu-Martins, Artiga-Artigas, Hilsdorf Piccoli, Martín-Belloso, Salvia-Trujillo, 2020; Molet-Rodríguez, Martín-Belloso, & Salvia-trujillo, 2021). In this sense, the formation of stable $W_1/O/W_2$ emulsions with lipid phases consisting of CO or MCT with GS might be attributed to a decrease of water migration between aqueous phases after emulsion formation due to the physical barrier created by the adsorption of GS

crystals at the water/oil or oil/water interface. Therefore, the surface-active properties of the lipid or fat crystals may determine their location in the lipid phase, and consequently their ability to avoid inner water migration. In agreement with these results, research conducted by Herzi & Essafi (2018) evidenced that the retention of the inner water phase in $W_1/O/W_2$ emulsions formulated with mixtures of cocoa butter (located at the bulk lipid phase) and MCT increased with the percentage of fat crystals, whereas for $W_1/O/W_2$ emulsions with fat fractions located at the water/oil interface, the rate of inner water content release was independent of the percentage of fat crystals.

4.1.2 *Droplet size*

The lipid phase composition had a significant impact on the W_1/O droplet size of $W_1/O/W_2$ emulsions with liquid lipid phase stabilized with Tween 80, being significantly smaller when using MCT (9.90 ± 0.15 μm) as compared to CO (13.14 ± 1.51 μm). In addition, the viscosity values of the W_1/O emulsions formulated with MCT, were significantly lower (68.7 ± 1.5 mPa·s) than the ones with CO (150.3 ± 1.5 mPa·s). Other authors have reported a relationship between the dispersed lipid phase viscosity and the final O/W emulsion droplet size, obtaining smaller droplet sizes when using a low viscosity dispersed lipid phase (Qian & McClements, 2011; Weiss & Muschiolik, 2007). Thus, this might be also applicable when the dispersed phase is a W_1/O emulsion, such as in the case of $W_1/O/W_2$ emulsions. Contrarily, the emulsifier type (Tween 80 or lecithin) used to stabilize the CO-W_1/O droplets dispersed in the W_2 phase did not cause a significant effect on their droplet size, which ranged between 13.14 and 14.54 μm. Both emulsifiers are classified as small-molecule emulsifiers, thus occupying the same space at the oil/water interface and consequently leading to the formation of droplets with similar sizes (Kralova & Sjöblom, 2009). Regarding the lipid phase state, non-significant differences in the W_1/O average oil droplet size of $W_1/O/W_2$ emulsions with gelled lipid phase consisting of MCT and GS (1% w/w) were observed in comparison to their respective liquid emulsions. Nevertheless, increasing the GS concentration to 5% (w/w) resulted in smaller W_1/O droplet sizes due to GS emulsifying properties.

4.1.3 *ζ-potential*

The lipid phase composition did not influence the ζ-potential of Tween 80-stabilized $W_1/O/W_2$ emulsions with liquid lipid phase, since the electrical charge of the W_1/O

droplets using MCT (-24.65 ± 3.44 mV) was similar to using CO (-26.92 ± 5.02 mV). On the contrary, the hydrophilic emulsifier type affected the electrical charge of the W_1/O droplets. For instance, $W_1/O/W_2$ emulsins formulated with CO presented more negative ζ-potential values using lecithin (-70.95 ± 4.81 mV) than Tween 80 (-26.92 ± 5.02 mV). The strongly negative ζ-potential values of $W_1/O/W_2$ emulsions stabilized with lecithin might be due to the anionic nature of this emulsifier, which is rich in phosphate groups (PO_3^{4-}) (Artiga-Artigas, Lanjari-Pérez, & Martín-Belloso, 2018; Zhang et al., 2012). On the contrary, Tween 80 is a non-ionic emulsifier, meaning it does not give a charge when adsorbed at the interface. However, it is well-known that anionic hydroxyl groups (OH^-) present in the water or oil used to prepare the $W_1/O/W_2$ emulsion can give small negative charges (McClements, 2015). When the lipid phase was gelled with GS (1% w/w), lecithin led to less negatively charged W_1/O droplets in comparison to its respective liquid $W_1/O/W_2$ emulsion. In fact, ζ-potential values were -70.95 ± 4.81 and -57.52 ± 7.61 mV for CO-$W_1/O/W_2$ emulsions with liquid and gelled lipid phase, respectively. This might be attributed to the ability of GS to displace a certain amount of anionic lecithin molecules from the oil droplet surface (Gaonkar & Borwankar, 1991), thus contributing to the less negatively ζ-potential values observed. The displacement of emulsifier from the interface by GS (1% w/w) has not been observed in $W_1/O/W_2$ emulsions stabilized with Tween 80, which showed similar ζ-potential values when formulated with liquid or gelled lipid phase. This might be because Tween 80 strongly adsorbs at the oil/water interface, which prevents its displacement by GS molecules, hence maintaining its interfacial electrostatic characteristics (Nash & Erk, 2017).

4.2 Colloidal stability of chlorophyllin-loaded $W_1/O/W_2$ emulsions

4.2.1 Cold storage conditions

In chapter IV, the colloidal stability of $W_1/O/W_2$ emulsions with liquid (MCT or CO) or gelled lipid phase (MCT or CO + GS 1% w/w) was studied by monitoring their ΔBS during 12 days of dark storage at 4 °C in order to simulate common storage conditions. Clarification, measured as ΔBS at the bottom of the tube, was influenced by the lipid phase state. In general, $W_1/O/W_2$ emulsions with a liquid lipid phase showed a significant increase in BS values during storage time at 4 °C, whereas their respective $W_1/O/W_2$ emulsions with a gelled lipid phase remained without changes, which evidenced their higher stability against clarification. According to Fernández-Martín, Freire, Bou,

Cofrades, & Jiménez-Colmenero (2017), the crystallization of a lipid phase would increase its viscosity offering a higher resistance to a viscous flow. Regarding the BS changes in the $W_1/O/W_2$ emulsions with liquid lipid phases, they presented ΔBS values below 5 during the first 2 days of storage but experimented with an increase after 5 days. At that point, clarification rather depended on the type of hydrophilic emulsifier used to disperse the W_1/O droplets into the W_2 phase, than on the lipid phase composition, with ΔBS values of around 20 and below 15 for lecithin and Tween 80, respectively. Nevertheless, at the end of the storage time, differences in the ΔBS were predominantly due to the lipid phase composition. For instance, $W_1/O/W_2$ emulsions stabilized with Tween 80 presented ΔBS values of 11.64 ± 1.08 and 23.88 ± 0.74 for MCT and CO, respectively. This might be due to the reduced initial oil droplet size of the $W_1/O/W_2$ emulsions formulated with MCT as compared to CO, which is known to cause droplets to be closely packed, retarding their migration to the upper part of the tube (McClements et al., 2007).

4.2.2 *In vitro gastrointestinal conditions*

The lipid phase composition and state determined the ability of $W_1/O/W_2$ emulsion to maintain their colloidal stability upon gastric conditions. The average W_1/O particle size of the $W_1/O/W_2$ emulsion with liquid lipid phase (MCT) after gastric conditions was significantly smaller (5.88 ± 0.43 μm) than that of the initial emulsion (7.88 ± 0.15 μm). It is well established that $W_1/O/W_2$ emulsions are susceptible to osmotic pressure changes. For instance, Liu et al. (2020) have reported that under an external applied osmotic gradient, W_1/O droplets in $W_1/O/W_2$ emulsions might experience swelling or shrinkage. These instability mechanisms could be explained by considering the osmolarity difference between the inner water droplets and the external aqueous phase. In the present study, salts present in the SGF solution could promote the partial migration of water from the inner to the outer aqueous phase of the $W_1/O/W_2$ emulsion with MCT, and consequently, the shrinkage of its W_1/O droplets. In contrast, the W_1/O droplet size of $W_1/O/W_2$ emulsions with gelled lipid phase formulated with a blend of MCT and GS (5% w/w) did not change significantly from their initial size, thus they remained stable upon the gastric conditions. This could be explained by the ability of the gelled lipid phase to act as a barrier and avoid water migration between aqueous phases (Herzi & Essafi, 2018; Liu et al., 2020; Molet-Rodríguez et al., 2021; Weiss & Muschiolik, 2007). In the

case of the $W_1/O/W_2$ emulsion with gelled lipid phase using HPO, its initial average W_1/O particle size did not change after gastric conditions, yet it continued exhibiting phase separation.

Regarding the W_1/O droplet size after the small intestinal digestion, both $W_1/O/W_2$ emulsions (MCT and MCT-GS) showed a bimodal size distribution. It is well-known that lipolysis during small intestinal digestion of emulsion-based delivery systems leads to lipid droplets break-up. Both $W_1/O/W_2$ emulsions (MCT and MCT-GS) had complete lipid hydrolysis, suggesting that the smaller particle observed in their size distribution graph would correspond to lipolysis subproducts in the digest. The bigger particles could be attributed to the presence of complex association colloids, such as vesicles and lamellar structures, formed in the digestion medium as a result of the interactions of lipid digestion products, bile salts, phospholipids, and calcium micelles (Gasa-Falcon, Odriozola-Serrano, Oms-Oliu, & Martín-Belloso, 2017). In the case of the $W_1/O/W_2$ emulsion with HPO, it had an increase in the average particle size after being subjected to *in vitro* small intestinal digestion (from 2.22 ± 1.07 to 5.37 ± 0.43 μm) and monomodal size distribution. It might be attributed to the presence of both digested products and non-digested lipid particles in the digest, as observed in its microscopy image after the small intestinal phase. In concordance, $W_1/O/W_2$ emulsions with HPO showed an uncomplete lipid digestibility.

4.3   Functionality of chlorophyllin-loaded $W_1/O/W_2$ emulsions

4.3.1   Encapsulation efficiency

The ability of the $W_1/O/W_2$ emulsions with liquid or gelled lipid phase to encapsulate CHL in the inner aqueous phase was evaluated. $W_1/O/W_2$ emulsions both with liquid and gelled lipid phases showed CHL encapsulation efficiency (EE) values higher than 98%. Our results are in agreement with a previous study where the CHL EE values in liquid lipid $W_1/O/W_2$ emulsions were around 91% (Artiga-Artigas, Molet-Rodríguez, Salvia-Trujillo, & Martín-Belloso, 2018a). In particular, $W_1/O/W_2$ emulsions stabilized with lecithin had the highest CHL EE (> 99%), which might be due to a possible interaction between the phosphate ions of lecithin and the hydroxyl groups of the encapsulated compound, being capable of forming H-bonds with the CHL (Artiga-Artigas et al., 2018b).

4.3.2 Lipid digestibility

The lipid digestibility of the $W_1/O/W_2$ emulsions was measured as the percentage of FFAs released during the *in vitro* small intestinal digestion (chapter V). Gelling the lipid phase by adding GS (5% w/w) to MCT or with pure HPO did not affect the lipid digestibility rate of $W_1/O/W_2$ emulsions, which behaved as liquid lipid $W_1/O/W_2$ emulsions possibly due to the melting of the lipid phase during intestinal conditions. Similar to our findings, it has been recently reported no significant differences between the lipid digestibility kinetics of O/W nanoemulsions stabilized with MCT and blends of MCT and GS (Abreu-Martins et al., 2020). Nevertheless, the lipolysis kinetics of solid lipid O/W nanoemulsions have been observed to be highly related to the specific crystalline state of the solid fat used at the intestinal temperature conditions (Abreu-Martins et al., 2020). In this regard, several authors have observed a delay in the lipolysis initiation of O/W nanoemulsions using lipid phases consisting of HPO, tripalmitin, fully hydrogenated soybean oil and cocoa butter, which was attributed to their high melting temperatures (Bonnaire et al., 2008; Guo, Bellissimo, & Rousseau, 2017; Hart, Lin, Thilakarathna, Wright, 2018; Abreu-Martins et al., 2020). The absence of differences in the lipid digestibility rate of $W_1/O/W_2$ emulsions formulated with MCT-GS or HPO may suggest that the presence of W_1 droplets within the oil droplets could have affected the type of HPO crystals formed and consequently, their crystalline state during the intestinal phase. Accordingly, Andrade, Wright, & Corredig (2018) have observed no significant differences in the initiation time of the lipolysis reaction between $W_1/O/W_2$ emulsions with liquid (soybean oil) or gelled lipid phases (soybean oil + trimyristin). In addition, the higher lipid droplet size in $W_1/O/W_2$ emulsions in comparison with that of the O/W nanoemulsions could minimize the effect of lipid phase gelling on lipid digestibility.

Lipid digestion end-point values were observed to be dependent on the fatty acid composition of each lipid phase used. $W_1/O/W_2$ emulsions with pure MCT and a blend of MCT and GS (5% w/w) presented FFAs values of $115.46 \pm 1.35\%$ and $110.49 \pm 7.39\%$, respectively. Their final amount of FFA released greater than 100% can be explained by the conversion of monoacylglycerol into glycerol and FFAs, which was not taken into account in the calculations (Carey, Small & Bliss, 1983). In the case of the $W_1/O/W_2$ emulsion with HPO, it showed a final FFA release of $33.40 \pm 0.52\%$. MCT oils are known to be digested by lipase more rapidly than LCT, such as those present in HPO, explaining

the lower FFA released of the $W_1/O/W_2$ emulsion formulated with HPO compared to the ones with MCT or MCT-GS (Salvia-Trujillo et al., 2013b). This has been attributed to the ability of medium-chain fatty acids to migrate more rapidly to the aqueous phase, while long-chain fatty acids tend to accumulate at the oil/water interface, thus hindering the lipase activity (Li et al., 2011). Despite the lower lipolysis of lipid droplets formed mainly by LCT, other authors have observed higher FFAs release values than the ones obtained in the present study. The visual appearance of the $W_1/O/W_2$ emulsion formulated with HPO showed an upper cream layer of non-emulsified oil, which has been reported to have a slower digestibility by lipase than emulsified oils (Zhang et al., 2016).

4.3.3 *Chlorophyllin bioaccessibility*

The CHL bioaccessibility was linked with the lipid digestion extent during *in vitro* small intestinal digestion of $W_1/O/W_2$ emulsions, which in turn depended on the lipid phase composition (see section 4.3.2). The FFA release end-point was higher for $W_1/O/W_2$ emulsions formulated with MCT ($115.46 \pm 1.35\%$) and MCT-GS ($110.49 \pm 7.39\%$) compared to HPO ($33.40 \pm 0.52\%$). Accordingly, higher CHL bioaccessibility values were obtained for $W_1/O/W_2$ emulsions formulated with MCT ($88.97 \pm 7.12\%$) and MCT-GS ($81.05 \pm 3.99\%$) than HPO ($67.12 \pm 6.82\%$). Thus, our results evidenced that a higher lipid digestibility of $W_1/O/W_2$ emulsions formulated with MCT oils in comparison with LCT during the *in vitro* small intestinal digestion results in higher CHL bioaccessibility (Lamba, Sathish, & Sabikhi, 2015). Nevertheless, the lipid phase gelation did not influence the CHL bioaccessibility of $W_1/O/W_2$ emulsions at the end of the small intestinal phase. In agreement with these results, Andrade et al. (2018) have reported that the release of hydrophilic molecules, vitamin B12, from the inner to the outer aqueous phase during *in vitro* gastrointestinal conditions did not differ between $W_1/O/W_2$ emulsions with liquid phase (soybean oil) and gelled lipid phase (soybean oil + trimyristin).

5   Chlorophyllin-loaded $W_1/O/W_2$ emulsions with liquid or gelled lipid phase into whole milk

5.1   Physicochemical properties of chlorophyllin-loaded $W_1/O/W_2$ emulsions once incorporated into whole milk

The behaviour of $W_1/O/W_2$ emulsions in terms of W_1/O particle size once incorporated into whole milk depended on their lipid phase composition, being MCT, a blend of MCT and GS (5% w/w) or HPO. The average particle sizes of $W_1/O/W_2$ emulsions formulated with pure MCT or a blend of MCT and GS (5% w/w) were 7.88 ± 0.15 and 4.30 ± 0.63 μm, respectively, whereas after their incorporation into whole milk average particle sizes of 1.60 ± 0.10 and 1.16 ± 0.18 μm, were observed, respectively. In addition, their monomodal distribution (particle population > 1 μm) changed to bimodal when whole milk was present, with a new population of submicron particles. This population might be due to the presence of fat globules (0.39 ± 0.06 μm) and casein micelles ($\sim$ 50-500 nm) dispersed in the outer aqueous phases, whereas the micrometric peak would correspond to W_1/O droplets. Thus, the average W_1/O particle size of $W_1/O/W_2$ emulsions (MCT or MCT-GS) was not altered after their incorporation into whole milk. Regarding the $W_1/O/W_2$ emulsion with gelled lipid phase (HPO) into whole milk, it showed improved stability, as observed in its homogeneous visual appearance in comparison with the $W_1/O/W_2$ emulsion (HPO) itself that presented phase separation. In this context, it might be possible that the oil/water interface of the $W_1/O/W_2$ emulsion with HPO had not been fully saturated by Tween 80 during emulsion formation (Molet-Rodríguez et al., 2021). As a consequence, milk protein, which is well-known to have surface-active properties, could have been absorbed at the oil/water interface of W_1/O particles, enhancing the $W_1/O/W_2$ emulsion colloidal stability (Gomes et al., 2018). In concordance with the absorption of milk protein at the oil/water interface, the average W_1/O particle size of $W_1/O/W_2$ emulsion with HPO was reduced after its incorporation into whole milk (from 3.60 ± 3.25 to 0.59 ± 0.07 μm).

5.2 Colloidal stability during *in vitro* gastrointestinal conditions of chlorophyllin-loaded $W_1/O/W_2$ emulsions co-digested with whole milk

The colloidal stability of the $W_1/O/W_2$ emulsions into whole milk after gastric conditions depended also on the lipid phase composition. The average W_1/O particle size of $W_1/O/W_2$ emulsions formulated with MCT or MCT-GS into whole milk was not affected by the gastric conditions. Although both formulations experimented with a significant increase in their average particle size after the gastric phase (from 1.60 ± 0.10 to 8.06 ± 0.18 μm and from 1.16 ± 0.18 to 4.17 ± 0.62 μm for MCT and MCT-GS, respectively), their microscopic images did not show changes in the W_1/O particle size. Instead, aggregates of proteins could be observed in the outer aqueous phase. Casein micelles are known to deprotonate and form aggregates via hydrophobic attractions and van der Waals interactions at pH close to their isoelectric point (around 4.5-4.8), that is, upon gastric pH conditions. Thus, milk proteins aggregation upon gastric conditions could be responsible for the increased particle size in $W_1/O/W_2$ emulsions formulated with MCT and MCT-GS into whole milk after gastric phase conditions, rather than W_1/O droplets instability. In the case of the $W_1/O/W_2$ emulsion formulated with HPO into whole milk, its visual appearance after the gastric phase presented two phases (cream and serum), thus suggesting that W_1/O droplets suffer destabilization and further phase separation has occurred. Taking into account the possible absorption of milk protein at the oil/water interface once the $W_1/O/W_2$ emulsion formulated with HPO was incorporated into whole milk (see section 5.1), the gastric phase pH of 3 may have caused absorbed proteins to deprotonate and subsequently, W_1/O droplets to attract each other's, explaining the observed $W_1/O/W_2$ emulsion phase separation.

As in the case of the $W_1/O/W_2$ emulsions, the particle size after the small intestinal digestion of $W_1/O/W_2$ emulsions into whole milk depended on the lipid droplets hydrolysis and break-up. Thus, small particle sizes could be due to free lipolysis products, whereas high particle size would correspond to lipolysis products complexation and undigested oil droplets aggregation (Salvia-Trujillo et al., 2013a). In addition, Marwah et al. (2018) have shown that one-tailed amphiphilic molecules such as GS, can form large aggregates in an aqueous medium containing hydrophilic molecules such as protein and lactose. In addition, the remaining non-digested SC and WPI could have aggregated, explaining the big particle sizes observed (Chang & McClements, 2016).

5.3 Functionality during *in vitro* small intestinal digestion of chlorophyllin-loaded $W_1/O/W_2$ emulsions co-digested with whole milk

5.3.1 Lipid digestibility

The $W_1/O/W_2$ emulsions formulated with MCT and MCT-GS into whole milk presented a final percentage of FFAs released ≥ 96%, suggesting a complete lipid digestibility. In the case of the $W_1/O/W_2$ emulsion formulated with HPO, its co-digestion with whole milk led to higher percentages of FFA release (57.71 ± 3.06%) compared to the $W_1/O/W_2$ emulsion (33.40 ± 0.52%). In this case, the lipolysis of other lipid components in the system, such as fat globules from whole milk, could explain the differences in the FFA release after the intestinal digestion of the $W_1/O/W_2$ emulsion formulated with HPO before and after being incorporated into whole milk. In addition, milk proteins could also have contributed to the observed increased lipid digestibility by *(i)* contributing to the NaOH needed to neutralize the acid released due to the hydrolyzation of proteins into amino acids in the small intestine (Mat et al. 2016); *(ii)* improving the $W_1/O/W_2$ emulsion stability and consequently the lipid digestibility extent, as emulsified oils are well known to present a faster lipid digestibility than non-emulsified oils (Zhang et al., 2016); and *(iii)* enhancing the access of lipase to the lipid droplets as a result of their smaller size and the increase of the surface area (Salvia-Trujillo et al., 2013a).

5.3.2 Chlorophyllin bioaccessibility

The CHL bioaccessibility after *in vitro* small intestinal digestion of $W_1/O/W_2$ emulsion (MCT) co-digested with whole milk was lower (66.07 ± 8.29%) compared to its respective $W_1/O/W_2$ emulsion (88.97 ± 7.12%). Instead, $W_1/O/W_2$ emulsion with gelled lipid phases (MCT-GS and HPO) co-digested with whole milk showed non-significant differences in the CHL bioaccessibility (91.87 ± 13.64 and 67.88 ± 10.26%, respectively) with their respective $W_1/O/W_2$ emulsion with gelled lipid phase (81.05 ± 3.99 and 67.12 ± 6.82%, respectively). It could be possible that the CHL in the digest of the $W_1/O/W_2$ emulsion (MCT) would have interacted with milk macromolecules, thus hindering the adsorption of CHL in the small intestine. Interestingly, these interactions would be avoided by $W_1/O/W_2$ emulsion lipid phase gelation.

6 References

Abreu-Martins, H., Artiga-Artigas, M., Hilsdorf Piccoli, R., Martín-Belloso, O., & Salvia-Trujillo, L. (2020). The lipid type affects the in vitro digestibility and β-carotene bioaccessibility of liquid or solid lipid nanoparticles. *Food Chemistry*, *311*, 126024.

Ahmed, K., Li, Y., McClements, D. J., & Xiao, H. (2012). Nanoemulsion- and emulsion-based delivery systems for curcumin: Encapsulation and release properties. *Food Chemistry*, *132*(2), 799–807.

Andrade, J., Wright, A. J., & Corredig, M. (2018). In vitro digestion behavior of water-in-oil-in-water emulsions with gelled oil-water inner phases. *Food Research International*, *105*, 41–51.

Artiga-Artigas, M., Molet-Rodríguez, A., Salvia-Trujillo, L., & Martín-Belloso, O. (2018a). Formation of Double (W1/O/W2) Emulsions as Carriers of Hydrophilic and Lipophilic Active Compounds. *Food and Bioprocess Technology*, *12*, 422–435.

Artiga-Artigas, M., Lanjari-Pérez, Y., & Martín-Belloso, O. (2018b). Curcumin-loaded nanoemulsions stability as affected by the nature and concentration of surfactant. *Food Chemistry*, *266*, 466–474.

Bonnaire, L., Sandra, S., Helgason, T., Decker, E. A., Weiss, J., & McClements, D. J. (2008). Influence of lipid physical state on the in vitro digestibility of emulsified lipids. *Journal of Agricultural and Food Chemistry*, *56*(10), 3791–3797.

Borreani, J., Leonardi, C., Moraga, G., Quiles, A., & Hernando, I. (2019). How do Different Types of Emulsifiers/Stabilizers Affect the In Vitro Intestinal Digestion of O/W Emulsions? *Food Biophysics*, *14*(3), 313–325.

Brummer, Y., Defelice, C., Wu, Y., Kwong, M., Wood, P. J., & Tosh, S. M. (2014). Textural and rheological properties of oat beta-glucan gels with varying molecular weight composition. *Journal of Agricultural and Food Chemistry*, *62*(14), 3160–3167.

Carey, M. C., Small, D. M., & Bliss, C. M. (1983). Lipid digestion and absorption. *Annual Review of Physiology, 45*, 651–677.

Chang, & McClements, D. J. (2016). Influence of emulsifier type on the in vitro digestion of fish oil-in-water emulsions in the presence of an anionic marine polysaccharide (fucoidan): Caseinate, whey protein, lecithin, or Tween 80. *Food Hydrocolloids*, *61*, 92–101.

Chang Y., McLandsborough, L., & McClements, D. J. (2012). Physical properties and antimicrobial efficacy of thyme oil nanoemulsions: Influence of ripening inhibitors. *Journal of Agricultural and Food Chemistry*, *60*(48), 12056–12063.

Chuacharoen, T., & Sabliov, C. M. (2016). The potential of zein nanoparticles to protect entrapped b -carotene in the presence of milk under simulated gastrointestinal (GI) conditions. *LWT - Food Science and Technology*, *72*, 302–309.

De Bont, P. W., Van Kempen, G. M. P., & Vreeker, R. (2002). Phase separation in milk protein and amylopectin mixtures. *Food Hydrocolloids*, *16*(2), 127–138.

Di Mattia, C. D., Sacchetti, G., & Pittia, P. (2011). Interfacial Behavior and Antioxidant Efficiency of Olive Phenolic Compounds in O/W Olive oil Emulsions as Affected by Surface Active Agent Type. *Food Biophysics*, *6*(2), 295–302.

Dickinson, E. (2001). Milk protein adsorbed layers and the relationship to emulsion stability and rheology. *Studies in Surface Science and Catalysis*, *132*, 973–978.

Dickinson, E., & Hong, S. T. (1994). Surface Coverage of β-Lactoglobulin at the Oil-Water Interface: Influence of Protein Heat Treatment and Various Emulsifiers. *Journal of Agricultural and Food Chemistry*, *42*(8), 1602–1606.

Fernández-Martín, F., Freire, M., Bou, R., Cofrades, S., & Jiménez-Colmenero, F. (2017). Olive oil based edible W/O/W emulsions stability as affected by addition of some acylglycerides. *Journal of Food Engineering*, *196*, 18–26.

Francis, M. J., Glover, Z. J., Yu, Q., Povey, M. J., & Holmes, M. J. (2019). Acoustic characterisation of pH dependant reversible micellar casein aggregation. *Colloids and Surfaces A: Physicochemical and Engineering Aspects*, *568*, 259–265.

Gao, B., Luo, Y., Lu, W., Liu, J., Zhang, Y., & Yu, L. (2017). Triacylglycerol compositions of sunflower, corn and soybean oils examined with supercritical CO2 ultra-performance convergence chromatography combined with quadrupole time-of-flight mass spectrometry. *Food Chemistry*, *218*, 569–574.

Gaonkar, A. G., & Borwankar, R. P. (1991). Competitive adsorption of monoglycerides and lecithin at the vegetable oil-water interface. *Colloids and Surfaces*, *59*(C), 331–343.

Gasa-Falcon, A., Odriozola-Serrano, I., Oms-Oliu, G., & Martín-Belloso, O. (2017). Influence of mandarin fiber addition on physico-chemical properties of nanoemulsions containing β-carotene under simulated gastrointestinal digestion conditions. *LWT - Food Science and Technology*, *84*, 331–337.

Gasa-Falcon, A., Odriozola-Serrano, I., Oms-Oliu, G., & Martín-Belloso, O. (2019). Impact of emulsifier nature and concentration on the stability of β-carotene enriched nanoemulsions during: In vitro digestion. *Food and Function*, *10*(2), 713–722.

Gill, A. O., Delaquis, P., Russo, P., & Holley, R. A. (2002). Evaluation of antilisterial action of cilantro oil on vacuum packed ham. *International Journal of Food Microbiology*, *73*(1), 83–92.

Goh, K. K. T., Sarkar, A., & Singh, H. (2014). Milk Protein–Polysaccharide Interactions. In H. Singh, M. Boland, & A. Thompson (2nd ed.)*, Milk Proteins From Expression to Food* (pp. 387-419). Academic Press.

Gomes, A., Costa, A. L. R., & Cunha, R. L. (2018). Impact of oil type and WPI/Tween 80 ratio at the oil-water interface: Adsorption, interfacial rheology and emulsion features. *Colloids and Surfaces B: Biointerfaces*, *164*, 272–280.

Guo, Q., Bellissimo, N., & Rousseau, D. (2017). The Physical State of Emulsified Edible Oil Modulates Its in Vitro Digestion. *Journal of Agricultural and Food Chemistry*, *65*(41), 9120–9127.

Halabi, A., Croguennec, T., Bouhallab, S., Dupont, D., & Deglaire, A. (2020). Modification of protein structures by altering the whey protein profile and heat treatment affects: In vitro static digestion of model infant milk formulas. *Food and Function*, *11*(8), 6933–6945.

Hart, S. M., Lin, X., Thilakarathna, S. H., & Wright, A. J. (2018). Emulsion droplet crystallinity attenuates early in vitro digestive lipolysis and beta-carotene bioaccessibility. *Food Chemistry*, *260*, 145–151.

Hassan, A. N., Frank, J. F., Farmer, M. A., Schmidt, K. A., & Shalabi, S. I. (1995). Formation of Yogurt Microstructure and Three-Dimensional Visualization as Determined by Confocal Scanning Laser Microscopy. *Journal of Dairy Science*, *78*(12), 2629–2636.

Herzi, S., & Essafi, W. (2018). Different magnesium release profiles from W/O/W emulsions based on crystallized oils. *Journal of Colloid and Interface Science*, *509*, 178–188.

Hsu, J. P., & Nacu, A. (2003). Behavior of soybean oil-in-water emulsion stabilized by nonionic surfactant. *Journal of Colloid and Interface Science*, *259*(2), 374–381.

Hur, S. J., Decker, E. A., & McClements, D. J. (2009). Influence of initial emulsifier type on microstructural changes occurring in emulsified lipids during in vitro digestion. *Food Chemistry*, *114*(1), 253–262.

Jo, Y. J., & Kwon, Y. J. (2014). Characterization of β-carotene nanoemulsions prepared by microfluidization technique. *Food Science and Biotechnology*, *23*(1), 107–113.

Karupaiah, T., & Sundram, K. (2007). Effects of stereospecific positioning of fatty acids in triacylglycerol structures in native and randomized fats: A review of their nutritional implications. *Nutrition and Metabolism*, *4*(16), 1–17.

Keowmaneechai, E., & McClements, D. J. (2002). Effect of CaCl2 and KCl on Physiochemical Properties of Model Nutritional Beverages Based on Whey Protein Stabilized Oil-in-Water Emulsions. *Journal of Food Science, 67*(2), 665-671.

Knudsen, K. E. B. (2014). Fiber and nonstarch polysaccharide content and variation in common crops used in broiler diets. *Poultry Science*, *93*(9), 2380–2393.

Kossena, G. A., Boyd, B. J., Porter, C. J. H., & Charman, W. N. (2003). Separation and characterization of the colloidal phases produced on digestion of common formulation lipids and assessment of their impact on the apparent solubility of selected poorly water-soluble drugs. *Journal of Pharmaceutical Sciences*, *92*(3), 634–648.

Kralova, I., & Sjöblom, J. (2009). Surfactants used in food industry: A review. *Journal of Dispersion Science and Technology*, *30*(9), 1363–1383.

Lamba, H., Sathish, K., & Sabikhi, L. (2015). Double Emulsions: Emerging Delivery System for Plant Bioactives. *Food and Bioprocess Technology*, *8*(4), 709–728.

Law, A. J. R., & Leaver, J. (2000). Effect of pH on the thermal denaturation of whey proteins in milk. *Journal of Agricultural and Food Chemistry*, *48*(3), 672–679.

Li, Y., Hu, M., & McClements, D. J. (2011). Factors affecting lipase digestibility of emulsified lipids using an in vitro digestion model: Proposal for a standardised pH-stat method. *Food Chemistry*, *126*(2), 498–505.

Li, Y., & Mcclements, D. J. (2010). New mathematical model for interpreting ph-stat digestion profiles: Impact of lipid droplet characteristics on in vitro digestibility. *Journal of Agricultural and Food Chemistry*, *58*(13), 8085–8092.

Liu, J., Kharat, M., Tan, Y., Zhou, H., Muriel Mundo, J. L., & McClements, D. J. (2020). Impact of fat crystallization on the resistance of W/O/W emulsions to osmotic stress: Potential for temperature-triggered release. *Food Research International*, *134*, 109273.

Lubary, M., Hofland, G. W., & ter Horst, J. H. (2011). The potential of milk fat for the synthesis of valuable derivatives. *European Food Research and Technology*, *232*(1), 1–8.

Luo, J., Wang, Z. W., Wang, F., Zhang, H., Lu, J., Guo, H. Y., & Ren, F. Z. (2014). Cryo-SEM images of native milk fat globule indicate small casein micelles are constituents of the membrane. *RSC Advances*, *4*(90), 48963–48966.

Mackie, A. R., Rafiee, H., Malcolm, P., Salt, L., & van Aken, G. (2013). Specific food structures supress appetite through reduced gastric emptying rate. *American Journal of Physiology - Gastrointestinal and Liver Physiology*, *304*(11), 1038–1043.

Maldonado-Valderrama, J., Wilde, P., Macierzanka, A., & Mackie, A. (2011). The role of bile salts in digestion. *Advances in Colloid and Interface Science*, *165*(1), 36–46.

Marinova, K. G., Alargova, R. G., Denkov, N. D., Velev, O. D., Petsev, D. N., Ivanov, I. B., & Borwankar, R. P. (1996). Charging of Oil - Water Interfaces Due to Spontaneous Adsorption of Hydroxyl Ions. *Langmuir, 12*(8), 2045–2051.

Maragò, E., Iacopini, P., Camangi, F., Scattino, C., Ranieri, A., Stefani, A., & Sebastiani, L. (2015). Phenolic profile and antioxidant activity in apple juice and pomace: Effects of different storage conditions. *Fruits*, *70*(4), 213–223.

Marwah, M., Magarkar, A., Ray, D., Aswal, V., Bunker, A., & Nagarsenker, M. (2018). Glyceryl Monostearate: Probing the Self Assembly of a Lipid Amenable To Surface Modification for Hepatic Targeting. *The Journal of Physical Chemistry C*, *122*(38), 22160–22169.

Mason, T. G., Wilking, J. N., Meleson, K., Chang, C. B., & Graves, S. M. (2006). Nanoemulsions: formation, structure, and physical properties. *Journal of Physics: Condensed Matter*, *18*(41), R635–R666.

Mat, D. J. L., Le Feunteun, S., Michon, C., & Souchon, I. (2016). In vitro digestion of foods using pH-stat and the INFOGEST protocol: Impact of matrix structure on digestion kinetics of macronutrients, proteins and lipids. *Food Research International*, *88*(B), 226–233.

McClements, D. J., Decker, E. A., & Weiss, J. (2007). Emulsion-based delivery systems for lipophilic bioactive components. *Journal of Food Science*, *72*(8), 109–124.

McClements, D. J. (2015). *Food Emulsions: Principles, Practices, and Techniques* (3rd ed.). CRC Press, Taylor & Francis Group.

Molet-Rodríguez, A., Martín-Belloso, O., & Salvia-trujillo, L. (2021). Formation and Stabilization of W1/O/W2 Emulsions with Gelled Lipid Phases. *Molecules*, *26*(2), 312.

Mulet-Cabero, A. I., Mackie, A. R., Wilde, P. J., Fenelon, M. A., & Brodkorb, A. (2019). Structural mechanism and kinetics of in vitro gastric digestion are affected by process-induced changes in bovine milk. *Food Hydrocolloids*, *86*, 172–183.

Mulet-Cabero, A. I., Torcello-Gómez, A., Saha, S., Mackie, A. R., Wilde, P. J., & Brodkorb, A. (2020). Impact of caseins and whey proteins ratio and lipid content on in vitro digestion and ex vivo absorption. *Food Chemistry*, *319*, 126514.

Mun, S., Kim, Y. R., Shin, M., & McClements, D. J. (2015). Control of lipid digestion and nutraceutical bioaccessibility using starch-based filled hydrogels: Influence of starch and surfactant type. *Food Hydrocolloids*, *44*, 380–389.

Nash, J. J., & Erk, K. A. (2017). Stability and interfacial viscoelasticity of oil-water nanoemulsions stabilized by soy lecithin and Tween 20 for the encapsulation of bioactive carvacrol. *Colloids and Surfaces A: Physicochemical and Engineering Aspects*, *517*, 1–11.

Nguyen, H. T. H., Gathercole, J. L., Day, L., & Dalziel, J. E. (2020). Differences in peptide generation following in vitro gastrointestinal digestion of yogurt and milk from cow, sheep and goat. *Food Chemistry*, *317*, 126419.

Pihlanto, A. (2006). Antioxidative peptides derived from milk proteins. *International Dairy Journal*, *16*(11), 1306–1314.

Pinheiro, A. C., Lad, M., Silva, H. D., Coimbra, M. A., Boland, M., & Vicente, A. A. (2013). Unravelling the behaviour of curcumin nanoemulsions during in vitro digestion: Effect of the surface charge. *Soft Matter*, *9*(11), 3147–3154.

Qian, C, & McClements, D. J. (2011). Formation of nanoemulsions stabilized by model food-grade emulsifiers using high-pressure homogenization: Factors affecting particle size. *Food Hydrocolloids*, *25*(5), 1000–1008.

Qian, C., Decker, E. A., Xiao, H., McClements, D.J. (2012). Physical and chemical stability of b-carotene-enriched nanoemulsions: Influence of pH, ionic strength, temperature, and emulsifier type. *Food Chemistry, 132*(3), 1221-1229.

Regand, A., Tosh, S. M., Wolever, T. M. S., & Wood, P. J. (2009). Physicochemical properties of glucan in differently processed oat foods influence glycemie response. *Journal of Agricultural and Food Chemistry*, *57*(19), 8831–8838.

Roth, S., Murray, B. S., & Dickinson, E. (2000). Interfacial shear rheology of aged and heat-treated β-lactoglobulin films: Displacement by nonionic surfactant. *Journal of Agricultural and Food Chemistry*, *48*(5), 1491–1497.

Roye, C., Bulckaen, K., De Bondt, Y., Liberloo, I., Van De Walle, D., Dewettinck, K., & Courtin, C. M. (2020). Side-by-side comparison of composition and structural properties of wheat, rye, oat, and maize bran and their impact on in vitro fermentability. *Cereal Chemistry*, *97*(1), 20–33.

Salvia-Trujillo, L., Qian, C., Martín-Belloso, O., & McClements, D. J. (2013a). Modulating β-carotene bioaccessibility by controlling oil composition and concentration in edible nanoemulsions. *Food Chemistry*, *139*(1–4), 878–884.

Salvia-trujillo, L., Qian, C., Martín-belloso, O., & Mcclements, D. J. (2013b). Influence of particle size on lipid digestion and β-carotene bioaccessibility in emulsions and nanoemulsions. *Food Chemistry*, *141*(2), 1472–1480.

Salvia-Trujillo, L., Verkempinck, S.H.E., Sun, L., Van Loey, A.M., Grauwet, T., & Hendrickx, M.E. (2017). Lipid digestion, micelle formation and carotenoid bioaccessibility kinetics: Influence of emulsion droplet size. *Food Chemistry, 229,* 653–662.

Sarantis, S. D., Eren, N. M., Kowalcyk, B., Jimenez–Flores, R., & Alvarez, V. B. (2021). Thermodynamic interactions of micellar casein and oat β-glucan in a model food system. *Food Hydrocolloids*, *115*, 106559.

Schempp, H., Christof, S., Mayr, U., & Treutter, D. (2016). Phenolic compounds in juices of apple cultivars and their relation to antioxidant activity. *Journal of Applied Botany and Food Quality*, *89*, 11–20.

Schmidts, T., Dobler, D., Guldan, A. C., Paulus, N., & Runkel, F. (2010). Multiple W/O/W emulsions-Using the required HLB for emulsifier evaluation. *Colloids and Surfaces A: Physicochemical and Engineering Aspects*, *372*(1–3), 48–54.

Skandamis, P., Tsigarida, E., & Nychas, G. J. E. (2000). Ecophysiological attributes of Salmonella typhimurium in liquid culture and within a gelatin gel with or without the addition of oregano essential oil. *World Journal of Microbiology and Biotechnology*, *16*(1), 31–35.

Sun, C., Gunasekaran, S., & Richards, M. P. (2007). Effect of xanthan gum on physicochemical properties of whey protein isolate stabilized oil-in-water emulsions. *Food Hydrocolloids*, *21*(4), 555–564.

Timm-Heinrich, M., Xu, X., Nielsen, N. S., & Jacobsen, C. (2003). Oxidative stability of structured lipids produced from sunflower oil and caprylic acid. *European Journal of Lipid Science and Technology*, *105*(8), 436–448.

Tosh, S. M., Brummer, Y., Wood, P. J., Wang, Q., & Weisz, J. (2004). Evaluation of structure in the formation of gels by structurally diverse (1 → 3)(1 → 4)-β-D-glucans from four cereal and one lichen species. *Carbohydrate Polymers*, *57*(3), 249–259.

Urakami, A. M., Ukada, K. F., Amano, Y. Y., & Ohtani, S. G. (2005). *Effects of Sucrose on Emulsification of Triglyceride by Polyglycerin Fatty Acid Ester*. *54*(6), 335–340.

Vasbinder, A. J., Alting, A. C., & De Kruif, K. G. (2003). Quantification of heat-induced casein-whey protein interactions in milk and its relation to gelation kinetics. *Colloids and Surfaces B: Biointerfaces*, *31*(1–4), 115–123.

Verkempinck, S. H. E., Salvia-Trujillo, L., Moens, L. G., Charleer, L., Van Loey, A. M., Hendrickx, M. E., & Grauwet, T. (2018). Emulsion stability during gastrointestinal conditions effects lipid digestion kinetics. *Food Chemistry*, *246*, 179–191.

Wackerbarth, H., Stoll, T., Gebken, S., Pelters, C., & Bindrich, U. (2009). Carotenoid-protein interaction as an approach for the formulation of functional food emulsions. *Food Research International*, *42*(9), 1254–1258.

Weiss, J., & Muschiolik, G. (2007). Factors affecting the droplet size of water-in-oil emulsions (W/O) and the oil globule size in Water-in-oil-in-water emulsions (W/O/W). *Journal of Dispersion Science and Technology*, *28*(5), 703–716.

Wu, J., Zhang, Y., Wang, L., Xie, B., Wang, H., & Deng, S. (2006). Visualization of Single and Aggregated Hulless Oat (Avena nuda L.) (1→3),(1→4)-β- d -Glucan Molecules by Atomic Force Microscopy and Confocal Scanning Laser Microscopy . *Journal of Agricultural and Food Chemistry*, *54*(3), 925–934.

Zhang, H. Y., Tehrany, E. A., Kahn, C. J. F., Ponc, M., Linder, M., & Cleymand, F. (2012). Effects of nanoliposomes based on soya , rapeseed and fish lecithins on chitosan thin films designed for tissue engineering. *Carbohydrate Polymers, 88*(2), 618–627.

Zhang, R., Zhang, Z., Zou, L., Xiao, H., Zhang, G., Decker, E. A., & McClements, D. J. (2016). Enhancement of carotenoid bioaccessibility from carrots using excipient emulsions: Influence of particle size of digestible lipid droplets. *Food and Function*, *7*(1), 93–103.

Zulueta, A., Esteve, M. J., Frasquet, I., & Frígola, A. (2007). Vitamin C, vitamin A, phenolic compounds and total antioxidant capacity of new fruit juice and skim milk mixture beverages marketed in Spain. *Food Chemistry*, *103*(4), 1365–1374.

CONCLUSIONS

The results obtained in this doctoral thesis contributed to elucidating the behaviour of emulsion-based delivery systems (*i.e.,* O/W emulsions, O/W nanoemulsions and $W_1/O/W_2$ emulsions) carrying active compounds once incorporated into complex food matrices in terms of physicochemical properties, colloidal stability and functionality. The main findings obtained are organized in two sections depending on the emulsion-based delivery system used.

Section I: O/W emulsions and nanoemulsions

- The incorporation of essential oils-O/W nanoemulsions into apple juice-based beverage enhanced their colloidal stability and antioxidant activity, which can be probably attributed to the presence of polyphenols in this food matrix. Nevertheless, their antimicrobial activity was diminished into apple juice-based beverage compared to water, presumably due to the ability of sugars to repair damaged cells.

- The colloidal stability of β-carotene-loaded O/W emulsions into dairy products during *in vitro* gastrointestinal digestion conditions was not altered. However, their lipid emptying was faster because of the ability of the dairy protein to form a sedimented network entrapping the lipid droplets, thus being emptied at early gastric times. In addition, the incorporation of O/W emulsions into dairy products enhanced their lipid digestibility, which might be due to the higher lipid digestion of dairy fat globules and/or oil droplets stabilized with denatured protein. Their β-carotene retention was also increased, probably due to the antioxidant properties of protein. Nevertheless, the β-carotene bioaccessibility of O/W emulsions into dairy products was diminished, presumably because of its lower micellarization as a result of the interaction with dairy protein.

- The incorporation of β-carotene-loaded O/W emulsion into complex meals consisting of whole milk and oatmeal did not compromise its colloidal stability during *in vitro* gastrointestinal digestion. Nevertheless, their lipid emptying was delayed due to the ability of β-glucan within oat grains to form gels, which slowed down the emptying. The β-carotene retention of O/W emulsions into the meals

during *in vitro* gastrointestinal digestion was enhanced, probably due to the antioxidant properties of both protein and polysaccharides within the meals.

Section II: $W_1/O/W_2$ emulsions

- The successful formation of stable $W_1/O/W_2$ emulsions with gelled lipid phase was strongly dependent on the lipid phase composition. Gelling the lipid phase neither alter the lipid digestibility nor the chlorophyllin bioaccessibility, which was also influenced by the lipid phase composition. $W_1/O/W_2$ emulsions with gelled lipid phase formulated adding an oleogelator to medium-chain triglycerides were digested to a higher extent than using long-chain triglycerides, which ultimately resulted in enhanced chlorophyllin bioaccessibility.

- The colloidal stability, lipid digestibility and chlorophyllin bioaccessibility of $W_1/O/W_2$ emulsions with gelled lipid phase into whole milk depended on the lipid phase composition. The $W_1/O/W_2$ emulsion with a gelled lipid phase consisting of medium-chain triglycerides with an oleogelator was not affected by its incorporation into whole milk, whereas the colloidal stability, lipid digestibility and consequently the chlorophyllin bioaccessibility were improved when a $W_1/O/W_2$ emulsion with gelled lipid phase formulated using a long-chain triglyceride oil was incorporated into whole milk.

FUTURE RESEARCH

The work presented in this doctoral thesis is one of the first to evaluate the colloidal stability and functionality of emulsion-based delivery systems into food products. From the results obtained, remaining gaps in knowledge and some aspects where future work is needed were identified and briefly discussed below:

- The present doctoral thesis particularly focuses on emulsion-delivery systems with aqueous continuous phases and stabilized with Tween 80 into water-based food matrices. There are several types of emulsion-based delivery systems and food matrices with different physicochemical properties, thus having the possibility to use a large number of combinations for the development of functional foods. In this sense, knowing the behaviour of other emulsion formulations and types in combination with different food matrices would be useful to modulate the formulation of the emulsion-based delivery system to obtain food products with specific functionality. Thus, future investigations may consider the study of other emulsions into different food matrices than the ones used in this doctoral thesis.

- The lipid digestion of emulsions before and after being incorporated into food products during the small intestinal phase was monitored with a pH-stat method. This allows understanding the lipid digestion rate and extent, as well as, bioactive compound bioaccessibility of emulsions co-ingested with food products as a whole system. In this sense, there is a need to complement pH-stat results with the quantitative determination of the lipid digestion species present during digestion, being free fatty acids, monoglycerides, diglycerides and triglycerides to gain insight on the contribution of lipid digestion from emulsions or food matrix when co-digested together, as well as, on the relationship between lipid digestion products and mixed micelles composition and solubilization capacity.

- Lipid digestion rate and extent were based on the action of pancreatic lipase in the small intestinal phase, as it is the main enzyme responsible for the digestion of triglycerides during gastrointestinal digestion. The study of the lipid digestion in the gastric phase by the action of gastric lipase would further enhance the understanding of the lipid digestion during the gastrointestinal tract from a more

realistic point of view, as well as, the possible implications to the gastric emptying of chyme and its subsequent lipolysis during the small intestinal digestion.

- The focus in this doctoral thesis was on lipid digestibility, as it serves as a carrier of active compounds into water-based food products and plays a key role in bioactive compound bioaccessibility. Nevertheless, results from chapter II point out a possible absorption of yogurt proteins at the oil/water interface of the O/W emulsion oil droplets, which may affect lipid digestion and consequently the bioactive compound bioaccessibility. Thus, the study of the protein digestion throughout the gastric phase would help in explaining the possible effect of protein-containing food matrices on the emulsion's lipid digestibility and bioaccessibility.